

**Tissue Engineering the TMJ Condyle using Human Umbilical Cord  
Mesenchymal Stromal Cells**

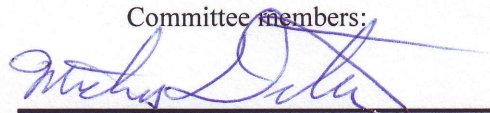
By

**Limin Wang**

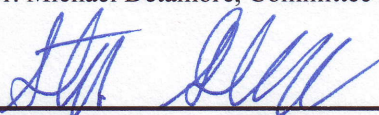
B.S., Chemical Engineering, Daqing Petroleum Institute, Daqing, China, 2001  
M.S., Chemical Engineering, China Petroleum University, Beijing, China, 2004

Submitted to Department of Chemical and Petroleum Engineering and the Faculty of  
the Graduate School of the University of Kansas in Partial Fulfillment of the  
Requirements for the Degree of Doctor of Philosophy

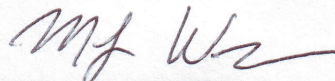
Committee members:



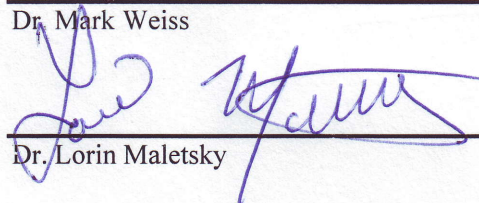
Dr. Michael Detamore, Committee chair



Dr. Stevin Gehrke



Dr. Mark Weiss



Dr. Lorin Maletsky



Dr. Cory Berkland

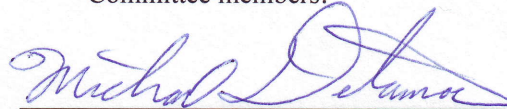
08/25/2008

Date defended

The Dissertation Committee for Limin Wang certifies  
that this is the approved version of the following dissertation:

Tissue Engineering the TMJ Condyle using  
Human Umbilical Cord Mesenchymal Stromal Cells

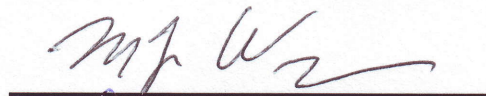
Committee members:



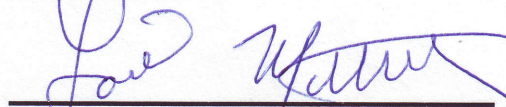
Dr. Michael Detamore, Committee Chair



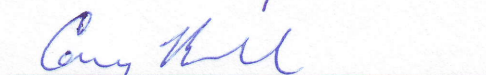
Dr. Stevin Gehrke



Dr. Mark Weiss



Dr. Lorin Maletsky



Dr. Cory Berkland



Date Approved

## ABSTRACT

The temporomandibular joint (TMJ), associated with everyday activities, such as chewing, yawning, talking, and laughing, is one of the most complex but least studied joints in the musculoskeletal system. Patients suffering from TMJ disorders (TMDs) may experience a variety of agonizing symptoms, such as earaches, headaches, neck pain, and difficulty opening the mouth, while current treatments are inefficacious owing to a poor understanding of TMJ disorder pathologies. Prior to this thesis, human umbilical cord mesenchymal stromal cells (hUCMSCs), identified as multipotent cells only in this decade, had not yet been used for TMJ tissue engineering. Hence, this thesis proposed a revolutionary tissue engineering approach in which hUCMSCs and mature hyaline cartilage cells, scaffolds, and growth factors were integrated to create TMJ condylar bone and cartilage *in vitro* to substitute for deteriorated native tissues. hUCMSCs were successfully differentiated along chondrogenic and osteogenic lineages in a 3D biomaterial-based environment, supporting the feasibility of using these cells for TMJ cartilage and bone tissue engineering. In TMJ cartilage regeneration, hUCMSCs demonstrated significant advantages over both mature TMJ cells and human bone marrow mesenchymal stromal cells (hBMSCs), with faster cell proliferation and superior biosynthesis. As an additional alternative, hyaline cartilage cells also surpassed TMJ cells in that they produced considerably more extracellular matrix. Following the initial efforts, the cell culture environment was refined, including cell seeding densities and signaling strategies. Higher cell seeding densities (>25 million cells/ml) were recommended for

both cartilage and bone tissue engineering, mainly due to their benefits to differentiation and biosynthesis. Insulin-like growth factor I (IGF-I) enhanced the chondrogenesis of pre-differentiated hUCMSCs while having no effect on osteogenically induced hUCMSCs. Therefore, the work on the successful differentiation of hUCMSCs in 3D biomaterials has been pioneering, and the culture parameters for *in vitro* TMJ tissue engineering have been refined. Moreover, this innovative work has tremendous implications for a broader area (e.g., musculoskeletal tissue engineering).

## ACKNOWLEDGMENTS

I would like to acknowledge Drs. Detamore, Gehrke, Weiss, Maletsky and, Berkland for serving on my dissertation committee and for their valuable mentorship as I researched and wrote this Ph.D. thesis. I want to give special recognition to my advisor, Dr. Michael Detamore, for his insight, support, and advice regarding personal and professional matters. His encouragement, experience, and enthusiasm provide motivation for my academic pursuits every day. Dr. Mark Weiss was especially helpful in providing help on stem cell isolation and critical comments on manuscripts. I also want to thank Dr. Lynda Bonewald for offering insightful suggestions regarding osteogenic differentiation and assistance in techniques related to bone-related protocols as well as reviewing the manuscript.

I would like to thank those who have provided assistance with this thesis project over the years. In particular, I would like to thank Milind Singh for his initial guidance in performing mechanical tests, Kiran Seshareddy for teaching me how to harvest cells from umbilical cords, Drs. Xinkun Wang and Qian Chen for their guidance in performing the RT-PCR technique, Dr. Liang Zhao for his guidance concerning flow cytometry, Jennifer Rosser for her assistance in doing bone assays, and Nathan Dormer and Paul Glatt for proofreading the manuscripts and this thesis.

I would like to thank Lauren Tice, Jaret Flores, Chris Conti, Ryan Boehler, Bryn Gardner, Mihael Lazebnik, Travis Miller, Ivy Tran, and Lana Johnson, Mark Bailey, undergraduates who completed projects under my supervision. In particular, I

extend thanks to Mihael Lazebnik for his intelligent and intuitive work on the development of bone assays, the execution of the OC experiment, and the maintenance of lab equipment.

I want to thank my parents, Yingxian and Zhili, for their great love and endless encouragement. Most importantly, I offer my special thanks to my wife Meina for sharing my happiness and sadness and for giving me unconditional and selfless support during this four-year period.

## TABLE OF CONTENTS

ACCEPTANCE PAGE .....	i
ABSTRACT .....	ii
ACKNOWLEDGEMENTS .....	iv
TABLE OF CONTENTS .....	vi
LIST OF FIGURES .....	xi
LIST OF TABLES .....	xiii
<b>CHAPTER 1: Introduction</b> .....	<b>1</b>
<b>CHAPTER 2: Tissue Engineering the Mandibular Condyle</b> .....	<b>6</b>
ABSTRACT .....	6
INTRODUCTION .....	7
ANATOMY .....	8
STRUCTURE AND FUNCTION OF MANDIBULAR CONDYLAR CARTILAGE .....	10
<i>Cell type and extracellular matrix</i> .....	10
<i>Biomechanic</i> .....	12
STRUCTURE AND FUNCTION OF MANDIBULAR CONDYLAR BONE ..	13
CELL SOURCES FOR MANDIBULAR CONDYLE TISSUE ENGINEERING .....	14
<i>Cell harvest from the condyle</i> .....	14
<i>Cell sources</i> .....	15
<i>Cell expansion</i> .....	18
SCAFFOLDS FOR BONE AND CARTILAGE TISSUE ENGINEERING .....	19
EFFECTS OF GROWTH FACTORS ON MANDIBULAR CONDYLAR CELLS .....	21
BIOREACTORS FOR CARTILAGE AND BONE TISSUE ENGINEERING ..	26
TISSUE ENGINEERING THE MANDIBULAR CONDYLE .....	32
DISCUSSION AND CONCLUSIONS .....	36
<b>CHAPTER 3: Tissue Engineering with Human Umbilical Cord Mesenchymal Stromal Cells</b> .....	<b>42</b>
ABSTRACT .....	42
INTRODUCTION .....	43
CELL CHARACTERIZATION .....	44
DIFFERENTIATION AND TISSUE ENGINEERING .....	47
<i>Chondrogenic differentiation and cartilage tissue engineering</i> .....	47
<i>Osteogenic differentiation and bone tissue engineering</i> .....	50

<i>Undifferentiated hUCMSCs and cardiovascular tissue engineering</i> .....	52
<i>Adipose differentiation and tissue engineering</i> .....	54
ESCS AND BMSCS .....	55
DISCUSSION, CONCLUSION AND FUTURE DIRECTIONS .....	56
<b>CHAPTER 4: Effects of Growth Factors and Glucosamine on Porcine Mandibular Condylar Cartilage Cells and Hyaline Cartilage Cells for Tissue Engineering Applications .....</b>	<b>61</b>
ABSTRACT.....	61
INTRODUCTION.....	62
MATERIALS AND METHODS .....	63
<i>Cell isolation</i> .....	63
<i>Growth factor</i> .....	64
<i>Measurement of cell number and biosynthesis</i> .....	64
RESULTS .....	65
<i>Cell number</i> .....	65
<i>GAG content</i> .....	67
<i>Collagen content</i> .....	68
DISCUSSION.....	70
<b>CHAPTER 5: Hyaline cartilage cells outperform mandibular condylar cartilage cells in a TMJ fibrocartilage tissue engineering application .....</b>	<b>74</b>
ABSTRACT.....	74
INTRODUCTION.....	75
MATERIALS AND METHODS .....	79
<i>Cell harvesting</i> .....	79
<i>Cell seeding and growth factor incorporation</i> .....	80
<i>Biochemical analysis and immunohistochemical staining</i> .....	81
<i>Statistical analysis</i> .....	82
RESULTS .....	82
<i>Cell number</i> .....	83
<i>GAG content</i> .....	84
<i>Hydroxyproline content</i> .....	85
<i>IHC analyses</i> .....	86
DISCUSSION.....	88
<b>CHAPTER 6: A Comparison of Human Umbilical Cord Matrix Stem Cells and TMJ Condylar Chondrocytes for Tissue Engineering TMJ Condylar Cartilage .....</b>	<b>95</b>
ABSTRACT.....	95
INTRODUCTION.....	96
MATERIALS AND METHODS .....	99
RESULTS .....	104
DISCUSSION.....	110

<b>CHAPTER 7: A Comparison of Human Bone Marrow-Derived Mesenchymal Stem Cells and Human Umbilical Cord-Derived Mesenchymal Stromal Cells for Cartilage Tissue Engineering</b> .....	<b>115</b>
ABSTRACT .....	115
INTRODUCTION .....	116
MATERIALS AND METHODS .....	118
<i>Cell harvest</i> .....	118
<i>Cell seeding</i> .....	119
<i>Biochemical analysis</i> .....	120
<i>Immunohistochemistry for types I and II collagen and aggrecan</i> .....	121
<i>RNA isolation and gene expression analysis</i> .....	122
<i>Statistical analysis</i> .....	123
RESULTS .....	123
<i>Cell number</i> .....	123
<i>GAG and HYP content</i> .....	125
<i>Immunohistochemistry</i> .....	126
<i>RT-PCR analysis</i> .....	128
DISCUSSION .....	129
<b>CHAPTER 8: The Effect of Initial Seeding Density on Human Umbilical Cord Mesenchymal Stromal Cells for Fibrocartilage Tissue Engineering</b> .....	<b>133</b>
ABSTRACT .....	133
INTRODUCTION .....	134
MATERIALS AND METHODS .....	136
<i>Cell harvest</i> .....	136
<i>Cell seeding</i> .....	138
<i>Biochemical analysis</i> .....	139
<i>Immunohistochemistry for types I and II collagen, and aggrecan</i> .....	140
<i>Mechanical integrity</i> .....	141
<i>Statistical analysis</i> .....	142
RESULTS .....	142
<i>Scaffold morphology</i> .....	142
<i>Cell number</i> .....	142
<i>GAG and hydroxyproline content</i> .....	144
<i>Immunohistochemical results</i> .....	148
<i>Mechanical properties</i> .....	150
DISCUSSION .....	150
<b>CHAPTER 9: Insulin-like Growth Factor-I Improves Chondrogenesis of Pre-differentiated Human Umbilical Cord Mesenchymal Stromal Cells</b> .....	<b>157</b>
ABSTRACT .....	157
INTRODUCTION .....	158
MATERIALS AND METHODS .....	159
<i>Cord collection and cell isolation</i> .....	159

<i>Cell seeding and culture</i> .....	160
<i>Assessment of biosynthesis and cell proliferation</i> .....	161
<i>Immunohistochemistry for types I and II collagen and aggrecan</i> .....	161
<i>RNA isolation and real-time RT-PCR</i> .....	162
<i>Statistics and data analysis</i> .....	163
RESULTS .....	163
<i>Cell number</i> .....	163
<i>GAG content</i> .....	164
<i>HYP content</i> .....	165
<i>Immunohistochemistry</i> .....	167
<i>RT-PCR analysis</i> .....	169
DISCUSSION .....	169
<b>CHAPTER 10: Osteogenic Differentiation of Human Umbilical Cord</b>	
<b>Mesenchymal Stromal Cells for Bone Tissue Engineering</b> .....	<b>173</b>
ABSTRACT .....	173
INTRODUCTION .....	174
MATERIALS AND METHODS .....	176
<i>Cell harvest</i> .....	176
<i>Cell culture and seeding</i> .....	177
<i>Cell number and hydroxyproline (HYP) content</i> .....	178
<i>Alkaline phosphatase (ALP) activity</i> .....	179
<i>Calcium content</i> .....	179
<i>Histology</i> .....	180
<i>Statistical analysis</i> .....	180
RESULTS .....	181
<i>Scaffold morphology and cell number</i> .....	181
<i>HYP content</i> .....	183
<i>ALP activity</i> .....	184
<i>Calcium content and von Kossa staining</i> .....	185
DISCUSSION .....	186
<b>CHAPTER 11: Signaling Strategies for Osteogenic Differentiation of Human</b>	
<b>Umbilical Cord Mesenchymal Stromal Cells for 3D Bone Tissue Engineering</b>	<b>192</b>
ABSTRACT .....	192
INTRODUCTION .....	193
MATERIALS AND METHODS .....	195
<i>Isolation and culture of hUCMSCs</i> .....	195
<i>Scaffold preparation, cell seeding and differentiation</i> .....	196
<i>Biochemical assays</i> .....	197
<i>Histology</i> .....	198
<i>RNA isolation and real-time RT-PCR</i> .....	199
<i>Statistical analysis</i> .....	199
RESULTS .....	200

<i>Cell number</i> .....	200
<i>HYP content</i> .....	201
<i>Calcium content</i> .....	203
<i>Histology</i> .....	205
<i>Gene expression levels of CI, Runx2, and OCN</i> .....	206
DISCUSSION AND CONCLUSION .....	206
<b>CHAPTER 12: Conclusion</b> .....	<b>210</b>
<b>REFERENCES</b> .....	<b>213</b>

## LIST OF FIGURES

### CHAPTER 1

No Figures

### CHAPTER 2

Figure 2.1: Schematic of the strategy to tissue engineer TMJ condyle ..... 37

### CHAPTER 3

Figure 3.1: Structure of UCs and differentiation schematic of hUCMSCs ..... 45

### CHAPTER 4

Figure 4.1: Cell number per well ..... 66

Figure 4.2: GAG content per well ..... 68

Figure 4.3: Collagen content per well ..... 69

### CHAPTER 5

Figure 5.1: Cell number per construct ..... 83

Figure 5.2: GAG content per construct ..... 84

Figure 5.3: Hydroxyproline (HYP) content per construct ..... 86

Figure 5.4: Immunohistochemical (IHC) test for types I and II collagen ..... 87

Figure 5.5: Double IHC staining for types I (CI) and II collagen (CII) ..... 88

Figure 5.6: IHC staining for aggrecan ..... 89

### CHAPTER 6

Figure 6.1: Diagram of experimental design ..... 101

Figure 6.2: Mean cell number per construct ..... 105

Figure 6.3: Mean GAG biosynthesis ..... 107

Figure 6.4: The left column is Safranin-O/fast green staining ..... 108

Figure 6.5: IHC staining for CI and CII ..... 109

### CHAPTER 7

Figure 7.1: Seeding efficiency and cell number ..... 124

Figure 7.2: GAG and HYP contents per construct and per cell ..... 126

Figure 7.3: IHC staining for CI, CII, and aggrecan ..... 127

Figure 7.4: Gene expression for CI, CII, and aggrecan ..... 128

### CHAPTER 8

Figure 8.1: Scaffold size and cell density ..... 143

Figure 8.2: Cell number per construct ..... 144

Figure 8.3: GAG content per construct (A) and per cell (B) ..... 145

Figure 8.4: HYP content per construct (A) and per cell (B) ..... 146

Figure 8.5: IHC staining for CI, CII, and aggrecan ..... 148

Figure 8.6: Mechanical testing of unseeded PGA and seeded constructs	149
--	-----

## **CHAPTER 9**

Figure 9.1: Cell number	164
Figure 9.2: GAG content per construct and per cell	165
Figure 9.3: HYP content per construct and per cell	166
Figure 9.4: IHC staining for CI, CII, and aggrecan	167
Figure 9.5: Gene expression for CI, CII, and aggrecan	168

## **CHAPTER 10**

Figure 10.1: Construct volume (A) and cell number per construct (B)	181
Figure 10.2: Seeding efficiency	182
Figure 10.3: HYP content per construct (A) and per cell (B)	183
Figure 10.4: Alkaline phosphatase activity	184
Figure 10.5: Calcium content per construct (A) and per cell (B)	185
Figure 10.6: von Kossa staining	186

## **CHAPTER 11**

Figure 11.1: Cell number per construct	200
Figure 11.2: HYP content per construct (A) and per cell (B)	202
Figure 11.3: Calcium content per construct (A) and per cell (B)	203
Figure 11.4: Alizarin Red S staining and von Kossa staining	204
Figure 11.5: Gene expression for CI, Runx2, and OCN	205

## **CHAPTER 12**

No Figures

## LIST OF TABLES

### CHAPTERS 1-2 and 4-12

No Tables

### CHAPTER 3

Table I: Criteria for cell source selection in tissue engineering ..... 58

## CHAPTER 1: Introduction

Temporomandibular joint disorders (TMDs) are a multifactorial and complex set of dysfunctional conditions in the area of the jaw joint, with various symptoms including headaches, neck pain, and difficulty in daily activities such as eating, talking, and yawning. The pathology of TMDs is poorly understood and current treatments are inefficient. Tissue engineering, aiming to create a substitute *in vitro* to replace deteriorated temporomandibular joint (TMJ) structures, is an ideal solution to these problems. Human umbilical cord mesenchymal stromal cells (hUCMSCs) are a multipotent and primitive stromal population with numerous advantages over adult stem cells and mature TMJ cells, including inexpensive and painless collection, extensive availability, no ethical controversy, no donor site morbidity, and great *in vitro* expansion ability. The overall objective of this strategy was thus to tissue engineer cartilage and bone in the TMJ condyle *in vitro* using hUCMSCs. To achieve this goal, three specific aims were designed:

- 1) To identify suitable cell sources for engineering the TMJ condylar cartilage:

To achieve this aim, a comparison was conducted among porcine TMJ condylar cartilage cells, porcine hyaline cartilage cells, human bone marrow stromal cells (hBMSCs), and hUCMSCs. *The hypothesis was that hUCMSCs would outperform mature TMJ condylar cartilage cells as a mesenchymal stromal cell (MSC) source and that hyaline cartilage cells would outperform TMJ cells as a mature autologous cell source.*

- 2) To refine culture parameters for engineering the TMJ condylar cartilage using hUCMSCs:

Endeavoring to attain this goal, parameters were refined for cartilage tissue engineering in two phases: cell seeding density and growth factor selection. The first phase was to select an initial cell seeding density in the scaffolds. The second phase was to identify the effects of insulin-like growth factor-I (IGF-I) added after the initial chondrogenic differentiation of hUCMSCs using the seeding density selected during the first phase. *The hypothesis was that a higher seeding density (50 million cells/ml), coupled with IGF-I (100 ng/ml), would promote cell proliferation and differentiation and extracellular matrix synthesis better than a lower density without IGF-I incorporation.*

- 3) To refine culture parameters for engineering the TMJ condylar bone using hUCMSCs:

Using the osteogenic media for bone tissue engineering, the experimental design of Aim 3 was analogous to Aim 2. *The hypothesis was that the combination of a higher seeding density and a higher IGF-I concentration would enhance extracellular matrix synthesis to a greater extent.*

The remaining chapters are organized as follows:

Chapters 2 – 3 serve as a comprehensive review, providing background information for subsequent chapters. In Chapter 2, the recent progress in TMJ condyle biology is documented, and the three main factors in TMJ tissue engineering

are described: cell sources, growth factors, and scaffolds. In Chapter 3, the biology of hUCMSCs and their application in tissue engineering and regenerative medicine are discussed, and the rationale for using hUCMSCs for TMJ tissue engineering in this thesis is explained.

In Chapters 4 – 7, the first above-mentioned goal, that is, to select cell sources for TMJ condylar cartilage tissue engineering, is fulfilled. Chapter 4 serves as a cell biology study, screening different growth factors and glucosamine sulfate with TMJ condylar and hyaline cartilage cells in a 2D monolayer environment for the following tissue engineering studies. As the criterion, biochemical contents, including cell number, glycosaminoglycans (GAGs), and collagen, were evaluated during the 3-week culture period. Chapter 5 is a side-by-side comparison of TMJ and hyaline cartilage cells, with the stimulation of bioactive signals selected from Chapter 4, in a 3D biomaterial-based environment for TMJ tissue engineering. Biochemical assays and immunohistochemical techniques were used to assess cell proliferation, matrix synthesis, and aggrecan and collagen distribution. Chapter 6 is a comparison of TMJ cells and hUCMSCs and serves as the introduction of hUCMSCs to musculoskeletal tissue engineering, demonstrating that TMJ cells themselves may be not the best option for TMJ tissue engineering. In Chapter 7, hUCMSCs were further compared to hBMSCs, the current “gold standard” in musculoskeletal tissue engineering, to illustrate that hUCMSCs may be a viable alternative to hBMSCs based on cell proliferation, matrix synthesis, and chondrogenic differentiation ability.

Chapters 8 – 9 delineate the second above-mentioned goal. In the first phase, Chapter 8 investigated the effects of three different seeding densities, 5, 25, and 50 million cells per ml of scaffolds on hUCMSCs, which provided the critical parameter for Chapter 9. Except for the evaluation of biochemical contents and differentiation, a compressive mechanical test was used to determine Young's elastic modulus and the relaxation modulus of tissue-engineered constructs. In the second phase, an optimal seeding density, determined from Chapter 8, was used to seed hUCMSCs in scaffolds, and then a sequential signaling of transforming growth factor beta3 (TGF- $\beta$ 3) and IGF-I on hUCMSCs was applied. hUCMSCs were exposed to a differentiation medium containing TGF- $\beta$ 3 for 3 weeks to induce chondrogenesis and then exposed to an anabolic medium containing IGF-I for another 3 weeks to promote cell proliferation and matrix synthesis. In addition to biochemical and immunohistochemical assays, a real-time reverse transcriptase polymerase chain reaction (RT-PCR) was used to evaluate chondrogenic differentiation at a gene level.

Chapters 10 – 11 focus on the third goal, for which the experimental design was analogous to Aim 2. The difference is that osteogenic differentiation of hUCMSCs, in place of chondrogenic differentiation in Aim 2, was induced in Aim 3 for bone tissue engineering. Biochemical assays were used to examine cell number, collagen and calcium contents, and alkaline phosphatase (ALP) activity. Histology, including Alizarin red S staining and von Kossa staining, was used to visualize the mineralization during osteogenesis of hUCMSCs. RT-PCR was used to quantify the relative gene expression level of bone-specific markers. The significance of these two

studies in Aim 3 was to first demonstrate osteogenic differentiation of hUCMSCs in 3D biomaterials, thus supporting the feasibility of utilizing these cells for bone tissue engineering.

Chapter 12 is the conclusion, summarizing all the findings and serving as a reference for future studies using hUCMSCs. Moreover, the next steps en route to TMJ condyle tissue engineering are addressed in this chapter.

## **CHAPTER 2: Tissue Engineering the Mandibular Condyle\***

### **ABSTRACT**

Tissue engineering provides the revolutionary possibility for curing temporomandibular joint (TMJ) disorders. Although characterization of the mandibular condyle has been extensively studied, tissue engineering of the mandibular condyle is still in an inchoate stage. The purpose of this review is to provide a summary of advances relevant to tissue engineering of mandibular cartilage and bone, and to serve as a reference for future research in this field. A concise anatomical overview of the mandibular condyle is provided, and the structure and function of the mandibular condyle are reviewed, including the cell types, extracellular matrix composition, and biomechanical properties. Collagens and proteoglycans are distributed heterogeneously (topographically and zonally). The complexity of collagen types (including types I, II, III, and X) and cell types (including fibroblast-like cells, mesenchymal cells, and differentiated chondrocytes) indicates that mandibular cartilage is an intermediate between fibrocartilage and hyaline cartilage, with a fibrocartilaginous fibrous zone at the surface being separated from hyaline-like mature and hypertrophic zones below by a thin and highly cellular proliferative zone. Mechanically, the mandibular condylar cartilage is anisotropic under tension (stiffer anteroposteriorly) and heterogeneous under compression (anterior region stiffer than posterior). Tissue engineering of mandibular condylar cartilage and bone is reviewed, consisting of cell culture, growth factors, scaffolds,

---

\*Chapter published as Wang and Detamore. "Tissue engineering the mandibular condyle," *Tissue Eng* 13, 1955, 2007. (Special Issue on Emerging Technologies and New Basic Science Directions in Tissue Engineering.)

and bioreactors. Ideal engineered constructs for mandibular condyle regeneration must involve two distinct yet integrated stratified layers in a single osteochondral construct to meet the different demands for the regeneration of cartilage and bone tissues. We conclude this review with a brief discussion of tissue engineering strategies, along with future directions for tissue engineering the mandibular condyle.

## INTRODUCTION

Temporomandibular joint disorders (TMDs) are a common subgroup of orofacial pain disorders, which cause trouble with chewing, swallowing, talking, pain and tenderness in the jaw, and even can be relevant to other afflictions, such as headaches and neck pain. All of these symptoms can be associated with mandibular condyle dysfunctions, including internal derangement, osteoarthritis and traumas. Tissue engineering of the articular cartilage and bone, intending to create an osteochondral replacement, offers the opportunity to overcome current surgical limitations with both biologically and mechanically functional regeneration. Three elements are generally believed to be essential to engineered tissues: cells, signals, and scaffolds.<sup>1</sup> Cells can be driven by specific bioactive molecules and other physical factors to proliferate, differentiate, migrate and secrete the extracellular matrix.<sup>2</sup> The differentiation of mesenchymal stem cells into chondrocytes and osteoblasts makes it possible to culture an osteochondral graft from a single cell source.<sup>3-5</sup> The scaffolds are central for tissue engineering constructs, which provide the necessary support for cells to proliferate and maintain their differentiated functions. In addition, the

architecture of scaffolds defines the ultimate shape of the new tissue engineered cartilage and bone. Recent emerging scaffold fabrication techniques, including electrospinning,<sup>6</sup> rapid prototyping,<sup>7</sup> fused deposition modeling (FDM),<sup>8</sup> and other solid free-form (SFF) methods,<sup>9-11</sup> have been applied to fabricate complex osteochondral scaffolds with controlled degradation rate and specific porosity.

Tissue engineering the mandibular condyle is not the regeneration of a single tissue, but involves two integrated tissues (cartilage and bone) with dramatic distinctions in structure and function.<sup>12</sup> Ideally, an osteochondral construct in the shape of the mandibular condyle would have heterogeneous physical and mechanical properties similar to native tissue. The scaffolds would be seeded with chondrocytes or chondrogenic cells, and osteoblasts or osteogenic cells to create a functional substitute of the mandibular condyle. This review begins with the anatomy of mandibular condyles, the characterization of cells and the extracellular matrix, and the mechanical properties of mandibular condylar cartilage and the underlying bone. The subsequent tissue engineering sections cover the discussion of cell culture conditions, growth factors, scaffolds, and bioreactors.

## **ANATOMY**

Numerous studies have been done on the anatomy of human and various animal TMJs during the past four decades.<sup>13-19</sup> This section provides a concise anatomical overview of the mature mandibular condyle. It should be noted that growth of the condyle during the postnatal period is accompanied by a significant

thickness increase in the fibrous zone and an obvious thickness decrease in the hypertrophic zone, with an overall decrease in the cartilage thickness.<sup>20</sup> The condyle is longer mediolaterally than anteroposteriorly, forming an elliptical shape in the transverse plane.<sup>14</sup> Anteriorly and posteriorly, the condyle is connected to the disc via collateral ligaments, which set a mechanical limitation on anteroposterior disc movement. Medially and laterally, the condyle is attached tightly to the capsule and disc through the poles of condyle. The mandibular condyle is covered by a zonal cartilage layer from the articular surface to the underlying bone, which serves to absorb shock and contribute to bone remodeling. There are several zonal categorizations of the mandibular cartilage,<sup>14, 21-25</sup> which result from subtle differences in the cell types and extracellular matrix contents in the different layers. The classification scheme of four zones, consisting of the fibrous, proliferative, mature, and hypertrophic zones, will be used in this review. Essentially, the proliferative zone serves as a separating barrier between the fibrocartilaginous fibrous zone and the hyaline-like mature and hypertrophic zones. Below the cartilage is the mandibular bone, with cancellous bone covered by a layer of compact cortical plate.<sup>14, 17</sup> Hansson *et al.*<sup>26, 27</sup> divided the human condyle anteroposteriorly into three parts, anterior, superior, and posterior regions, and mediolaterally into four parts, lateral, lateralcentral, mediocentral, and medial regions. Anteroposteriorly, the thickest region of the mandibular cartilage is the superior area (0.4-0.5 mm). Mediolaterally, the cartilage of the healthy human condyle has greater thickness in the lateralcentral and mediocentral parts than in the medial and lateral parts. For the

underlying bone, the cortical bone is much denser in the lateral region than in the medial part of the condyle, which may suggest a greater stress on the lateral part.<sup>17</sup> In the cancellous bone of the mandibular condyle, the compressive cancellous trabeculae are oriented vertically, extending into the cortical bone.<sup>17</sup> The tensile cancellous trabeculae intersect perpendicularly with compressive trabeculae, forming an interconnected architecture that serves an important role in the biomechanical properties of the bone.<sup>17</sup>

## **STRUCTURE AND FUNCTION OF MANDIBULAR CONDYLAR CARTILAGE**

### ***Cell type and extracellular matrix***

The articular fibrous zone is comprised of fibroblast-like cells,<sup>13, 28</sup> which have a flat shape and endoplasmic reticulum surrounded by dense cytoplasm.<sup>16</sup> In addition to the mitotic activity of the fibroblast-like cells contributing to the growth of the fibrous zone,<sup>28</sup> the underlying proliferative zone produces cells for the fibrous zone.<sup>29, 30</sup> However, it remains a question whether the fibrous zone or the proliferative zone plays the predominant role in the growth of the cellularity of the fibrous zone.<sup>28</sup> The proliferative zone indeed plays an important role as a cell reservoir, which has mesenchymal cells distributed heterogeneously as chondrocyte precursors for the underlying zones.<sup>15, 31, 32</sup> Thus, it is likely that these mesenchymal cells partly contribute to the changes in the thickness and shape of mandibular condylar cartilage in adaptation.<sup>31</sup> Differentiated chondrocytes are found in the mature and hypertrophic

zones, where the degeneration of chondrocytes has been noted closer to the subchondral bone.<sup>16</sup>

Collagen provides mandibular cartilage with tensile and shear resistance.<sup>33</sup> In the fibrous zone, collagen fibers are oriented parallel to the cartilage surface but angled together to form a sheet-like structure.<sup>16, 34</sup> The proliferative zone is composed primarily of cellular components and few collagen fibers are observed in this zone.<sup>34</sup> In the mature and hypertrophic zones, the collagen fibers demonstrate a random arrangement by crossing each other through a radial orientation.<sup>34</sup> Regarding the collagen types, collagen type I is found throughout all of the mandibular condylar cartilage zones,<sup>35</sup> which indicates a key difference between the mandibular articular cartilage and hyaline cartilage, the latter of which contains collagen type II predominantly. Collagen type II and collagen type X, while absent in the fibrous zone, are abundant in the mature and hypertrophic zones.<sup>36</sup>

Proteoglycans are glycoproteins that consist of a protein core with covalently attached highly anionic glycosaminoglycan (GAG) chains. The primary proteoglycan in mandibular condylar cartilage is negatively charged aggrecan, capable of binding with a hyaluronan chain to form large aggregates.<sup>37</sup> It has been immunologically verified that aggrecan is mainly located in the hypertrophic and mature zones.<sup>33, 38</sup> The major function of aggrecan is to provide osmotic swelling pressure to the cartilage and enable it to resist compressive forces, which results from the anionic character of the GAG chains.<sup>33, 38-40</sup> In addition to aggrecan, other proteoglycans, such as versican and decorin, have been detected in the mandibular condylar cartilage as

well. Versican, consisting exclusively of chondroitin sulfate, was identified in the articular fibrous zone<sup>33, 38</sup> and in the proliferative zone.<sup>38</sup> Decorin, a regulator of collagen fibrillogenesis, has been reported in all zones of the rat mandibular condylar cartilage.<sup>41</sup>

### ***Biomechanic***

The mandibular condylar cartilage is a nonlinear viscoelastic material, with an initial toe region and a quasi-linear profile under tension.<sup>42</sup> Anisotropy of the mechanical properties in mandibular condylar cartilage is confirmed by greater average tensile strength, tensile stiffness and energy absorption in the anteroposterior direction than in the mediolateral direction, but lower average failure strain in the anteroposterior direction than in the mediolateral direction.<sup>42</sup> The reported Young's moduli in the anteroposterior and mediolateral directions were respectively  $9.0 \pm 1.7$  MPa and  $6.6 \pm 1.2$  MPa.<sup>42</sup>

Kuboki *et al.*<sup>43</sup> investigated the response of the mandibular condyle cartilage-bone system under compression. Indentation testing demonstrated that the deformation pattern of mandibular condylar cartilage was similar to the hyaline articular cartilage from the knee or hip joint. The deformation of the cartilage was notably associated with magnitude of compression, and was greater in sustained compression than in the intermittent compression. Moreover, Hu *et al.*<sup>44</sup> examined the compressive properties in different regions of the mature rabbit mandibular condylar cartilage using atomic force microscopy, which was divided into the anteromedial

(AM), anterolateral (AL), posteromedial (PM), and posterolateral (PL) regions. The Young's moduli (AM>AL>PM>PL) and Poisson's ratios (AM>AL>PM>PL) for the four regions indicated significantly different abilities to resist sustained compression among regions. A further study from the same group demonstrated rather uniform compressive properties on 7 day old rabbits, revealing the mechanical development of the mandibular condyle.<sup>45</sup> In a macroscopic indentation study on porcine condylar cartilage, Tanaka and colleagues<sup>46</sup> discovered that the moduli (dynamic complex, storage, and loss) were higher in the anterior region than in the posterior region, in agreement with the nanoindentation findings of Hu *et al.*<sup>44</sup>

In summary, the condylar cartilage appears to be anisotropic and heterogeneous. It is stiffer anteriorly than anteriorly under compression, and stiffer in the anteroposterior direction than in the mediolateral direction under tension.

## **STRUCTURE AND FUNCTION OF MANDIBULAR CONDYLAR BONE**

Bone is clearly a distinct connective tissue from the overlying cartilage in structure and function. The predominant collagen type in the subchondral bone is type I, which is distributed throughout the cancellous and cortical bones. Giesen *et al.*<sup>47</sup> investigated the mechanical anisotropy of the cancellous bone under compression in the human mandibular condyle. The results indicated that the cancellous bone was 3.4 times stiffer and 2.8 times stronger in axial loading than in transverse loading, which was confirmed by micro-computed tomography techniques and finite element

modeling.<sup>48</sup> The Young's moduli under the axial and transverse compressive loading were  $431 \pm 217$  MPa and  $127 \pm 92$  MPa, respectively.<sup>47</sup> Further investigation demonstrated that decreased mechanical loading could reduce the density, stiffness, and strength of the cancellous bone in the mandibular condyle.<sup>49</sup> Regarding the properties of the cortical bone, scanning acoustic microscopy revealed that the mechanical properties of the cortical bone were transversely isotropic with respect to the anteroposterior direction, and the cortical bone in the anteroposterior direction was stiffer than in the mediolateral and superiorinferior directions.<sup>50</sup> Schwartz-Dabney and Dechow,<sup>51</sup> using ultrasonic techniques, investigated the mechanical variations of the cortical bone throughout the human dentate mandible. The elastic and shear moduli of the condylar part respectively ranged from 12.2 to 29.8 GPa and from 4.9 to 7.7 GPa.

## **CELL SOURCES FOR MANDIBULAR CONDYLE TISSUE ENGINEERING**

### ***Cell harvest from the condyle***

Many tissue engineering studies choose mature chondrocytes or osteoblasts for cartilage and bone regeneration. The traditional harvest method for articular cartilage is that the tissue slices are excised from the cartilage surface, minced with a scalpel, and then digested by successive enzymes.<sup>52</sup> Takigawa *et al.*<sup>53</sup> developed a method for harvesting mandibular condylar cartilage cells, whereby a rabbit mandibular condyle and disc were removed as a whole and stored in calcium-free and

magnesium-free balanced salt solution (pH 7.4). After the removal of the disc and ligament, the mandibular condylar cartilage was separated and minced, then digested in collagenase solution. The cells obtained through this method include various cell types from the different layers in the mandibular condyle. Another method for harvesting chondrocytes is to allow the cells from cultured explants to migrate out and grow onto a specific substrate. Subsequently, the cells are released from the substrate and suspended in medium. Tsubai *et al.*<sup>54</sup> used this method to isolate the fibroblast-like cells from the fibrous zone of a fetal rabbit mandibular condyle. The mandibular condyle was collected and then washed in Hanks' Balanced Salt Solution (HBSS), and the tip of the condyle was allowed to contact with a gelfoam surgical sponge for 1 week. After this period, the gelfoam sponge was treated with collagenase to liberate the cells. The cell suspension was centrifuged, and then the cells were resuspended in minimum essential medium (MEM). To date, there have been no procedures described to isolate either the proliferative cells from the proliferative zone or the chondrocytes from the mature and hypertrophic zones for tissue engineering studies, although techniques developed for hyaline cartilage could perhaps be adapted to condylar cartilage to accomplish this.<sup>55, 56</sup>

### ***Cell sources***

Differentiated autologous cells for tissue engineering, such as chondrocytes and osteoblasts, could raise several problems. First, the patients suffer from donor site morbidity.<sup>5</sup> Second, in large-scale tissue-engineered constructs, a high initial cell

density is necessary to obtain sufficient cartilage and bone for clinical use, which is difficult to achieve with autologous articular chondrocytes and osteoblasts.<sup>57</sup> Furthermore, autologous mandibular condylar cartilage cells are not mandatory for tissue engineering the mandibular condyle, although the characterization of these cells will be valuable for validating engineered constructs. Recent efforts have been employed to explore stem cells in tissue engineering applications. Exposed to specific growth factors, stem cells, including adult marrow-derived mesenchymal stem cells (MSCs), embryonic stem cells (ESCs), and human umbilical cord matrix (HUCM) stem cells, have the pluripotent capability of differentiating into multiple cell lineages that can result in the formation of cartilage, bone, tendon and other connective tissues.<sup>58-66</sup> In the United States in 2006, we would argue that MSCs are currently the best option because they are autologous, well characterized, and politically benign. It has been proven that marrow-derived MSCs have the ability to differentiate into chondrocytes and osteoblasts for tissue engineering the mandibular condyle.<sup>5, 57, 67, 68</sup> However, MSCs have their own limitations, such as the limited self-renewal and proliferative ability, the decrease in available cell numbers with age, and donor-site morbidity.<sup>69</sup> It should be noted that an individual would be expected to have an adequate number of MSCs to regenerate their own mandibular condyles. ESCs demonstrate considerable promise for chondrogenic and osteogenic differentiation with self-renewal capacity.<sup>61, 62, 69-74</sup> However, tissue engineered constructs from donor ESCs could involve immune rejection. HUCM stem cells, which develop from extraembryonic mesoderm that forms the umbilical cord matrix, may be a potential

alternative to ESCs.<sup>75</sup> They have been shown to be multipotential stem cells with properties between ESCs and adult stem cells.<sup>75-78</sup> There is a lower incidence of graft vs. host disease than with bone marrow transplants, and a significant absence of major histocompatibility complexes, suggesting that umbilical cord cells may have an innate mechanism to evade the immune system.<sup>77, 79, 80</sup> Only recently have HUCM stem cells been considered for tissue engineering,<sup>64-66, 76, 81-83</sup> and for the most part have been focused on vascular tissue engineering.<sup>65, 81-83</sup> Bailey *et al.*<sup>66</sup> investigated the potential of HUCM stem cells in mandibular condylar cartilage tissue engineering. The extracellular matrix formation, including collagens types I and II, and GAGs, revealed that HUCM stem cells may have the ability to differentiate into chondrocyte-like cells. Furthermore, a comparison of HUCM stem cells and mandibular condylar chondrocytes demonstrated that HUCM stem cells actually outperformed the mandibular condylar chondrocytes, producing higher cell numbers and higher collagen and GAG content. In a related study, a German group reported that they were able to differentiate HUCM stem cells into cells with osteoblastic properties.<sup>64</sup> Therefore, HUCM stem cells may be an alternative cell source for mandibular condyle tissue engineering, and more broadly for orthopaedic osteochondral tissue engineering as well. In summary, although differentiated autologous cells and stem cells are acceptable for engineering an osteochondral mandibular condyle, stem cells in general may be better candidates, based on the inherent limitations of mature autologous cells. While marrow-derived MSCs are

currently the preferred type of stem cells for this application, HUCM stem cells and ESCs represent a promising alternative for the future.

### ***Cell expansion***

In order to get enough cells for tissue-engineered constructs, the harvested cells are usually multiplied and expanded *in vitro* in cell culture medium. Using mandibular condylar chondrocytes, Takigawa *et al.*<sup>53</sup> investigated the effect of the initial cell seeding density on cell proliferation in monolayer culture and concluded that a high initial cell density benefited cell proliferation. When the initial cell density was  $2.5 \times 10^4$  cells/cm<sup>2</sup>, the cells failed to proliferate after 11 days of culture. However, after the initial cell density was raised to  $5 \times 10^4$  cells/cm<sup>2</sup>, the cell number appeared to increase logarithmically.

Monolayer expansion is an effective way to obtain adequate cell numbers for tissue-engineered constructs. However, the expansion of chondrocytes results in cell dedifferentiation with the increase of culture time and passage number,<sup>84, 85</sup> which will lead to the loss of chondrocyte phenotype and affect matrix synthesis.<sup>86, 87</sup> The dedifferentiated cells have a fibroblast-like appearance, less production of proteoglycans, and a shift of the synthesized collagen types from type II to type I,<sup>87</sup> indicative of fibrous tissue formation. Several studies have shown that hydrogel encapsulation can be used successfully as a carrier to foster the phenotype retention of chondrocytes and the re-expression of the dedifferentiated chondrocytes harvested from the goat knee,<sup>84, 85</sup> human femoral condyles,<sup>88</sup> and rabbit and human auricular

cartilage.<sup>88, 89</sup> In addition, a study by Darling and Athanasiou<sup>84</sup> demonstrated that an aggrecan-coated surface had the ability to retain chondrocyte phenotype in monolayer culture, which may be an attractive alternative to hydrogel encapsulation as a means to retain phenotype. Recently, Chang *et al.*<sup>90</sup> investigated human mandibular condylar chondrocytes in alginate gel beads suspended in culture medium. After 4 weeks of culture, most of the cells were round or elliptical, and immunological studies revealed the presence of type II collagen and aggrecan, indicating the sustainability of a chondrogenic phenotype in alginate with mandibular condylar cartilage cells.

## **SCAFFOLDS FOR BONE AND CARTILAGE TISSUE ENGINEERING**

The function of scaffolds in tissue engineering is to provide a mechanical and structural support for tissue reconstruction and to serve as a carrier for the cells to attach, migrate, proliferate, and differentiate.<sup>91</sup> The scaffolds in mandibular condyle tissue engineering must fulfill both the biological and mechanical requirements for cartilage and bone regeneration. These requirements include high porosity and surface area, mechanical stiffness and strength, controlled degradation, and biocompatibility for cell growth and extracellular matrix formation. Besides these criteria, a craniofacial scaffold must be designed with a complex shape, defined by clinical imaging data.<sup>10</sup> Several new techniques, such as SFF and electrospinning, have been applied to accurately control scaffold dimensions. Using these approaches, scaffolds with specific shapes and porosities have been fabricated from a range of

biomaterials including hydroxyapatite (HA), tri-calcium phosphate (TCP), HA/TCP composites, polyglycolic acid (PGA), poly lactic-co-glycolic acid (PLGA), and polypropylene fumarate/tri-calcium phosphate (PPF/TCP) composites.<sup>9, 10, 92</sup>

Due to the few scaffold studies on tissue engineering mandibular condylar cartilage and bone, a brief review related to general cartilage and bone tissue engineering studies will be imperative. Various scaffolds have been fabricated for articular cartilage tissue engineering. Synthetic scaffolds include PGA,<sup>93</sup> polylactic acid (PLA),<sup>94, 95</sup> and copolymers of PGA/PLA. The disadvantage of these synthetic scaffolds is relatively poor cell adhesion due to the hydrophobic surface. Natural scaffolds, such as collagen, fibrin, and chitosan, demonstrate the ability to improve cell attachment. Collagen is a natural component of cartilage and a collagen scaffold is known to play an important role during cell adhesion as well as chondrocyte and osteoblast differentiation.<sup>96-98</sup> Surface modification of synthetic biomaterials, with the intent to improve adhesion and biocompatibility, has been extensively studied. Collagen-coating<sup>99</sup> and RGD immobilization<sup>100</sup> on the scaffold surface can be achieved by chemical techniques.<sup>100, 101</sup> The immobilization of RGD peptides on PLA and PLGA scaffolds has been shown to promote cell attachment and mineralized matrix deposition.<sup>100, 102</sup> Detailed reviews of scaffolds for cartilage tissue engineering, including relevant hydrogels, can be found in various reviews.<sup>103-106</sup>

Scaffolds for bone tissue engineering, also reviewed elsewhere in detail,<sup>107-112</sup> require higher mechanical stiffness. Ceramics, such as hydroxyapatite [ $\text{Ca}_{10}(\text{PO}_4)_6(\text{OH})_2$ ] and  $\beta$ -tricalcium phosphate [ $\text{Ca}_3(\text{PO}_4)_2$ ,  $\beta$ -TCP], are widely used

in bone tissue engineering because of their biocompatible and osteoinductive properties.<sup>110</sup> Synthetic polymers such as poly( $\epsilon$ -caprolactone) (PCL), PGA, polyethylene glycol (PEG), and polypropylene fumarate (PPF) could be modified and optimized to meet specific demands. The mechanical properties of polymers in general, however, must be improved for bone tissue engineering. Nanofiber scaffolds are emerging with the use of electrospinning techniques. To date, PCL, PLA, PGA, and PLGA have been fabricated via electrospinning methods.<sup>6, 113-116</sup> These nanofibers form nonwoven meshes to provide enhanced mechanical properties such as tensile strength and elasticity as well as enhanced cell attachment due to similarities between the nanofiber and native ECM.<sup>101</sup> Shin *et al.*<sup>117</sup> examined nanofibrous PCL using MSCs *in vivo* and found that cells and ECM formation were observed throughout the constructs. In addition, mineralization and type I collagen were also detected.<sup>117</sup> Referring back to cartilage tissue engineering, Li and coworkers<sup>118</sup> found that nanofibrous PCL acted as a biologically preferred scaffold/substrate for proliferation and maintenance of the chondrocyte phenotype in comparison to monolayer culture.

### **EFFECTS OF GROWTH FACTORS ON MANDIBULAR CONDYLAR CELLS**

Jiao *et al.*<sup>119</sup> found that 10 ng/ml bFGF had the greatest stimulatory effect on the proliferation of mandibular condylar chondrocytes compared to 10 ng/ml TGF- $\beta$  and 10 ng/ml insulin-like growth factor-I (IGF-I) in both low serum (0.4% newborn

calf serum) and high serum conditions (10% serum) in monolayer culture. At the low serum concentration, the groups treated with bFGF had a moderate increase in cell numbers, while the effects of TGF- $\beta$  and IGF-I demonstrated no statistically significant differences in comparison to the control group. At the high serum concentration, all three growth factors promoted cell proliferation, with an increase of 65% with bFGF, 24% with IGF-I, and 13% with TGF- $\beta$  compared to the control group. The synergetic effect of these three growth factors was also reported in this study. The combination of IGF-I, bFGF and TGF- $\beta$ , the combination of IGF-I and bFGF, the combination of TGF- $\beta$  and bFGF, and the combination of TGF- $\beta$  and IGF-I increased cell proliferation by 68%, 66%, 65%, and 57%, respectively, compared to the control group. The fact that the combinations that included bFGF had greater cell numbers indicated that bFGF seemed to be the leading effective factor in the synergetic promotion of proliferation. Besides the investigation of the isolated mandibular condylar cells, the effect of bFGF in the explant culture of mandibular condylar cartilage was studied. Fuentes *et al.*<sup>120</sup> demonstrated that bFGF promoted cell proliferation with a 43% increase in cell number after 2 days of mandibular condylar explant culture in serum-free DMEM medium. Delatte *et al.*<sup>121</sup> examined biosynthesis in addition to proliferation, reporting that bFGF stimulated cell proliferation while it inhibited GAG and collagen synthesis after 2 weeks of mandibular condylar explant culture, with Iscove's Modified Dulbecco's Medium (IMDM) supplemented with 0.1% bovine serum albumin (BSA). This study also revealed that bFGF inhibited the effect of IGF-I on GAG production. Recently, an

inhibitory effect of bFGF on chondrogenesis in the mandibular condyle was reported when fetal rat condylar explants were cultured in serum-free modified Fitton-Jackson BGJb medium.<sup>122</sup> After 2 days of explant culture, the group treated with bFGF in the perichondrium had lower cell numbers than the untreated groups. After 5 days, the hypertrophic chondrocyte number in the bFGF-treated condyle was less than in the untreated groups as well.

Regarding IGF-I, Yang *et al.*<sup>123</sup> investigated its effect on the proliferation of cultured mandibular condylar chondrocytes at six concentrations (1, 5, 10, 50, 100, 500 ng/ml). After a 24-hr period, the proliferation at all concentrations was enhanced in comparison to the control group, and the highest concentration led to the greatest cell proliferation. With rat condylar explant culture, Fuentes *et al.*<sup>120</sup> demonstrated that an increased cell proliferation elicited by IGF-I was greater than with bFGF or TGF- $\beta$ . Delatte *et al.*<sup>124</sup> demonstrated that not only could cell proliferation be increased, but also the production of GAG and collagen could be up-regulated significantly by IGF-I in rat condylar explant culture. Delatte *et al.*<sup>121</sup> also reported that the increases in cell proliferation and GAG synthesis stimulated by IGF-I were greater than TGF- $\beta$  and bFGF in newborn rat condylar explant culture. Furthermore, local injection of IGF-I into rat mandibular condylar cartilage confirmed the positive effect of IGF-I on cell proliferation and matrix synthesis by increasing the thickness of the cartilaginous layer.<sup>125</sup>

TGF- $\beta$  has an inhibitory or stimulatory effect on cell growth and extracellular matrix formation, depending on the serum concentration in the culture medium. Song

*et al.*<sup>126</sup> examined the effect of TGF- $\beta$  on rat mandibular condylar cells in DMEM medium with 15% fetal bovine serum. The fourth passage chondrocytes were divided into 20 groups with four different TGF- $\beta$  concentrations (0, 0.1, 1, and 10 ng/ml) for 0, 6, 12, 18, and 24 hrs. Cell proliferation was evaluated by the proliferative index (PI). For each concentration group, the PI increased between 0 and 18 hrs and demonstrated a decreasing trend between 18 and 24 hrs. The PIs of all concentration groups were higher than the control group between 0 and 24 hrs. The PI increased with increasing concentration during all time periods. This study used fourth passage chondrocytes as a cell source in order to get enough cells; however, future phenotype research may be warranted to compare the result to lower passage cells since chondrocytes appear to lose their phenotype after several passages.<sup>85</sup> In a related study, Jiao *et al.*<sup>119</sup> found that TGF- $\beta$  had an inhibitory effect on mandibular condylar chondrocyte proliferation with low bovine serum concentration (0.4%), and had a stimulatory influence with high bovine serum concentration (10%) after 3 days of culture. With respect to explant culture of mandibular condyles of newborn rats in IMDM medium supplemented with 0.1% BSA, TGF- $\beta$  did not promote cell proliferation and collagen production, although 10 ng/ml TGF- $\beta$  upregulated GAG content with a 23% increase relative to the control group.<sup>121</sup>

Tsubai *et al.*<sup>54</sup> investigated the effect of epidermal growth factor (EGF) on the mandibular condylar explants of fetal rabbits and on isolated fibroblast-like cells from the fibrous zone. For the isolated fibroblast-like cells, EGF accelerated the cell cycle in contrast with the control group. For explant culture, the cell numbers in all zones

were higher with the stimulation of EGF in comparison with the control group. However, the absolute cell numbers decreased with time with respect to initial cell numbers, which indicated that the mitosis of cells gradually decreased as the fetal period ended. Moreover, the thicknesses of the fibrous zone and hypertrophic zone with the EGF group were significantly greater than the initial thickness due to the increase of extracellular matrix.

For bone tissue engineering, growth factors are not only needed to promote osteogenic regeneration, but also to support vascularization. Extensive reviews of the effects of growth factors on bone regeneration have been made by Zhang *et al.*,<sup>127</sup> Mistry and Mikos,<sup>110</sup> and Gittens and Uludag.<sup>128</sup> BMPs, the most common cytokines of the TGF superfamily, stimulate osteogenic differentiation of MSCs and proliferation of osteoblasts. BMP-2 and BMP-7, the most extensively studied BMPs, can induce endochondral bone formation in numerous primate models.<sup>128</sup> TGF- $\beta$  can promote the proliferation of osteoblasts, although it could also enhance bone resorption at certain concentrations.<sup>110</sup> Platelet-derived growth factor (PDGF) has been shown to promote bone regeneration only when combined with IGF-I or dexamethasone.<sup>129-131</sup> Other growth factors such as IGF-I and FGFs have multifaceted regulatory effects on bone formation, and further investigation is needed.<sup>132-134</sup>

In summary, bFGF at high serum concentration is the best stimulator of proliferation in mandibular condylar chondrocytes, followed by IGF-I. IGF-I is a potent promoter of cell proliferation and biosynthesis, especially GAG production. TGF- $\beta$  can induce biosynthesis significantly, including GAG and collagen formation.

However, further investigation of the mechanism of the effect of serum concentration in TGF- $\beta$  treated medium on cell proliferation is needed to resolve inconsistencies between studies. EGF is a potent inducer of proliferation in fibroblast-like cells isolated from the fibrous zone. Therefore, a combination or sequence of bFGF and IGF-I may be an advisable choice for both cell proliferation and biosynthesis with mature condylar cartilage cells. A combination of different factors may be required with stem cells, promoting proliferation, then moving to differentiation and matrix synthesis. Finally, given that these growth factors each have different effects on bone and cartilage, perhaps a specific growth factor, such as IGF-I, could be delivered to an osteochondral construct, promoting the growth of bone and cartilage in their respective capacities.

## **BIOREACTORS FOR CARTILAGE AND BONE TISSUE ENGINEERING**

The purpose of a bioreactor for tissue engineering is to enhance cell growth and the formation of extracellular matrix by creating a dynamic and controlled environment. The primary focus of this section in our review is on mass transfer bioreactors. The driving force for mass transfer in static culture is passive molecular diffusion, which can lead to undesirable nutrient and waste gradients and a resulting heterogeneity. The enhanced mass transfer within bioreactors strives to promote uniform distribution of cells in the scaffold, exchange of nutrients and wastes between cells and culture medium, and mechanical stimulation of cell growth.

According to the magnitude of the shear force that bioreactors create, a bioreactor can be classified as high-shear or low-shear.<sup>135</sup> High shear force can be achieved by mixed flasks, orbital shakers and direct perfusion bioreactors. Low shear force can be obtained using rotating wall bioreactors. The following paragraphs will provide a recapitulative overview of current representative bioreactors for cartilage and bone tissue engineering, including stirred spinner flasks, direct perfusion bioreactors, and rotating wall bioreactors, which will be followed by a brief mention of mechanical stimulation bioreactors.

In the stirred spinner flask, a magnetic stir bar at the flask bottom drives fluid flow, which can dramatically improve the exchange rate of oxygen and nutrients between the medium and the inner scaffold, and can thus result in more cells and extracellular matrix in the central section of scaffolds than with static culture.<sup>136</sup> Although the increase of mixing intensity may enhance cell proliferation and biosynthesis, it could increase the release of GAG from the tissue construct.<sup>137</sup> For bone tissue engineering, Meinel *et al.*<sup>138</sup> examined MSC-derived osteoblasts in spinner flasks and found that the scaffolds in the spinner flask contained more cells and mineralized matrix than those in static culture or in the perfusion system. The velocity field created by the vortex of the stir bar was non-uniform, as the cells and matrix on the surface were exposed to a greater shear force than internally.<sup>136</sup> Due to greater mechanical stimulation on the surface, accumulation of mineralized matrix at the periphery was found in bone tissue engineering using the spinner flask.<sup>138</sup> Similarly, in cartilage tissue engineering, a thick fibrous capsule was seen

surrounding the scaffolds and native tissue explants in the stirred spinner flask after 6 weeks of *in vitro* culture, despite the fact that continuous cartilaginous matrix was formed in the inner scaffold.<sup>139, 140</sup> It should be noted that spinner flask seeding requires that the constructs are skewed on a wire, resulting in a hole in the constructs. Perhaps due in part to this inherent limitation, spinner flasks are primarily used for cell seeding.

In rotating bioreactors, the medium consisting of cell-seeded scaffolds is filled either in a single cylinder or between two concentric cylinders, where the objective is to suspend constructs in perpetual free fall, such that they are relatively stationary with respect to an observer.<sup>135, 136, 141</sup> The laminar flow in the rotating wall bioreactor generates a low shear force, which is much lower than other types of bioreactors, in an effort to stimulate cell proliferation and biosynthesis and to avoid the shear-related damage to cell growth. Increased GAG and collagen content has been reported for cartilage regeneration in rotating wall bioreactors.<sup>140, 142-144</sup> With the culture time increasing up to 7 months, the GAG content has achieved the same wet weight fraction as explanted native cartilage.<sup>145</sup> However, a study by Detamore and Athanasiou<sup>141</sup> demonstrated the neutral performance of a rotating bioreactor in tissue engineering with the TMJ disc. They found that the rotating bioreactor did not induce uniform distribution of extracellular matrix or a significant increase in total matrix content and compressive stiffness in comparison to static culture, although a dense matrix and cellular composition was reported in the rotating bioreactor. It was

suggested that a static culture period of 3-4 weeks prior to bioreactor use may lead to improved results with the rotating bioreactor.

In comparison with spinner flasks and rotating wall bioreactors, mass transport in perfusion bioreactors is especially enhanced in the interior scaffold with the forced flow penetrating the scaffold pores.<sup>135, 146, 147</sup> Whereas spinner flasks and rotating bioreactors replenish the surrounding medium to maintain maximum concentration gradients and thus to facilitate passive diffusion, perfusion bioreactors impart a pressure gradient to drive nutrient and waste transport via convection. Perfusion of a scaffold seeded with chondrocytes has been shown to upregulate cell growth and extracellular matrix biosynthesis in a time-dependent and velocity-dependent manner,<sup>148, 149</sup> and to promote better distribution of cells throughout the constructs as well.<sup>147</sup> For bone marrow stromal osteoblasts in the perfusion system, significantly more mineralized matrix deposition accumulated on titanium fiber meshes<sup>150</sup> and PLLA scaffolds<sup>151</sup> after 16 days in comparison to static culture, with the increased shear force from perfusion not only accelerating mineralized matrix deposition but also improving extracellular matrix distribution. In an experiment by Sikavitsas *et al.*,<sup>150</sup> change of shear force was achieved by changing the viscosity of the fluid at a constant fluid superficial velocity. The double and triple of the viscosity resulted in a 4-fold and 7-fold increased mineralized matrix deposition, respectively. Although uniform distribution of mineralized matrix was reported by Meinel *et al.*,<sup>138</sup> they found that the perfusion bioreactor provided reduced proliferation and mineralized matrix deposition compared to the spinner flask configuration, where the

mineralized matrix mainly formed at the outer rim of the collagen scaffold. A couple of potential limitations with perfusion bioreactors are that unidirectional flow could result in the alignment of cells and extracellular matrix parallel with the flow direction,<sup>148</sup> and that dense matrix formation can result on the surface facing the oncoming medium flow.<sup>135</sup> A possible solution might be oscillating perfusion bioreactors, in which the medium flow direction would reverse at a specific frequency.<sup>152</sup> In our group, we are exploring intermittent perfusion as another alternative, whereby uncoupling mass transport and shear stress may lead to the greatest overall benefit.

Mechanical stimulation as a secondary phenomenon, such as shear stress in bioreactors, may regulate cell differentiation and extracellular matrix synthesis. Generally, chondrocytes and osteoblasts respond to specific magnitudes and frequencies of mechanical loading with increased cell proliferation and biosynthesis.<sup>147</sup> Mechanical load may also modulate cell adhesion.<sup>153, 154</sup> Mechanical stimulation bioreactors in cartilage regeneration rely on direct compression, shear stress, or hydrostatic pressure, which have been reviewed by Darling and Athanasiou in detail.<sup>155</sup> With bone regeneration, a pair of reviews has been provided by Hughes-Fulford<sup>156</sup> and Anselme.<sup>153</sup> Generally speaking, oscillatory stimulation has proven most effective for both cartilage and bone regeneration, with a notable exception being TMJ disc cells.<sup>157</sup> Future work in this field may look to develop new bioreactors to combine these mechanical stimuli with current mass transfer

bioreactors, in an effort to provide multiple stimuli to maximize the stimulatory effect on cell growth and matrix synthesis.<sup>135</sup>

Although bioreactors provide a stimulatory dynamic environment for tissue regeneration, parameters such as the mixing intensity, rotation rate and perfusion rate are still far from being optimized. The traditional trial-and-error approach is time consuming for multiple changes of operation conditions. Modeling of bioreactor environments, involving computational fluid dynamics, may improve bioreactor designs significantly.<sup>158</sup> Venkat *et al.*<sup>159</sup> investigated hydrodynamics in the impeller region of spinner-flask bioreactors using particle tracking velocimetry. Full experimental and computational fluid models for spinner flasks were established by Sucusky *et al.*<sup>160</sup> and Bilgen *et al.*<sup>161</sup> The velocity field was measured by particle-image velocimetry followed by the calculations of shear-stress field, flow periodicity, Reynolds-stress field and turbulence-intensity field according to the distribution of velocity. For rotating-wall perfused-vessel bioreactors, Begley and Kleis<sup>162</sup> developed a mathematical model originating from the momentum and continuity equations, which were solved by numerical methods. The fluid dynamics and shear stress were characterized in the bioreactor, and then validated by experimental data with less than 5% difference. To enhance the understanding of tissue growth in the scaffold in response to mechanical shear stress in the rotating wall bioreactor, mathematical models of tissue growth were introduced by Lappa<sup>163</sup> to explain the interplay between increasing tissue size and the structure of the flow field, and to predict tissue growth and progression of extracellular matrix deposition under the stimulation of fluid shear

stress. In a perfusion system, the dynamic environment was characterized to evaluate the effect of different parameters such as scaffold porosity and flow rate on the local shear stress distribution in the perfused scaffold.<sup>164</sup> The simulation results demonstrated that the pore size influenced the predicted shear stress level, whereas the porosity was related to the statistical distribution of the shear stresses.<sup>164</sup>

In summary, bioreactors can lead to significantly improved cell proliferation and biosynthesis. In comparison to spinner flasks, rotating and perfusion bioreactors generally appear to provide more uniform distribution of cells and extracellular matrix. However, the spinner flask is an effective cell seeding method for controlled cell density and uniform cell distribution.<sup>165</sup> Although there are no direct comparisons between rotating and perfusion bioreactors, the forced flow in perfusion bioreactors leads to better mass transfer than with rotating bioreactors, which perhaps may be advantageous in producing osteochondral tissues in a full-scale. In addition, the development of modeling bioreactors will provide accurate parameters for building and operating bioreactors.

## **TISSUE ENGINEERING THE MANDIBULAR CONDYLE**

Whereas characterization of the native condyle began more than four decades ago, tissue engineering of the mandibular condyle is in its infancy, with fewer than 20 condylar tissue engineering studies published, all in this decade.<sup>5, 9-11, 57, 68, 91, 92, 166-172</sup> An early attempt conducted by Weng *et al.*<sup>91</sup> produced a homogenous PGA/PLA

scaffold in the shape of the human mandibular condyle for mandibular condylar reconstruction. The scaffold was seeded with osteoblasts harvested from bovine periosteum-derived explant culture, and bovine chondrocytes from the forelimbs were painted onto the scaffold surface as a cartilage layer. 12 weeks of implantation demonstrated that the scaffold maintained the condylar shape, and an interface was formed between the bone and cartilage. The significance of this study was in demonstrating the feasibility of creating the tissue engineered mandibular condyle in the form of two stratified layers using differentiated autologous cells. Histology was used in this study in lieu of quantified biochemical assays, thus cell numbers, GAG content, and collagen content data were not available.

Ueki *et al.*<sup>169</sup> implanted a PLGA and gelatin sponge complex (PGS) following condylectomy in rabbits. Three groups were compared: PGS without BMP-2, PGS with BMP-2, and the control. After 24 weeks, the new tissue in the control group was composed of a mixture of fibrous tissue, fibro-cartilage and hypercellular cartilage, without new bone formation. In both PGS groups, the growth of bone and cartilage-like tissue was observed with hematoxylin-eosin staining. Although BMP-2 was considered to be an osteoinductive signal, no significant differences were found between the PGS and BMP-treated PGS groups. Essentially, the cartilage-like and bone tissue were derived from MSCs in the underlying bone marrow. In order to enhance tissue regeneration, it was recommended that PGS be seeded with MSCs before implantation. This study also revealed that a PGS complex could be a good candidate for tissue engineering, because both PGS with or without BMP-2 could

induce the formation of cartilage-like and bone tissues. A concern here was that the new tissue regenerated in this way had a mixture of cartilage and bone together as opposed to cartilage and bone located in separate layers.

Subsequent research was focused intensively on seeking new cell sources and on developing osteochondral scaffolds. Abukawa *et al.*<sup>168</sup> seeded MSCs into PLGA scaffolds in the shape of the mandibular condyle, which were prepared by the particulate-leaching technique. 6 weeks of *in vitro* culture in a rotational bioreactor revealed the presence of osteocytes and bone matrix. Similar studies conducted by Chen *et al.*<sup>167, 170</sup> demonstrated the feasibility of using porous natural coral seeded with MSCs for bone regeneration with the evidence of bone neogenesis in condylar-shaped scaffolds. The significance of both studies was to reveal osteogenesis of MSCs in 3D scaffolds while the scaffolds maintained the original shape. However, both studies focused on only bone tissue engineering in a single scaffold. Furthermore, Mao and colleagues<sup>5, 57, 67, 68, 171</sup> differentiated MSCs into chondrocytes and osteoblasts, which were seeded in different layers of a PEG-based hydrogel fabricated by photopolymerization. The osteogenic and chondrogenic cells were entrapped in the PEG-based hydrogel suspension, and then sequentially loaded into a hollow human mandibular condyle-shaped polyurethane mold and photopolymerized. After 4 weeks of *in vivo* implantation, histology showed that the chondrogenic layer had scattered chondrocyte-like cells and intercellular matrix, and the osteogenic layer contained osteoblast-like cells in island-like structures. The results of these studies showed the possibility of engineering the mandibular condyle in the shape of the

human mandibular condyle from a single population of bone marrow-derived chondrogenic and osteogenic cells.

With respect to the development of new scaffolds, image-based design (IBD) and SFF were introduced by Hollister and colleagues<sup>9-11, 92, 166, 172</sup> to design and fabricate craniofacial composites with specific physical and mechanical properties, which included not only the specific shape and porosity, but also the desired elasticity and permeability. PCL scaffolds have been fabricated successfully via selective laser sintering (SLS), an indirect SFF method, in the mandibular condyle shape with mechanical properties similar to trabecular bone.<sup>11</sup> These scaffolds were seeded with bone morphogenetic protein (BMP) transduced fibroblasts, and after implantation into mice for 5-8 weeks, bone formation was verified by histological staining and CT scans. Furthermore, a PLA/HA composite was fabricated for tissue engineering the mandibular condyle.<sup>172</sup> The PLA and HA scaffolds were designed and fabricated to meet the different requirements of the regeneration of cartilage and bone, and were joined tightly with PLA rods. This composite was seeded with chondrocytes in the polymeric PLA phase and transduced fibroblasts with BMP-7 in the ceramic HA phase. 4 weeks of *in vivo* culture in mice demonstrated GAG formation, indicated by Safranin O staining in the polymeric layer, and bone formation with marrow space in the ceramic layer, as indicated by hematoxylin and eosin (H&E). The advantage of IBD and SFF is that accurate control over biomaterials made the patient-specific scaffolds possible and allowed more detailed experiments to build optimized scaffolds.

To the best of our knowledge, to date, there is only one study using a bioreactor to tissue engineer the mandibular condyle. As we discussed earlier, Abukawa *et al.*<sup>168</sup> cultured MSC-derived osteoblasts in a rotational bioreactor system. The PLGA scaffolds were seeded with osteoblasts and placed in gas-permeable centrifuge tubes, which rotated for 6 weeks at 6 rpm. A layer of new tissue-engineered bone, consisting of cells and densely staining osteoid, was formed uniformly on the surfaces of the constructs. In the internal section, osteocytes and bone matrix were observed. This important study will lead the way for future bioreactor studies in mandibular condyle tissue engineering.

## **DISCUSSION AND CONCLUSIONS**

A tissue-engineered osteochondral mandibular condyle construct would be a promising and improved treatment for severe TMJ disorders. A schematic of our approach to tissue engineer the mandibular condyle, which will eventually be combined with a tissue engineered disc,<sup>173</sup> is provided in Fig. 2.1. Chondrocytes and osteoblasts can be either directly harvested, or indirectly derived from stem cells, such as ESCs, bone marrow-derived MSCs or HUCM stem cells. Passaging these cells is imperative for obtaining sufficient cell numbers for large scale cell seeding. Then these cells can be seeded statically or dynamically into 3D scaffolds as a stratified cartilage layer and bone layer. The shape of these scaffolds can be pre-

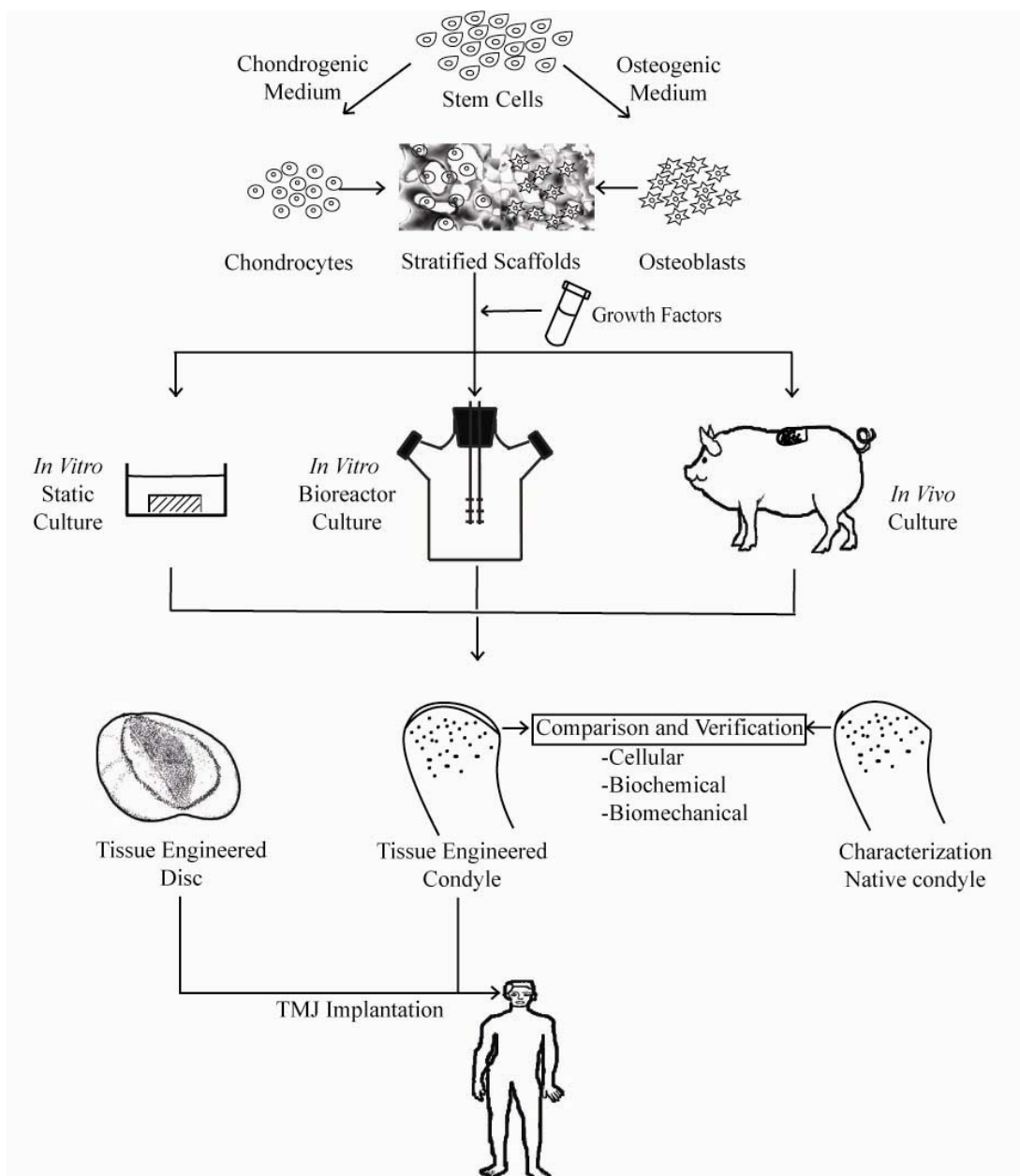


**Figure 2.1:** Schematic of our strategy to tissue engineer the mandibular condyle.

First, the product must be developed in vitro (static or bioreactor) or in vivo, and compared to the native condyle. This developed technology in clinical application may then be combined with an engineered TMJ disc to treat patients with severe TMJ disorders.

defined according to clinical imaging data and fabricated with desired porosity to meet the mechanical strength and biological function requirements. Optimized selection of the types, concentrations and timing of growth factors can accelerate the proliferation of chondrocytes and osteoblasts and the formation of extracellular matrix. Further culture of cells in the scaffolds can be achieved *in vitro* (static or bioreactor) or *in vivo*. Bioreactors are recommended because they can not only enhance the mass transfer of nutrients and wastes, but also provide mechanical stimulation as a means to not only promote biosynthesis, but also to facilitate matrix organization and consequently improve mechanical function. Finally, the biologically and mechanically functional comparison between tissue engineered products and native tissue will be necessary as validation before clinical application, emphasizing the need for native characterization data.

En route to tissue engineering a functional mandibular condyle, a number of challenges need to be considered. A native tissue characterization of the mandibular condyle, including both the surface cartilage and underlying bone, should be examined systematically for tissue engineering studies. Further investigation should focus on quantification of biochemical compositions in the cartilage. Age-related variations of these compositions should go to further the understanding of the adaptation to specific biomechanical loading.<sup>22</sup> The molecular level mechanism of growth factors on chondrocytes and osteoblasts must be further investigated to conciliate conflicting results in previous studies. Understanding how cells respond to exogenous growth factors will be critical not only for the selection of growth factors,

but also for the usage of the optimized dosage for maximized benefit to cell proliferation and biosynthesis. Due to the insufficient mass transfer within large scaffolds, the scale-up of osteochondral constructs may be limited by the inability to achieve homogenous cell densities and maintain cell viability and differentiated function in the dimensions of the human condyle.

Although tremendous strides have been made for both cartilage and bone regeneration, tissue engineering of osteochondral tissues is still in its infancy. Only recently has the musculoskeletal tissue engineering community begun to acknowledge the significance of osteochondral tissue engineering, which is not merely a simple combination of cartilage and bone tissue engineering. Osteochondral tissue engineering is an “autocatalytic” process in the sense that the mutually inductive nature of chondrocytes and osteoblasts push the other down their respective lineages, which may be a missing key ingredient in the isolated approaches of engineering cartilage or bone alone. Gerstenfeld *et al.*<sup>174</sup> strongly supported this point, demonstrating that only co-culture with chondrocytes (as opposed to osteoblasts and fibroblasts) was successful at promoting osteogenesis of mesenchymal stem cells. We are aware of only a select number of groups who have published osteochondral tissue engineering studies, and methodologies vary widely.<sup>3, 5, 8, 68, 91, 171, 175-182</sup> Some groups have used mesenchymal stem cells,<sup>3, 5, 68, 171, 176, 177, 181</sup> while others relied on differentiated cartilage and/or bone cells.<sup>8, 91, 178-180</sup> From the viewpoint of translational research, a single stem cell source may offer advantages over obtaining both bone and cartilage biopsies from a patient. With respect to growth

factors, it is necessary to further examine the synergistic effect since the regeneration of the complex tissue may require the combination of several growth factors. With respect to scaffolds, it is essential to improve the design and fabrication techniques of osteochondral scaffolds to make a multilayered composite, with controlled spatial distribution of physical and mechanical properties in two layers for cartilage regeneration and bone formation. Moreover, there is no easy solution to integrating the two layers, and researchers should be commended for their creative approaches heretofore, which include layering of chondro- and osteo-induced regions,<sup>5, 8, 68, 171</sup> painting chondrocytes onto an osteoblast-containing construct,<sup>91</sup> suturing<sup>179</sup> or press-fitting<sup>180, 181</sup> the two layers together, use of a fibrin sealant<sup>3</sup> to adhere the two, and simply relying on *in vivo* conditions.<sup>176, 177</sup> In addition, the cartilage layer would ideally resemble zonal organization in native cartilage,<sup>183</sup> and vascularization within the osseous portion of the construct is still a challenge, which depends on the regeneration of blood vessels.

As TMJ tissue engineering progresses, we must be cognizant of practical issues with clinical application on the horizon. Attaching engineered tissues in this highly complex joint will not be an easy feat. For example, surgeons may prefer to attach an engineered TMJ disc to an *engineered* condyle rather than attempt to attach it to the *existing* condyle in certain cases, as making the challenging medial attachments to an existing degenerated condyle may not be an attractive option. Nevertheless, attaching the engineered disc and condyle will be a challenge, as will connecting surrounding soft tissues and anchoring the engineered condyle to the

ascending ramus. We urge the TMJ tissue engineering community to keep these factors in mind as the field matures, such that we can prepare for these clinical hurdles.

In conclusion, the ultimate goal of tissue engineering the mandibular condyle is to reconstruct a functional replacement equivalent to the native tissues in cellular and biochemical composition and organization, and in biomechanical properties and behavior. The native tissue characterizations of mandibular condylar cartilage and bone must be investigated further to provide a basis for tissue engineering design and validation. The cell sources are not limited to autologous differentiated cells, as MSCs, ESCs and HUCM stem cells are promising choices. Despite the abundance of growth factor studies, inconsistencies must be resolved, and both synergistic and sequential effects need to be identified to engineer the mandibular condyle. We must emphasize the need to design and fabricate seamless stratified osteochondral constructs as a single unit. Furthermore, it may be advantageous for investigators to develop composite mechanical stimulation and mass transfer bioreactors for tissue engineering osteochondral tissues. The end goal is to create an engineered condyle that a surgeon could affix to the ascending ramus of the mandible, and perhaps attach to an engineered disc and to existing and/or engineered attachment tissues. This combination of engineered tissues would be a revolutionary treatment to a community of TMJ surgeons and patients desperate for answers.

## CHAPTER 3: Tissue Engineering with Human Umbilical Cord Mesenchymal Stromal Cells\*

### ABSTRACT

Multipotent mesenchymal stromal cells (MSCs) hold tremendous promise for tissue engineering and regenerative medicine, yet with so many sources of MSCs, what are the primary criteria for selecting leading candidates? Certainly the cells of a given source must be multipotential, and ideally will be inexpensive, easy and painless to collect, readily available in large numbers, immunocompatible, free of ethical controversy (politically benign), developmentally primitive, expandable *in vitro* for several passages, and obtained without donor site morbidity. Bone marrow MSCs do not meet all of these criteria, neither do embryonic stem cells. However, a promising new cell source is emerging in tissue engineering that appears to meet all of these criteria: umbilical cord mesenchymal stromal cells (UCMSCs). UCMSCs are derived from the Wharton's jelly of umbilical cords, the jelly-like connective tissue supporting the umbilical vessels. Exposed to appropriate culture conditions, UCMSCs differentiate along several cell lineages such as the chondrocyte, osteoblast, adipocyte, myocyte, neuronal, pancreatic, or hepatocyte lineages. In animal models, hUCMSCs demonstrate great immunocompatibility with host organs/tissues, even in xenotransplantation, although it is unlikely that immunocompatibility is retained after differentiation or activation. However, UCMSCs can be banked at birth, as is commonly done with cord blood today, and accessed either as an autologous cell source or as a tremendous resource of MHC-matched allogeneic cells. Cumulatively,

---

\*Chapter submitted to Tissue Eng Part B as Wang, Seshareddy, Weiss, and Detamore. "Tissue engineering with human umbilical cord mesenchymal stromal cells," August 2008.

the advantages of UCMSCs render them an attractive source of multipotent cells for tissue engineering applications. In this review, we address their cellular characteristics, multipotent differentiation ability and potential for tissue engineering with an emphasis on musculoskeletal tissue engineering.

## INTRODUCTION

Increased efforts have been employed in the identification of cell sources that can be utilized for tissue engineering and regenerative medicine.<sup>184-186</sup> Multipotent mesenchymal stromal cells (MSCs) reside in a variety of tissues, such as bone marrow, adipose tissue, blood, synovial fluid, dermis, muscle, dental pulp, and can differentiate along several mesenchymal lineages such as cartilage, bone, and adipose tissue.<sup>187-193</sup> However, there are significant differences in their proliferation and differentiation abilities, and harvesting procedure among these MSCs,<sup>194</sup> which may limit their application in tissue engineering. In recent years, the Wharton's jelly (WJ) of human umbilical cords has been discovered as a reservoir of MSCs.<sup>195</sup> Cells isolated from WJ are referred to as umbilical cord mesenchymal stromal cells (UCMSCs) in the following sections. Recent evidence supports that human UCMSCs (hUCMSCs) are a multipotent stromal cell population that share MSC surface markers such as CD73, CD90, and CD105, and are non-hematopoietic cells.<sup>196</sup>

Before the 21<sup>st</sup> century, umbilical cord research focused on the structure of umbilical cords and the characterization of extracellular matrix and stroma cells as early as the 1940s.<sup>197, 198</sup> Following the recognition of their neural differentiation

ability demonstrated early in the current decade,<sup>75</sup> hUCMSCs have evoked a rapidly growing interest with over 30 studies published during the last 5 years.<sup>64, 75-77, 80, 81, 186, 195, 196, 199-220</sup> It has been reported that hUCMSCs can differentiate along several cell lineages in all three germ layers including chondrogenic, osteogenic, adipogenic, myogenic, pancreatic, neurogenic, and hepatogenic.<sup>75, 81, 195, 199, 215</sup> *In vivo* transplantation of these cells has been demonstrated to prevent progressive deterioration with brain injury and to rescue the eye from retinal disease in a rodent model.<sup>213, 214</sup> Recent tissue engineering studies with hUCMSCs have focused on cardiovascular tissue engineering,<sup>65, 81, 82, 205, 221, 222</sup> and on musculoskeletal tissue engineering.<sup>66, 207</sup> In this review, we have emphasized the mesenchymal differentiation of hUCMSCs and their potential for musculoskeletal tissue engineering. Cell biology and transplantation reviews of hUCMSCs can be found in detail in the literature.<sup>196, 200, 223</sup>

## CELL CHARACTERIZATION

The human umbilical cord includes one vein, two arteries, and a surrounding connective tissue known as Wharton's jelly (Fig. 3.1). The connective tissue may be divided into three zones: subamniotic, intervacular, and perivascular stromata.<sup>195</sup> hUCMSC-like cells, called prechondrocytes, were isolated by McElreavey *et al.*<sup>224</sup> in the early 90s using the explant method. Enzyme digestion of trypsin and/or collagenase has been recently utilized to extract hUCMSCs with fast isolation and high yield.<sup>76, 77, 80, 195</sup> UCMSCs include cells from all three stromata, and the

umbilical cord perivascular cells, obtained via enzyme digestion of the area surrounding umbilical vessels, may isolate a subpopulation.<sup>77, 218, 225</sup> hUCMSCs resemble fibroblasts in their morphology (Fig. 3.1) and have been defined as myofibroblasts based on their positive expression of vimentin, desmin, and/or  $\alpha$ -smooth muscle actin (ASMA) in native tissue or with *in vitro* cultured

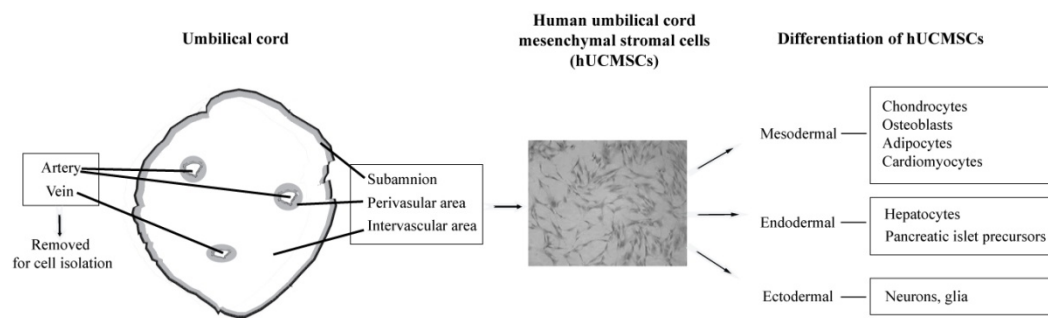


**Figure 3.1:** Structure of umbilical cords (UC) and differentiation schematic diagram of human mesenchymal stromal cells (hUCMSCs).

cells.<sup>75, 226, 227</sup> In a recent review,<sup>196</sup> UCMSCs were proposed to be a primitive stromal population that possess characteristics of bone marrow MSCs (BMSCs) defined by the International Society for Cellular Therapy (ISCT).<sup>196</sup> hUCMSCs express surface markers that have been identified in other MSCs, including CD10,<sup>80</sup> CD13,<sup>80, 199, 204, 208</sup> CD29,<sup>76, 80, 204, 208</sup> CD44,<sup>76, 77, 80, 195, 199, 204, 208</sup> CD49e,<sup>80, 225</sup> CD51,<sup>76</sup> CD73/SH3,<sup>76, 77, 195, 199, 204</sup> CD90 (Thy-1),<sup>77, 80, 199, 208, 225</sup> CD105/SH2,<sup>76, 77, 80, 195, 199, 204</sup> CD106,<sup>204</sup> CD117,<sup>75, 77, 199</sup> CD146,<sup>225</sup> CD166,<sup>199, 204, 208</sup> and HLA-1/HLA-ABC;<sup>77, 80, 204, 208</sup> and are negative for hematopoietic markers (e.g., CD14, CD31, CD34, CD38, CD45, HLA-DR).<sup>64, 65, 75-77, 80, 81, 83, 195, 199, 201, 204, 208, 209, 225</sup> On the other hand, hUCMSCs

express pluripotency markers such as Oct-4, Nanog, and Sox-2 at the transcription level in porcine umbilical cord cells, although at a lower level than embryonic tissues,<sup>201</sup> indicating that hUCMSCs may have a subpopulation that share properties of both pluripotent and non-pluripotent stem cells.<sup>201</sup> The perivascular cells express STRO-1 (~1%),<sup>225</sup> an MSC surface marker that has been used to enrich fibroblast colony-forming units (CFU-F) cells from bone marrow.<sup>228</sup> Therefore, hUCMSCs present adherent cells with a non-hematopoietic and non-endothelial (CD34 negative) phenotype and share a similar set of surface markers with other adult MSCs.

hUCMSCs demonstrate the ability to differentiate along several cell lineages of mesodermal origin and along a neural lineage of ectodermal origin (Fig. 3.1).<sup>75, 81, 195, 199</sup> Furthermore, recent studies reported that hUCMSCs were able to differentiate both *in vivo* and *in vitro* into hepatocyte-like cells and pancreatic islet precursors of endodermal origin.<sup>199, 215</sup> Exposed to a hepatogenic culture medium, hUCMSCs expressed hepatic markers including albumin,  $\alpha$ -fetoprotein, cytokeratin-19, connexin-32, and dipeptidyl peptidase IV.<sup>199</sup> This study provided the foundation for the application of hUCMSCs for liver regeneration. Work from Chao *et al.*<sup>215</sup> suggests that UCMSCs may be differentiated into pancreatic islet precursors, produce human insulin, and respond to a glucose challenge for up to 12 weeks in a xenotransplantation type I DM model. As a fetal-derived cell source, hUCMSCs have a rapid proliferation rate with shorter doubling time than other adult stem cells.<sup>196</sup> Following cell harvesting, hUCMSCs can be passaged for 7 times to achieve a 300-fold increase in cell number while the differentiation potential is maintained.<sup>195</sup> The

rapid proliferation rate, accompanied by the wide availability of umbilical cords, is highly desirable for tissue engineering as it is possible to obtain a large number of cells in a short time.

## **DIFFERENTIATION AND TISSUE ENGINEERING**

### *Chondrogenic differentiation and cartilage tissue engineering*

Cartilage, which plays a critical role in load bearing and distribution, has limited self-regeneration capabilities after injury. Compared to the current clinical approaches such as microfracture, artificial prosthesis, and cell-based implantation, tissue engineering may be an ideal method to fully restore the cartilage function.<sup>229</sup> Cell dedifferentiation of mature chondrocytes during monolayer expansion makes it difficult to obtain enough cells for tissue engineering.<sup>85</sup> Thus, the application of MSCs in tissue engineering is promising mainly due to their self-renewal and differentiation ability. Chondrogenic differentiation of MSCs can be triggered by the transforming growth factor- $\beta$  isoforms (TGF- $\beta$ 1,  $\beta$ 2, and  $\beta$ 3) and be enhanced by the addition of dexamethasone.<sup>230-232</sup> Insulin-like growth factor-I (IGF-I), an important anabolic agent, remains controversial with its role in chondrogenic differentiation.<sup>232-</sup>  
<sup>234</sup> However, a recent study reported that IGF-I and TGF- $\beta$  had equal chondroinductive ability with MSCs after the removal of insulin from insulin-transferrin-selenious acid Premix (ITS Premix), a substitute for FBS in serum-free chondrogenic medium.<sup>234</sup>

Like other MSCs, hUCMSCs are able to differentiate along a chondrogenic lineage under the stimulation of TGF- $\beta$ s in 3D cell pellets and polyglycolic acid (PGA) scaffolds.<sup>66, 76, 195, 225, 235</sup> In the late 1990s, Naughton *et al.*<sup>235</sup> reported the chondrogenic differentiation of hUCMSCs on 3D PGA scaffolds in a conference abstract. Exposed to TGF- $\beta$  for 6 weeks, constructs formed a dense fibrocartilage-like tissue with both types I and II collagen. The significance of the study is that it was not only the first to report the chondrogenic differentiation of hUCMSCs in biomaterials, but also to suggest their potential for cartilage tissue engineering. In the following cell pellet studies, the chondrogenic ability of hUCMSCs was also supported by Alcian blue staining for glycosaminoglycans (GAGs),<sup>76, 225</sup> and immunohistochemical staining for type II collagen.<sup>76, 195</sup> However, the chondrogenic studies of hUCMSCs have had inconsistent results in the literature.<sup>76, 195</sup> In a study by Wang *et al.*,<sup>76</sup> untreated cells in the control group (no TGF- $\beta$ 1) also demonstrated positive staining for GAGs and collagen type II. In contrast, no type II collagen was observed with the control group in a study by Karahuseyinoglu *et al.*,<sup>195</sup> although only a trace of type II collagen was detected with human BMSCs (hBMSCs), in contrast to the formation of abundant type II collagen in previous hBMSC studies.<sup>58, 236</sup> Type I collagen was also identified in this study in both hBMSCs and hUCMSCs. Nevertheless, larger pellets were observed in the hUCMSC group with a better filamentous extracellular matrix than hBMSCs.<sup>195, 225</sup> Moreover, the GAG quantification revealed that the perivascular cells, a subpopulation of hUCMSCs, produced a quantity of GAGs comparable to hBMSCs after 21 days, although the perivascular groups had fewer GAGs than

hBMSC groups during the first week. Therefore, the better differentiation ability compared to hBMSCs and the co-existence of types I and II collagen in both cell pellets and biomaterial-based culture indicate that hUCMSCs may be considered as a MSC source for fibrocartilage tissue engineering applications such as for the temporomandibular (TMJ) disc, intervertebral disc, and knee meniscus. In our group, following the initial effort in cartilage tissue engineering by Naughton *et al.*,<sup>235</sup> we applied hUCMSCs for musculoskeletal tissue engineering.

The first full-length study of hUCMSCs for musculoskeletal tissue engineering was a comparison of hUCMSCs to TMJ condylar cartilage cells *in vitro* for TMJ regeneration.<sup>66</sup> Both types of cells were cultured in PGA scaffolds over a 4-week period. The hUCMSC constructs formed a fibrocartilage-like tissue similar to the native TMJ cartilage and outperformed TMJ condylar cartilage cells with higher cellularity and biosynthesis of collagen and GAGs. Based on the limited availability of TMJ cells relative to umbilical cord cells and the superior biosynthesis of hUCMSCs, hUCMSCs were suggested as a promising alternative to mature condylar cartilage cells for TMJ tissue engineering. In a 3D comparison of hUCMSCs and hBMSCs for cartilage tissue engineering, hUCMSCs also demonstrated superior extracellular matrix synthesis with more GAGs and collagen than hBMSCs (unpublished data). We further explored cell seeding density for fibrocartilage tissue engineering using hUCMSCs.<sup>207</sup> hUCMSCs were seeded in PGA scaffolds at 5 (low), 25 (middle), or 50 (high) million cells/ml of scaffold. After a 4-week culture period, the high and medium density groups possessed significantly higher cell numbers and

extracellular matrix content per construct and per cell than the lower density group. More importantly, constructs in the high and medium density groups maintained their mechanical integrity, which was confirmed by unconfined compression testing. Therefore, a seeding density greater than 25 million cells/ml was recommended for related future fibrocartilage tissue engineering studies. In a parallel study (unpublished data), we revealed that a sequential signaling strategy, switching from a chondrogenic signal (TGF- $\beta$ 3) to an anabolic agent (IGF-I) in the middle of the culture period, promoted cartilage-like matrix synthesis and type II collagen gene expression better than continuing with TGF- $\beta$ 3 alone throughout the culture period.

In summary, the formation of fibrocartilage-like tissue in cell pellet culture and biomaterial-based tissue engineering studies indicates that hUCMSCs may be an excellent cell source candidate for fibrocartilage regeneration. In addition, a further modified chondrogenic environment, perhaps including the investigation of factors such as bioactive chemical signals (e.g., growth factors, aggrecan), oxygen tension, co-culture, mechanical stimulation and/or *in vivo* regulation, will be needed to enhance chondrogenesis to apply hUCMSCs in hyaline cartilage tissue engineering.

### ***Osteogenic differentiation and bone tissue engineering***

Unlike cartilage, bone is a vascularized tissue with an innate self-healing and remodeling ability.<sup>237</sup> Although bone defects can be treated by autologous bone grafts, the current gold standard, this method is limited by donor site morbidity, malformation and infection.<sup>238</sup> Moreover, there is no satisfactory treatment for some

severe bone injuries.<sup>111</sup> As a tissue engineering approach, BMSCs can be incorporated into biomaterials for direct implantation, with or without prior *in vitro* culture in osteogenic media. A typical osteogenic medium includes osteogenic signals of dexamethasone and/or BMP-2, in addition to  $\beta$ -glycerophosphate and ascorbic acid to aid in matrix synthesis. Exposure of BMSCs to this medium before implantation allows the delivery of more mature osteogenic cells to defects and thus accelerating the *in vivo* bone regeneration.<sup>111</sup>

To date, there have been no 3D bone tissue engineering studies published with UCMSCs. However, osteogenic induction of hUCMSCs in 2D (monolayer) has been accomplished by treatment with dexamethasone and  $\beta$ -glycerophosphate.<sup>76, 77, 195, 204, 208, 225</sup> During the course of osteogenic differentiation in monolayer culture, positive alkaline phosphatase (ALP) activity was observed,<sup>76, 77, 225</sup> osteopontin gene expression was confirmed,<sup>76, 204</sup> the bone-specific immunostaining of osteonectin, osteocalcin and bone sialoprotein-2 was visualized,<sup>195</sup> and mineralization was verified by von Kossa staining and Alizarin red staining.<sup>76, 77, 195, 204, 208</sup> Like hBMSCs, mineralization was observed with hUCMSCs in 2-weeks<sup>76, 195, 204, 208</sup> and similar side-by-side gene expression was also observed during this period.<sup>204</sup> It appears that hUCMSCs had less mineralization than hBMSCs as evidenced by Alizarin red staining.<sup>195</sup> However, perivascular cells from the umbilical cord demonstrated better osteogenic potential with higher ALP activity and richer bone-specific extracellular matrix than both BMSCs and the whole population of hUCMSCs.<sup>77, 225</sup> Exposed to osteogenic medium, the perivascular cells differentiated faster along the osteogenic

lineage with the formation of bone nodules after only 4-5 days.<sup>77</sup> When hUCMSCs were cultured for 7 days in monolayer with a medium containing osteoinductive biomaterials such as demineralized bone matrix,<sup>239</sup> their proliferation was inhibited, their morphology appeared shortened and flattened, and ALP activity increased significantly. These phenomena indicated that hUCMSCs may differentiate along the osteogenic lineage,<sup>239</sup> while long-term culture will be needed to verify the presence of late stage osteogenic markers.

Therefore, in monolayer culture, hUCMSCs demonstrate osteogenic differentiation ability after exposure to chemical signals and osteoinductive biomaterials, and perivascular cells appear to exhibit superior osteogenesis compared to hUCMSCs and hBMSCs. The osteogenic differentiation in 3D biomaterials is still unexplored in the literature and future tests are warranted to utilize hUCMSCs for bone tissue engineering. In fact, in our group (unpublished data), hUCMSCs did differentiate along the osteogenic lineage when placed in poly(L-lactic acid) (PLLA) and PGA scaffolds. Osteogenic differentiation was concluded based on ALP activity, collagen production, and calcium deposition, which were greater with higher cell seeding densities. In the future, it will be valuable to make a 3D osteogenic comparison among hUCMSCs, the perivascular cells, and hBMSCs. Moreover, *in vivo* studies and methods to improve osteogenic differentiation will be high priority areas of future investigation.

### ***Undifferentiated hUCMSCs and cardiovascular tissue engineering***

Detailed reviews regarding the application of hUCMSCs in cardiovascular tissue engineering can be found in the literature,<sup>240, 241</sup> so only a brief overview will be provided here. hUCMSCs were utilized for cardiovascular tissue engineering prior to the identification of multipotent differentiation,<sup>81</sup> and in subsequent studies have been shown to be a suitable cell source for this application.<sup>65, 82, 205, 221, 222</sup> In monolayer culture, undifferentiated hUCMSCs expressed a positive staining of ASMA and vimentin with the deposition of types I and III collagen in 2 weeks in a culture medium containing only Dulbecco's Modified Eagle's Medium and 10% fetal bovine serum, which was phenotypically similar to the native cells in heart valve leaflets.<sup>81</sup> This similarity provided the rationale for using these cells for cardiovascular regeneration.<sup>81</sup> The culture of hUCMSCs on 3D PGA/poly-4-hydroxybutyrate (PGA/P4HB)<sup>65, 81, 82, 205, 222</sup> or P4HB<sup>221</sup> scaffolds produced a layered tissue with types I and III collagen, GAGs, elastin, and a mechanical stiffness comparable to native cardiovascular tissue. These tissue-engineered constructs can be endothelialized under cyclic strain with human umbilical cord blood endothelial progenitor cells (UC-EPCs) to provide a functional endothelial layer.<sup>205</sup> Hence, the approach using hUCMSCs for cardiovascular tissue engineering is attractive, since UC-EPCs can also be obtained at birth along with the hUCMSCs. This alone, will not solve the problem of tissue rejection. However, if the umbilical cord is collected from children who have a congenital heart defect, then UC-EPCs and UCMSCs can be used to construct bilaminar constructs.

### ***Adipose differentiation and tissue engineering***

Traditional autologous fat tissue transplantation suffers from the loss of graft volume with time.<sup>242</sup> When tissue engineering is applied to adipose tissue regeneration, the usage of mature adipocytes is limited by the inferior *in vitro* proliferation and expansion ability of these cells, and stem cells thus have been proposed.<sup>243</sup> Adipose differentiation of hUCMSCs has been induced in monolayer culture by dexamethasone, insulin, indomethacin, and isobutylmethylxanthine, and has been verified by lipid deposits that were detected by Oil Red O staining.<sup>76, 195, 204, 208, 225</sup> Following adipogenic differentiation, adipose-related genes, such as peroxisome proliferator-activated receptor  $\gamma$  2 (PPAR $\gamma$ 2),<sup>76</sup> lipoprotein lipase,<sup>204</sup> and plasminogen activator inhibitor-1 (PAI-1),<sup>195</sup> were detected in hUCMSCs by RT-PCR. Compared to hBMSCs, hUCMSCs took a longer period to achieve adipose differentiation (40 days vs. 21 days, respectively).<sup>195</sup> A similar observation has been made between fetal MSCs and adult MSCs. In addition, hBMSCs formed more homogeneous lipid droplets and had a more round morphology than the hUCMSCs.<sup>195</sup> However, in a 2-week study by Lu *et al.*,<sup>204</sup> no significant difference was found in the percentage of adipogenic positive cells between hUCMSCs and hBMSCs (69.4% vs. 57.3%, respectively). In another study,<sup>219</sup> after long-term exposure to adipogenic medium, 90% of hUCMSCs differentiated toward the adipogenic lineage and formed mature adipocytes. Therefore, the adipose differentiation ability of hUCMSCs makes them a promising alternative to autologous

fat cells for adipose tissue engineering, despite the fact that hUCMSCs have not yet been used for adipose tissue engineering.

## ESCS AND BMSCS

An ideal cell source for tissue engineering should satisfy requirements including ease of access, sufficient cell number and immunocompatibility. Mature autologous cells have commonly been used in previous studies, due to the advantages of already being differentiated and immunocompatibility. In contrast to mature autologous cells, ESCs are a major area of contemporary research interest, and offer significant potential to treat or even cure a plethora of diseases. They can differentiate into a wide range of cell lineages in all three germ layers, such as hematopoietic cells, insulin-secreting cells, and keratinocytes, which BMSCs may not be able to differentiate into or are inefficiently differentiated into. The self-renewal ability of ESCs also allows a large number of undifferentiated cells to be produced for tissue engineering applications. However, ESCs suffer from a series of constraints including *in vitro* culture, political concerns, availability, difficulty in obtaining a viable line, and potential immunorejection. Although induced pluripotent (iPS) cells have the potential to overcome the immunorejection obstacle,<sup>244, 245</sup> a great deal of work remains before they can be developed into a safe therapy in humans.

BMSCs are the most extensively investigated MSCs for tissue engineering applications and have been considered as the “gold standard” cell source in musculoskeletal tissue engineering. In bone marrow, MSCs create a

microenvironment for hematopoiesis and also provide a stem cell reservoir for bone repair and turnover. BMSCs have the ability to differentiate *in vitro* and *in vivo* into several connective tissues such as cartilage, bone, and adipose tissues. The main advantage of using BMSCs is to provide an autologous cell source for tissue engineers to avoid potential immunorejection. They are also easy to access, but have limited self-renewal ability. hBMSCs are the first stem cell source that were used via a tissue engineering approach to treat bone defects in clinical studies.<sup>246, 247</sup> In a 7-year clinical trial,<sup>246, 247</sup> porous ceramic scaffolds seeded with undifferentiated, *in vitro*-expanded autologous hBMSCs were implanted to treat a large bone (4-8 cm) defect. After 5–7 months, the implants were completely integrated together with the host bone and no post-surgery complications were observed in all 3 patients. In the 7<sup>th</sup> year follow-up,<sup>247</sup> this integration was maintained and no further fractures were observed. This pilot study demonstrated the feasibility of a tissue engineering approach in human bone regeneration with long-term durability, which provided a substitute method for autologous bone grafts. However, there are some known hurdles which limit the applications of BMSCs. The relative number of hBMSCs in the marrow, their proliferation ability, and their differentiation potential decrease significantly with age.<sup>248</sup> Moreover, the invasive harvesting procedure may lead to complications and morbidity.<sup>249</sup>

## **DISCUSSION, CONCLUSION AND FUTURE DIRECTIONS**

In this review, hUCMSCs were introduced to the tissue engineering community as an alternative to mature cells, ESCs, and BMSCs, with clear advantages over each (Table I). Practically speaking, hUCMSCs are much easier and less expensive to harvest and culture. In addition, hUCMSCs are less controversial in the current political climate than ESCs. In terms of availability and harvesting efficiency, hUCMSCs offer a major advantage over ESCs, as there is an endless supply of umbilical cords and hUCMSCs can be prepared from close to 100% of cord samples. With regard to their self-renewal ability, hUCMSCs, as fetus-derived MSCs, have a better *in vitro* expansion capability than adult stem cells, perhaps due to their longer telomeres.<sup>250</sup> The rapid proliferation rate compared to BMSCs and their extensive availability make it possible to obtain a tremendous number of hUCMSCs cells in a short time (orders of magnitude larger than BMSCs) to meet the need of tissue engineering applications. As for their differentiation ability, hUCMSCs have been shown to differentiate along mesenchymal lineages and cross germ layer boundaries. With regard to their immunocompatibility, hUCMSCs thus far appear to be more immunocompatible than ESCs.<sup>251, 252</sup> hUCMSCs can be also used as an autologous MSC source, which can be cryogenically frozen, and thus it is possible to avoid immunorejection. Even if evidence of immunogenicity is discovered after differentiation,<sup>253</sup> allogeneic hUCMSCs would be a viable option with the availability of cord cell banks, as routine tissue-typing (HLA/MHC matching) with a tremendous donor selection would be straightforward and would thus reduce any potential immunogenicity along with immunosuppressants, as is done for transplant patients

(but without waiting indefinitely for a donor). Nevertheless, as an allogeneic source, hUCMSCs have demonstrated their immunocompatibility and even immunosuppressive nature in animal models.<sup>77, 78, 80, 216, 217, 254</sup> In xenotransplantation studies, UCMSCs survived without immune response and displayed a rescue phenomenon in retinal and Parkinson's disease.<sup>78, 213</sup> The immunogenicity of hUCMSCs was only observed in one study after repeated injection of hUCMSCs into the same diseased region.<sup>254</sup> With all of these characteristics, we believe that hUCMSCs will be a suitable, attractive, and potentially preferred cell source for tissue engineering.

**Table I:** Criteria for cell source selection in tissue engineering

<b>Factor</b>	<b>Mature</b>	<b>BMSCs</b>	<b>ESCs*</b>	<b>UCMSCs</b>
Large supply (availability)				X
Easy to obtain and to use	X	X		X
Low immunogenicity	X	X		X
Politically non-controversial	X	X		X
Pluripotent		X	X	X
No donor site morbidity			X	X
Developmentally primitive cells			X	X
Multiple passaging			X	X

BMSC = bone marrow mesenchymal stromal cell, ESC = embryonic stem cell,  
hUCMSCs = umbilical cord mesenchymal stromal cell

\* = includes embryonic germ cells

Although it is still unclear whether hUCMSCs are a true stem cell population due to no available evaluation of their long-term engraftment or *in vivo* differentiation and self-renewal ability in the literature,<sup>196</sup> hUCMSCs can differentiate into various cell lineages and have great *in vitro* expansion ability, which certainly support the contention that these cells may indeed act as true stem cells. En route to the application of hUCMSCs in tissue engineering, a number of concerns remain to be

addressed, including cell-biomaterial surface interaction, cell culture environment, and safety. Tissue engineering strategies require hUCMSC to adhere efficiently to biomaterials. Indeed, high seeding efficiency with hUCMSCs, coupled with fast proliferation, can reduce the quantity of cords and the cost of culture reagents significantly. Tissue engineering strategies also require an optimal culture environment that can maintain cell growth, differentiation potential, phenotype, and genomic stability.<sup>255</sup> Currently, the most common medium for hUCMSCs involves the usage of bovine serum which may cause disease transmission and the immune reaction to foreign proteins. As tissue engineering using hUCMSCs is translated into clinical practice, a serum-free medium may be preferred to avoid these problems. In fact, a low-serum medium has been successfully used to culture hUCMSCs. It includes only 2% bovine serum, 1X serum substitute (ITS), and growth factors containing epidermal growth factor (EGF) and platelet-derived growth factor (PDGF).<sup>80</sup> In this medium, cells grew robustly and most of the initial surface markers were maintained after 4 passages. In the future of clinical practice, human autologous serum may be an option to replace this 2% animal serum, although clearly a serum-free medium would be ideal. Moreover, to engineer large-scale tissues, typical scale-up problems need to be addressed as the diffusion of nutrients and wastes is hindered in large constructs.<sup>256</sup>

In conclusion, UCMSCs represent an exciting MSC source for tissue engineering applications with clear advantages over other cell sources including but not limited to the ease to access, extensive availability (e.g., 4.1 million births in the

United States alone in 2005<sup>257</sup>), non-invasive harvesting, and *in vitro* expansion ability. Investigations of hUCMSCs in cartilage and cardiovascular tissue engineering have shown encouraging results based on the *in vitro* evaluation, and *in vivo* tissue engineering studies of hUCMSCs are warranted en route to clinical trials. Following the current successes in cartilage and cardiovascular tissue engineering, we believe that hUCMSCs have the potential to be successfully used in other tissue engineering areas such as adipose, bone, and neural tissue. Future work should include the optimization of cell culture environment, scaffold design, and bioreactor development, all of which can be integrated in stem cell-based tissue engineering strategies toward clinical application.

## **CHAPTER 4: Effects of Growth Factors and Glucosamine on Porcine Mandibular Condylar Cartilage Cells and Hyaline Cartilage Cells for Tissue Engineering Applications\***

### **ABSTRACT**

Temporomandibular joint (TMJ) condylar cartilage is a distinct cartilage that has both fibrocartilaginous and hyaline-like character, with a thin proliferative zone that separates the fibrocartilaginous fibrous zone at the surface from the hyaline-like mature and hypertrophic zones below. In this study, we compared the effects of insulin-like growth factor-I (IGF-I), basic fibroblast growth factor (bFGF), transforming growth factor beta1 (TGF- $\beta$ 1), and glucosamine sulfate on porcine TMJ condylar cartilage and ankle cartilage cells in monolayer culture. In general, TMJ condylar cartilage cells proliferated faster than ankle cartilage cells, while ankle cells produced significantly greater amounts of glycosaminoglycans (GAGs) and collagen than TMJ condylar cartilage cells. IGF-I and bFGF were potent stimulators of TMJ cell proliferation, while no signals statistically outperformed controls for ankle cell proliferation. IGF-I was the most effective signal for GAG production with ankle cells, and the most potent upregulator of collagen synthesis for both cell types. Glucosamine sulfate promoted cell proliferation and biosynthesis at specific concentrations and outperformed growth factors in certain instances. In conclusion, hyaline cartilage cells had lower cell numbers and superior biosynthesis compared to TMJ condylar cartilage cells, and we have found IGF-I at 100 ng/mL and

---

\*Chapter published as Wang and Detamore. "Effects of growth factors and glucosamine on porcine mandibular condylar cartilage cells and hyaline cartilage cells for tissue engineering applications," Arch Oral Biol, Epub ahead of print, 2008.

glucosamine sulfate at 100  $\mu\text{g}/\text{mL}$  to be the most effective signals for these cells under the prescribed conditions.

## INTRODUCTION

Temporomandibular joint (TMJ) condylar cartilage is categorized as secondary cartilage formed by periosteum or endosteum. It has both fibrocartilaginous and hyaline-like character, with a thin proliferative zone that separates the fibrocartilaginous fibrous zone at the surface from the hyaline-like mature and hypertrophic zones below. The complexities of TMJ condylar cartilage distinguish it from both well-characterized hyaline cartilage and the TMJ disc, which we have investigated before.<sup>258, 259</sup> There are only three studies from a single group about the differences between the cell types from hyaline cartilage and TMJ condylar cartilage, all of which investigated the effects of growth factors on cell behavior in rat explant culture.<sup>35, 121, 124</sup> The first study found that the DNA content with TMJ condylar cartilage was significantly increased by 25 ng/mL IGF-I, while the femoral head cartilage was not affected. The second and third studies revealed that three growth factors, bFGF, IGF-I and TGF- $\beta$ 1, stimulated higher cell proliferation in the TMJ condylar explants than in the femoral head explants, while no significant difference in GAG content was discovered between these two types of cartilage.

Glucosamine remains virtually untested in tissue engineering applications, with the exception of a few recent studies that presented conflicting results. Some studies revealed that glucosamine did enhance GAG<sup>260, 261</sup> and collagen<sup>262, 263</sup>

synthesis, and upregulate the gene expression of aggrecan<sup>260, 262, 263</sup> and type II collagen<sup>262, 263</sup> in a concentration-dependent manner. However, other studies seem to suggest that its effects are mostly based on inhibiting catabolic activities rather than on anabolic ability to rebuild cartilage, indicated by the down-regulation of aggrecan and type II collagen.<sup>264, 265</sup> To date, there have been no studies that have investigated the effects of glucosamine on TMJ condylar cartilage cells. The goal of the current study was to examine the *in vitro* effects of glucosamine sulfate and three growth factors, namely bFGF, IGF-I and TGF- $\beta$ 1, on proliferation and extracellular matrix synthesis of cells obtained from porcine TMJ condylar and ankle cartilage.

## MATERIALS AND METHODS

### *Cell isolation*

One head and two ankles were obtained from the same hog (Chester white breed, female, age 8 months), acquired from Santa Fe Trail Meats (Overbrook, Kansas, USA). TMJ condylar cartilage cells and ankle hyaline cartilage cells were harvested by enzyme digestion.<sup>66</sup> Briefly, for each cell type, two joints were sterilized using an iodine pad, the joint capsule was broken, and cartilage was obtained and minced. Following enzyme digestion overnight, the cells were resuspended, and cultured in the flasks containing cell culture medium consisting of Dulbecco's modified Eagle medium (Invitrogen; Carlsbad, CA), 10% fetal bovine serum (Gemini; West Sacramento, CA), 25  $\mu$ g/mL ascorbic acid (Sigma; St. Louis, MO),

1% non-essential amino acids (Invitrogen) and 1% penicillin-streptomycin-fungizone (Invitrogen). Cells were fed every other day until confluent and labelled as passage 1.

### ***Growth factor***

All growth factors were purchased from PeproTech, Inc. Cells were seeded in 12-well plates at 150,000 cells/cm<sup>2</sup> with 1 mL of medium per well. A total of 12 groups (n = 4) were examined for each cell type, consisting of three growth factors tested at two concentrations each, glucosamine tested at five concentrations, and one control group (cell culture medium without growth factors or glucosamine). No synergistic effects were investigated. IGF-I and bFGF were each examined at 10 and 100 ng/mL,<sup>259</sup> TGF- $\beta$ 1 was examined at 5 and 30 ng/mL,<sup>259</sup> and D-glucosamine 6-sulfate was examined at 0.02, 0.1, 20, 100, and 700  $\mu$ g/mL (corresponding to 0.08, 0.39, 77.2, 385.8 and 2700.3  $\mu$ M). Half of the media was changed every two days for 3 weeks of culture.

### ***Measurement of cell number and biosynthesis***

After 3 weeks, medium was removed from each well and replaced with 1.5 mL papain (120  $\mu$ g/mL) for digestion. Plates were kept at 60 °C overnight and then stored at -20 °C. Cell number and biosynthesis were measured as described previously.<sup>266</sup> Cell number was evaluated by measuring DNA content (PicoGreen Kit, Molecular Probes; Eugene, OR). A conversion factor of 7.7 pg DNA/cell was determined previously. Biosynthesis was evaluated by measuring total GAG and

collagen content. GAG content was measured using a dimethylmethylene blue (DMMB) dye binding assay kit (Biocolor; Newtownabbey, Northern Ireland). Collagen content was determined by using a modified hydroxyproline assay. A collagen standard (Accurate Chemical and Scientific Corporation; Westbury, NY) was used instead of hydroxyproline standards to alleviate the need for approximating a conversion from hydroxyproline to collagen and thus to directly provide collagen content values. All data were expressed as means  $\pm$  standard deviations and analyzed by a single-factor analysis of variance (ANOVA) followed by a Fisher's Protected Least Significant Difference *post-hoc* test.

## RESULTS

### *Cell number*

With regard to cell morphology, there did not appear to be any significant morphological differences over the duration of the study between the two cell types in this high density culture environment. For TMJ condylar cartilage cells, all growth factor groups and glucosamine groups, except for TGF- $\beta$ 1 groups, had an increased cell number compared to the control group (Fig. 4.1). Both 100 ng/mL IGF-I and bFGF groups increased TMJ cell proliferation by 30% compared to the control group ( $p < 0.005$ ). 10 ng/ml IGF-I resulted in 23% more cells than the control ( $p < 0.05$ ). As an exception, TGF- $\beta$  decreased cell proliferation with 16% and 35% fewer cells than the control at 5 ng/mL and 30 ng/mL ( $p < 0.005$ ), respectively. Glucosamine promoted TMJ cell proliferation with 11%, 24%, 26%, 25%, and 17% increases at

0.02, 0.1 ( $p < 0.05$ ), 20 ( $p < 0.05$ ), 100 ( $p < 0.05$ ), and 700  $\mu\text{g/mL}$ , respectively, compared to the control.

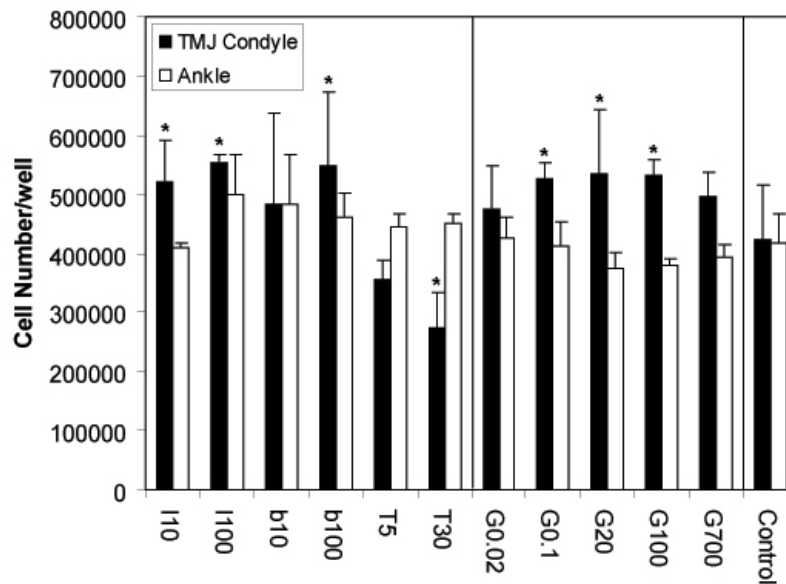


**Figure: 4.1:** Cell number per well via PicoGreen DNA assay ( $n = 4$ ). TMJ cells outperformed ankle cells. I=IGF-I, b=bFGF, T=TGF- $\beta$ , G=glucosamine sulfate, and number corresponds to concentration. Error bars represent standard deviations. \* = significant difference compared to control.

With regard to ankle cartilage cells, all growth factor groups, except for the 10 ng/mL IGF-I group, had a moderate increase in cell proliferation, ranging from 7% to 20% compared to the control, although none of these differences were statistically significant. All concentrations of glucosamine inhibited cell proliferation with an average of a 6% decrease compared to the control, without statistically significant differences. As for a comparison between TMJ cells and ankle cells, all growth

factors and glucosamine concentrations, with the exception of TGF- $\beta$ , promoted higher cell proliferation with TMJ cells than with ankle cells ( $p < 0.001$ ).

### ***GAG content***

For TMJ condylar cartilage cells, it must be noted that all three growth factor groups at low concentrations produced higher mean values for GAG content than the groups at high concentrations, and that GAG content in all growth factor groups had no significant differences compared to the control (Fig.4.2). Glucosamine groups produced a higher average amount of GAGs than growth factor groups. Specific concentrations of glucosamine enhanced GAG synthesis drastically compared to the control. The glucosamine groups at 0.02  $\mu\text{g/mL}$  and 100  $\mu\text{g/mL}$  produced 80% ( $p < 0.05$ ) and 82% ( $p < 0.05$ ) more GAGs than the control, respectively.

For ankle cartilage cells, all growth factor groups produced significantly more GAGs than the control, except for 5 ng/mL TGF- $\beta$  (Fig. 4.2). The 100 ng/mL IGF-I group had the highest GAG production with 3.3 times more GAGs than the control ( $p < 0.00001$ ), and the 10 ng/mL IGF-I and bFGF groups had 2.0 and 2.1 times more GAGs than the control ( $p < 0.00005$ ). The other three growth factor groups led to increases in the range of 12-53%. High concentrations of growth factors, except for bFGF, stimulated more GAG formation than low concentrations ( $p < 10^{-6}$ ). The pattern of glucosamine acting on GAG production with ankle cartilage cells was similar to the pattern with TMJ condylar cartilage cells, with a 75% increase in GAG content for the 0.02  $\mu\text{g/mL}$  concentration ( $p < 0.005$ ) and a 120% increase for the 100

$\mu\text{g/mL}$  concentration ( $p < 0.00001$ ) compared to the control. The  $0.1 \mu\text{g/mL}$  glucosamine group had 49% more GAG production than the control ( $p < 0.05$ ). Additionally, the comparison between cell types indicated that ankle cartilage cells produced 86% more GAGs than TMJ condylar cartilage cells ( $p < 10^{-9}$ ).

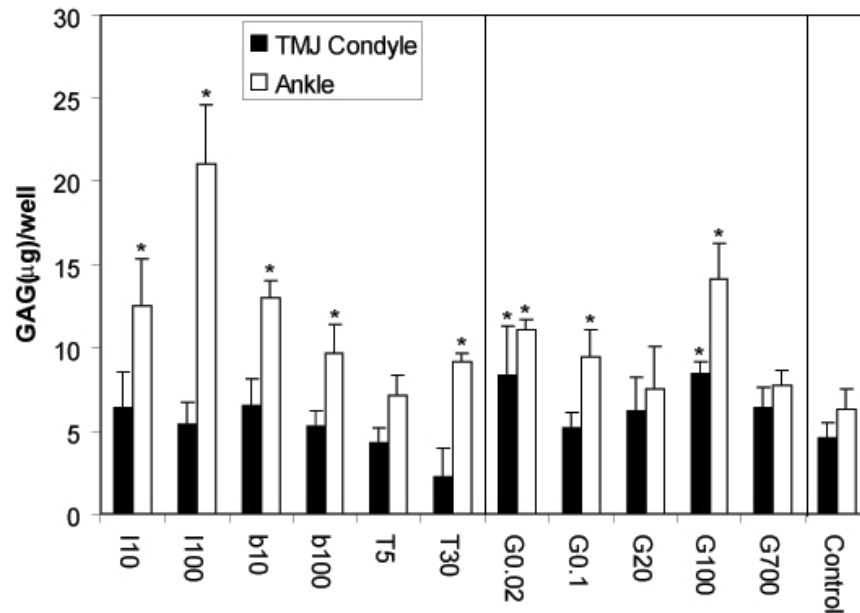


**Figure 4.2:** GAG content per well ( $n = 4$ ). Ankle cells produced much more GAGs than TMJ cells. Error bars represent standard deviations. \* = significant difference compared to control.

### *Collagen content*

TMJ condylar cartilage cells produced more collagen at low concentrations of growth factors than at high concentrations without statistical significance (Fig. 4.3). For collagen production with TMJ cells, it must be noted that only the  $10 \text{ ng/mL}$  IGF-I group statistically outperformed the control, with a 2.8-fold increase in collagen content ( $p < 0.05$ ). Higher concentrations of glucosamine stimulated TMJ condylar

cartilage cells to produce more collagen without statistical significance. Glucosamine groups at 100  $\mu\text{g}/\text{mL}$  and 700  $\mu\text{g}/\text{mL}$  produced 2.2 and 2.0 times more collagen than the control, respectively.

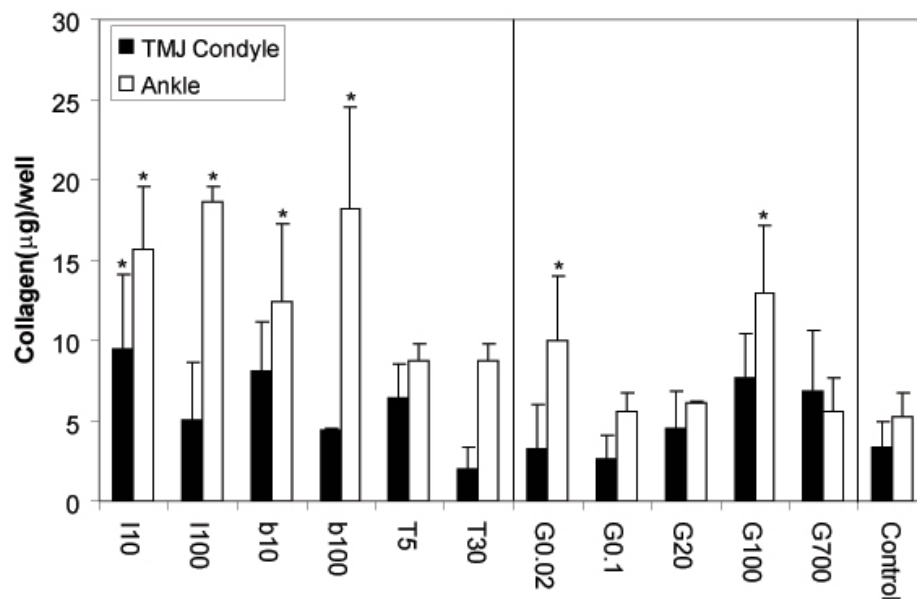


**Figure 4.3:** Collagen content per well ( $n = 4$ ). Ankle cells outperformed TMJ cells in collagen production. Error bars represent standard deviations. \* = significant difference compared to control.

For ankle cartilage cells, high concentrations of growth factors promoted collagen biosynthesis better than low concentrations without statistical significance (Fig. 4.3). The groups treated with 100  $\text{ng}/\text{mL}$  IGF-I and bFGF had the highest collagen production with 3.6 times ( $p < 0.00005$ ) and 3.5 times ( $p < 0.0001$ ) more collagen than the control, respectively. 10  $\text{ng}/\text{mL}$  IGF-I and bFGF had 3.0 times ( $p < 0.0005$ ) and 2.4 times ( $p < 0.05$ ) more collagen than the control, respectively. 0.02  $\mu\text{g}/\text{mL}$  and 100  $\mu\text{g}/\text{mL}$  of glucosamine were the best stimulators for collagen

formation with 1.9 and 2.5 times more collagen than the control, respectively ( $p < 0.05$ ). Other concentrations of glucosamine groups had no statistically significant effects on ankle cartilage cells. With regard to the comparison between the two types of cartilage cells, ankle cartilage cells outperformed TMJ condylar cartilage cells, with 2 times more collagen than TMJ cells ( $p < 0.000005$ ).

## DISCUSSION

This study revealed a distinct portrait of cell proliferation and biosynthesis between TMJ condylar cartilage cells and ankle cartilage cells and demonstrated that glucosamine sulfate at specific concentrations was comparable to growth factors. Passage 1 cells were used in the current study to prevent excessive chondrocyte dedifferentiation.<sup>84-87</sup> The final cell density was less than the initial seeding density (150,000 cells/cm<sup>2</sup>), which revealed cell detachment during the culture period. The average number of TMJ condylar cartilage cells after 3 weeks was significantly higher than with the ankle cartilage cells, which could be explained by the heterogeneous cell populations in TMJ condylar cartilage. Fibroblasts in the fibrous zone of TMJ condylar cartilage have a faster proliferation rate than chondrocytes, resulting in higher cell numbers for TMJ condylar cartilage cells compared to the ankle cartilage groups. Another possible reason is that mesenchymal cells in the proliferative zone of TMJ condylar cartilage may proliferate faster than chondrocytes or may differentiate into fibroblasts. With regard to GAG and collagen content, ankle cells produced significantly more extracellular matrix than TMJ condylar cartilage

cells, which is similar to the native configurations in the two types of cartilages. We are aware that the comparison of the collagen type is critical for tissue engineering applications. In fact, TMJ condylar cells in polyglycolic acid (PGA) scaffolds expressed mainly type I collagen, while hyaline cartilage cells produced dominantly type II collagen (unpublished data).

The current study demonstrated that glucosamine sulfate stimulated TMJ condylar cartilage cells to proliferate while inhibiting ankle cartilage cell proliferation. The same inhibition effect was observed with chondrocyte proliferation in 2D and 3D culture.<sup>262, 267</sup> Glucosamine promoted GAG synthesis for both types of cells, and 0.02 and 100  $\mu\text{g}/\text{mL}$  were optimal concentrations, a bimodal effect that was not expected. We can only speculate as to the biochemical pathways leading to the observed response, which may differ between these two ranges, although there are clearly two efficacious ranges that warrant further investigation. With regard to collagen synthesis, 0.02 and 100  $\mu\text{g}/\text{mL}$  were again the best concentrations for ankle cells, while 100 and 700  $\mu\text{g}/\text{mL}$  were superior for TMJ cells. It was interesting to note that, with ankle cells, 100  $\mu\text{g}/\text{mL}$  glucosamine outperformed all growth factor groups for GAG synthesis except for 100 ng/mL IGF-I, and also surpassed 10 ng/mL IGF-I and bFGF and both concentrations of TGF- $\beta$  ( $p < 0.05$ ) for collagen synthesis. The TGF- $\beta$  concentrations were relatively high, and perhaps lower concentrations (e.g., 0.1 – 1 ng/mL) may prove more efficacious in the future. It must be noted that the total GAG content might include both endogenous GAG biosynthesis (with glucosamine acting as a bioactive signal) and exogenous glucosamine incorporation

(where glucosamine acts as a building block). Exogenous glucosamine, whether bound to cells or incorporated into the synthesized matrix, should be included in measuring the GAG content of an engineered construct because it is indeed part of the construct. Based on the results of both our and previous studies, we speculate that glucosamine may act primarily as a signal rather than as a building block alone. First, the GAG content did not increase with increasing concentrations of glucosamine to achieve a plateau effect, but rather acted in a concentration-dependent manner.<sup>262, 263, 267</sup> Second, a notable increase in collagen synthesis was also observed,<sup>6, 7</sup> as was especially evident in this study with 100  $\mu\text{g}/\text{mL}$  of glucosamine with ankle cells, a phenomenon independent of exogenous incorporation. Furthermore, Varghese *et al.*<sup>262</sup> proposed that the up-regulation of TGF- $\beta$ 1 gene expression triggered by the exogenous glucosamine might be related to the increase of cartilage specific matrix production through the hexosamine pathway.<sup>268</sup> To further isolate the effects of glucosamine, a TGF- $\beta$ 1 blocking agent may be advantageous in future studies.

In conclusion, TMJ condylar cartilage cells were more proliferative than ankle cartilage cells, whereas ankle cartilage cells prevailed over condylar cartilage cells in extracellular matrix production. 10 ng/mL and 100 ng/mL IGF-I were the best concentrations for TMJ condylar cartilage cells and ankle cartilage cells, respectively, due to an outstanding performance in promoting cell proliferation and GAG and collagen production. In addition, glucosamine demonstrated an ability to significantly promote biosynthesis and outperform growth factors in certain instances. In the future, experiments will include exploring synergistic effects of growth factors and

glucosamine sulfate and making comparisons in 3D culture to evaluate the differences between the 2D and 3D environments, for example to determine whether catabolic activity is observed with glucosamine in 3D.<sup>262</sup> Moreover, it will be crucial to further investigate the mechanisms underlying the bimodal phenomenon observed with glucosamine signaling in 2D, and perhaps more importantly, to investigate whether this effect is also observed in 3D. Finally, it will be meaningful to investigate the cell behavior of subpopulations of TMJ condylar cartilage cells from the different zones.

## **CHAPTER 5: Hyaline cartilage cells outperform mandibular condylar cartilage cells in a TMJ fibrocartilage tissue engineering application\***

### **ABSTRACT**

**Objective:** To compare temporomandibular joint (TMJ) condylar cartilage cells *in vitro* to hyaline cartilage cells cultured in a three-dimensional environment for tissue engineering of mandibular condylar cartilage.

**Design:** Mandibular condylar cartilage and hyaline cartilage cells were harvested from pigs and cultured for 6 weeks in polyglycolic acid (PGA) scaffolds. Both types of cells were treated with glucosamine sulfate (0.4 mM), insulin-like growth factor (IGF-I) (100 ng/ml) and their combination. At weeks 0 and 6, cell number, glycosaminoglycan (GAG) and collagen content were determined, types I and II collagen were visualized by immunohistochemistry and GAGs were visualized by histology.

**Results:** Hyaline cartilage cells produced from half an order to a full order of magnitude more GAGs and collagen than mandibular condylar cartilage cells in 3D culture. IGF-I was a highly effective signal for biosynthesis with hyaline cartilage cells, while glucosamine sulfate decreased cell proliferation and biosynthesis with both types of cells. *In vitro* culture of TMJ condylar cartilage cells produced a fibrous tissue with predominantly type I collagen, while hyaline cartilage cells formed a fibrocartilage-like tissue with types I and II collagen. The combination of IGF and

---

\*Chapter published as Wang, Lazebnik, and Detamore. "Hyaline cartilage cells outperform mandibular condylar cartilage cells in a TMJ fibrocartilage tissue engineering application," *Osteoarthritis Cartilage*, In Press, 2008

glucosamine had a synergistic effect on maintaining the phenotype of TMJ condylar cells to generate both types I and II collagen.

**Conclusion:** Given the superior biosynthetic activity by hyaline cartilage cells and the practical surgical limitations of harvesting cells from the TMJ of a patient requiring TMJ reconstruction, cartilage cells from elsewhere in the body may be a potentially better alternative to cells harvested from the TMJ for TMJ tissue engineering. This finding may also apply to other fibrocartilages such as the intervertebral disc and knee meniscus in applications where a mature cartilage cell source is desired.

## INTRODUCTION

Temporomandibular joint (TMJ) disorders resulting from arthritis, ankylosis, traumas, internal derangement and/or other afflictions can ravage TMJ structures that have limited capacity for regeneration. Tissue engineering may provide an ideal solution, especially when severe degeneration occurs.<sup>173, 269</sup> Although our long-term goal is to regenerate the whole mandibular condyle of the TMJ, the specific focus of the current study was the condylar cartilage, where cell sources and signals were investigated. The purpose of this study was to compare the behavior of mandibular condylar cartilage cells and ankle (hyaline) cartilage cells under the regulation of insulin-like growth factor-I (IGF-I) and glucosamine sulfate.

The composition and structure of mandibular condylar cartilage (henceforth referred to as TMJ condylar cartilage) differ from hyaline cartilage. Hyaline cartilage

cells are chondrocytes, and hyaline cartilage can be divided into four zones: superficial, middle, deep and calcified. In contrast, TMJ condylar cartilage has both fibrocartilaginous and hyaline-like character, with a thin proliferative zone that separates the fibrocartilaginous fibrous zone at the surface from the hyaline-like mature and hypertrophic zones below. Unlike hyaline cartilage, TMJ condylar cartilage contains predominantly fibroblasts and collagen I in the superficial fibrous zone.<sup>16, 22, 35</sup> Undifferentiated mesenchymal cells are distributed in the proliferative zone, serving as a cell reservoir to provide cells for the fibrous zone and underlying zones.<sup>15, 29-32</sup> The underlying mature and hypertrophic zones include differentiated chondrocytes and the collagen is both types I and II.<sup>16, 22, 35, 36</sup> From the standpoint of embryonic origin, TMJ condylar cartilage is categorized as a secondary cartilage formed by periosteum or endosteum, while hyaline cartilage is a primary cartilage, which precedes bone formation. TMJ condylar cartilage falls under the classification of fibrocartilage, with a strong presence of both collagen types I and II.<sup>35, 36</sup> However, hyaline cartilage contains predominately collagen type II in all zones.<sup>270</sup> These contrasting structures make it imperative to investigate and compare the responses of TMJ condylar cartilage cells and hyaline cartilage cells to biological signals and biodegradable scaffolds.

Previous tissue engineering studies of TMJ condylar cartilages utilized cells from the condyle itself,<sup>66</sup> hyaline cartilage cells,<sup>91</sup> fibroblasts<sup>10, 172</sup> and stem cells<sup>5, 57, 66-68, 167, 168, 170, 171</sup> as cell sources. An early attempt conducted by Weng *et al.*<sup>91</sup> seeded bovine hyaline chondrocytes from the forelimbs onto the surface of a polyglycolic

acid/polylactic acid (PGA/PLA) scaffold as a cartilage layer. Hollister and colleagues<sup>10, 172</sup> also seeded bone morphogenetic protein (BMP)-transduced fibroblasts into scaffolds. In both studies, cartilage formation was observed after implantation by Safranin-O staining. Furthermore, bone marrow and umbilical cord matrix mesenchymal stromal cells<sup>5, 57, 66-68, 167, 168, 170, 171</sup> were introduced to TMJ tissue engineering, demonstrating the feasibility of creating a tissue engineered mandibular condyle in the form of two stratified layers. In these studies, the positive immunohistochemical (IHC) staining for types I and II revealed the existence of a fibrocartilage. Although most previous studies used stem cells for TMJ tissue engineering,<sup>5, 57, 66-68, 167, 168, 170, 171</sup> an advantage that mature cells possess over various types of stem cells is the absence of the variable of differentiation and reduced possibility of metaplasia. This study thus aimed to compare TMJ condylar cartilage cells to hyaline cartilage cells for tissue engineering applications.

Although the cell behavior of TMJ condylar cartilage and hyaline cartilage has been extensively investigated, there are only three studies comparing the respective cell types, performed in newborn rat explant culture by a single group.<sup>35, 121, 124</sup> These studies revealed that basic fibroblast growth factor (bFGF), IGF-I and transforming growth factor beta (TGF- $\beta$ ) stimulated higher cell proliferation in the TMJ condylar explants than in the femoral head explants. IGF-I increased glycosaminoglycan (GAG) formation, while bFGF and TGF- $\beta$  decreased GAG production in both types of cartilage. It must be noted that these studies used newborn rat condyles, which grew faster than mature condyles,<sup>20</sup> whereas in the current study,

cells were isolated from mature porcine mandibular condylar and ankle cartilage. In a two-dimensional environment (2D) using mature cells,<sup>271</sup> IGF-I promoted cell proliferation and biosynthesis for both types of cells. Therefore, based on both explant and monolayer cell culture, IGF-I was chosen in our three-dimensional (3D) study to regulate cell growth and biosynthesis.

Glucosamine has been scarcely tested in tissue engineering applications, with a handful of recent studies. One recent investigation revealed that glucosamine hydrochloride up-regulated matrix production at concentrations between 0 and 2 mM<sup>262</sup>. Glucosamine sulfate has been shown *in vitro* to promote aggrecan production,<sup>260, 261</sup> and to inhibit matrix degrading protein production in chondrocytes.<sup>260</sup> In our 2D monolayer culture,<sup>271</sup> glucosamine sulfate also demonstrated an ability to significantly promote GAG and collagen production and to outperform growth factors in certain instances (between 0 and 0.4 mM) for both TMJ condylar cartilage cells and ankle cartilage. Consequently, besides IGF-I at 100 ng/ml, glucosamine at 0.4 mM was adopted and the synergistic effects of IGF-I and glucosamine were also investigated in the current study.

Non-woven polyglycolic acid (PGA) scaffolds have been broadly exploited in both hyaline<sup>165, 272, 273</sup> and fibrocartilage cartilage<sup>141, 259, 274</sup> tissue engineering, due to its good biocompatibility and biodegradability. Our previous study<sup>66</sup> also demonstrated that non-woven PGA meshes did support proliferation and biosynthesis of TMJ condylar cartilage cells as evidenced by a significant increase in cell number and the presence of types I and II collagen and GAGs throughout the constructs.

Therefore, in this study, non-woven PGA scaffolds were seeded with porcine cartilage cells from mature TMJ condylar cartilage and hyaline cartilage from ankles. Exogenous signals including glucosamine sulfate (0.4 mM) and IGF-I (100 ng/ml) and their combination were employed to regulate cell proliferation and extracellular matrix production. The comparison between these two types of cells provide critical steps in demonstrating that hyaline cartilage cells may be a promising mature cell source for TMJ condylar cartilage tissue engineering.

## **MATERIALS AND METHODS**

### ***Cell harvesting***

Hog heads and ankles (Chester white breed, female, age 8 months) were acquired from Winchester Meat Processing (Winchester, KS, USA). The TMJ was first removed *en bloc* with capsule intact and placed into 100% ethanol for 20 min. The TMJ was scrubbed using a sterile iodine pad, then the joint capsule was broken and the disc was removed in a sterile manner with a scalpel in a tissue culture hood. TMJ condylar cartilage was removed by chopping cartilage from the surface of the TMJ condyle, washed with sterile phosphate buffered saline (PBS), minced, and digested for 24 hrs in 2 mg/ml type II collagenase (394U/mg; Worthington Biochemical; Lakewood, NJ, USA). The cell solution was centrifuged and cells were resuspended in a cell culture medium, consisting of Dulbecco's Modified Eagle medium (Invitrogen; Carlsbad, CA, USA), 10% fetal bovine serum (FBS; Gemini; West Sacramento, CA, USA), 25 µg/ml ascorbic acid (Sigma; St. Louis, MO, USA),

1% non-essential amino acids (Invitrogen) and 1% penicillin-streptomycin-fungizone (Invitrogen). Cells were fed every other day until confluent. The confluent cell population was trypsinized and labeled as passage 1. The procedure to obtain cartilage cells from ankles was similar to harvesting TMJ condylar cartilage cells, although more straightforward. Briefly, skin was removed, the joint was sterilized using an iodine pad, the joint capsule was broken, and cartilage was obtained and minced. After digestion, the cells were resuspended, cultured in the flasks, and labeled as passage 1.

#### ***Cell seeding and growth factor incorporation***

A non-woven PGA mesh (50 mg/cc; Synthecon; Houston, TX, USA) was punched into disc-shape scaffolds with a 5 mm diameter and 2 mm thickness, and then sterilized with ethylene oxide. After sterilization, the scaffolds were aired in sterilization pouches under a fume hood for one day, then wetted with sterile filtered ethanol for 5 min and two washes of sterile PBS. The scaffolds were then soaked in the cell culture medium for 1 day and then removed for cell seeding. P1 cells were seeded on the PGA scaffolds at 50 million cells per ml of scaffold. Highly concentrated cell solution (500  $\mu$ l) was dispensed slowly onto scaffolds in 24-well plates, which were set on an orbital shaker at 150 rpm for 12 hrs. After 12 hrs, 500  $\mu$ l of fresh medium was added. After 24 hrs, an additional 1 ml of medium was added and cells were allowed to attach statically in the medium for another day. After allowing 2 days for seeding and attachment (recorded as day 1), the medium was

replaced by 2 ml of either fresh medium or the medium supplemented with either growth factor or glucosamine. There were a total of eight groups in this study, including the TMJ condylar and hyaline cartilage cells treated by IGF (100 ng/ml; Pepro Tech; Rocky Hill, NJ, USA), D-glucosamine 6-sulfate (0.4 mM, corresponding to 100 mg/ml; Sigma) and their combination (100 ng/ml IGF and 0.4 mM glucosamine) and their respective controls (cultured in fresh medium without IGF and glucosamine treatment). Scaffolds were cultured in 2 ml of medium for 6 weeks and half of the medium was changed every other day.

#### ***Biochemical analysis and immunohistochemical staining***

Scaffolds were examined at weeks 0 and 6 for cell number, GAG and hydroxyproline content. Cell number was measured using a Picogreen assay (Molecular Probes; Eugene, OR, USA) with a conversion factor of 7.7 pg DNA/cell.<sup>258</sup> The GAG content was quantified by a dimethylmethylene blue (DMMB) dye assay (Biocolor; Newtownabbey, Northern Ireland).<sup>258</sup> The hydroxyproline content was examined by a hydroxyproline assay (Accurate; Westbury, NY, USA).<sup>258</sup> A conversion factor of 11.5 was determined in a preliminary study for converting hydroxyproline mass to collagen mass. Histological analysis was performed using a Safranin-O/fast green stain. Immunohistochemical (IHC) staining of types I and II collagen was performed in a Biogenex i6000 autostainer (San Ramon, CA, USA).<sup>66</sup> The mouse monoclonal IgG anti-collagen I (1:1500 dilution) (Accurate Chemical, Westbury, NY, USA), mouse monoclonal IgG anti-collagen II

(1:1000 dilution) (Chondrex, Redmond, WA, USA) and mouse monoclonal IgG anti-aggrecan (1:50 dilution) (Abcam, Cambridge, MA, USA) antibodies were chosen as primary antibodies. The streptavidin-linked horse anti-mouse IgG secondary antibody, ABC detection kit, and DAB (brown) and VIP (purple) substrate kits were obtained from Vector Laboratories (Burlingame, CA, USA). Double IHC staining of types I and II collagen was performed for sagittal sections of native ankle and TMJ tissues. Type I collagen staining was first conducted by following the above procedure with VIP as the substrate, avidin and biotin (Vector Laboratories) were then added in a blocking step to prevent the interaction between the first and second sets of labeling reagents, and type II collagen staining was finally performed with DAB as the substrate. Negative controls were prepared by omitting the primary antibodies, and the absence of non-specific staining was confirmed.

### ***Statistical analysis***

All data were expressed as means  $\pm$  one standard deviation and analyzed by an analysis of variance (ANOVA) followed by a Fisher's Protected Least Significance Difference post hoc test. Three-way ANOVAs with interaction were used to determine whether there were differences among time-points, different treatments, or cell types. A statistical threshold of  $p < 0.05$  was used to indicate whether there were statistically significant differences among groups.

## **RESULTS**

### Cell number

Over 6 weeks of culture, the ankle groups had significantly more cells than the TMJ groups ( $p < 10^{-12}$ ) (Fig. 5.1). At week 0, there were 1.44 times more cells attached to scaffolds in ankle groups than in TMJ groups ( $p < 0.05$ ), although two types of cells were seeded onto scaffolds at the same density (1.96 million cells per

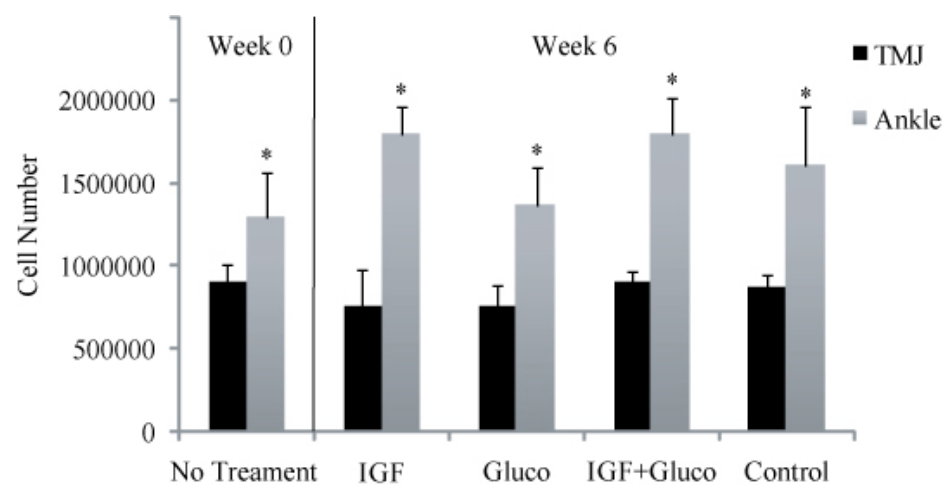


**Figure 5.1:** Cell number per construct at weeks 0 and 6 ( $n = 4$ ). Gluco denotes glucosamine. Symbol \* means statistically significant difference between ankle groups and TMJ groups. Error bars represent standard deviations.

construct). At week 6, the average cell number of ankle groups was 1.63 million cells per construct, while the cell count of TMJ groups was 0.82 million cells per construct ( $p < 10^{-12}$ ). With regard to IGF and glucosamine, ankle cells were more sensitive than TMJ cells. In all ankle groups, except for the glucosamine group, cell numbers increased from week 0 to week 6 ( $p < 10^{-4}$ ), while cell numbers in TMJ groups did not exhibit any statistically significant differences from week 0 to week 6. In

comparison to their respective controls, significant differences in cell numbers were not observed for either cell type. However, IGF and the combination of IGF and glucosamine in ankle groups promoted cell number compared to the glucosamine group ( $p < 0.001$ ). In fact, the glucosamine groups had 15% and 13% decreases in cell number compared to the control for both the ankle and TMJ groups (not statistically significant), respectively.

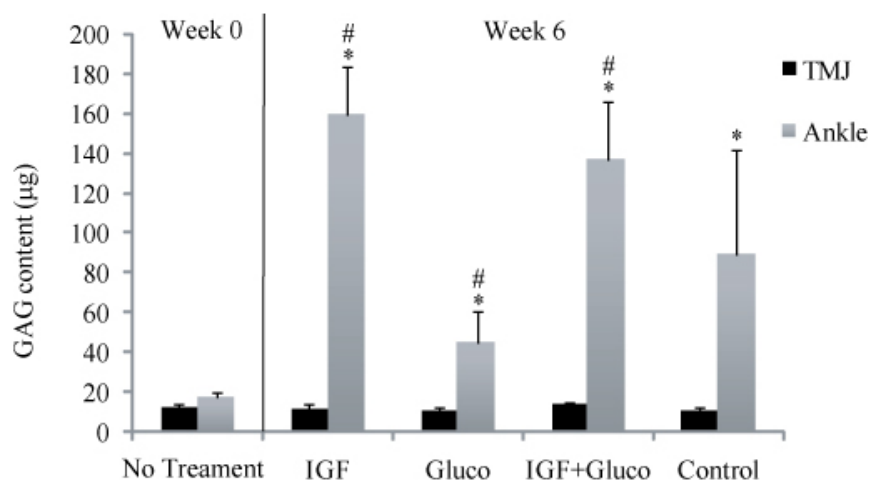


**Figure 5.2:** GAG content per construct at weeks 0 and 6 ( $n = 4$ ). Gluco denotes glucosamine. Symbol \* means statistically significant difference between ankle groups and TMJ groups. Symbol # means statistically significant difference compared to the respective control group. Error bars represent standard deviations.

### *GAG content*

There was no significant difference in GAG content at week 0 between ankle and TMJ cells (Fig. 5.2). The average GAG production per construct of 107.4  $\mu\text{g}$  in ankle groups was an order of magnitude higher than the average content of 11.3  $\mu\text{g}$  per construct in TMJ groups after 6 weeks of culture ( $p < 10^{-11}$ ). Ankle groups at week 6, with the exception of the glucosamine group, had drastically increased GAG production over time, as the IGF, combination and the control groups had 8.3 ( $p < 10^{-9}$ ), 7.0 ( $p < 10^{-8}$ ), and 4.1 ( $p < 10^{-4}$ ) times higher GAG contents than at week 0, respectively, while there was no significant difference among TMJ groups. Both IGF and the combination promoted GAG production, with 1.79 and 1.49 times more GAGs in ankle groups than in the control ( $p < 10^{-4}$  and 0.05, respectively), whereas glucosamine lessened the GAG production by 49% ( $p < 0.01$ ).

### ***Hydroxyproline content***

As with cell number and GAG content, hydroxyproline content in ankle groups was significantly higher than in TMJ groups ( $p < 10^{-11}$ ) (Fig. 5.3). Despite the fact that the ankle group had 5.8 times more hydroxyproline than the TMJ group at week 0, there was no statistically significant difference between them. In comparison to week 0, hydroxyproline content in ankle groups at week 6 increased over time by 8.9, 5.2, 8.0, and 6.0 times with the IGF group ( $p < 10^{-9}$ ), the glucosamine group ( $p < 10^{-4}$ ), their combination ( $p < 10^{-8}$ ) and the control ( $p < 10^{-5}$ ) respectively, while no significant differences were detected among TMJ groups. IGF and the combination in

ankle groups had 26.0 and 24.0  $\mu\text{g}$  of hydroxyproline per construct, which were 48% ( $p < 0.005$ ) and 35% ( $p < 0.05$ ) increases compared to the control, respectively.

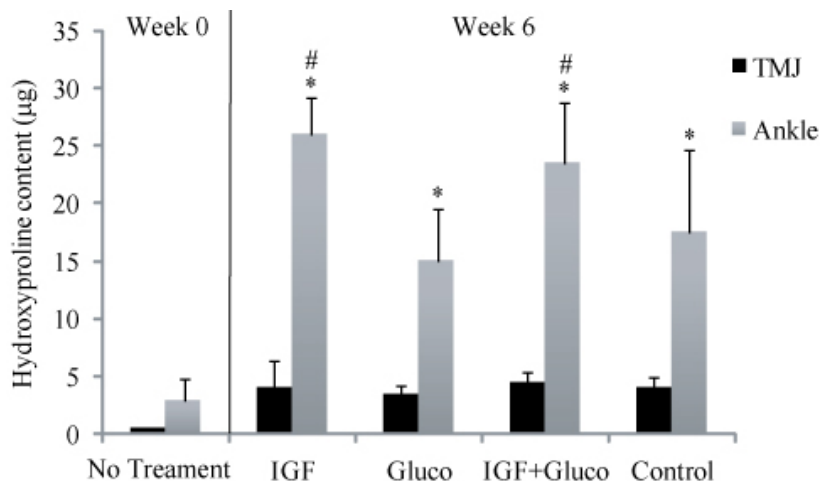


**Figure 5.3:** Hydroxyproline content per construct at weeks 0 and 6 ( $n = 4$ ) (multiply by a factor of 11.5 for collagen content). Gluco denotes glucosamine. Symbol \* means statistically significant difference between ankle groups and TMJ groups. Symbol # means statistically significant difference compared to the respective control group. Error bars represent standard deviations.

### *IHC analyses*

At week 6, immunohistochemical analysis revealed a moderate staining of type I collagen and an intense staining of type II collagen in ankle groups (Fig. 5.4), with especially intense regions of collagen II staining in the IGF-glucosamine combination group. In the native ankle cartilage, type II collagen was dominant (Fig. 5.5). The constructs in TMJ groups demonstrated a significant presence of type I collagen and a minute amount of type II collagen (Fig. 5.4). It must be noted that the group combining IGF and glucosamine in the TMJ group demonstrated much more

intense staining of type II collagen than all other TMJ groups. In native TMJ condylar cartilage, type I collagen was dominant in the superficial zone, abundant type I and moderate II collagen were observed in the proliferative zone, and type II collagen was dominant in the mature and hypertrophic zone (Fig. 5.5). In general, ankle cells had a weaker staining of type I collagen than TMJ cells and a stronger staining of type II collagen. IHC also revealed a more abundant presence of aggrecan in the IGF and the combination groups with ankle cells, compared to other ankle groups and all TMJ groups (Fig. 5.6), which was further confirmed by the GAG content from DMMB assays.

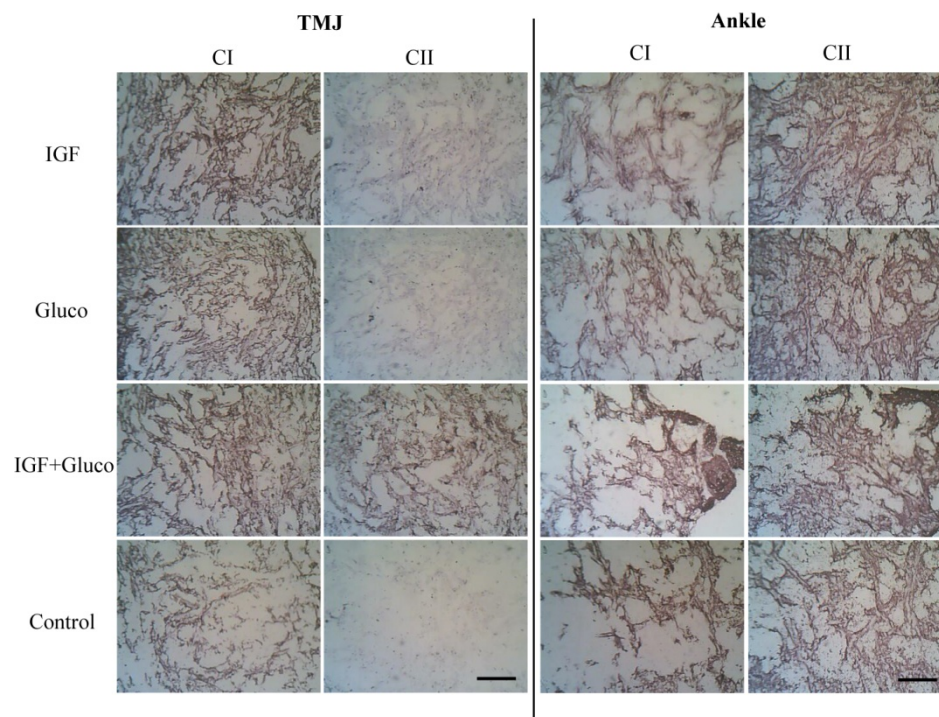


**Figure 5.4:** Immunohistochemical test for types I and II collagen at week 6 (n =2). Positive staining is purple in color. The scale bar is 100 μm. CI = type I collagen, CII = type II collagen.

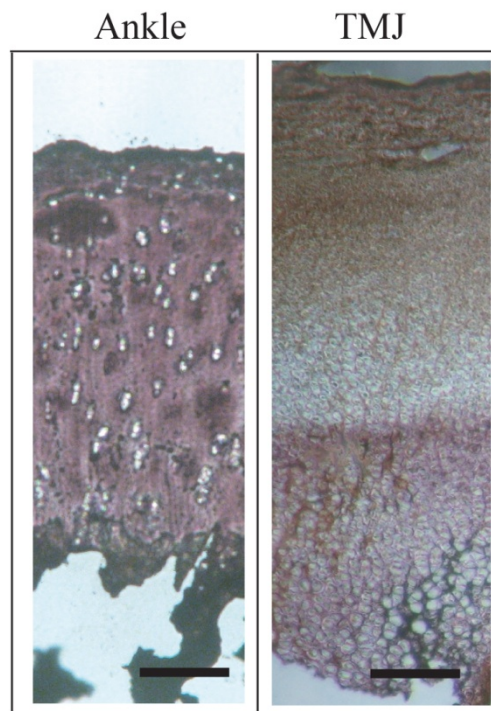


**Figure 5.5:** Double immunohistochemical staining for types I and II collagen in sagittal sections from native tissues. Positive staining of type I collagen is brown in color. Positive staining of type II collagen is purple in color. Note that the hyaline cartilage is stained almost exclusively for type II collagen, whereas in sharp contrast the mandibular condylar cartilage consists of distinct zones dominated either by collagen I (superficial zone) or collagen II (mature and hypertrophic zones) staining. The scale bar is 100  $\mu\text{m}$ .

## DISCUSSION

In this study, mature porcine cartilages were used since the pig has been identified as a suitable model for TMJ tissue engineering strategies,<sup>46, 173, 275-277</sup> although the different species and ages<sup>278</sup> might lead to different results. The two types of cartilage cells were shown to differ *in vitro* in cell proliferation, GAG and

collagen production, and collagen type. In addition, the results revealed that the compositions of tissue engineered cartilages were different from their respective native tissues. Loading conditions may contribute to the different behaviors of the respective cell types, although it should be made clear that the TMJ is a load-bearing joint.<sup>275, 279</sup> To the best of our knowledge, this was the first effort to compare cartilage cell sources for TMJ tissue engineering, as a first step in demonstrating that it may not be necessary to use cells from the same tissue when selecting a mature cell source for fibrocartilage regeneration. Moreover, this is the first example of collagen I and II double immunostaining of condylar cartilage, to the best of our knowledge.

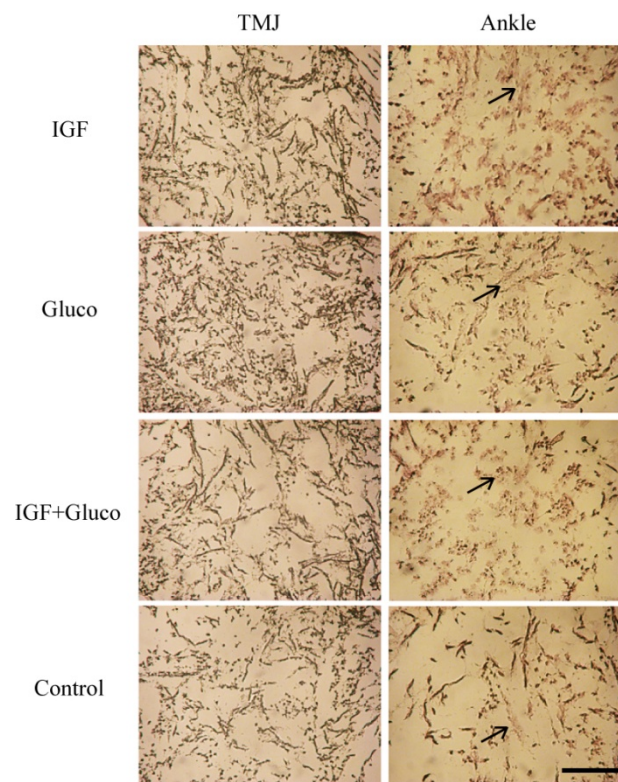


**Figure 5.6:** Immunohistochemical staining for aggrecan at week 6 (n =2). Arrows indicate examples of positive staining of aggrecan (light purple color). The black color indicates PGA debris. The scale bar is 400  $\mu$ m.

Compared to hyaline cartilage cells, TMJ condylar cells were less proliferative in a 3D environment. The significant difference at week 0 in cell number between TMJ condylar cells and hyaline cartilage cells revealed that TMJ condylar cells had an inferior ability to attach onto PGA scaffolds compared to hyaline cartilage cells. This inferior attachment ability would likely explain the lower cellularity of TMJ groups at 6 weeks, given the superior proliferation rate of TMJ condylar cartilage cells in monolayer culture.<sup>280</sup> The exploration of new biomaterials may enhance the adhering ability of TMJ cells, such as Arg-Gly-Asp (RGD)-modified poly(lactic-co-glycolic acid) (PLGA)<sup>281</sup> and poly-L-lactic acid (PLLA).<sup>282</sup> During the 6 weeks of culture, TMJ condylar cells maintained a relatively constant cell number, indicating that TMJ condylar cartilage cells exhibited a behavior more similar to fibrocartilage cells such as TMJ disc cells and knee meniscus cells, although they were more proliferative in monolayer culture than ankle hyaline cartilage.<sup>280</sup> In fact, Almarza and Athanasiou<sup>274</sup> reported that *in vitro* culture of fibrocartilage cells (TMJ disc cells) even demonstrated a decrease in cell number over a 4-week period. Mesenchymal stem cells (human umbilical cord mesenchymal stromal cells) in a chondrogenic medium also had a decreased or stable cell number in PGA scaffolds over 4 weeks of culture in a fibrocartilage tissue engineering application.<sup>207</sup> The relatively invariable cellularity with TMJ condylar cells implied that a higher seeding density might be necessary.

TMJ condylar cells were inferior in extracellular matrix synthesis to hyaline cartilage cells. The ratios of GAG to collagen content in the TMJ groups were 0.25 on

average, which is higher than the ratios in native tissues, while this ratio in the ankle groups was 0.47, which is comparable to native tissues.<sup>283-285</sup> The dominance of type I relative to type II collagen in TMJ groups (except for the combination of IGF and glucosamine) might be unexpected since there is abundant type II collagen present in the mature and hypertrophic zones of native TMJ condylar cartilage, though type I collagen produced by fibroblasts in the fibrous zone likely contributed to collagen production. A strong IHC staining of type II collagen and a moderate staining of type I collagen were observed in hyaline cartilage groups, indicating the formation of a fibrocartilage-like tissue, which is the goal with TMJ condylar cartilage regeneration. The abundant type I collagen in TMJ groups and moderate type I collagen presence in ankle groups together suggest the inevitable shift of TMJ and ankle cell phenotypes during *in vitro* culture, due to the differences between the *in vitro* and *in vivo* microenvironments, such as mechanical conditions, bioactive signals, and the exchange of nutrients and wastes. The dedifferentiated hyaline chondrocytes may be redifferentiated in an agarose gel,<sup>86</sup> alginate beads,<sup>286</sup> by use of high density culture,<sup>287</sup> by substituting serum with the combination of TGF- $\beta$ 2 and IGF-I,<sup>288</sup> or by coating a surface with chondrogenic molecules such as aggrecan.<sup>84, 85</sup> However, it is still questionable whether redifferentiated chondrocytes have the ability to generate a properly assembled matrix.<sup>289</sup>

TMJ condylar cells were less responsive to the stimulation of exogenous signals than hyaline cartilage cells, in that the IGF and IGF/glucosamine combination both significantly upregulated collagen and GAG biosynthesis with hyaline cartilage

cells, whereas no signals produced statistically significant differences for the TMJ cells compared to the control. It was unanticipated that glucosamine at 0.4 mM exhibited a noticeable inhibition of biosynthesis with ankle cartilage cells, although this concentration was the best for the up-regulation of GAG and collagen in our preliminary monolayer studies,<sup>271</sup> indicating that further optimization of glucosamine concentrations in a 3D environment is required. However, Mroz and Silbert<sup>290, 291</sup> also revealed that glucosamine chloride did not stimulate the formation of chondroitin sulfate with rat chondrocytes and even inhibited it at specific concentrations. Glucosamine is an important building block of proteoglycans in cartilage. However, a previous study<sup>290</sup> revealed that exogenous glucosamine did not participate in the pathway to produce GAGs, but rather played a role as a signal to regulate GAG and collagen production. Indeed, in the current study, the combination of IGF and glucosamine demonstrated a critical ability to retain type II collagen synthesis with TMJ condylar cells during *in vitro* culture, although the inherent mechanism needs to be further investigated in the future.

Ideally, tissue-engineered TMJ condylar cartilage should mimic the native zonal structure to achieve a functional condylar replacement. One strategy to accomplish this could be to separately harvest cells from the different zones of the condylar cartilage. However, the separation of different cell populations from their respective layers is limited by the accurate dissection of different layers of TMJ condylar cartilage due to the irregular zonal distribution. Countercurrent centrifugation, a technique extensively used with hematopoietic progenitor cells, was

utilized in a previous study to elutriate five different fractions of cells from TMJ condylar cells based on the different sizes of cells.<sup>292</sup> Characterization of these cells suggested that fibroblast-like cells, mesenchymal stem cells and hypertrophic cells might be identified from these five populations according to cell volume, alkaline phosphatase content, proteoglycan production, and collagen types. Seeding these cells into a stratified scaffold would be interesting but challenging work in the future.

*In vitro* culture of both types of cartilage cells appeared to exhibit a phenotypic shift during the 6 weeks of culture in PGA scaffolds. *In vitro* tissue engineering of TMJ condylar cartilage using mature cells produced a fibrous tissue with dominant type I collagen. The combination of IGF and glucosamine demonstrated the ability to maintain the expression of both types I and II collagen with TMJ condylar cartilage cells. *In vitro* culture of hyaline cartilage cells resulted in the fibrocartilage-like tissue genesis with both types I and II collagen. Most importantly, cell number and extracellular matrix content in the hyaline cartilage cell groups were significantly higher than in the TMJ condylar cartilage cell groups. Furthermore, from a clinical perspective, it is more reasonable to obtain cells from hyaline cartilage (or perhaps costal cartilage) than from degenerated TMJ condylar cartilage, in which the healthy cells are very limited, or from a healthy contralateral TMJ, which may lead to bilateral dysfunction. Therefore, given the importance of the superior biosynthetic activity by hyaline cartilage cells, and the clinical difficulty in obtaining donor cartilage, hyaline cartilage cells may be a more promising mature cell source than the TMJ itself for TMJ condylar cartilage tissue engineering, a principle

which may also apply to other fibrocartilages such as the intervertebral disc and knee meniscus. In the future, experiments will include optimizing glucosamine concentrations in 3D culture, designing zonal scaffolds for seeding different populations of cells, and evaluating mechanical properties of tissue-engineered constructs for long-term culture (> 6 weeks).

## **CHAPTER 6: A Comparison of Human Umbilical Cord Matrix Stem Cells and TMJ Condylar Chondrocytes for Tissue Engineering TMJ Condylar Cartilage\***

### **ABSTRACT**

The temporomandibular joint (TMJ) presents many problems in modern musculoskeletal medicine. Patients who suffer from TMJ disorders often experience a major loss in quality of life due to the debilitating effects that TMJ disorders can have on everyday activities. Cartilage tissue engineering can lead to replacement tissues that could be used to treat TMJ disorders. In this study, a spinner flask was used for a period of 6 days to seed polyglycolic acid (PGA) scaffolds with either TMJ condylar chondrocytes or mesenchymal-like stem cells derived from human umbilical cord matrix (HUCM). Samples were then statically cultured for 4 weeks either in growth medium containing chondrogenic factors or in control medium. Immunohistochemical staining of HUCM constructs after 4 weeks revealed a strong presence of collagen I and minute amounts of collagen II, whereas TMJ constructs revealed little collagen I and no collagen II. The HUCM constructs were shown to contain more GAGs than the TMJ constructs quantitatively at week 0 and histologically at week 4. Moreover, the cellularity of HUCM constructs was 55% higher at week 0 and nearly twice as high after 4 weeks, despite being seeded at the same density. The increased level of biosynthesis and higher cellularity of HUCM constructs clearly demonstrates that the HUCM stem cells outperformed the TMJ condylar cartilage cells under the prescribed conditions. HUCM stem cells may

---

\*Chapter published as Bailey, Wang, Bode, Mitchell, and Detamore. "A comparison of human umbilical cord matrix stem cells and temporomandibular joint condylar chondrocytes for tissue engineering temporomandibular joint condylar cartilage," *Tissue Eng* 13, 2003, 2007. (Special Issue on Emerging Technologies and New Basic Science Directions in Tissue Engineering.)

therefore be an attractive alternative to condylar cartilage cells for TMJ tissue engineering applications. Furthermore, given the availability and ease of obtaining HUCM stem cells, these findings may have far-reaching implications, leading to novel developments in both craniofacial and orthopaedic tissue replacement therapies.

## INTRODUCTION

The complexity of the temporomandibular joint (TMJ), or jaw joint, makes it difficult to treat its disorders such as arthritis, internal derangement, and ankylosis. TMJ disorders can restrict the range of mouth opening, and can make routine activities such as eating, talking, and yawning severely painful. Fortunately, tissue engineering may be able to address these problems. Our current efforts focus on the articular cartilage of the mandibular condyle. Native mandibular condylar cartilage is composed of four distinct layers, namely the fibrous zone with fibroblast-like cells, proliferative zone with mesenchymal cells, mature zone with differentiated chondrocytes, and hypertrophic zone with differentiated chondrocytes. Collagen type I is distributed throughout all of the zones,<sup>35</sup> and collagen type II is abundant in the mature and hypertrophic zones.<sup>36</sup> The major proteoglycan in the mandibular condyle is negatively charged aggrecan, in which GAG chains consist predominately of chondroitin sulfate and keratan sulfate.<sup>37</sup> Ideally, tissue engineering aims to create the mandibular condylar cartilage with the same biochemical composition as the native cartilage. Much of the work in TMJ tissue engineering to date has focused on the TMJ disc, and has demonstrated the usefulness of poly(glycolic acid) (PGA) as a

scaffolding material.<sup>293, 294</sup> Only a handful of condylar tissue engineering studies have been done, all published in this decade.<sup>5, 10, 11, 68, 91, 92, 166-172</sup> These studies have utilized a variety of different cell sources, scaffold materials and chemical signals. Thus, tissue engineering for the TMJ condyle is a field in its infancy, and in the current study we investigate the crucial factor of cell source.

Mature chondrocytes are a common choice for cartilage regeneration. However, autologous chondrocytes are faced with several potential limitations. First, in large-scale tissue-engineered constructs, a high initial cell density is necessary to obtain sufficient cartilage for clinical applications. The availability of sufficient cell numbers from autologous chondrocytes is limited due to their limited ability to expand in culture.<sup>57</sup> Second, articular chondrocytes tend to lose their phenotype after passaging in monolayer culture.<sup>295</sup> Adult mesenchymal stem cells (MSCs) derived from bone marrow have the capability to differentiate into multiple cell lineages *in vitro* including bone, cartilage, tendon, and other connective tissues.<sup>58-60</sup> Exposed to specific growth factors, MSCs can differentiate into osteoblasts, chondrocytes, and periodontal ligament cells that could be used for replacement or regeneration of oral tissue in dental and craniofacial tissue engineering.<sup>57, 296</sup>

Recent developments in the field of tissue engineering have shown that porcine TMJ disc cells seeded on bioresorbable polymer scaffolds showed promising proliferative and biosynthetic activity, which could ultimately lead to a viable material for TMJ disc replacement.<sup>259</sup> Studies have shown that polyglycolic acid (PGA), as well as poly(lactic-co-glycolic acid) (PLGA)<sup>294, 297</sup> can be used as a

suitable three dimensional scaffold for cell seeding. It has also been demonstrated by Almarza and Athanasiou<sup>294</sup> that a spinner flask bioreactor can provide the necessary dynamic culture environment to seed PGA scaffolds with TMJ disc cells.

In order to overcome the various limitations related to currently available cell sources, we propose the use of a promising new cell source for musculoskeletal tissue engineering. It has been shown that cells isolated from Wharton's jelly, or the human umbilical cord matrix (HUCM), are multipotent stem cells that express mesenchymal stem cell (MSC) markers<sup>76, 298</sup> Studies have analyzed the differentiation capacity of umbilical cord matrix cells and have shown that these cells are capable of differentiating into cells with osteogenic phenotypes.<sup>64, 76</sup>

There are several options for cell sources, including mature cartilage and bone cells (or even skin or fat cells),<sup>299</sup> mesenchymal stem cells (MSCs) from bone marrow, and embryonic stem cells. HUCM stem cells, which are multipotential stem cells with properties between embryonic stem cells and adult stem cells,<sup>75-78</sup> offer several advantages for cell-based therapies. Umbilical cord stem cells are believed to be a type of mesenchymal stem cell because in addition to expressing a significant number of mesenchymal stem cell markers (*e.g.*, CD10, CD13, CD29, CD44, CD90, SH2, SH3) and negative expression of hematopoietic markers (*e.g.*, CD14, CD34, CD45, HLA-DR), they have demonstrated mesenchymal cell-lineage capacities for osteogenic, chondrogenic, myogenic and adipogenic differentiation in several instances.<sup>64, 76, 77, 80, 300-308</sup> Although they have much in common with bone marrow derived MSCs, HUCM stem cells have distinct advantages in that they are easily

obtained and are in abundant supply, have no donor site morbidity, are developmentally more primitive cells, and can be expanded for several passages. Furthermore, HUCM stem cells can be expanded and cryogenically stored for years without losing viability or their stem cell properties. There is a lower incidence of graft vs. host disease than with bone marrow transplants, and a significant absence of major histocompatibility complexes, suggesting that umbilical cord cells may have an innate mechanism to evade the immune system.<sup>77, 79, 80</sup> As human cells with low immunogenicity, HUCM stem cells are natural candidates for translational research. Use of HUCM stem cells is a new technology, and this is their first application in musculoskeletal tissue engineering, to the best of our knowledge. All indicators point to HUCM stem cells as having the potential to be a highly desirable cell source for musculoskeletal tissue engineering in the future.

The current study examined the biosynthetic and proliferative activity of HUCM stem cells cultured in three-dimensional PGA scaffolds in the presence of factors that promote chondrogenic differentiation. These cells were compared to TMJ condyle cartilage cells, with the hypothesis being that HUCM stem cells would produce comparable or superior engineered constructs under the given conditions.

## **MATERIALS AND METHODS**

HUCM stem cells were harvested as described by Mitchell *et al.*<sup>75</sup> with minor modifications. Human umbilical cords were obtained from a local obstetrician, washed in betadine, rinsed in sterile phosphate buffered saline (PBS), incubated in

hyaluronidase (40 U/mL) (MP Biomedical, Aurora, OH) and collagenase type I (0.4 mg/mL) (Sigma) for 30 min at 37°C, and rinsed with sterile PBS. After removal of vascular tissue, the cords were finely minced, plated in six-well plates, and maintained in defined media (DM), which is composed of DMEM (Invitrogen) and MCDB-201 medium (Sigma) supplemented with 1× insulin-transferrin-selenium (Invitrogen), 0.15% lipid-rich bovine serum albumin (Albumax, Invitrogen), 0.1 nM dexamethasone (Sigma), 10 μM ascorbic acid-2-phosphate (Sigma), 1× penicillin/streptomycin (Fisher), 2% fetal bovine serum (FBS, HyClone; Logan, UT), 10 ng/mL recombinant human epidermal growth factor, and 10 ng/mL human platelet-derived growth factor BB (R&D Systems, Inc.). After one week in culture, cord remnants were removed and the attached cells were maintained in DM. Cells were passaged by lifting with 0.05% trypsin EDTA and replated to maintain a density between 30 to 80%.

Cartilage tissue was harvested in a manner similar to that described by Detamore and Athanasiou.<sup>141, 258, 259</sup> Briefly, the head of a Yorkshire male hog, age 6-7 months, was obtained from a local butcher. TMJs were removed en bloc, and then both mandibular condyles were aseptically disengaged from the TMJ. The cartilage was removed from the condyle with a scalpel and placed in a Petri dish. The resected tissue was digested for 24 hrs in a 30 mL solution of 2 mg/mL collagenase (Type 2, 394U/mg; Worthington Biochemical, Lakewood, NJ). The resulting cell solution was centrifuged and the cells resuspended in DMEM-high glucose, 10% FBS (Gemini BioProducts, Woodland, CA), 25 μg/mL ascorbic acid (Sigma-Aldrich; St. Louis,

MO), 1% non-essential amino acids (NEAA) (Invitrogen Corporation; Grand Island, NY), and 1% penicillin-streptomycin-fungizone (Invitrogen Corporation; Grand Island, NY). Approximately 21 million cells were obtained per condyle. Cells were plated and fed every other day until confluent, after which the cells were lifted and labeled as passage 1.

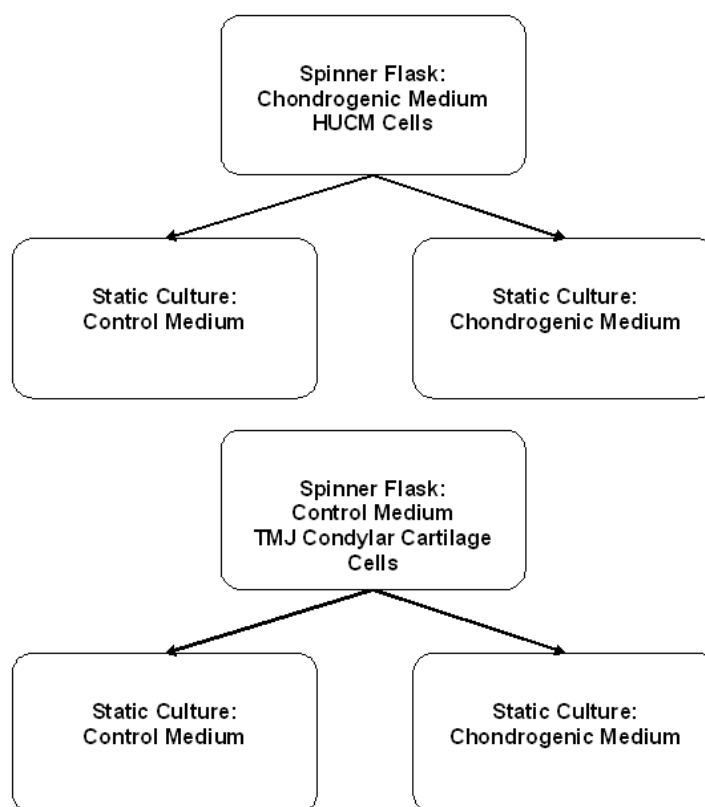


**Figure 6.1:** Diagram of experimental design. HUCM stem cells were seeded onto PGA scaffolds in chondrogenic medium, and TMJ condylar chondrocytes were seeded in control medium. Constructs from both flasks were then split and cultured in either chondrogenic or control medium.

Control medium was prepared by supplementing DMEM-high glucose with 10% FBS, 50  $\mu\text{g/mL}$  ascorbic acid, 1% NEAA, and 1% penicillin/streptomycin.

Chondrogenic medium was prepared by supplementing the above control medium with 10 ng/mL of recombinant human transforming growth factor- $\beta$ 1 (TGF- $\beta$ 1) (PeproTech, Inc.; Rocky Hill, NJ), and 50 mg/mL insulin transferrin-selenium plus 1 premix (ITS+1) (Sigma-Aldrich; St. Louis, MO).

The experiment was set up using two spinner flasks, one containing chondrogenic medium and one containing control medium (Fig. 6.1). The HUCM stem cells were cultured in chondrogenic medium to produce an initial differentiation, and the condylar cartilage cells were cultured in control medium in order to produce two populations of cell-seeded scaffolds for comparison. After seeding, scaffolds were removed from the spinner flasks and cultured in either control or chondrogenic medium for an additional 4 weeks. Spinner flasks were prepared as described by Detamore and Athanasiou.<sup>141, 259</sup> A polyglycolic acid (PGA) non-woven mesh (Concordia Manufacturing, Coventry, RI) with a thickness of 1.5 mm was used as the scaffold. A circular brass tube fitting and a surgical scalpel were used to cut 5 mm diameter scaffolds. The scaffolds were then skewered onto a steel wire, alternating with two glass beads, until a total of 16 scaffolds were placed on the wire in each flask. The spinner flasks, along with the scaffolds, were sterilized with ethylene oxide and then aired under a fume hood for 2 days. The scaffolds were then wetted with sterile filtered ethanol, and two washes of sterile PBS.

This was followed by adding 200 mL of medium to each flask, and the flasks were then incubated at 37°C in 5% CO<sub>2</sub> overnight.  $3.4 \times 10^6$  HUCM stem cells were then added to the flask containing chondrogenic medium, and an equivalent number

of porcine mandibular condyle cartilage cells were added to the flask containing control medium. The flasks were incubated at 37°C in 5% CO<sub>2</sub> and stirred continuously at 90 RPM. Stirring was stopped after 3 days, and an additional 1% pen-strep was added to each flask. The cells were given an additional 3 days to adhere to the scaffolds. Scaffolds were then carefully transferred to two 24-well plates with each well coated with 600 µL of 2% agarose. Scaffolds from each group were cultured for 4 weeks in 1 mL of either chondrogenic medium or control medium. Half of the medium was changed every 2 days.

Scaffolds were analyzed biochemically, histologically and immunohistochemically for biosynthesis and proliferation at week 0 and week 4. Week 0 refers to the time immediately after the 6 day seeding period. Proliferation was measured using a Picogreen assay (Molecular Probes; Eugene, OR).<sup>258</sup> A conversion factor of 7.7 pg DNA/cell was used for both condyle and HUCM stem cells.<sup>258</sup> A dimethylmethylene blue (DMMB) dye assay was used to determine the amount of glycosaminoglycan (GAG) produced using a chondroitin sulfate standard (Biocolor; Newtownabbey, Northern Ireland).<sup>258</sup> A hydroxyproline assay using a collagen standard (Accurate Chemical and Scientific Corporation; Westbury, NY) was used to quantify the amount of collagen produced.<sup>258</sup>

Immunohistochemical analysis of collagen I and II was performed as described by Detamore *et al.*<sup>141, 309</sup> Staining was performed using a Biogenex i6000 autostainer (San Ramon, CA). Slides were placed in the autostainer and rehydrated with PBS for 5 min. Endogenous peroxidase activity was quenched with 1%

hydrogen peroxide in methanol for 30 min, followed by blocking in 3% horse serum for 20 min. Samples were then stained with a primary antibody for 60 min. The mouse monoclonal IgG anti-collagen I (1:1500 dilution) and mouse monoclonal IgG anti-collagen II (1:1000 dilution) antibodies were obtained from Accurate Chemical and Scientific (Westbury, NY) and Chondrex, LLC (Redmond, WA), respectively. The primary antibody was followed by incubation with a streptavidin-linked horse anti-mouse IgG secondary antibody (Vector Laboratories, Burlingame, CA) for 30 min. This was followed by incubation with avidin-biotinylated enzyme complex (Vector Laboratories) for 30 min and then 3,3'-diaminobenzadine for 4 min. The slides were counterstained with Harris hematoxylin, dehydrated with graded ethanol, and then mounted. Immunohistochemistry of chondroitin-4-sulfate (C4S) and chondroitin-6-sulfate (C6S) was conducted in the same manner, except a digestion for 2 hr using 0.2 U/mL chondroitinase ABC (Seikagaku America) was added before serum blocking, as required by the first antibody manufacturer.<sup>141</sup> The C4S (1:100) and C6S (1:100) antibodies were obtained from Chemicon. Histological analysis was performed using a Safranin O/fast green stain with Harris hematoxylin.

An analysis of variance (ANOVA) was used to determine statistical significance ( $p < 0.05$ ). Comparisons among groups were done using a Fisher's Protected Least Significant Difference *post-hoc* test. Sample sizes were  $n = 4$  for all biochemical tests.

## RESULTS

We hypothesized that due to the high proliferative capacity of HUCM stem cells in monolayer cell culture compared to condylar cartilage cells, that they may have a similar advantage when grown on PGA scaffolds. Indeed, despite beginning with equivalent cell numbers, there were approximately  $140 \pm 22 \times 10^3$  cells per HUCM construct compared to  $90 \pm 9 \times 10^3$  cells per TMJ construct at week 0 ( $p < 0.01$ ) (Fig. 6.2), corresponding to  $4.75 \times 10^6$  and  $3.06 \times 10^6$  cells/mL, respectively.

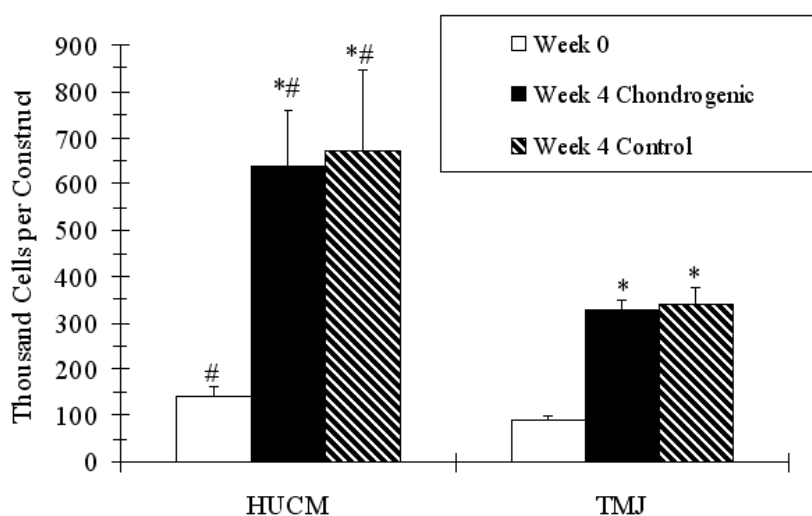


**Figure 6.2:** Mean cell number per construct  $\pm$  standard deviation ( $n = 4$ ). HUCM refers to the human umbilical cord cell-seeded constructs and TMJ refers to condylar cartilage cell-seeded constructs. Values are given in thousands of cells per construct. \* indicates a significant difference from week 0 for the same cell type and # indicates a significant difference between HUCM and condylar cartilage at a given time point.

At week 4, the cell content increased to  $638 \pm 121$  and  $674 \pm 173 \times 10^3$  cells per HUCM construct cultured in chondrogenic and control medium, respectively (Fig.

6.2). There was a significant increase in cell number between the HUCM week 0 group and both of the HUCM week 4 groups ( $p < 0.00002$ ). Condylar cartilage cells cultured in chondrogenic and control media also increased significantly from week 0 to  $327 \pm 19 \times 10^3$  and  $339 \pm 38 \times 10^3$  cells per TMJ construct, respectively ( $p < 0.002$ ). There was also a significant difference in cell number between HUCM and TMJ constructs at week 4 in both chondrogenic and control media ( $p < 0.0001$ ).

We next wanted to evaluate the potential of HUCM cells to produce extracellular matrix molecules required for cartilage formation compared to the native cartilage-forming cells. To achieve this, we measured the GAG and collagen content and examined the distribution of GAGs and collagen types I and II at week 0 and week 4 post-seeding for all groups.

At week 0, the GAG content was  $8.6 \pm 1.1 \mu\text{g}$  and  $11.3 \pm 2.3 \mu\text{g}$  per construct ( $93 \pm 17$  and  $80 \pm 21 \text{ pg per cell}$ ) for the TMJ and HUCM groups, respectively (Fig. 6.3). There was a significant decrease in GAG content from week 0 to week 4 for both the HUCM and TMJ constructs cultured in either medium ( $p < 0.00004$ ). However, there was no significant difference in GAG synthesis between chondrogenic and control media at 4 weeks within the HUCM group or within the TMJ group. The production of GAGs was supported by Safranin-O staining, which revealed a larger concentration of GAGs in HUCM constructs in both control and chondrogenic medium compared to the concentration in TMJ constructs cultured in either control or chondrogenic media (Fig. 6.4). At week 4, immunohistochemistry presented positive staining of chondroitin-4-sulfate and chondroitin-6-sulfate more

intensely in the HUCM group than in the TMJ group, which was consistent with the Safranin-O staining (C4S shown in Fig. 6.4).

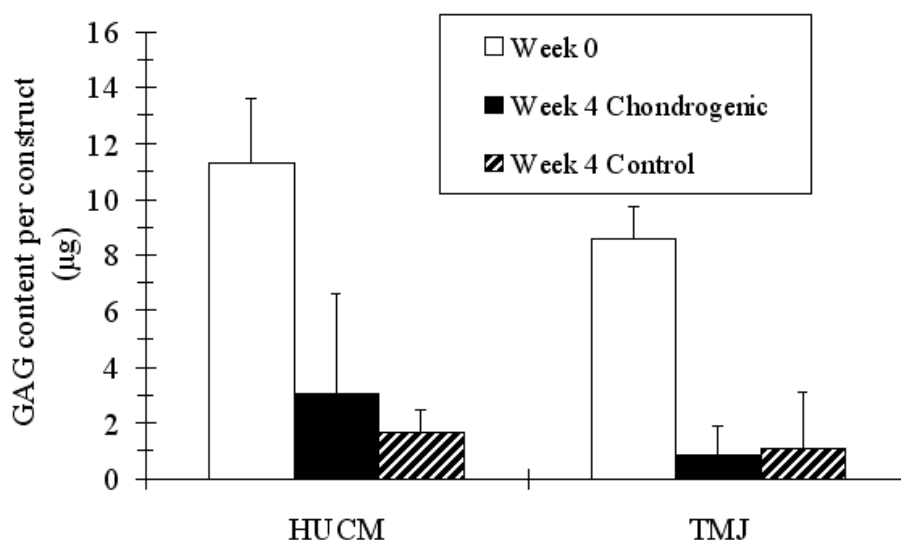


**Figure 6.3:** Mean GAG biosynthesis per construct  $\pm$  standard deviation ( $n = 4$ ). HUCM refers to the human umbilical cord cell-seeded construct. Chondrogenic and control refer to the culture medium.

While immunohistochemical staining attempts on TMJ condyle constructs were unsuccessful at week 0 (constructs washed off slides during processing), immunohistochemical analysis of the HUCM constructs at week 0 revealed the presence of type I collagen, and minute amounts of type II collagen (data not shown). The detection of collagen with immunohistochemical analysis was supported by the results of the hydroxyproline assay at week 0, which reported  $4.6 \pm 1.0$   $\mu\text{g}$  of collagen per HUCM construct, compared to  $6.0 \pm 1.1$   $\mu\text{g}$  of collagen per TMJ construct, which was not a significant difference.

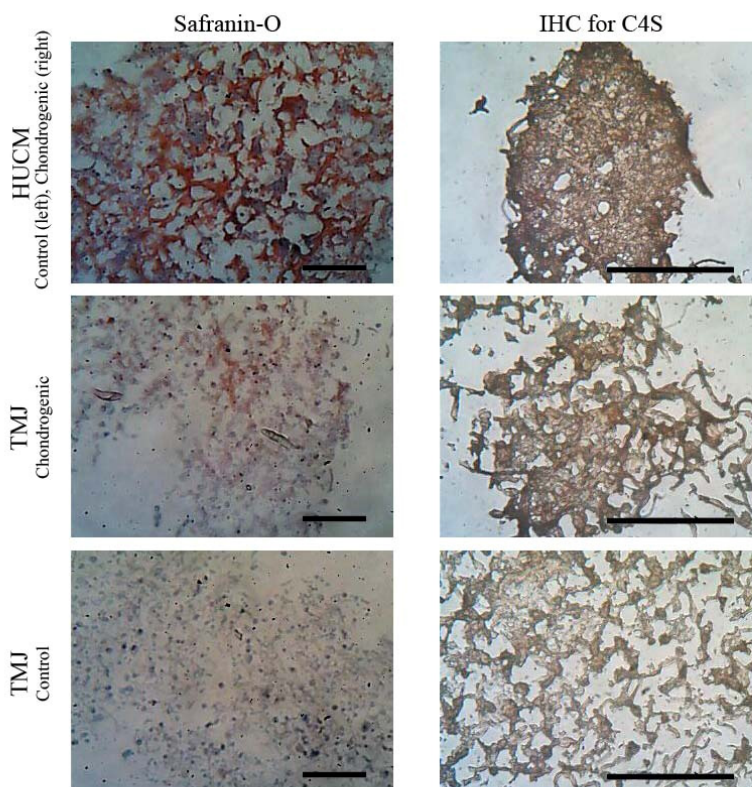


**Figure 6.4:** The left column is Safranin-O/fast green staining after 4 weeks. The right column is immunohistochemical staining of chondroitin-4-sulfate (C4S) after 4 weeks. From the top row to the bottom is HUCM stem cells in control (left) or chondrogenic (right) medium, TMJ cartilage cells in chondrogenic medium, and TMJ cartilage cells in control medium. This evidence suggests the ability of HUCM stem cells to progress down a chondrogenic lineage in 3D after initial exposure to chondrogenic signals. Moreover, the significantly higher intensity of staining for both Safranin-O and C4S immunohistochemistry (IHC) in the HUCM constructs demonstrates that the HUCM stem cells significantly outperform TMJ cartilage cells in GAG synthesis. The scale bars are 25  $\mu$ m.

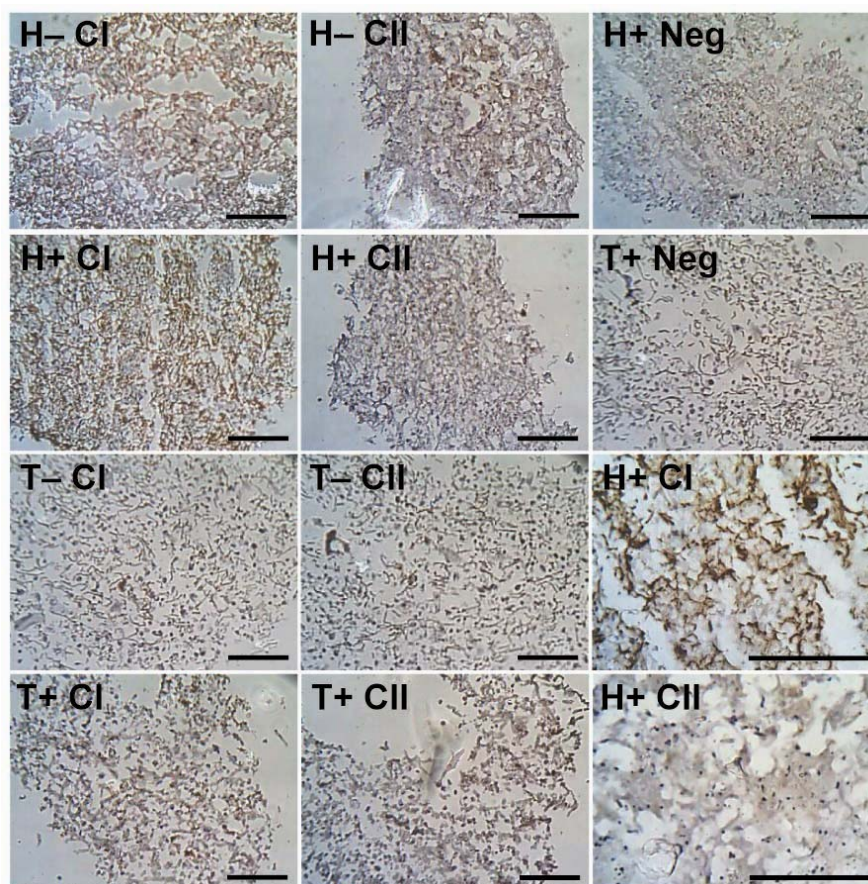


**Figure 6.5:** HUCM and TMJ construct sections from constructs cultured in chondrogenic and control media after 4 weeks. Photos are taken after immunohistochemical staining for collagen types I and II, plus background staining. H, T, +, -, CI, CII, and Neg refer to HUCM stem cells, TMJ condylar cartilage cells, chondrogenic medium, control medium, collagen type I, collagen type II, and negative control groups, respectively. The brown areas indicate a positive stain, and dark purple stains are cell nuclei. The last two pictures provide high magnification examples of HUCM constructs. The scale bars are 25  $\mu\text{m}$ .

At week 4, immunohistochemical analysis of HUCM constructs cultured in control medium revealed the presence of type I collagen, and minute amounts of type II collagen (Fig. 6.5). Immunohistochemical analysis of the HUCM constructs cultured in chondrogenic medium revealed a significant presence of type I collagen and minute amounts of type II collagen (Fig. 6.5). The results of the hydroxyproline assay at week 4, however, were inconclusive for both HUCM groups because the collagen content was below the detection limit of the assay, as was also the case for the TMJ constructs at week 4.

Immunohistochemical staining of TMJ constructs cultured in control medium did not conclusively reveal the presence of type I collagen or type II collagen (Fig. 6.5). However, immunohistochemical staining of the TMJ constructs cultured in chondrogenic medium revealed a weak presence of type I and type II collagen (Fig. 6.5).

## **DISCUSSION**

To the best of our knowledge, this is the first attempt to evaluate the potential value of HUCM stem cells for musculoskeletal tissue engineering, and to culture condylar cartilage cells in 3D for tissue engineering. Comparing these two cell types is an important early step in our effort to engineer condylar cartilage.

In general, the presence of the chondrogenic medium after seeding did not seem to have a large effect on the biosynthetic and proliferative activity of the HUCM stem cells, although there were slight differences in collagen I and II biosynthesis

suggested by immunohistochemistry. HUCM stem cells have been shown to express bmi-1 and p21, genes which are both involved in anti-apoptotic pathways (unpublished data). This could possibly explain in part the greater cell numbers in the HUCM constructs than in the TMJ cell constructs at week 0 and week 4. Another explanation could be that the HUCM stem cells are better able to adhere to the construct than cartilage cells, which tend to interact less with their tissue environment than other cells. The increase in cell number in both groups at week 4 is likely due to continued cell proliferation, or a shorter doubling time of cells in 3D culture. Comparisons of doubling times of these cell types in both media types in monolayer vs. 3D-culture needs to be done to support this contention. Most importantly, it was demonstrated that HUCM cells remained highly proliferative in this environment and supported our hypothesis that they would be more proliferative than condylar cartilage cells.

HUCM constructs cultured in chondrogenic medium contained approximately the same number of cells as HUCM constructs cultured in control medium. The same trend was also observed with the TMJ constructs. Based on this observation, it appears that the TGF- $\beta$ 1 and the ITS+1 at the concentrations used did not significantly affect cell proliferation for either group during the 4-week culture period.

The sharp decrease in collagen synthesis reported by the hydroxyproline assay in both the HUCM and the TMJ groups at week 4 was unexpected. The immunohistochemical staining indicated the presence of collagen I and II in the

HUCM groups. Contraction of the constructs was also observed, which would produce a denser collagen matrix. The contraction of the construct would increase the visual density of the collagen (immunohistochemical results), despite the fact that the total quantity may be less than before (hydroxyproline assay results).

The large concentration of GAG produced by the HUCM constructs at week 0 could be due in part to the presence of heparin or heparan sulfate, both of which are sulfated glycosaminoglycans. According to the manufacturer of the DMMB dye assay (Accurate Chemical), the assay will detect the presence of both heparin and heparan sulfate. Heparin is commonly found in connective tissue and residual amounts might have been present in the HUCM cell culture or more likely produced by the HUCM stem cells themselves. However, this higher metabolic activity could also mean that functional proteoglycans such as aggrecan and decorin are being synthesized. Indeed, the intense immunohistochemical staining for chondroitin sulfates in the HUCM constructs confirms that the primary GAG component of aggrecan has a strong presence, and is thus largely responsible for the high sulfated GAG concentration revealed by Safranin-O staining.

The decrease in the observed GAG content at week 4, as indicated by the DMMB assay, could be due to the degradation of the polymer construct, as discussed previously by Detamore and Athanasiou.<sup>259</sup> In this case, some polymer fibers dislodge as the scaffold degrades, falling from the construct along with the GAGs attached to those fibers. This occurs when the rate of polymer degradation exceeds the rate of tissue formation, which might be most appropriately addressed by higher

cell seeding densities in the future. This observation could also be due in part to the contraction of the constructs at week 4. The decrease in GAG at week 4 was not, however, supported by the Safranin-O staining, which showed a dramatic increase in GAG concentration for the HUCM constructs.

The higher amount of collagen and GAGs present in the HUCM constructs after static culture, as indicated by the immunohistochemical staining for collagen I, collagen II, and chondroitin sulfates, and by the Safranin-O histology, in addition to the higher cell numbers in the HUCM constructs, indicate that the HUCM stem cells may be a better candidate for cartilage tissue engineering applications than the TMJ condylar chondrocytes.

The logical next steps will be to optimize the chondrogenic medium components and to compare HUCM stem cells to mesenchymal stem cells (MSCs) derived from bone marrow. It must be noted that though HUCM stem cells are themselves considered to be MSCs, they provide clear advantages over MSCs in that HUCM stem cells are easily obtained from a normally discarded tissue, are in abundant supply, have no donor site morbidity, are developmentally more primitive cells, and can be expanded for several passages (>p10) prior to senescence or differentiation.

The results of the present study have demonstrated that constructs seeded with HUCM stem cells can be induced to proliferate and biosynthesize collagen I and glycosaminoglycans. While synthesis of collagen I is a successful outcome for engineering fibrocartilages like the TMJ condylar cartilage, extensions of this work

into engineering hyaline cartilages as in the knee and hip will require a much higher production of collagen II. Based on the difficulty in obtaining donor cartilage for tissue engineering applications, and the superior biosynthetic activity by HUCM stem cells, we conclude that HUCM stem cells may have a significant potential therapeutic value for tissue engineering applications in the future.

## **CHAPTER 7: A Comparison of Human Bone Marrow-Derived Mesenchymal Stem Cells and Human Umbilical Cord-Derived Mesenchymal Stromal Cells for Cartilage Tissue Engineering\***

### **ABSTRACT**

Bone marrow-derived mesenchymal stem cells (BMSCs) have long been considered the gold standard for stem cell sources in musculoskeletal tissue engineering. The true test of stem cell source is a side-by-side comparison with BMSCs. Human umbilical cord-derived mesenchymal stromal cells (hUCMSCs), one such candidate with high potential, are a fetus-derived stem cell source collected from a discarded tissue (Wharton's jelly) after birth. Compared to human BMSCs (hBMSCs), hUCMSCs have the advantages of abundant supply, painless collection, no donor site morbidity, and faster and longer self-renewal *in vitro*. In this 6-week study, a chondrogenic comparison was conducted between hBMSCs and hUCMSCs in a 3D scaffold for the first time. Cells were seeded on polyglycolic acid (PGA) scaffolds at 25M cells/ml and then cultured in identical conditions. Cell proliferation, biosynthesis, and chondrogenic differentiation were assessed at weeks 0, 3, and 6 after seeding. At weeks 3 and 6, hUCMSCs produced more glycosaminoglycans (GAGs) than hBMSCs. At week 6, the hUCMSC group had 3 times more collagen than the hBMSC group. Immunohistochemistry revealed the presence of collagen types I and II and aggrecan with both groups. However, type II collagen staining was more intense for hBMSCs than hUCMSCs. Quantitative RT-PCR revealed a decrease

---

\*Chapter submitted to Tissue Eng Part A as Wang, Ivy, Seshareddy, Weiss, and Detamore. "A comparison of human bone marrow-derived mesenchymal stem cells and human umbilical cord-derived mesenchymal stromal cells for cartilage tissue engineering," July 2008.

of type I collagen mRNA and an increase of type II collagen mRNA with both cell types. Therefore, it was concluded that hUCMSCs may be a better option for use as a MSC cell source for cartilage tissue engineering than hBMSCs, given the numerous advantages and superior biosynthesis of hUCMSCs in a 3D matrix. However, further investigation into signals that best promote chondrogenesis specifically for hUCMSCs is warranted.

## INTRODUCTION

Mesenchymal stem cells (MSCs) can differentiate along a variety of cell lineages that can be used for tissue engineering and regenerative medicine. MSCs reside in many tissues including bone marrow,<sup>187</sup> adipose tissue,<sup>188</sup> blood,<sup>189</sup> synovial fluid,<sup>190</sup> dermis,<sup>191</sup> muscle,<sup>192</sup> and dental pulp.<sup>193</sup> Among them, human bone marrow stem cells (hBMSCs) are the most commonly used MSCs for scientific and clinical purposes. They are isolated via plastic adhesion or negative selection from bone marrow aspirate that includes a highly heterogeneous cell population such as hematopoietic cells, endothelial cells, and adipocytes.<sup>310</sup> However, there are some limitations of hBMSCs. The relative number of hBMSCs in the marrow and their differentiation potential decrease significantly with age increase.<sup>248</sup> Moreover, the harvesting procedure is painful and invasive and may lead to complications and morbidity.<sup>249</sup> Due to all the disadvantages associated with hBMSCs, efforts have been employed to find alternative sources of mesenchymal stem cells that function as well as hBMSCs but overcome these key limitations.

In recent years, umbilical cord-derived mesenchymal stromal cells (UCMSCs) have been explored as a MSC source with clear advantages over hBMSCs. UCMSCs are extracted through enzyme digestion or explant culture method from Wharton's jelly of umbilical cords,<sup>200</sup> a discarded tissue in abundant supply. The harvesting procedure is not invasive or painful and there is no donor site morbidity. The enzyme extraction yields  $10\text{-}50 \times 10^3$  cells per cm of cord,<sup>80, 195</sup> corresponding to approximately  $2\text{-}10 \times 10^5$  primary cells per cord, and can be expanded 300-fold for over seven passages without the loss of differentiation potential.<sup>195</sup> hUCMSCs strongly express surface markers that have been identified with other MSCs, including CD10,<sup>80</sup> CD13,<sup>80, 199, 204, 208</sup> CD29,<sup>76, 80, 204, 208</sup> CD44,<sup>76, 77, 80, 195, 199, 204, 208</sup> CD49e,<sup>80, 225</sup> CD51,<sup>76</sup> CD73/SH3,<sup>76, 77, 195, 199, 204</sup> CD90 (Thy-1),<sup>77, 80, 199, 208, 225</sup> CD105/SH2,<sup>76, 77, 80, 195, 199, 204</sup> CD106,<sup>204</sup> CD117,<sup>75, 77, 199</sup> CD146,<sup>225</sup> CD166,<sup>199, 204, 208</sup> and HLA-1/HLA-ABC,<sup>77, 80, 204, 208</sup> and are negative for hematopoietic markers (e.g., CD14, CD31, CD34, CD38, CD45, HLA-DR).<sup>64, 65, 75-77, 80, 81, 195, 199, 201, 204, 208, 209, 225</sup> Moreover, the presence of Oct-4, Nanog, and Sox-2 transcription factors indicated that a subpopulation of UCMSCs might share some properties of both embryonic and non-embryonic stem cells.<sup>201</sup> hUCMSCs have the ability to differentiate into mesenchymal cell-lineages such as osteogenic, chondrogenic, myogenic, and adipogenic.<sup>64, 76, 77, 195, 225</sup> Moreover, the number of fibroblast colony-forming units (CFU-F) is significantly higher in hUCMSCs than hBMSCs.<sup>204</sup>

In the past four years, only five previous studies demonstrated the chondrogenic differentiation of hUCMSCs in cell pellet culture<sup>76, 195, 225</sup> or

poly(glycolic acid) (PGA) scaffolds.<sup>66, 207</sup> Wang *et al.*<sup>76</sup> first revealed evidence of chondrogenesis by a positive immunohistochemical (IHC) staining of type II collagen, which was also observed with non-differentiated cells. Other than a conference abstract,<sup>235</sup> the first application of hUCMSCs in 3D musculoskeletal tissue engineering were performed by our group.<sup>66, 207</sup> In these studies, we demonstrated that 3D culture of hUCMSCs in PGA scaffolds led to a fibrocartilage with intense type I collagen, and moderate collagen type II and aggrecan immunostaining.<sup>66, 207</sup> Here, our objective is to compare hUCMSCs and hBMSCs *in vitro* in a cartilage tissue engineering application. Both types of cells were cultured in PGA scaffolds, and we evaluated their proliferation, biosynthesis, and chondrogenic differentiation over a period of 6 weeks.

## MATERIALS AND METHODS

### *Cell harvest*

hUCMSCs were harvested following our previous methods, with IRB approval and informed consent.<sup>80</sup> The cells were plated and recorded as P0 in six well plates containing a low-serum medium at a density of 10,000 cells/cm<sup>2</sup>. The medium was composed of low-glucose Dulbecco's modified Eagle's medium (DMEM-LG; Invitrogen, Carlsbad, CA) and MCDB-201 medium (Sigma, St. Louis, MO) supplemented with 1× insulin-transferrin-selenium (Invitrogen), 0.15% lipid-rich bovine serum albumin (Albumax; Invitrogen), 0.1 nM dexamethasone (Sigma), 10 μM ascorbic acid-2-phosphate (Sigma), 1× penicillin/streptomycin (Fisher Scientific,

Pittsburgh, PA), 2% fetal bovine serum (FBS; Invitrogen), 10 ng/mL recombinant human epidermal growth factor (Invitrogen), and 10 ng/mL human platelet-derived growth factor BB (R&D Systems, Minneapolis, MN). Cells in the well plates were fed every two to three days and maintained in a cell culture incubator (NuAire, Autoflow, 5% CO<sub>2</sub>, 37°C and 90% humidity). Cells were then detached at 80-90% confluence and plated into 25 cm<sup>2</sup> flasks. At P1, cells were resuspended at the density of 1 million cells per ml of freezing medium composed of 90% FBS and 10% dimethyl sulfoxide (DMSO; Fishersci). The cell suspension was transferred into cryotubes, which were stored in Mr. Frosty freezing containers (Nalgene, Rochester, NY) at -80°C overnight, and then transferred to a liquid nitrogen cryogenic storage system at -196°C for future use. P0 frozen hBMSCs were obtained from StemCell Technologies, with IRB approval. The bone marrow was extracted from the posterior iliac crest from a maximum of 4 sites/donor (25 ml/site). The phenotype of P0 hBMSC was evaluated by flow cytometry and cells included CD29 (>90%), CD44 (>90%), CD105 (>90%), CD166 (>90%), CD14 (<1%), CD34 (<1%) and CD45 (<1%).

### ***Cell seeding***

Both types of cells were thawed and expanded with a plating density of 5000-6000 cells/cm<sup>2</sup> in 300 cm<sup>2</sup> flasks to P4 in a medium containing DMEM-LG, 10% fetal bovine serum (StemCell Technologies), 1% penicillin/streptomycin (Invitrogen), and 1% non-essential amino acids (NEAA; Invitrogen). Non-woven PGA meshes (50

mg/cc; Synthecon, Houston, TX) were punched to cylindrical scaffolds with a 5 mm diameter and 2 mm thickness, and then sterilized with ethylene oxide. After sterilization, the scaffolds were aired under a fume hood for one day, then wetted with sterile filtered ethanol and two washes of sterile PBS. The scaffolds were then soaked in the medium for one day and the medium was removed for cell seeding. Both cell types, at P4, were seeded at 20 million cells per ml of scaffold via orbital shakers onto PGA scaffolds at 150 rpm for 24 hrs. Finally, the medium was replaced by 2 ml of chondrogenic-differentiation medium consisting of high-glucose DMEM (DMEM-HG; Invitrogen), 1% NEAA, 1× insulin-transferrin-selenium premix (ITS premix; BD Biosciences, San Jose, CA), 10 ng/ml transforming growth factor beta-1 (TGF-β1; PeproTech, Rocky Hill, NJ), 100 nM dexamethasone (Sigma), 50 µg/ml ascorbic acid 2-phosphate (Sigma), 100 mM sodium pyruvate (Fisher), and 40 µg/ml L-proline (Sigma). This time point was recorded as week 0. Medium was changed every other day over a period of 6 weeks.

### ***Biochemical analysis***

At weeks 0, 3 and 6, constructs were digested by adding 1.1 ml papain solution (120 µg/ml) at 60 °C overnight, and then constructs were stored at -20 °C for future assays. Cell number was determined by measuring DNA content via a PicoGreen kit (Invitrogen). A conversion factor of 8.5 pg DNA/cell was determined in preliminary studies. Biosynthesis was evaluated by measuring total GAG and hydroxyproline (HYP) contents. GAG content was measured using a

dimethylmethylene blue (DMMB) dye binding assay kit (Biocolor, Belfast, UK). From each sample, 100  $\mu\text{L}$  was added to 1 ml of DMMB and allowed 30 min to bind. Solutions were then centrifuged, supernatant was discarded, and the pellet was resuspended and read at 656nm. HYP content was determined by using a modified HYP assay.<sup>311</sup> Briefly, 400 $\mu\text{L}$  of each sample was hydrolyzed with an equal volume of 4N sodium hydroxide at 121°C for 30 min, neutralized with an equal volume of 4N hydrochloric acid, and then titrated to an approximate pH range between 6.5 and 7.0. One ml of this solution was combined with 0.5 ml Chloramine-T (14.1 g/L) in the buffer (50 g/l citric acid, 120 g/l sodium acetate trihydrate, 34 g/l sodium hydroxide and 12.5 g/l acetic acid), and the resulting solution was then combined with 0.5 ml of 1.17 mM p-dimethylaminobenzaldehyde in perchloric acid and read at 550 nm. A conversion factor of 11.5 can be used to convert HYX mass to collagen mass based on our preliminary studies.

### ***Immunohistochemistry for types I and II collagen and aggrecan***

Immunohistochemical analysis was performed in a BioGenex i6000 autostainer (BioGenex, San Ramon, CA). Scaffolds were frozen and sliced into thin sections (10  $\mu\text{m}$ ) that were fixed in chilled acetone (4 °C) for 10 min before staining. Slides were (n = 2) rehydrated with PBS for 5 min. Endogenous peroxidase activity was inhibited using 1% hydrogen peroxide in methanol for 30 min. Each section was blocked in 3% horse serum for 20 min and incubated with a primary antibody for an hour. Primary antibodies used in this study included the mouse monoclonal IgG anti-

collagen I (1:1500 dilution; Accurate Chemical and Scientific, Westbury, NY), mouse monoclonal IgG anti-collagen II (1:1000 dilution; Chondrex, Redmond, WA), and mouse monoclonal IgG anti-aggrecan (1:50 dilution; Abcam, Cambridge, MA). Following primary antibody incubation, the sections were incubated with a streptavidin-linked horse anti-mouse IgG secondary antibody (Vector Laboratories, Burlingame, CA) for 30 min. After secondary antibody incubation, the sections were incubated with an avidin-biotinylated enzyme complex (ABC complex; Vector Laboratories) for 30 min, and then VIP substrate (purple color) (Vector Laboratories) was applied on sections for 6 min. Protocols run with the primary antibody omitted served as negative controls.

### ***RNA isolation and gene expression analysis***

Real-time reverse transcriptase polymerase chain reaction (real time RT-PCR) was used to quantify the relative gene expression level of types I and II collagen, and aggrecan. The constructs were collected at weeks 3 and 6 and homogenized with an electrical homogenizer in 1 ml of Trizol reagent (Invitrogen) to extract mRNA according to the manufacturer's protocol. Total mRNA was reverse transcribed to cDNA using a High-Capacity cDNA Archive kit (Applied Biosystems, Foster City, CA). Real-time RT-PCR reactions were run in an Applied Biosystems 7500 Fast Sequence Detection System. TaqMan gene expression assay kits (Applied Biosystems), including two pre-designed primers and one probe, were used for transcript levels of the proposed genes. 2  $\mu$ l of cDNA from each sample was mixed

with 7  $\mu$ l of RNase/DNase free water, 1  $\mu$ l of 20  $\times$  TaqMan gene expression assay reagent, and 10  $\mu$ l of 2  $\times$  TaqMan universal PCR master mix. Assay IDs of TaqMan gene expression assays were Hs00164004\_m1 for type I collagen, Hs00156568\_m1 for type II collagen, Hs00153936\_m1 for aggrecan, and Hs99999905\_m1 for glyceraldehyde 3-phosphate dehydrogenase (GAPDH). Relative mRNA expression level for each target gene was evaluated using a  $2^{-\Delta\Delta C_t}$  method.<sup>312</sup> The  $C_t$  values of target genes were first normalized by subtracting the  $C_t$  values of the TaqMan human housekeeping gene GAPDH to obtain  $\Delta C_t$  values. They were then normalized by subtracting the  $C_t$  value of the calibrator sample, the hBMSC group at week 3, to get  $\Delta\Delta C_t$  values, which were finally calculated to acquire the fold changes. Each sample was analyzed in triplicate.

### ***Statistical analysis***

All data were expressed as means  $\pm$  one standard deviation and analyzed by analysis of variance (ANOVA) followed by Tukey's Honestly Significant Difference (HSD) post hoc tests. Two-way ANOVAs with interaction were performed with time-points and cell sources as statistical factors. A statistical threshold of  $p < 0.05$  was used to indicate whether there were statistically significant differences among different groups.

## **RESULTS**

### ***Cell number***

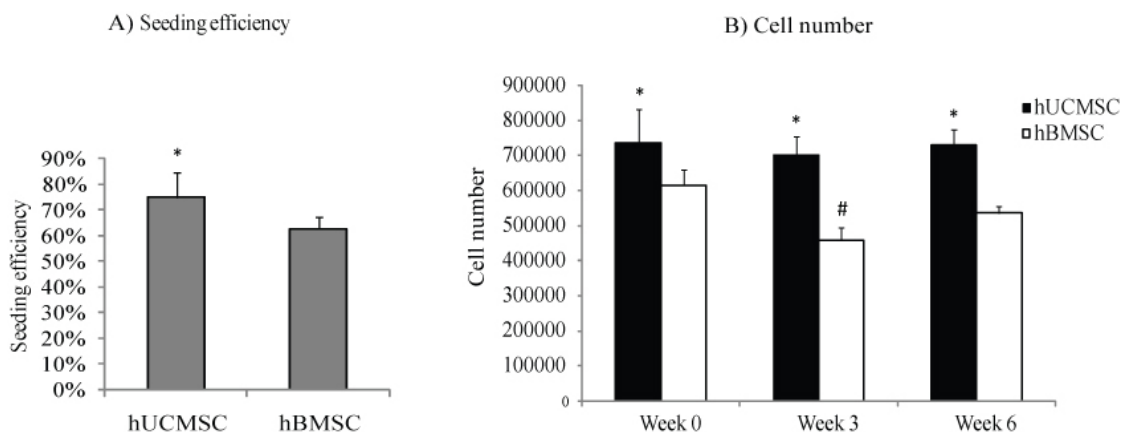


**Figure 7.1:** Seeding efficiency at week 0 (A) and cell number at weeks 0, 3, and 6 (B). \* = statistically significant difference between hUCMSC and hBMSC groups. # = statistically significant difference between weeks 0 and 3. Error bars represent standard deviations.

During the monolayer expansion prior to 3D seeding stage, hUCMSCs had a higher proliferation rate than hBMSCs. At the same plating density of 5000-6000 cells/cm<sup>2</sup>, hUCMSCs reached 80-90% confluence within 3-4 days, while hBMSCs took 4-6 days to reach the same confluence. At week 0, a seeding efficiency (defined as the percentage ratio of the number of attached cells to the number of seeded cells) of 75% was achieved with hUCMSCs, while a seeding efficiency of only 62% was observed with hBMSCs ( $p < 0.05$ ) (Fig. 7.1A). After the initial seeding period, both hUCMSC and hBMSC groups maintained cell numbers over 6 weeks, except for a drop ( $p < 0.05$ ) at week 3 in hBMSC groups. However, following the drop, a recovery increase in cell number occurred without significant difference. In comparison, the

cell number in the hUCMSC group was significantly higher than in the hBMSC group throughout the culture period ( $p < 0.05$ ) (Fig. 7.1B).

### ***GAG and HYP content***

There was a continuing increase in GAG content per construct in the hUCMSC group over 6 weeks ( $p < 0.05$ ), whereas the GAG content decreased in the hBMSC group from weeks 0 to 3 ( $p < 0.05$ ) and then increased from weeks 3 to 6 ( $p < 0.05$ ) (Fig. 7.2A). However, the increases did not lead to a significant difference between weeks 0 and 6 for either group. In comparison to the hBMSC group, the hUCMSC group had a 51% and 28% higher GAG content per construct at weeks 3 and 6, respectively ( $p < 0.05$ ). With regard to GAG content per cell, both the hUCMSC and hBMSC groups had a significant increase between weeks 0 and 6 (Fig. 7.2B) ( $p < 0.05$ ). There was also a significant increase in GAG content for the hBMSC group from weeks 3 to 6 ( $p < 0.05$ ). In comparison to the hBMSC group, the hUCMSC group at week 3 had a higher GAG content per cell ( $p < 0.05$ ), although there was no statistically significant difference between them at week 6.

HYP content both per construct and per cell increased markedly from weeks 0 to 3 in both the hUCMSC and hBMSC groups (Fig. 7.2C-D), while there was no increase in HYP content between weeks 3 and 6 for either group. Comparatively, the hUCMSC group had 2.5 and 2.9 times more HYP content per construct than the hBMSC group at weeks 3 and 6 ( $p < 0.05$ ), respectively. Similar to HYP content per construct, the HYP content per cell increased from weeks 0 to 3 ( $p < 0.05$ ) and then

maintained with no significant changes until week 6 for both groups. In comparison to each other, the hUCMSC group processed 1.7 and 2.1 times more HYP content per cell than the hBMSC group ( $p < 0.05$ ).

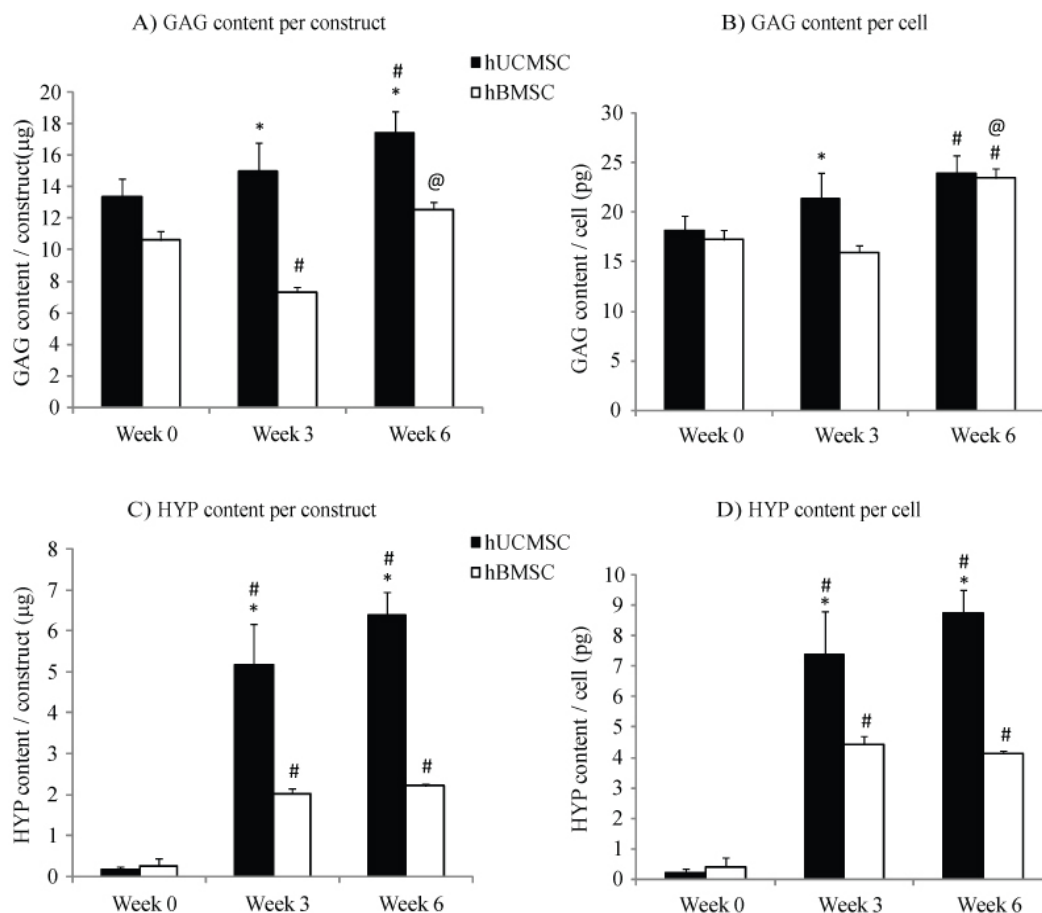


**Figure 7.2:** GAG and HYP contents per construct and per cell at weeks 0, 3, and 6. \* = statistically significant difference between hUCMSC and hBMSC groups at a specific time point. # = statistically significant difference between weeks 0 and 3 in either hUCMSC or hBMSC group. @ = statistically significant difference between weeks 3 and 6 in either hUCMSC or hBMSC group. Error bars represent standard deviations.

### *Immunohistochemistry*

Immunohistochemistry revealed positive staining for types I and II collagen and aggrecan with both the hUCMSC and hBMSC groups through the 6-week period (Fig. 7.3). At week 3, both the hBMSC and hUCMSC groups showed an abundant amount of type I collagen, a small amount of type II collagen, and a moderate amount of aggrecan. Relatively stronger staining of type I collagen and aggrecan was present in the hUCMSC group than in the hBMSC group. At week 6, both the hUCMSC and hBMSC groups presented a concentrated staining for type I collagen and a more intense staining for aggrecan than at week 3. There was a vast increase in type II collagen staining in the hBMSC group from weeks 3 to 6, while only a trace presence of type II collagen was detected in the hUCMSC group at week 6.

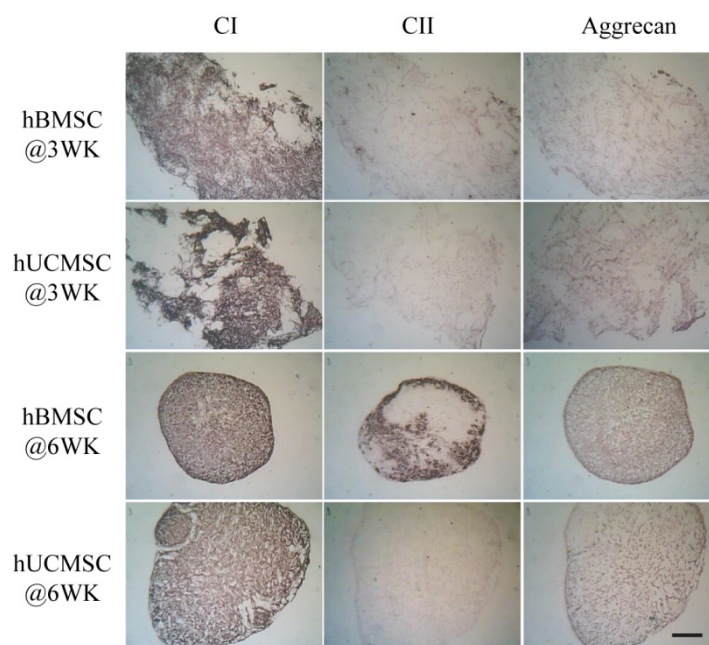


**Figure 7.3:** Immunohistochemical staining for types I and II collagen, and aggrecan. The scale bar is 500  $\mu\text{m}$ . CI = type I collagen, CII = type II collagen, @3WK = at week 3, and @6WK = at week 6.

### *RT-PCR analysis*

Compared to hBMSCs, hUCMSCs had a lower mRNA level of type I collagen at weeks 3 and 6 ( $p < 0.05$ ), a lower mRNA level of type II collagen at week 6, and the same level of aggrecan at weeks 3 and 6 (Fig.7.4). From weeks 3 and 6, in both the hUCMSC and hBMSC groups, type I collagen mRNA level decreased ( $p < 0.05$ ) and aggrecan mRNA level remained at the same level. Type II collagen mRNA level had a 3.8-fold increase in the hBMSC group from weeks 3 to week6 ( $p < 0.05$ ), while no change was observed in the hUCMSC group.

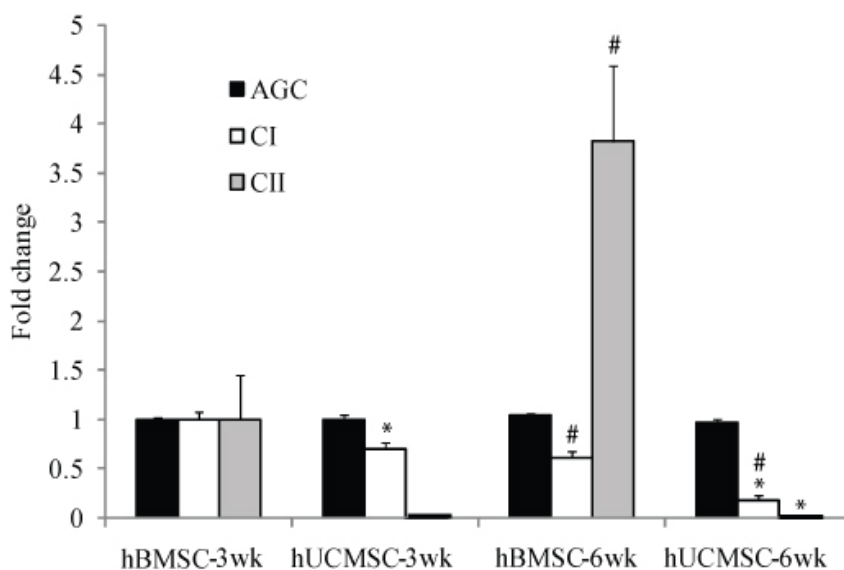


**Figure 7.4:** Gene expression for types I and II collagen, and aggrecan. CI = type I collagen, CII = type II collagen. \* = statistically significant difference between hUCMSC and hBMSC groups at a specific time point. # = statistically significant difference between weeks 3 and 6 in either hUCMSC or hBMSC group.

## DISCUSSION

It has been previously shown that hUCMSCs can differentiate toward a chondrogenic lineage.<sup>66, 76, 195, 225</sup> However, the application of these cells in musculoskeletal tissue engineering has been scarcely investigated.<sup>66, 207, 235</sup> This study, for the first time, specifically focused on the comparison between hUCMSCs and hBMSCs in a biomaterial-based 3D environment. This comparison is vital to the validation of hUCMSCs as a formidable cell source for cartilage—and more broadly, musculoskeletal—tissue engineering.

The faster proliferation rate of the hUCMSCs on monolayer culture provides for a larger number of cells in a shorter time period to better meet the needs of tissue engineering and clinical practice. The higher seeding efficiency with the hUCMSCs at week 0 indicated that hUCMSCs were more adherent to PGA scaffolds than hBMSCs. This higher seeding efficiency resulted in a higher cell number for the hUCMSC group, which was maintained over 6 weeks and likely contributed in part to the higher matrix production in the hUCMSC group. The decrease in cell number with hBMSCs from weeks 0 to 3 may be due to the degradation of the PGA scaffold, as we have noted in the past.<sup>207, 259</sup> In fact, the hUCMSC group also experienced a slight loss of cells (not statistically significant). The maintenance of cell numbers with hUCMSCs can be explained by the ability of hUCMSCs to proliferate at a higher rate as well as the higher matrix content that helps to retain cells in scaffolds. To overcome cell loss caused by PGA degradation, slowly degraded scaffolds such as PLLA and PLGA will be investigated in the future.

In this study, the hUCMSC group produced more GAGs than the hBMSC group. The higher GAG content per construct with hUCMSCs was due to the larger number of cells, as the GAG content per cell at week 6 was similar for the two groups. With regard to collagen production, both the hBMSC and hUCMSC groups showed an increase in collagen content throughout the 6-week culture, with the largest increase occurring between weeks 0 to 3. The higher porosity of cell-scaffold constructs in the first 3 weeks might contribute to higher collagen production, as it provided large space for matrix synthesis and nutrient diffusion. When compared directly to each other, the hUCMSC group produced 2.5 and 3.5 times more collagen per construct than the hBMSC group at weeks 3 and week6, respectively. More importantly, the hUCMSC group had more collagen per cell than the hBMSC group, indicating that hUCMSCs are better able to produce collagen than hBMSCs under the prescribed conditions. Thus, the high collagen content produced by hUCMSCs is attractive for cartilage tissue engineering.

Exposed to chondrogenic media, both types of cells produced a cartilage-like tissue with both types I and II collagen, and aggrecan. The chondrogenic differentiation of both cell types was accompanied by a down-regulation of type I collagen gene expression during this period. A higher type II collagen expression in the hBMSC group at both the mRNA and protein levels suggested that chondrogenic differentiation was more extensive with hBMSCs under the prescribed conditions. However, mRNA and protein expression of aggrecan was comparable between the

two groups, which suggests that hUCMSCs were at least in one capacity matching the apparent chondrogenesis of hBMSCs.

In previous hUCMSC pellet culture,<sup>76, 195</sup> plentiful type II collagen<sup>76, 195</sup> was observed with a little type I collagen<sup>19</sup> around the periphery. Limited oxygen (hypoxia) exists in the center of cell pellets due to low diffusion coefficient,<sup>313</sup> which may have contributed to the production of type II collagen.<sup>314</sup> It was unexpected that only a trace amount of type II collagen<sup>19</sup> was observed in hBMSC pellets because hBMSCs generally produced dominant type II collagen in pellets.<sup>315</sup> Compared to cell pellets, the constructs based on highly porous PGA scaffolds (> 95% porosity) in the current study had better diffusion, especially at the early stages. Moreover, the differences of chondrogenic media (TGF- $\beta$ 1 vs.  $\beta$ 3) and harvesting methods might explain these conflicting results between the pellet culture in the literature and the biomaterial-based culture in this study.

In conclusion, hUCMSCs proliferated faster, were seeded more efficiently, and demonstrated superior biosynthesis with nearly three times more collagen production. Although hBMSCs appeared to have progressed further down a chondrogenic lineage based on superior collagen II production, one may expect that the hUCMSCs will require a slightly modified set of signals to provide for optimal chondrogenesis. With the identification of this set of signals, it would be expected that hUCMSCs will be capable of producing a similar tissue in a drastically reduced time, which will translate to better patient care. hUCMSCs provide clear advantages over hBMSCs in that hUCMSCs are easily obtained from a discarded tissue, are in

abundant supply, have no donor site morbidity, and are highly expendable prior to senescence or differentiation. Moreover, in the future, if parents cryogenically save part of their child's umbilical cord, these hUCMSCs would also be available as an autologous cell source later in life with all of the aforementioned advantages. Based on these known advantages, and the results of this study, we therefore conclude that hUCMSCs are indeed a highly desirable cell source for cartilage tissue engineering, with significant and distinct advantages over the "gold standard" of hBMSCs.

## **CHAPTER 8: The Effect of Initial Seeding Density on Human Umbilical Cord Mesenchymal Stromal Cells for Fibrocartilage Tissue Engineering\***

### **ABSTRACT**

Cells derived from Wharton's jelly from human umbilical cords (called umbilical cord matrix mesenchymal stromal cells, here) are a novel cell source for musculoskeletal tissue engineering. In this study, we examined the effects of different seeding densities on seeding efficiency, cell proliferation, biosynthesis, mechanical integrity and chondrogenic differentiation. Cells were seeded on non-woven polyglycolic acid (PGA) meshes via orbital shaker, at densities of 5, 25 or 50 million cells/ml, then statically cultured for 4 weeks in chondrogenic medium. At week 0, initial seeding density did not affect seeding efficiency. Throughout the 4 week culture period, absolute cell numbers of the 25 and 50 million cells/ml (higher density) groups were significantly larger than the 5 million cells/ml (lower density) group. The presence of collagen types I and II and aggrecan was confirmed by immunohistochemical staining. GAG and collagen contents per construct in the higher density groups were significantly higher than in the lower density group. Constructs in the high density groups maintained their mechanical integrity, which was confirmed by unconfined compression testing. In conclusion, human umbilical cord matrix cells demonstrated the potential for chondrogenic differentiation in 3D tissue engineering, and higher seeding densities better promoted biosynthesis and mechanical integrity and thus a seeding density of at least 25 million cells per ml is

---

\*Chapter published as Wang, Seshareddy, Weiss, and Detamore. "The effect of initial seeding density on human umbilical cord matrix mesenchymal stromal cells for fibrocartilage tissue engineering." Tissue Eng Part A, In Press, 2008.

recommended for fibrocartilage tissue engineering with umbilical cord matrix mesenchymal stromal cells.

## INTRODUCTION

Fibrocartilage, is a primarily avascular tissue that is distinctly different from either fibrous tissues or hyaline cartilage.<sup>316, 317</sup> For example, fibrocartilage contains more type I collagen and less type II collagen and proteoglycans than hyaline cartilage.<sup>316</sup> Tissue engineering of fibrocartilage, aiming to create a functional replacement, offers promise for regenerative medicine with fibrocartilage defects. The approach of using differentiated adult cells is limited by insufficient cell availability and the loss of cell phenotype during *in vitro* expansion.<sup>84-87</sup> Tissue engineering with mesenchymal stem cells (MSCs) is attractive because of their expansion ability (self-renewal ability) and their ability to differentiate into cartilage, bone or other tissues *in vitro*.

Bone marrow-derived mesenchymal stem cells (BMSCs) are extensively used in musculoskeletal tissue engineering. They differentiate into multiple cell lineages including bone, cartilage, and other mesenchymal tissues when exposed to specific growth factors.<sup>58, 231, 318-320</sup> However, BMSCs have limited self-renewal ability and an age-dependent decrease in cell availability and proliferation. Furthermore, isolation of BMSCs requires an invasive and painful surgical procedure. Recently, umbilical cord matrix mesenchymal stromal cells (UCMSCs) have been shown to have extensive *in vitro* expansion capability, and ability to differentiate into mesenchymal cell-lineages

such as osteogenic, chondrogenic, myogenic, and adipogenic.<sup>64, 76, 77, 195, 225</sup> These cells are extracted through enzyme digestion or explant culture method from Wharton's jelly of umbilical cords.<sup>200</sup> The extraction yields  $10\text{-}50 \times 10^3$  cells per cm of cord,<sup>80, 195</sup> which can be expanded 300-fold for over seven passages without the loss of differentiation potential.<sup>195</sup> UCMSCs have the appearance of myofibroblasts, in terms of positive staining for the expression of vimentin, desmin, and/or  $\alpha$ -smooth muscle actin in native tissue or *in vitro* cultured cells.<sup>75, 226, 227</sup> UCMSCs possess markers found in BMSCs including CD29, CD44, CD90, CD105, and CD166.<sup>80, 195</sup> Moreover, the presence of Oct-4, Nanog, and Sox-2 transcription factors indicated that a subpopulation of UCMSCs might share some properties of both embryonic and non-embryonic stem cells.<sup>201</sup> Therefore, with the advantages of being easily obtained from a normally discarded tissue, abundant supply, no donor site morbidity, and expansion ability prior to senescence, UCMSCs are an attractive alternative for tissue engineering and regenerative medicine.

Recently, human UCMSCs (hUCMSCs) have been proposed for use in musculoskeletal tissue engineering.<sup>66</sup> The chondrogenic ability of hUCMSCs has been indicated by Alcian blue staining<sup>76, 225</sup> and toluidine blue staining for glycosaminoglycans (GAGs),<sup>195</sup> picrosirius red staining and Heidenhain's azan staining for collagen,<sup>195, 225</sup> and immunohistochemical staining for type I and II collagen.<sup>76, 195</sup> Our previous study compared hUCMSCs and mandibular condylar cartilage cells for tissue engineering mandibular condylar cartilage, the first full study with hUCMSCs in 3D musculoskeletal tissue engineering.<sup>66</sup> Both types of cells were

seeded on non-woven polyglycolic acid (PGA) meshes using spinner flasks and then statically cultured for 4 weeks in well plates containing either chondrogenic or control medium. The results demonstrated that hUCMSCs can be induced to produce type I collagen, chondroitin sulfates, and other GAGs. When compared to the tissue-engineered constructs using condylar cartilage cells, hUCMSC constructs had more cells and higher GAG production.

Toward tissue engineering using hUCMSCs, the initial cell density is critical for cell growth and extracellular matrix synthesis.<sup>274, 321, 322</sup> A previous study with fibrocartilage cells demonstrated that a lower cell density led to a loss of mechanical integrity, while a higher density benefited collagen production.<sup>274</sup> The goal of the current study was to demonstrate the fibrochondrogenic differentiation of hUCMSCs on non-woven PGA scaffolds and evaluate the effects of initial cell seeding density on cell number, biosynthesis and biomechanical properties. We hypothesized that hUCMSCs would form a fibrocartilage-like tissue with both types I and II collagen and aggrecan, and that a higher seeding density would maintain scaffold integrity and increase matrix synthesis per construct and per cell.

## **MATERIALS AND METHODS**

### ***Cell harvest***

Human umbilical cord collection and cell harvests were approved by the Kansas State University human subject board (IRB approval no. 3966). Cells were isolated via enzyme digestions as described by Weiss *et al.*<sup>80</sup> with minor

modifications. In brief, human umbilical cords were collected and cut into 3-5 cm pieces, and then vessels were removed from cord segments. Cord segments were incubated in hyaluronidase (1 mg/ml; Catalog# H2126; Sigma, St. Louis, MO) and collagenase type I (300 units/ml; Catalog# 17100-017; Invitrogen, Carlsbad, CA) for 1 hr at 37°C. After 1-hr incubation, the tissue pieces were crushed with tweezers to release cells from Wharton's jelly. The remaining segments were moved to new centrifuge tubes containing 0.1% trypsin/EDTA for another 30 min of incubation at 37°C and were then squeezed again to release additional cells from Wharton's jelly. Both vials containing cells from Wharton's jelly were combined and centrifuged at 250 x g for 5 min immediately after the second digestion. The cells were resuspended and plated in six well plates containing a low-serum medium at a density of 10,000 cells/cm<sup>2</sup>. The medium is composed of low-glucose Dulbecco's modified Eagle's medium (DMEM-LG; Catalog# 11885-092; Invitrogen) and MCDB-201 medium (Catalog# 045k8310; Sigma) supplemented with 1× insulin-transferrin-selenium (Catalog# 51300-044; Invitrogen), 0.15% lipid-rich bovine serum albumin (Catalog# 11020-021; Albumax, Invitrogen), 0.1 nM dexamethasone (Catalog# D2915; Sigma), 10 μM ascorbic acid-2-phosphate (Catalog# A-8960; Sigma), 1× penicillin/streptomycin (Catalog# 30-001-CI; Fisher Scientific, Pittsburgh, PA), 2% fetal bovine serum (FBS; Catalog# 16141079; Invitrogen), 10 ng/mL recombinant human epidermal growth factor (Catalog# 13247-051; Invitrogen), and 10 ng/mL human platelet-derived growth factor BB (Catalog# 220-BB-050; R&D Systems, Inc.). Cells in the well plates were recorded as P0 and were fed every two to three

days and maintained in a cell culture incubator (NuAire, Autoflow, 5% CO<sub>2</sub>, 37°C and 90% humidity). When cells had reached 80-90% confluence, they were detached and plated into 25 cm<sup>2</sup> flasks. At P1, cells were resuspended at a density of 1 million cells per ml freezing medium, composed of 90% FBS and 10% dimethyl sulfoxide (DMSO; Catalog# 61097-1000; Fisher Scientific). The cell suspension was transferred into cryotubes (Catalog# 5000-1020; Nalgene Labware, Rochester, NY), which were stored in Mr. Frosty freezing containers (Catalog# 5000-0001; Nalgene) at -80°C overnight, and transferred to a liquid nitrogen cryogenic storage system at -196°C for future use.

### ***Cell seeding***

Cells were thawed and expanded to P5 in the complete medium containing DMEM-LG, 10% fetal bovine serum (Catalog# 6472; StemCell Technologies), 1% penicillin/streptomycin (Catalog# 15140-122; Invitrogen), and 1% non-essential amino acids (NEAA; Catalog# 11140-050; Invitrogen). Non-woven PGA meshes (Concordia Manufacturing, Coventry, RI) were punched to round-shape scaffolds with a 5 mm diameter and 1.5 mm thickness, and then sterilized with ethylene oxide. After sterilization, the scaffolds were aired under a fume hood for one day, then wetted with sterile filtered ethanol and two washes of sterile phosphate buffered saline (PBS). The scaffolds were then soaked in complete medium for one day and then removed for cell seeding. P5 hUCMSCs were seeded at 5, 25 and 50 million cells per ml of scaffold via orbital shakers onto PGA scaffolds at 150 rpm for 24 hrs,

and were allowed to attach in the culture medium for another day. Finally, the complete medium was replaced by 2 ml chondrogenic medium including high-glucose DMEM (DMEM-HG; Catalog# 10566-016; Invitrogen), 1% NEAA, 1× Insulin-Transferrin-Selenium premix (Catalog# 354350; ITS premix; BD Biosciences, San Jose, CA), 10 ng/ml transforming growth factor beta-1 (TGF-β1; Catalog# 100-21C; PeproTech, Rocky Hill, NJ), 100 nM dexamethasone (Catalog# D4902; Sigma), 50 μg/ml ascorbic acid 2-phosphate (Catalog# A-8960; Sigma), 100 mM sodium pyruvate (Catalog# SH3023901; Fisher Scientific), and 40 μg/ml L-proline (Catalog# P5607-25G; Sigma). This time point was recorded as week 0. Medium was changed every other day for 4 weeks.

### ***Biochemical analysis***

At week 0, week 2, and week 4, constructs (n = 4) were digested by adding 1.1 ml papain solution (120 μg/ml) at 60 °C overnight, and then constructs were stored at -20 °C for biochemical assays. Cell number was determined by measuring DNA content, which was accomplished via a reaction between PicoGreen and DNA using a kit with provided DNA standards (Kit# P7589; Invitrogen). A conversion factor of 8.5 pg DNA/cell was determined in preliminary studies. Biosynthesis was evaluated by measuring total GAG and collagen content. GAG content was measured using a dimethylmethylene blue (DMMB) dye binding assay kit (Kit# B1500; Biocolor; Northern Ireland). Chondroitin sulfate provided with the kit was used as the GAG standard. From each sample, 100 μL was added to 1 ml of DMMB and allowed

30 min to bind. Solutions were then centrifuged, supernatant was discarded, and the pellet was resuspended and read at 656 nm. Hydroxyproline content was determined by using a modified hydroxyproline assay.<sup>311</sup> Briefly, 400  $\mu$ L of each sample was hydrolyzed with an equal volume of 4N sodium hydroxide at 121°C for 30 min, neutralized with an equal volume of 4N hydrochloric acid, and then titrated to an approximate pH range between 6.5 and 7.0. One ml of this solution was combined with 0.5 ml Chloramine-T (14.1 g/L) in the buffer (50 g/l citric acid, 120 g/l sodium acetate trihydrate, 34 g/l sodium hydroxide and 12.5 g/l acetic acid). The resulting solution was then combined with 0.5 ml of 1.17 mM p-dimethylaminobenzaldehyde in perchloric acid and read at 550 nm.

#### ***Immunohistochemistry for types I and II collagen, and aggrecan***

Immunohistochemical analysis was performed in a BioGenex i6000 autostainer (BioGenex, San Ramon, CA). Frozen sections of the 3D constructs (10  $\mu$ m) (n = 2) were rehydrated with PBS for 5 min and endogenous peroxidase activity was inhibited using 1% hydrogen peroxide in methanol for 30 min. The sections were then blocked in 3% horse serum for 20 min and incubated with a primary antibody for 1 hr. Primary antibodies used in this study included the mouse monoclonal IgG anti-collagen I (1:1500 dilution; Catalog# BYA6520-1; Accurate Chemical and Scientific, Westbury, NY), mouse monoclonal IgG anti-collagen II (1:1000 dilution; Catalog# 7005; Chondrex, Redmond, WA), and mouse monoclonal IgG anti-aggrecan (1:50 dilution; Catalog# ab3778-1; Abcam, Cambridge, MA). Following primary antibody

incubation, the sections were incubated with a streptavidin-linked horse anti-mouse IgG secondary antibody (Kit# PK-6102; Vector Laboratories, Burlingame, CA) for 30 min. After secondary antibody incubation, the sections were incubated with avidin-biotinylated enzyme complex (Kit# PK-6102; ABC complex; Vector Laboratories) for 30 min, and then VIP substrate (purple color) (Catalog# SK-4600; Vector Laboratories) was applied on sections for 4 min. Protocols run with the primary antibody omitted served as negative controls.

### ***Mechanical integrity***

At week 4, unconfined compression tests were performed using a uniaxial testing apparatus (Instron 5848). Hydrated samples ( $n = 4$ ) were placed on the testing platen in a custom-made bath, and a tare load of 0.01 N was applied. The bath was then filled with 0.1 M PBS at 37 °C to equilibrate under the tare load for 5 min. A 20% ramp strain was then applied at 1 mm/min, followed by stress relaxation for 1.5 hrs. Compressive elastic moduli were determined from the strain-stress curve. The stress relaxation following the ramp strain was fitted by the second order generalized Kelvin model as described by Fung:<sup>323</sup>

$$\sigma(t) = E_R \left[ 1 + \left( \frac{\tau_{\sigma_1}}{\tau_{\epsilon_1}} - 1 \right) \exp\left(-t/\tau_{\epsilon_1}\right) + \left( \frac{\tau_{\sigma_2}}{\tau_{\epsilon_2}} - 1 \right) \exp\left(-t/\tau_{\epsilon_2}\right) \right] \epsilon_0$$

where  $E_R$  is the equilibrium modulus,  $\sigma(t)$  is the stress profile,  $\epsilon_0$  is the ramp strain, and  $\tau_{\sigma}$  and  $\tau_{\epsilon}$  are the creep and stress relaxation time constants, respectively.

### ***Statistical analysis***

All data were expressed as means  $\pm$  one standard deviation, and analyzed by analysis of variance (ANOVA) followed by Tukey's Honestly Significant Difference (T-HSD) post hoc tests. Two-way ANOVAs with interaction were used to determine whether there were differences among either time-points or seeding densities. In addition, one-way ANOVAs were performed to specifically compare the differences among groups at specific time points or at specific densities. A statistical threshold of  $p < 0.05$  was used to indicate whether there were statistical significances among different groups.

## **RESULTS**

### ***Scaffold morphology***

After 4 weeks of culture, the dimensions of the scaffolds decreased to  $20.8 \pm 7.1\%$  of the original volume at the medium density and  $57.2 \pm 9.2\%$  at the high density (Fig. 8.1A). It was not possible to record accurate dimensions for the low density group due to the formation of tiny cell pellets with irregular shapes and poor mechanical integrity. The volume loss corresponded to an increase in the cell density of the scaffolds (Fig. 8.1B). Cell densities in the medium and high density groups each significantly increased from week 0 to week 4 ( $p < 0.05$ ).

### ***Cell number***

A) Volume change

Density	Week 0		Week 4	
	Unseeded	5 M	25 M	50 M
Morphology				
Volume (% of wk 0)	100%	Unstable	20.8±7.1%	57.2±9.2%

5 mm

B) Cell density change

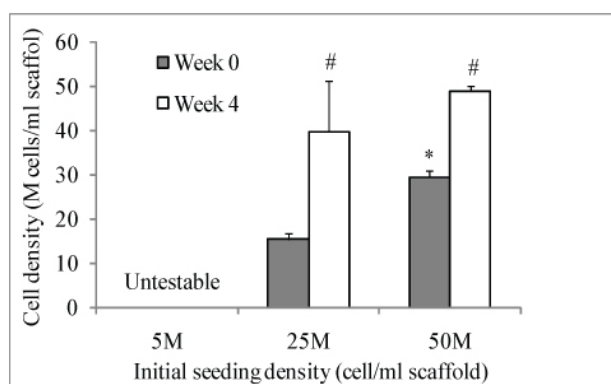


**Figure 8.1:** Scaffold size and cell density (cells per scaffold volume) ( $n = 4$ ). \* = statistically significant difference between the medium and high density groups. # = statistically significant difference between weeks 0 and 4. Error bars represent standard deviations.

There were no significant differences among the seeding efficiencies, with  $56.6 \pm 0.9\%$  at the low density,  $57.3 \pm 5.0\%$  at the medium density, and  $54.7 \pm 2.8\%$  at the high density. The cell numbers in all groups had moderate or significant decreases through the 4-week culture time (Fig. 8.2), despite the increase in cell density. All groups had a significant decrease in cell number between week 0 and week 2. Although the low seeding density group had a significant decrease from week

2 to week 4, there was no significant decrease in either the medium seeding density or high seeding density group between weeks 2 and 4. As expected, the high density group maintained higher cellularity than the medium group over the culture period ( $p < 0.05$ ) (Fig. 8.2). At week 2, the high density group had 2.4 and 14.1 times more cells than the medium group ( $p < 0.05$ ) and the low density group ( $p < 0.05$ ), respectively. At week 4, the high density group had 1.9 and 25.1 times more cells than the medium group ( $p < 0.05$ ) and the low density group ( $p < 0.05$ ), respectively.

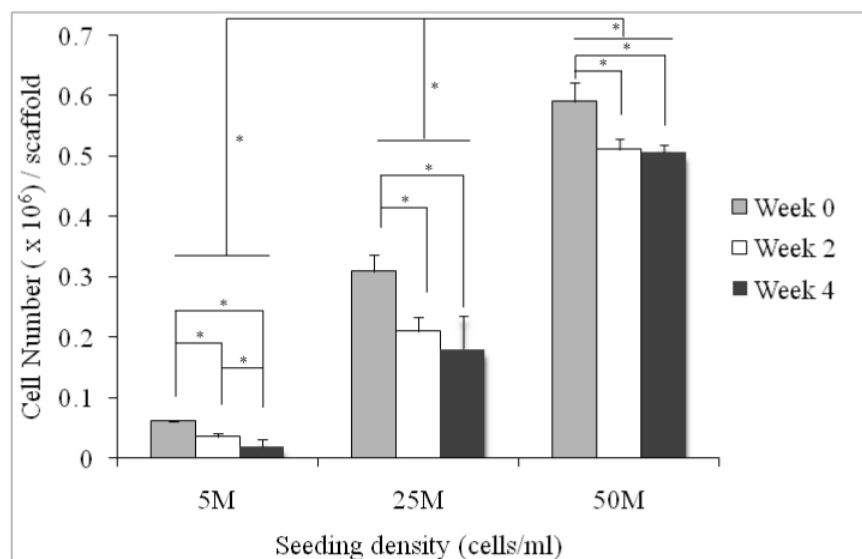
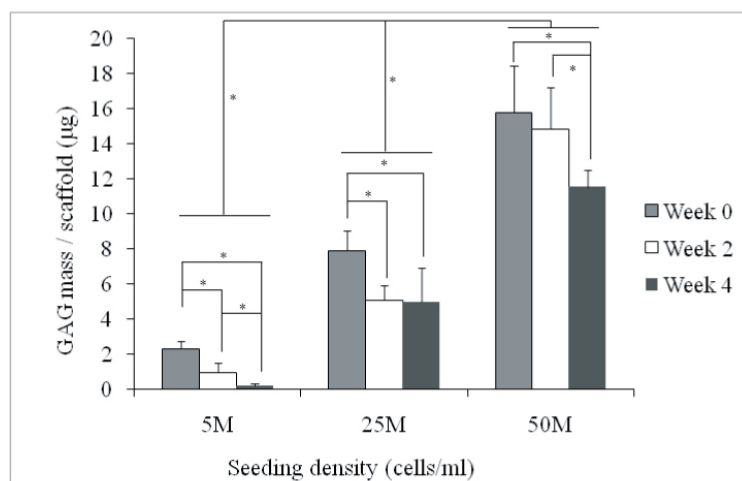


**Figure 8.2:** Cell number per construct with low, medium and high cell seeding density derived from DNA content ( $n = 4$ ). \* = statistically significant difference. Error bars represent standard deviations.

### ***GAG and hydroxyproline content***

There was a significant decrease in the GAG content per construct with all density groups from week 0 to week 4 (Fig. 8.3A). The low density group at week 4

A) GAG content per scaffold



B) GAG content per cell

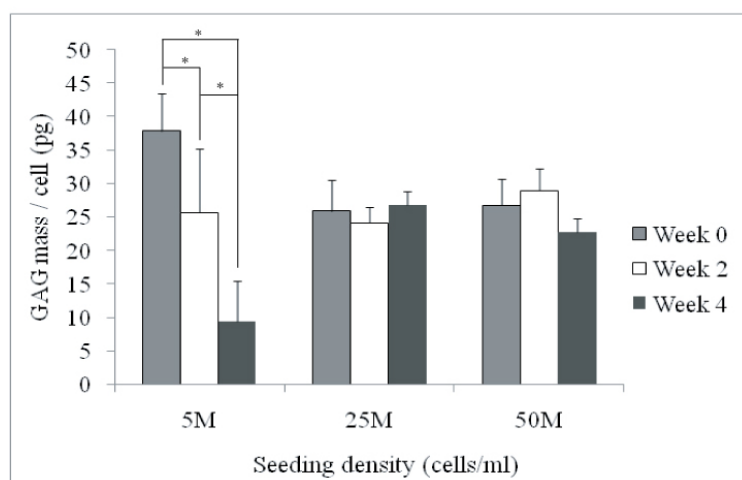
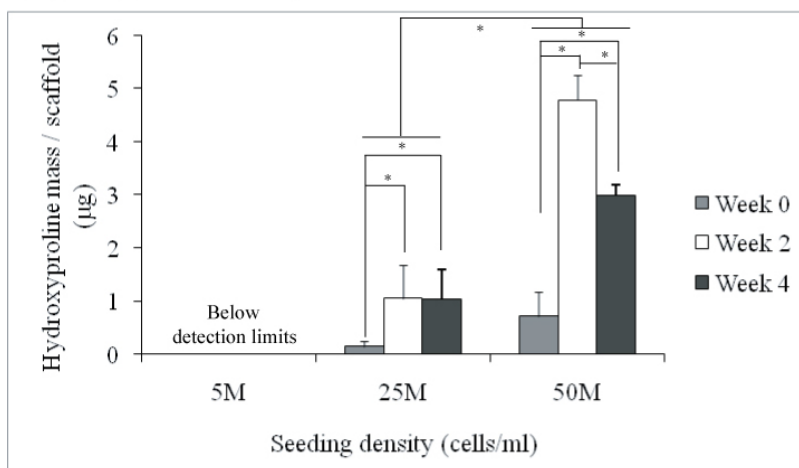


**Figure 8.3:** GAG content per construct (A) and per cell (B) with low, medium and high cell seeding density (n = 4). \* = statistically significant difference. Error bars represent standard deviations.

almost lost all GAG content (less than 1 µg), and the GAG content per cell in the low density group exhibited a decrease as well (Fig. 8.3B). The GAG content per cell in the low density group at week 0 was significantly higher than the medium and high

A) Hydroxyproline content per scaffold



B) Hydroxyproline content per cell

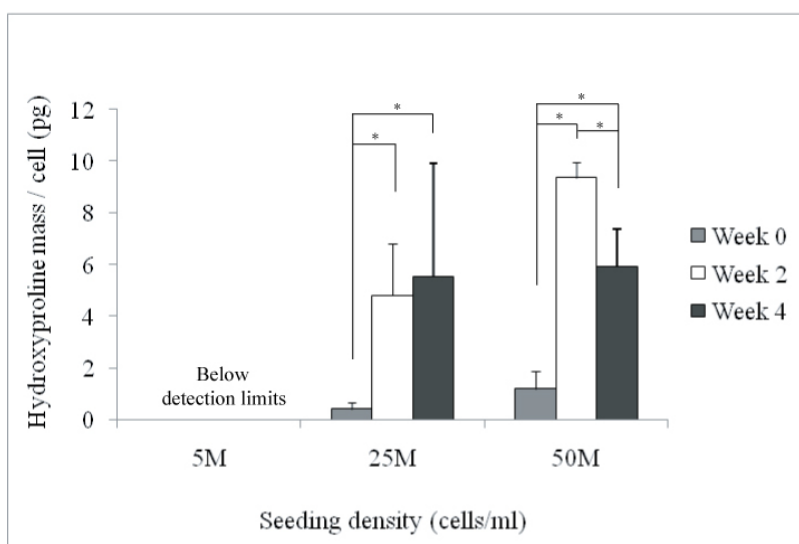


**Figure 8.4:** Hydroxyproline content per construct (A) and per cell (B) with low, medium and high cell seeding density (n = 4). \* = statistically significant difference. Note that the high density group had significantly higher hydroxyproline content per construct than the medium density group. Error bars represent standard deviations. For collagen content, multiply values by a conversion factor of 11.5.

density groups. However, the GAG contents per construct of the medium and high density groups at week 4 were 62.7% and 72.9% of their values at week 0, respectively, while the GAG content per cell between these two groups had no significant differences at any time point. The high density group possessed a higher GAG content per construct than the low and medium density groups at every time point ( $p < 0.05$ ). At week 2, the constructs in the high density group had 2.9 and 15.4 times more GAGs than the medium group ( $p < 0.05$ ) and the low density group ( $p < 0.05$ ), respectively. At week 4, the high density group had 2.3 and 59.6 times more GAGs than the medium ( $p < 0.05$ ) and the low density groups ( $p < 0.05$ ), respectively.

Both the hydroxyproline content per construct and per cell in the medium and high density groups increased significantly after 4 weeks of culture, although there was no detectable hydroxyproline in the low density group (Figs. 8.4). The hydroxyproline contents of the medium and high density groups increased from week 0 to week 2 ( $p < 0.05$ ). There was no difference in hydroxyproline content for the medium density group between weeks 2 to 4. It was interesting that the hydroxyproline content in the high density group decreased by 37.4% from week 2 to week 4 ( $p < 0.05$ ), and hydroxyproline content per cell also had significant decrease. The high density group maintained a higher hydroxyproline content than the medium group at every culture time point ( $p < 0.05$ ). At week 0, the high density group had 5.2 times more hydroxyproline per construct than the medium density group. At week 4, the high density group had 2.9 times more hydroxyproline per construct than the

medium density group ( $p < 0.05$ ). However, there was no significant difference in collagen *density* (content per ml of scaffold) between the low and high density groups at week 4. A conversion factor of 11.5 can be used to convert hydroxyproline mass to collagen mass, based on our preliminary studies (unpublished data).

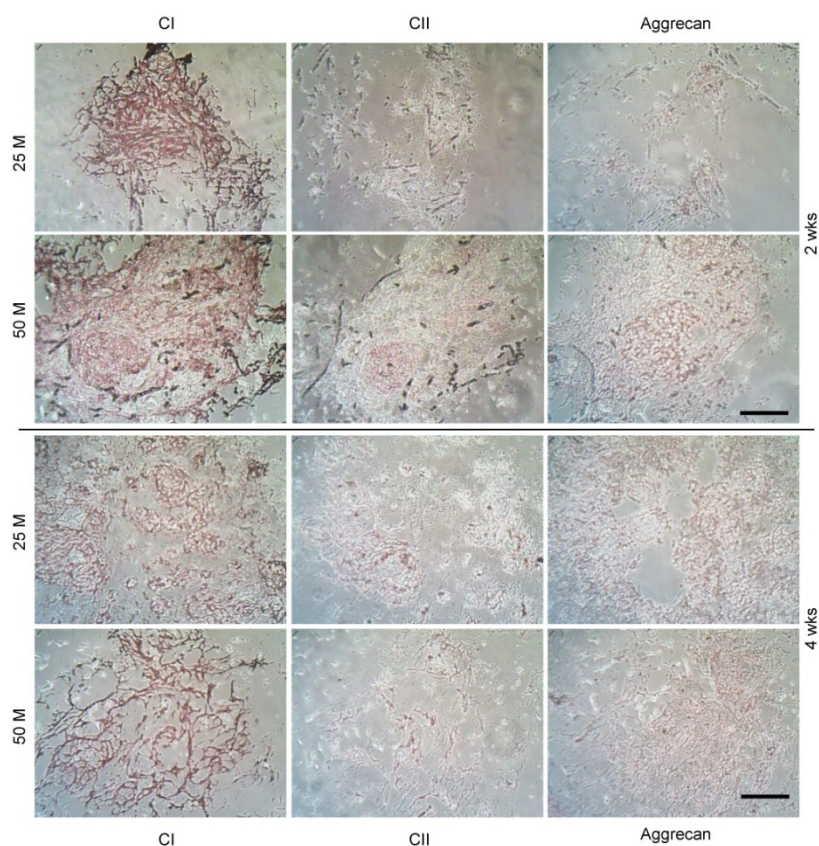


**Figure 8.5:** Immunohistochemical staining for types I and II collagen, and aggrecan.

The scale bar is 100  $\mu\text{m}$ . Moderate type II collagen and aggrecan staining indicates the chondrogenic differentiation of hUCMSCs. CI = type I collagen, CII = type II collagen.

### *Immunohistochemical results*

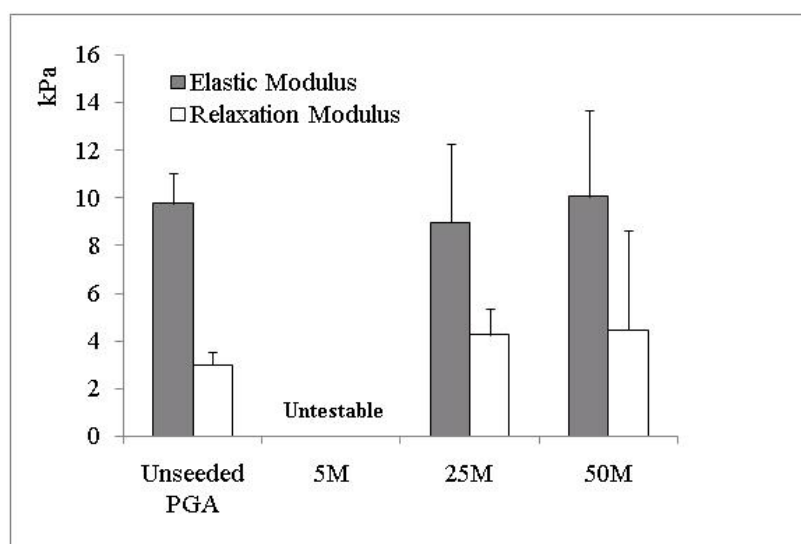


**Figure 8.6:** Mechanical testing of unseeded PGA at week 0 and seeded constructs at week 4. Compressive elastic modulus and relaxation modulus ( $n = 4$ ). \* = statistically significant difference. Error bars represent standard deviations.

Immunohistochemistry revealed positive staining for types I and II collagen, and aggrecan through the 4-week culture (Fig. 8.5). At week 2, immunohistochemical analysis demonstrated intense staining of type I collagen in the medium and high density groups. The high density group had moderate amounts of type II collagen and aggrecan, while the medium density group had no type II collagen and a minute amount of aggrecan. At week 4, both the medium and high density groups had strong staining of type I collagen and moderate staining of type II collagen and aggrecan. In comparison, there was more intense type I collagen staining in medium and high density groups at week 2 than at week 4, and more intense type II collagen and aggrecan staining at week 4 than at week 2. Moreover, the high density group

appeared to have stronger staining of types I and II collagen and aggrecan than the medium density group.

### ***Mechanical properties***

There were no significant differences in both compressive elastic moduli and relaxation moduli among unseeded PGA scaffolds at week 0 and the medium and high density groups at week 4 (Fig. 8.6). Mechanical tests could not be performed on the low density group due to the lack of mechanical integrity.

## **DISCUSSION**

hUCMSCs are fetus-derived cells and more primitive cells compared to adult-derived stem cells based upon their expansion ability *in vitro* and their tissue origin.<sup>200</sup> hUCMSCs have the ability to differentiate toward mesenchymal lineage cells such as cartilage, bone, adipose, and possibly neural cells of the ectodermal lineage.<sup>64, 66, 75-77, 80, 195, 202-204, 208, 210, 225</sup> Moreover, there have been studies in the past 3 yrs that have focused on cardiovascular tissue engineering using hUCMSCs and umbilical cord vein cells.<sup>65, 205, 222, 240, 241, 324</sup> Here, we explored chondrogenic differentiation in 3D PGA scaffolds, and the effects of initial cell seeding density of hUCMSCs for fibrocartilage engineering.

Seeding with orbital shakers demonstrated consistent efficiency (57% at the low density, 57% at the medium density, and 55% at the high density). In a parallel

study, we found higher rotation speeds improved efficiency (data not shown here). All groups decreased cell numbers between week 0 and week 2. At the low density, cell numbers were also significantly decreased from week 2 and week 4. These cell number decreases might be explained by degradation of the PGA scaffolds. In a previous study, quenched PGA demonstrated rapid mass decrease and water content increase after 10 days in PBS at 37 °C.<sup>325</sup> In a previous comparison to poly(lactic-co-glycolic acid) (PLGA; 82:18) and poly-L-lactic acid (PLLA), PGA fibers degraded faster, losing their integrity and becoming fiber fragments in the cell culture medium within 2 weeks.<sup>326</sup> Ideally, extracellular matrix created by hUCMSCs will fill the space created by scaffold degradation. In the low density group, insufficient extracellular matrix was produced due to the low cell number; leading to “contraction” (inward collapse) of the scaffolds. As observed under the microscope during culture, many cells and PGA debris fell into the cell culture medium, and scaffolds lost their mechanical integrity in the low seeding density cultures. In a future experiment, the measurement of cell number and matrix content in the medium can be done to correlate the relationship between scaffold degradation and the loss of cells and matrix. The medium and high seeding densities better maintained mechanical properties due to greater matrix production. Therefore, the medium and high cell seeding densities are recommended for future work with rapidly degrading scaffolds based on cell number and matrix production demands.

In this study, the high density group maintained a higher GAG content throughout the 4 week culture period, although all groups had lower GAG contents at

week 4 than at week 0. Some tissue engineering studies using mature chondrocytes reported the same phenomena of a GAG decrease in hyaluronic acid scaffolds with swine chondrocytes,<sup>327</sup> in poly(ethylene glycol)-co-PLLA hydrogels with calf chondrocytes,<sup>328</sup> and in PGA scaffolds with calf chondrocytes in a perfusion chamber.<sup>329</sup> In cartilage explant culture, medium molecular weight GAGs such as chondroitin and keratan sulfates have been shown to leach out.<sup>330, 331</sup> Thus, it is possible that the drop in GAG content in the current study could in part be attributed to some leaching out of GAGs. Scaffold degradation also may contribute to the decrease of GAG content as discussed in the above section. Extensive PGA scaffold degradation in the low density group not only influenced the direct GAG loss into the culture medium, but also decreased GAG content indirectly by the loss of cells (Fig. 8.3). In the medium and high density groups, the GAG decrease was most likely due to cell loss since the GAG content per cell remained constant. After the 2-day seeding period, the GAG content per cell in the medium and high density groups achieved an equilibrium over 4 weeks of culture. The dynamic environment in the orbital shaker might promote GAG synthesis during the seeding periods.<sup>332-334</sup> It must be noted that the highest GAG content at week 0 does not necessarily indicate the presence of GAGs specific to cartilage proteoglycans.

This study also demonstrated a significant increase in collagen content with the medium and high density groups during the 4-week culture period. At the low density, there was no detectable collagen by hydroxyproline assays due to the dissociation of PGA scaffolds. The rapid increases of hydroxyproline content

occurred between weeks 0 and 2, which helped to maintain the mechanical integrity. There was the same and even decreased hydroxyproline content with the medium density and high density from week 2 to week 4, respectively. During the first two weeks, there was enough space in the scaffolds for collagen synthesis; however, the scaffold shrinkage<sup>141</sup> led to a more dense packing of cells (Fig 8.1). The highly-packed cell and extracellular matrix (especially evident with the high density group at week 2) may limit the nutrient diffusion and also provide limited room for extracellular matrix synthesis, perhaps affecting the balance of the collagen metabolic activity in which collagen catabolism led to the loss of collagen. In native cartilage tissues, collagen contributes primarily to the tensile properties, while GAGs (when associated with aggrecan) contribute to compressive integrity. No such positive correlation was found between matrix content (GAG and collagen) and compressive stiffness, although high collagen content helped retain overall construct integrity. A weak correlation between GAG and collagen contents and mechanical integrity was previously observed in tissue engineering constructs using mature hyaline cartilage cells and fibrocartilage cells.<sup>274, 335</sup> It was not surprising that statistically significant differences in moduli were not observed between groups, as differences would only be expected with much larger increases in matrix content and organization over a longer period of time. Moreover, the larger matrix content in the higher density group was distributed over a larger volume, so it was also not surprising that the modulus variations between the medium and high density groups were minimal.

Compared to mature TMJ condylar cells in a prior study, hUCMSCs did demonstrate a superior performance with 2 times more cells and 4 times more GAGs.<sup>66</sup> However, the contraction was still observed with the highest density of 50 million cells/ml in the current study, along with a commensurate loss of cells and matrix as discussed earlier. More slowly degrading scaffolds such as PLGA or PLLA should be investigated in the future. In fact, PLLA has demonstrated its potential to maintain scaffold integrity with ample matrix production in fibrocartilage tissue engineering with TMJ disc cells.<sup>336</sup> On the other hand, the improvement of seeding technique and culture conditions can aid the tissue-genesis in PGA scaffolds. Highly-packed cells and matrix might block the pathway of nutrition and waste exchange, delaying the tissue-genesis inside of the scaffolds and contributing to the contraction of PGA scaffolds. Perfusion bioreactors might be used to provide a more homogenous cell distribution throughout scaffolds, assist in mass transport, and stimulate cell growth mechanically.<sup>149, 164, 329</sup> Moreover, bioactive signals such as IGF-I and TGF- $\beta$ 1 can enhance biosynthesis to help maintain the original shape of scaffolds.<sup>336</sup>

In the past four years, only four previous studies demonstrated the chondrogenic differentiation of hUCMSCs in cell pellet culture<sup>76, 195, 225</sup> or PGA scaffolds.<sup>66</sup> In comparison to BMSCs, larger pellets were observed in hUCMSC groups with a better filamentous extracellular matrix.<sup>195, 225</sup> hUCMSC pellets had more intense collagen staining than BMSC groups. In a parallel tissue engineering study (unpublished data), hUCMSCs also had a higher cell number, GAG content,

and collagen content than hBMSCs after 6 weeks of culture on PGA scaffolds. Slight type I collagen and plentiful type II collagen were observed with immunohistochemical staining in hUCMSC pellets, while only a trace amount of type II collagen was observed in BMSC pellets.<sup>195</sup> Here, intense type I collagen staining, and moderate collagen type II and aggrecan staining was shown; this is similar to native fibrocartilage. The decrease of type I collagen staining and increase in type II collagen and aggrecan staining from week 2 to week 4 suggests that further chondrogenic differentiation occurred during this period. Despite the lower amount of type II collagen produced in this study in comparison to hBMSCs in the literature,<sup>315</sup> hUCMSCs may progress further down a chondrogenic lineage with more collagen II production with the investigation of a slightly modified set of signals to provide for optimal chondrogenesis. The identification of these signals, with further validation via analysis of gene expression, will be an important area of future investigation.

In conclusion, human umbilical cord matrix mesenchymal stromal cells exhibited characteristics of differentiation along a fibrocartilaginous lineage. The production of an abundance of type I collagen, and a moderate amount of type II collagen and aggrecan suggest that hUCMSCs may be a suitable cell source for fibrocartilage-tissue engineering. A concentrated effort to drive hUCMSCs down an exclusively chondrogenic lineage (collagen II expression and production in lieu of collagen I) will be an exciting area of future investigation. As hypothesized, the constructs in the medium and high density groups had more cells and extracellular matrix (per construct and per cell) than the low density group over 4 weeks of culture,

and more importantly, retained their mechanical integrity, unlike the low density group. Thus, it is recommended that the cell seeding density in related future studies be not less than 25 million hUCMSCs per ml.

## **CHAPTER 9: Insulin-like Growth Factor-I Improves Chondrogenesis of Pre-differentiated Human Umbilical Cord Mesenchymal Stromal Cells\***

### **ABSTRACT**

Human umbilical cord mesenchymal stromal cells (hUCMSCs) are an attractive cell source for tissue engineering with numerous advantages over other adult stem cell sources such as great expansion ability *in vitro* and extensive availability. The objective of this 6-week study was to test the hypothesis that switching from chondrogenic transforming growth factor-beta3 (TGF- $\beta$ 3) to anabolic insulin-like growth factor-I (IGF-I) at the 3-week time point would produce more cartilage-like matrix than TGF- $\beta$ 3 alone. hUCMSCs were seeded into polyglycolic acid (PGA) scaffolds and then cultured in chondrogenic medium containing TGF- $\beta$ 3 for 3 weeks. The TGF- $\beta$ 3-treated hUCMSCs were then exposed for 3 more weeks to one of four different conditions: 1) continued in chondrogenic medium, 2) control medium (no TGF- $\beta$ 3), 3) control medium with 10 ng/ml IGF-I, or 4) control medium with 100 ng/ml IGF-I. Compared to continuing with TGF- $\beta$ 3, switching to IGF-I increased collagen production, and furthermore increased both collagen type II gene expression and immunostaining. In conclusion, the shift from TGF- $\beta$ 3 to IGF-I at week 3 resulted in a significant increase of cartilage-like extracellular matrix, confirming our hypothesis.

---

\*Chapter submitted to J Orthop Res as Wang and Detamore. "Insulin-like growth factor-I improves chondrogenesis of pre-differentiated human umbilical cord mesenchymal stromal cells," August 2008.

## INTRODUCTION

Umbilical cord mesenchymal stromal cells (UCMSCs), extracted from Wharton's jelly of umbilical cords,<sup>200</sup> are a primitive stromal population that possess the characteristics of mesenchymal stromal cells (MSCs) defined by the International Society for Cellular Therapy (ISCT).<sup>196</sup> Human UCMSCs (hUCMSCs) express surface markers that were identified with other mesenchymal stromal cells (MSCs) such as CD73, CD90, CD105, and are negative for hematopoietic markers such as CD34 and CD45.<sup>76, 195, 202, 204, 225</sup> hUCMSCs can differentiate along a variety of cell lineages that can be utilized for tissue engineering and regenerative medicine such as osteogenic, chondrogenic, myogenic, and adipogenic.<sup>64, 76, 77, 195, 225</sup>

In chondrogenic differentiation, transforming growth factor-beta isoforms (TGF- $\beta$ 1,  $\beta$ 2 and  $\beta$ 3) are known to play an important role.<sup>236</sup> In cell pellets, TGF- $\beta$ 1<sup>76</sup> or  $\beta$ 3<sup>195, 225</sup> have been incorporated into serum-free media to induce chondrogenic differentiation that were revealed by a positive immunostaining for type II collagen. In our group, we demonstrated that 3D culture of hUCMSCs in polyglycolic acid (PGA) scaffolds with chondrogenic medium containing TGF- $\beta$ 1 led to a fibrocartilage with intense type I collagen, and moderate type II collagen and aggrecan immunostaining.<sup>66, 207</sup> With hBMSCs, although both TGF- $\beta$ 1 and  $\beta$ 3 were chondro-inductive signals, TGF- $\beta$ 3 appeared to be more effective, leading to higher GAG production and earlier and more extensive type II collagen expression.<sup>236</sup> For this reason, TGF- $\beta$ 3 was chosen as the chondrogenic signal in the current study. Insulin-like growth factor-I (IGF-I), an important anabolic agent for several different

tissues in the body,<sup>337-339</sup> has been demonstrated by most studies to have little or no effect on chondrogenic differentiation,<sup>232, 234</sup> but promoted proliferation and biosynthesis *in vitro* of both mature hyaline cartilage and fibrocartilage cells.<sup>271, 340</sup> On the other hand, how IGF-I sequentially affect the TGF- $\beta$ -treated hUCMSCs and other MSCs is seldom reported in the literature.<sup>341</sup>

In the current study, we cultured hUCMSCs in chondrogenic medium containing TGF- $\beta$ 3 for 3 weeks to induce differentiation in PGA scaffolds, and then switched to IGF-I for another 3-week period. As controls, another group continued in TGF- $\beta$ 3, and another group continued without either TGF- $\beta$ 3 or IGF-I. The rationale for this approach was to determine whether it was possible to first steer the hUCMSCs along the desired path with a chondrogenic signal (TGF- $\beta$ 3), and then to provide a boost in matrix synthesis with an anabolic signal (IGF-I) to provide the best overall results. Therefore, we hypothesized that switching from TGF- $\beta$ 3 to IGF-I at the 3-week time point would produce more cartilage-like matrix than continuing with TGF- $\beta$ 3 for the entire 6-week duration.

## **MATERIALS AND METHODS**

### ***Cord collection and cell isolation***

One human umbilical cord (female, C-section, and 18 cm long) was obtained from the University of Kansas Medical Center (KU Medical Center IRB approval no. 10951, KU-Lawrence IRB approval no. 15402). Cords were first washed in sterile phosphate buffered saline (PBS) three times and then cut into 3-5 cm segments.

Vessels were pulled out from these segments, and the remaining segments were minced and digested in 0.75 mg/ml type II collagenase (298 U/mg; Worthington Biochemical; Lakewood, NJ) at 37°C in an incubator for 4 hrs. This cell solution was centrifuged, and the supernatant was discarded. Finally, cells in the bottom were resuspended in a complete culture medium consisting of low-glucose Dulbecco's modified Eagle's medium (DMEM-LG; Invitrogen, Carlsbad, CA), 10% MSC-qualified fetal bovine serum (FBS; StemCell Technologies, Canada), and 1% penicillin/streptomycin (PS; Invitrogen). Cells were seeded at 8000 cells/cm<sup>2</sup> (P0 cells) in cell culture flasks and the medium was replaced every 2-3 days. At 80-90% confluence, P0 cells were frozen for future use following a previously described procedure.<sup>207</sup>

### ***Cell seeding and culture***

Non-woven PGA meshes (50 mg/cc, >95% porosity) were purchased from Synthecon, Inc. (Houston, TX). The PGA sheets were punched into cylinder-shaped scaffolds that were 5 mm in diameter and 2 mm in thickness, to create a total of 54 scaffolds used in the study. The scaffolds were then processed and seeded into scaffolds at 50 million cells per ml of scaffold according to our previous procedure.<sup>207</sup> Scaffolds were then cultured in 2 ml of chondrogenic medium containing high-glucose DMEM (DMEM-HG; Invitrogen), 1% NEAA, 1× insulin-transferrin-selenium premix (ITS premix; BD Biosciences, San Jose, CA), 20 ng/ml TGF-β3 (RDI, Flanders, NJ, USA), 100 nM dexamethasone (Sigma), 100 mM sodium

pyruvate (Fisher Scientific), 40  $\mu\text{g/ml}$  L-proline (Sigma) and 50  $\mu\text{g/ml}$  ascorbic acid 2-phosphate (Sigma). This time point was recorded as week 0. After 3 weeks of culture, 2 ml of chondrogenic medium was removed and hUCMSCs were exposed for 3 more weeks to one of four different conditions: 1) continue in chondrogenic medium, 2) control medium (no TGF- $\beta$ 3), 3) control medium with 10 ng/ml IGF-I, or 4) control medium with 100 ng/ml IGF-I. Half of the medium was changed every other day over the 6-week period, except for the complete replacement at week 3.

#### ***Assessment of biosynthesis and cell proliferation***

At weeks 0, 3 and 6, constructs (n = 4 per group) were homogenized in 1.2 ml papain solution (120  $\mu\text{g/ml}$ ) and digested at 60 °C overnight for the following biochemical assays. Biosynthesis was evaluated by measuring total GAG and hydroxyproline (HYP) contents. GAG content was measured using a dimethylmethylene blue (DMMB) dye binding assay kit (Biocolor, Belfast, UK) according to the manufacturer's procedure. A modified HYP assay was used to test HYP content as described previously.<sup>207</sup> HYP mass can be converted to collagen mass by using a conversion factor of 11.5, based on our preliminary studies. A PicoGreen kit (Invitrogen) was used to measure DNA content. DNA content was converted to cell number by a conversion factor of 8.5 pg DNA/cell determined in preliminary studies.

#### ***Immunohistochemistry for types I and II collagen and aggrecan***

The primary antibodies were mouse monoclonal IgG anti-collagen I (1:1500 dilution; Accurate Chemical and Scientific, Westbury, NY), mouse monoclonal IgG anti-collagen II (1:1000 dilution; Chondrex, Redmond, WA), and mouse monoclonal IgG anti-aggrecan (1:50 dilution; Abcam, Cambridge, MA). A horse anti-mouse IgG secondary antibody was obtained from Vector Laboratories (Burlingame, CA). The frozen scaffolds were sliced into 10  $\mu\text{m}$  sections, which were then fixed in chilled acetone (4  $^{\circ}\text{C}$ ) for 10 min before staining. Specimens were hydrated and then treated with 1% hydrogen peroxide in methanol to quench endogenous peroxidase. The sections were then blocked in 3% horse serum and then incubated with the primary antibodies for 1 hr. After primary antibody incubation, the sections were incubated with the secondary antibody followed by an avidin-biotinylated enzyme complex (ABC complex; Vector Laboratories). Finally, the sections were visualized with VIP substrate (purple color) (Vector Laboratories). A negative control was designed with the primary antibodies omitted.

### ***RNA isolation and real-time RT-PCR***

The relative mRNA expression level of types I and II collagen, and aggrecan were quantified by using a real-time reverse transcriptase polymerase chain reaction (real time RT-PCR) in an Applied Biosystems (Foster City, CA) 7500 System (n = 4 per group). At weeks 3 and 6, the constructs were homogenized in 1 ml of Trizol reagent (Invitrogen) to isolate total mRNA according to the manufacturer's instruction. The mRNA samples were then converted to cDNA using a High-Capacity

cDNA Archive kit (Applied Biosystems). TaqMan gene expression assay kits (Applied Biosystems) were Hs00164004\_m1 for type I collagen, Hs00156568\_m1 for type II collagen, Hs00153936\_m1 for aggrecan, and Hs99999905\_m1 for glyceraldehyde 3-phosphate dehydrogenase (GAPDH). A  $2^{-\Delta\Delta Ct}$  method was used to evaluate relative the mRNA expression level for each target gene.<sup>312</sup> Briefly,  $\Delta Ct$  values were obtained by the difference between the Ct values of target genes and the GAPDH gene. They were then normalized by subtracting the  $\Delta Ct$  value of the calibrator sample, their respective groups at week 3, to obtain  $\Delta\Delta Ct$  values.

### ***Statistics and data analysis***

Statistical analysis was performed with one-way analysis of variance (ANOVA) followed by Tukey's Honestly Significant Difference (HSD) post hoc tests. The statistically significant differences were determined by a statistical threshold of  $p < 0.05$ .

## **RESULTS**

### ***Cell number***

After the initial seeding period, all groups at weeks 3 and 6 had fewer cells than at week 0 ( $p < 0.05$ ) (Fig. 9.1). However, the cell number was maintained between weeks 3 and 6 in all groups. At week 6, TGF- $\beta$ 3 stimulated cell proliferation with 22% more cells than the control group ( $p < 0.05$ ), whereas IGF-I at both concentrations had no effect on cell proliferation during the last 3 weeks. With regard

to the comparison between TGF- $\beta$ 3 and IGF-I, the TGF- $\beta$ 3 group had 20% more cells than the 10 ng/ml IGF-I group ( $p < 0.05$ ), and no statistically significant difference from the 100 ng/ml IGF-I group.

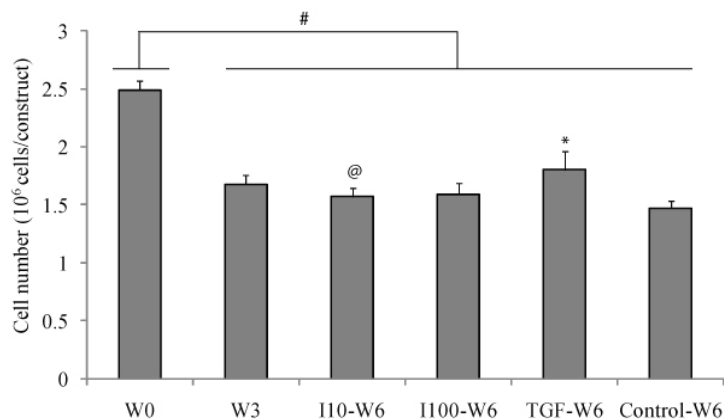


**Figure 9.1:** Cell number at weeks 0, 3, and 6 ( $n = 4$ ). W0 = week 0, W3 = week 3, W6 = week6, I10 = IGF at 10 ng/ml, I100 = IGF at 100 ng/ml, and TGF = TGF- $\beta$ 3 at 20 ng/ml. # = statistically significant difference ( $p < 0.05$ ). @ = statistically significant difference from the TGF- $\beta$ 3 group ( $p < 0.05$ ). \* = statistically significant difference between growth factor groups and the control group at week 6 ( $p < 0.05$ ). Error bars represent standard deviations.

### ***GAG content***

Similar to the cell number result, there was a 37% drop in the GAG content per construct from weeks 0 to 3 ( $p < 0.05$ ), and thus the GAG content per cell maintained the same level in this period (Fig. 9.2). Following this initial decrease of GAG content per construct, there was a recovery with an increase from weeks 3 to 6 ( $p < 0.05$ ) in all groups. The GAG content per construct at week 6 in the IGF-I groups

at 10 and 100 ng/ml, the TGF- $\beta$ 3 group, and the control group increased by 37%, 51%, 44%, and 19%, respectively, compared to at week 3. Among all growth factor groups, only the 100 ng/ml IGF-I group promoted the GAG content per construct with 28% more than the control ( $p < 0.05$ ). Despite a higher GAG content per construct in the TGF group than the control, there was no statistically significant difference between them. Like the GAG content per construct, the GAG content per cell in all groups increased from weeks 3 to 6 ( $p < 0.05$ ). However, there were no significant differences in GAG content per cell among all groups at week 6.

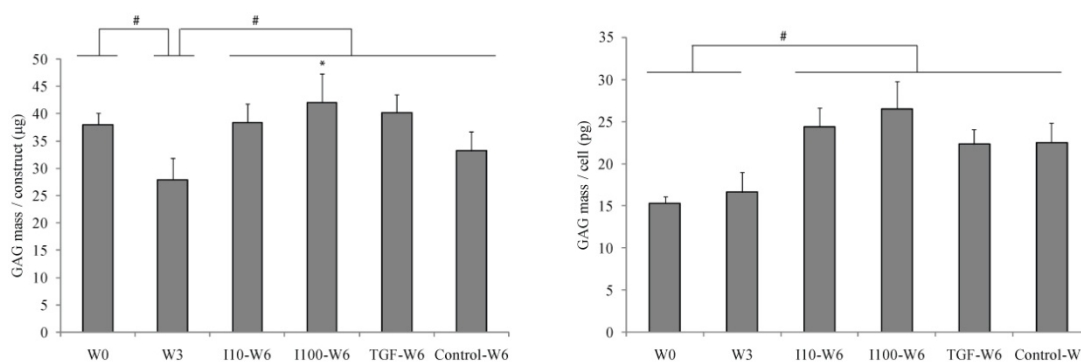


**Figure 9.2:** GAG content per construct and per cell at weeks 0, 3, and 6 ( $n = 4$ ). W0 = week 0, W3 = week 3, W6 = week6, I10 = IGF at 10 ng/ml, I100 = IGF at 100 ng/ml, and TGF = TGF- $\beta$ 3 at 20 ng/ml. # = statistically significant difference ( $p < 0.05$ ). \* = statistically significant difference between growth factor groups and the control group at week 6 ( $p < 0.05$ ). Error bars represent standard deviations.

### ***HYP content***

The HYP content both per construct and per cell increased continuously and markedly throughout the 6-week period ( $p < 0.05$ ) (Fig. 9.3). From weeks 0 to 3, the

HYP content per construct and per cell increased by 4.3 and 6.3 times, respectively ( $p < 0.05$ ). From weeks 3 to 6, the HYP content per construct and per cell increased by 1.5 and 1.6 times, respectively ( $p < 0.05$ ). In comparison to the control group, IGF at both 10 and 100 ng/ml stimulated collagen production with 1.3 and 1.6 times more HYP content per construct, respectively. Moreover, IGF at 100 ng/ml had 1.5 times more HYP content per cell than the control groups, while the TGF- $\beta$ 3 group did not affect the HYP synthesis. Compared to the TGF- $\beta$ 3 group, the 10 and 100 ng/ml IGF-I groups had 1.3 and 1.6 times more HYP content per cell, respectively, and the 100 ng/ml IGF-I group had 1.4 times more HYP content per construct ( $p < 0.05$ ).

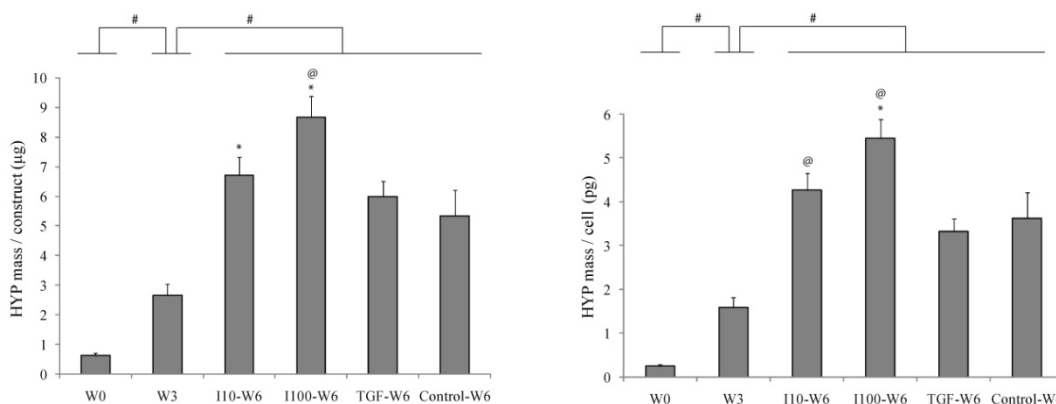


**Figure 9.3:** HYP content per construct and per cell at weeks 0, 3, and 6 ( $n = 4$ ). W0 = week 0, W3 = week 3, W6 = week6, I10 = IGF at 10 ng/ml, I100 = IGF at 100 ng/ml, and TGF = TGF- $\beta$ 3 at 20 ng/ml. # = statistically significant difference ( $p < 0.05$ ). @ = statistically significant difference from the TGF- $\beta$ 3 group ( $p < 0.05$ ). \* = statistically significant difference between growth factor groups and the control group at week 6 ( $p < 0.05$ ). Error bars represent standard deviations.

### *Immunohistochemistry*

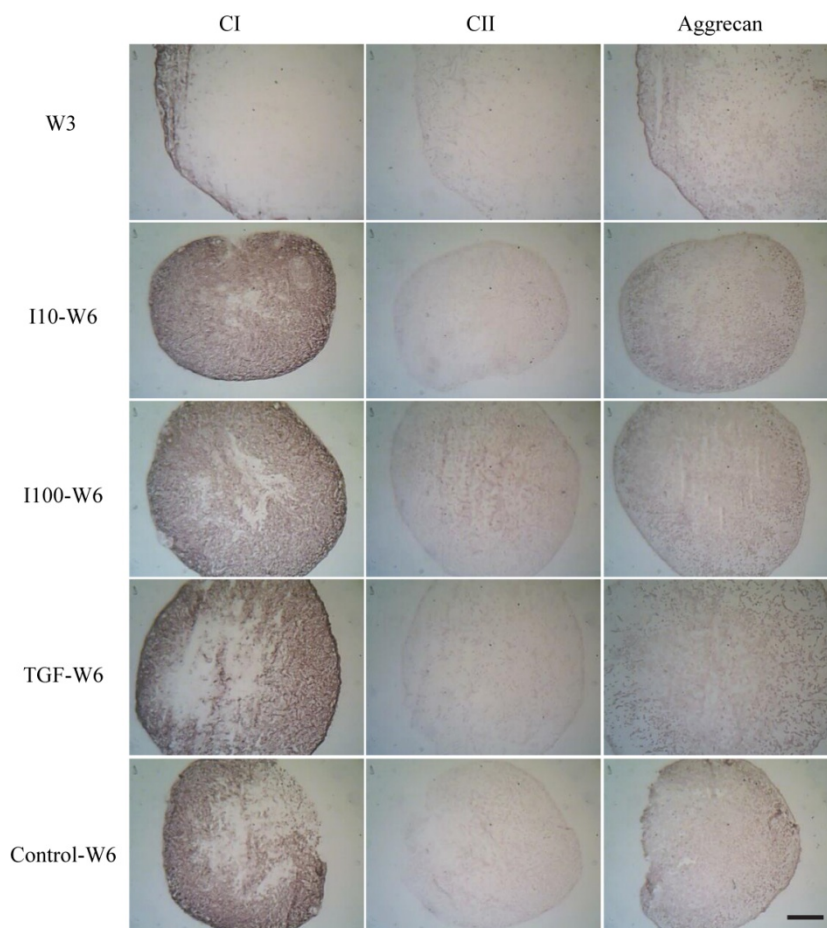


**Figure 9.4:** Immunohistochemical staining for types I and II collagen, and aggrecan (n = 2). CI = type I collagen, CII = type II collagen, W3 = week 3, W6 = week6, I10 = IGF at 10 ng/ml, I100 = IGF at 100 ng/ml, and TGF = TGF- $\beta$ 3 at 20 ng/ml. The scale bar is 500  $\mu$ m.

Immunohistochemistry revealed positive staining for types I and II collagen and aggrecan in all groups through the 6-week period (Fig. 9.4). After exposure to chondrogenic medium for 3 weeks, there was a small amount of type II collagen, a moderate amount of aggrecan throughout the constructs, and type I collagen was

distributed only around the periphery. At week 6, all groups presented a more intense staining for types I and II collagen and aggrecan than at week 3. It must be noted that type I collagen was the dominant collagen type, and that the 100 ng/ml IGF-I group had a stronger staining of type II collagen than other groups, albeit a lower level than type I collagen. With the two IGF-I groups, it was clear that the center of the constructs were more filled in with collagen than with the TGF- $\beta$ 3 and control groups, with type I collagen at both IGF-I concentrations and with type II collagen in the 100 ng/mL IGF-I group.

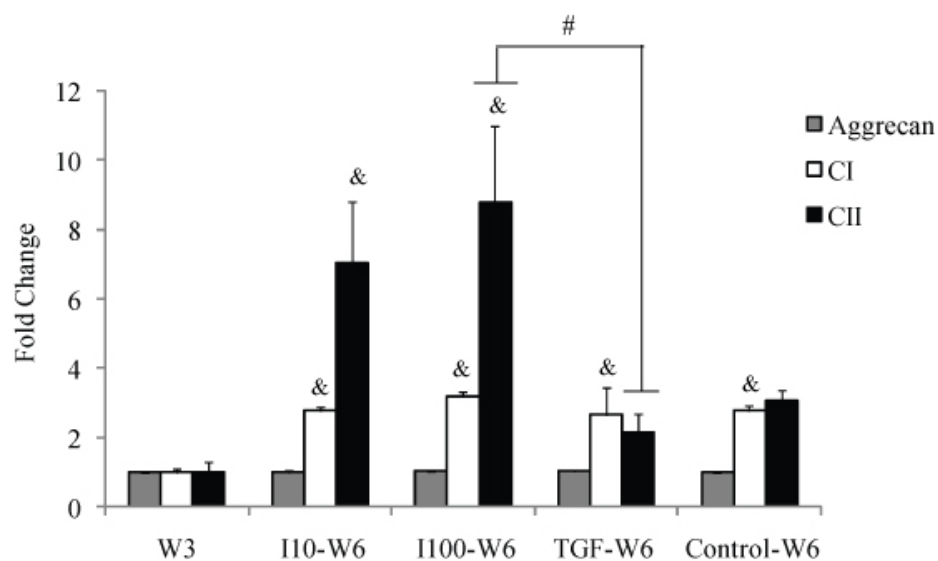


**Figure 9.5:** Gene expression for types I and II collagen, and aggrecan at weeks 3 and 6 (n = 4). CI = type I collagen, CII = type II collagen, W3 = week 3, W6 = week 6, I10 = IGF at 10 ng/ml, I100 = IGF at 100 ng/ml, and TGF = TGF- $\beta$ 3 at 20 ng/ml. # = statistically significant difference (p < 0.05). & = statistically significant difference from week 3 with specific genes (p < 0.05). Error bars represent standard deviations.

***RT-PCR analysis***

From weeks 3 to 6, the mRNA level of type I collagen for all groups and type II collagen for the IGF-I groups were up-regulated at week 6 ( $p < 0.05$ ), whereas aggrecan gene expression in all groups remained at the same level (Fig. 9.5). At week 6, all groups had no statistically significant differences in the gene expression of types I and II collagen and aggrecan from the control group, although the IGF-I groups at 10 and 100 ng/ml had 2.3 and 4.1 times higher gene expression than the control group. However, 100 ng/ml IGF-I did promote a type II gene expression that was 4.1 times higher than with the TGF- $\beta$ 3 group ( $p < 0.05$ ).

**DISCUSSION**

In recent years, hUCMSCs have been explored as a fetus-derived source alternative to other adult stem cells.<sup>196, 200</sup> hUCMSCs have only recently been applied in cartilage tissue engineering, with only two full studies conducted by our group.<sup>66, 207</sup> In the first application of these cells for fibrocartilage engineering, hUCMSCs outperformed native mandibular condylar cartilage cells, leading to higher cellularity and superior matrix production.<sup>66</sup> We further optimized the cell seeding density in PGA scaffolds and reported that a density larger than 25 million per ml was recommended to maintain the scaffold integrity and retain enough cells and extracellular matrix for fibrocartilage engineering.<sup>207</sup> In the current study, we specifically focused on the usage of bioactive signals (TGF- $\beta$ 3 and IGF-I) to better promote cell proliferation and enhance cartilage-specific matrix synthesis in a serum-

free medium. The chondrogenic ability of TGFs is well known and the combination of TGFs and IGF-I have been shown to enhance the chondrogenic differentiation and the GAG production of stem cells.<sup>232, 342</sup> However, there is a paucity of data on the sequential treatment of TGFs and IGF-I in the literature. This study revealed that the switching from TGF- $\beta$ 3 to IGF-I did promote HYP production and also up-regulated the gene expression of type II collagen, which confirmed our hypothesis.

In the first 3 weeks, the chondrogenic medium containing TGF- $\beta$ 3 induced hUCMSCs to differentiate toward a chondrogenic lineage with positive type II collagen and aggrecan immunostaining. During this period, the loss of both cells and GAGs was observed. The decrease in cell number has been found in our previous studies using PGA scaffolds, which degraded rapidly in 2-3 weeks.<sup>207, 259</sup> This degradation rate did not approximate the rate of extracellular matrix synthesis, which caused the contraction of PGA scaffolds and further cell loss into the culture medium.<sup>207, 259</sup> However, the cell number did not decrease further after 3 weeks, indicating that a more stable (confined) construct was achieved. The cell loss might be responsible for the GAG loss, given that the GAG content per cell did maintain at approximately the same level during the first 3 weeks. Therefore, more slowly degrading scaffolds such as poly(L-lactic acid) (PLLA) and poly(lactic-co-glycolic acid) (PLGA) would be beneficial in alleviating the cell and GAG loss in the future. Collagen content increased during this initial period, containing both types I and II collagen as revealed by immunostaining of types I and II collagen. It is interesting that the GAG content reached a high level at week 0 only after 2-day cell seeding,

although it is possible that these GAGs were non-cartilage-specific. After exposure to different medium conditions during the last 3 weeks, the extracellular matrix contents increased, which was consistent with stronger collagen and aggrecan staining. However, the intense type I collagen staining indicated that the increase of collagen mass was mainly due to type I collagen production.

IGF-I is an anabolic agent that regulates chondrocyte proliferation and biosynthesis at all stages of cartilage development.<sup>337, 343</sup> Indeed, after exposure to the medium containing IGF-I, the constructs were shown to have increased GAG and collagen contents compared to the control, while TGF- $\beta$ 3 did not significantly alter either of them relative to the control, despite the higher cell number in the TGF- $\beta$ 3 group. More importantly, in contrast to both the TGF- $\beta$ 3 and control groups, IGF-I had more collagen content per cell (and per construct at 100 ng/ml), indicating that IGF-I did promote collagen synthesis and/or inhibit collagen breakdown in the collagen metabolism process. It was unexpected that IGF-I increased type II gene expression, while continuing treatment of TGF- $\beta$ 3 had no effect on type II collagen gene expression. In spite of the 8.8-fold increase in type II gene expression in the 100 ng/ml IGF-I group from week 3 to 6, type II collagen immunostaining was not as strong as type I collagen. This may be due to the fact that immunostaining reflects the cumulative level of protein synthesized and retained in the construct over time, whereas the gene expression merely represents a snapshot of the cellular disposition at that point in time. The results could imply that with an extended culture period with IGF-I, significantly higher levels of collagen II protein synthesis may have been

observed. Therefore, in the future, a longer culture period will be useful to clarify this seemingly conflicting result. Nevertheless, in the 100 ng/ml IGF-I group, a stronger staining was observed compared to other groups. The up-regulated gene-expression of type II collagen due to the anabolic nature of IGF-I perhaps contributed to this increase.

In conclusion, these results indicated that a shift from a chondrogenic signal (TGF- $\beta$ 3) to an anabolic agent (IGF-I) in the middle of the culture period produced more cartilage-like matrix than continuing with TGF- $\beta$ 3 alone throughout the culture period. The IGF-I concentration of 100 ng/ml has been shown to promote biosynthesis and type II collagen gene expression with hUCMSCs following TGF- $\beta$ 3 treatment and is hence recommended for cartilage tissue engineering. This sequential signaling strategy is also meaningful for other tissue engineering areas using stem cells, as the ability of IGF-I to promote the respective matrix synthesis of a given tissue may prove highly advantageous following differentiation strategies in the initial culture period.

## **CHAPTER 10: Osteogenic Differentiation of Human Umbilical Cord Mesenchymal Stromal Cells for Bone Tissue Engineering\***

### **ABSTRACT**

Although human umbilical cord mesenchymal stromal cells (hUCMSCs) have been shown to differentiate along an osteogenic lineage in monolayer culture, the potential of these cells has never before been investigated in 3D scaffolds for bone tissue engineering applications. In this 6-week study, we demonstrated the osteogenic differentiation of hUCMSCs on polyglycolic acid (PGA) non-woven mesh scaffolds, and compared seeding densities for bone tissue engineering. Cells were seeded into PGA meshes with densities of 5, 25 or 50 x10<sup>6</sup> cells/ml scaffold and then cultured in osteogenic medium. Cell proliferation, osteogenic differentiation, and matrix formation were evaluated at weeks 0, 3, and 6. Osteogenic differentiation was observed based on the positive alkaline phosphatase activity (ALP) and an increase of collagen production and calcium incorporation into the extracellular matrix, which were greater with higher densities. In conclusion, hUCMSCs differentiated along an osteogenic lineage in 3D scaffolds, and higher cell density correlated with greater expression of osteoblast markers. A density greater than 25 x 10<sup>6</sup> cells/ml is recommended for bone tissue engineering with hUCMSCs.

---

\*Chapter submitted to Ann Biomed Eng as Wang, Bonewald, and Detamore. "Osteogenic differentiation of human umbilical cord mesenchymal stromal cells for bone tissue engineering," July 2008.

## INTRODUCTION

Autologous bone grafts are currently the most common clinical treatment of critical-sized bone defects.<sup>111</sup> However, there remain several drawbacks that limit their application, including limited availability, invasive bone tissue harvesting, and donor site morbidity.<sup>111, 344</sup> Bone tissue engineering, which aims to restore the biological and mechanical function of diseased and damaged bone, holds the greatest promise for future clinical practice.<sup>345, 346</sup> This approach integrates cells, bioactive molecules, and biocompatible scaffolds for direct implantation to facilitate bone regeneration *in vivo* or to create a replacement *in vitro* for implantation. Bone marrow-derived mesenchymal stem cells (BMSCs) have been extensively investigated as a cell source for bone tissue engineering.<sup>347</sup> However, the available cell number of BMSCs in bone marrow and their differentiation potential decreases significantly with age.<sup>248, 348</sup> Moreover, the harvesting procedure is painful, invasive, and may lead to complications and morbidity.<sup>249</sup>

Recently, umbilical cord mesenchymal stromal cells (hUCMSCs) have been explored as a promising cell source for tissue engineering and regenerative medicine.<sup>196</sup> UCMSCs are extracted through enzyme digestion from Wharton's jelly of umbilical cords,<sup>200, 206</sup> which yields  $10\text{-}50 \times 10^3$  cells per cm of cord, corresponding to approximately  $2\text{-}10 \times 10^5$  primary cells per cord. hUCMSCs express classic surface markers identified in BMSCs including CD29, CD44, CD90, CD105, and CD166<sup>80, 195</sup> and markers found in embryonic stem cells including Oct-4, Nanog, and Sox-2 transcription factors.<sup>201</sup> With exogenous signals such as dexamethasone<sup>76, 195, 204, 208</sup> or

osteoinductive biomaterials such as demineralized bone matrix,<sup>239</sup> hUCMSCs have been shown to differentiate along the osteogenic lineage, confirmed by positive von Kossa staining,<sup>76, 195, 204, 208</sup> Alizarin red staining,<sup>195</sup> alkaline phosphatase activity (ALP),<sup>76, 195, 204, 208, 239</sup> osteopontin gene up-regulation,<sup>76, 204</sup> and bone-related proteins such as osteopontin, osteonectin, osteocalcin, and bone sialoprotein-2.<sup>195</sup> Their osteogenic ability accompanied by numerous other advantages over hBMSCs indicates that hUCMSCs may be a promising candidate as a stem cell source for bone tissue engineering.

Osteogenic differentiation of hUCMSCs in three-dimensional (3D) scaffolds is heretofore unexplored in the literature, and is a significant leap forward from differentiation studies in monolayer culture. In a 3D environment, many parameters, such as the biocompatibility of materials, diffusion parameters, and cell seeding methods, are known to affect cell differentiation and proliferation and extracellular matrix synthesis.<sup>349</sup> In the current study, we focused on the effects of initial cell seeding density on hUCMSC differentiation. We have recently shown in a chondrogenic application of hUCMSCs that a seeding density above  $25 \times 10^6$  cells/mL was optimal.<sup>207</sup> In another study, a low cell seeding density resulted in a low seeding efficiency in a PLGA scaffold and delayed *in vivo* mineralization.<sup>350</sup> Furthermore, in collagen scaffolds, high seeding densities of hBMSCs augmented scaffold contraction<sup>351</sup> and a specific range of seeding densities ( $3\text{-}30 \times 10^6$  cells/ml) enhanced osteoblastic differentiation of osteosarcoma cell line.<sup>349</sup> The present study thus aimed to investigate how the seeding density of hUCMSCs affected their osteogenic

differentiation and subsequent matrix production in a 3D environment. The hypothesis for this study was that a higher seeding density would result in enhanced osteogenic differentiation with an increase in bone-related matrix synthesis.

## **MATERIALS AND METHODS**

### ***Cell harvest***

Human umbilical cord collection and cell harvests were approved by the University of Kansas human subject board (KU-Lawrence IRB approval no.15402, KU Medical Center IRB approval no.10951). One human umbilical cord (Female, C-section, 26cm long) was collected from the University of Kansas Medical Center and processed within 24 hrs. Cords were first cut into 3-5 cm pieces, and then vessels were removed from each cord segment. Cord segments were minced and incubated in 0.75 mg/ml type II collagenase (298 U/mg; Worthington Biochemical; Lakewood, NJ) at 37°C. After a 5-hr incubation, a homogenous gelatinous solution was obtained and diluted (1:8) in sterile phosphate buffered saline (PBS). The solution was centrifuged, the supernatant was discarded, and cells were resuspended in a complete culture medium consisting of low-glucose Dulbecco's modified Eagle's medium (DMEM-LG; Invitrogen, Carlsbad, CA), 10% MSC-qualified fetal bovine serum (FBS; StemCell Technologies, Canada), and 1% penicillin/streptomycin (PS; Invitrogen). Cells were plated in cell culture flasks at 8000 cells/cm<sup>2</sup> (P0 cells) and fed every two to three days. When cells had reached 80-90% confluence, they were detached by 1X trypsin (Invitrogen) and resuspended at a density of 1 x10<sup>6</sup> cells per

ml freezing medium, composed of 90% FBS and 10% dimethyl sulfoxide (DMSO; Fisher Scientific, Pittsburgh, PA). The cell suspension was transferred into cryotubes (Nalgene Labware, Rochester, NY), which were stored in “Mr. Frosty” freezing containers (Nalgene) at  $-80^{\circ}\text{C}$  overnight, and transferred to a liquid nitrogen cryogenic storage system at  $-196^{\circ}\text{C}$  for future use.

### ***Cell culture and seeding***

Cells were thawed and expanded to P4 in the complete medium. Non-woven PGA meshes (50 mg/cc; > 95% porosity; Synthecon, Houston, TX) were punched into 96 cylinder-shape scaffolds with a 5 mm diameter and 2 mm thickness, and then sterilized with ethylene oxide. After sterilization, the scaffolds were aired under a fume hood for one day, then wetted with sterile filtered ethanol and two washes of sterile phosphate buffered saline (PBS). The scaffolds were then soaked in the complete medium in 24-well plates for one day and then removed for cell seeding. P4 hUCMSCs were seeded at 5 (low), 25 (medium) and 50 (high)  $\times 10^6$  cells per ml of scaffold. 400  $\mu\text{l}$  of cell solution was transferred to well plates and pipetted 10 times through the scaffolds. Well plates were then set on orbital shakers at 150 rpm for 24 hours. In the medium and high density groups, this small amount of medium containing a large amount of cells yielded a highly concentrated cell solution, which caused the formation of several cell clusters in the medium, some of which attached lightly to the peripheral area of PGA scaffolds and detached from the edge when the medium was changed during the following culture. After the first 8 hours, the cell

clusters in the medium were removed and 400  $\mu$ l of medium was added. After the 24 hour orbital shaking period, cells were allowed to attach statically in the culture medium for another day. Finally, the complete medium was replaced by 2 ml osteogenic medium, which was the complete medium plus 100 nM dexamethasone (Sigma, St. Louis, MO), 10 mM  $\beta$ -glycerophosphate (Sigma), 50  $\mu$ g/ml ascorbic acid 2-phosphate (Sigma), and 10 nM  $1\alpha,25$ -Dihydroxyvitamin D<sub>3</sub> (BIOMOL International, Plymouth Meeting, PA). This time point was recorded as week 0. 1.5 ml of medium was changed every other day for 6 weeks. At weeks 3 and 6, separate groups of constructs were analyzed for hydroxyproline content, alkaline phosphatase activity, calcium content, and histological analysis. Hydroxyproline content was also measured at week 0 to demonstrate minimal initial differences in matrix content between groups.

#### ***Cell number and hydroxyproline (HYP) content***

Constructs (n = 4) were homogenized in 1.2 ml papain solution (120  $\mu$ g/ml) using a tissue homogenizer (Omni International, Marietta, GA), and incubated in this solution at 60 °C overnight, before storing at -20 °C for future biochemical assays. The DNA content was determined by using a PicoGreen kit (Invitrogen) according to the manufacturer's protocol. A conversion factor of 8.5 pg DNA/cell was determined in preliminary studies and used to convert DNA content to cell number. HYP content was determined by using a HYP assay as described previously.<sup>311</sup> Briefly, each sample was hydrolyzed with sodium hydroxide, neutralized with hydrochloric acid,

and then titrated to a pH range from 6.5 to 7.0. This solution was combined with Chloramine-T buffer and p-dimethylaminobenzaldehyde in perchloric acid and read spectrophotometrically at 550 nm. A conversion factor of 11.5 can be used to convert HYP mass to collagen mass, based on our preliminary studies.

#### ***Alkaline phosphatase (ALP) activity***

Constructs (n = 4) were homogenized in 500  $\mu$ l of 0.2% Triton X-100 (Sigma) and lysed twice using freeze–thaw cycles. The lysate was used to determine alkaline phosphatase activity following a previously described method.<sup>352</sup> In brief, 20  $\mu$ l of lysate was combined with 80  $\mu$ l of 1.5 M 2-amino-2-methyl-1-propanol (AMP; Sigma) buffer (pH 10.3) containing 5 mM p-nitrophenol phosphate substrate (Sigma). For the standard curve, serial dilutions of 0–20 nM p-nitrophenol (Sigma) were made in triton solution. The reaction was stopped by adding 100  $\mu$ l of 0.5 M NaOH. The solution was then read spectrophotometrically at 405 nm. ALP activity was normalized to total DNA content.

#### ***Calcium content***

Constructs (n = 4) were homogenized, suspended in 1N acetic acid overnight, and stored at -20 °C for future assays. An OCPC (ortho-cresolphthalein complexone) method was used to measure calcium content as described previously.<sup>353</sup> The OCPC solution consisted of 1 mg/ml OCPC in a buffer including 0.0063 N KOH and 0.0031 N acetic acid. The working solution contained 0.05 mg/ml OCPC solution, 0.74M

ethanolamine/boric acid buffer (pH 11), and 2% 8-hydroxyquinoline (5 g in 100 mL of 95% ethanol). 0–100 mg/ml  $\text{CaCl}_2$  solution (Sigma) was used as the standard. A solution including 50  $\mu\text{l}$  of culture sample and 250  $\mu\text{L}$  of working solution was incubated for 10 min at room temperature and then read spectrophotometrically at 575 nm.

### ***Histology***

Samples were embedded in an OCT compound (Tissue-Tek, Torrance, CA) and frozen sections (10  $\mu\text{m}$ ) ( $n = 2$ ) were cut using a cryostat (Micron HM-550 OMP, Vista, CA). Sections were incubated with 1% silver nitrate solution in a clear plastic Coplin jar, placed under ultraviolet light for 20 minutes and then rinsed in ultra-pure water. Finally, the samples were dehydrated through graded alcohol (95% and 100% twice each).

### ***Statistical analysis***

All data were expressed as means  $\pm$  one standard deviation, and analyzed by analysis of variance (ANOVA) followed by Tukey's Honestly Significant Difference post hoc tests. Two-way ANOVAs with interaction were used to determine whether there were differences among either time-points or seeding densities. A statistical threshold of  $p < 0.05$  was used to indicate whether there were statistical significances among different groups.

## RESULTS

### *Scaffold morphology and cell number*

The shape of the scaffolds changed from cylindrical at week 0 to spherical at weeks 3 and 6. Scaffold volume decreased in all groups over the course of the 6-week period, with higher density groups being larger than lower density groups (Fig. 10.1A). There were significant differences among the seeding efficiencies, with

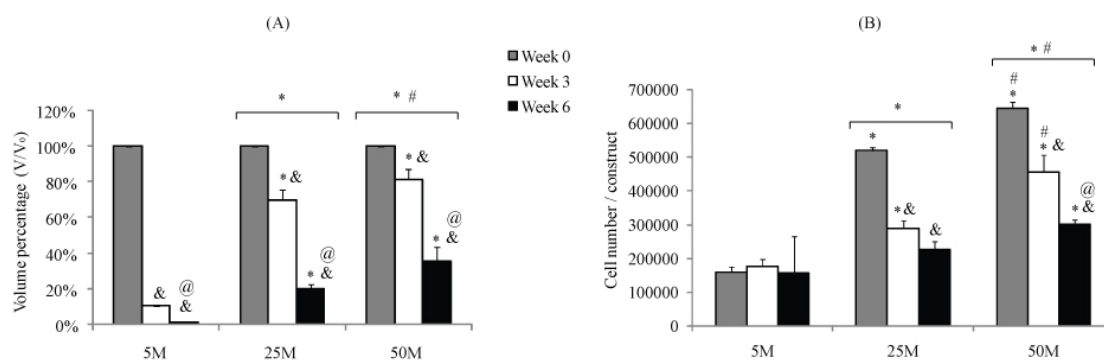


**Figure 10.1:** Construct volume (A) (n = 3) and cell number per construct (B) (n = 4).

\* = statistically significant difference (p < 0.05) from the low density group (5M). # = statistically significant difference between the medium density (25M) and high density (50M) groups. & = statistically significant difference from week 0. @ = statistically significant difference between weeks 3 and 6. The symbols in top brackets represent significant differences between the different density groups throughout the whole culture period. V in Part A represents the scaffold volume. V<sub>0</sub> in Part A represents the scaffold volume at week 0. Error bars represent standard deviations. A conversion factor of 8.5 pg DNA/cell was used to convert DNA content to cell number.

84.7 ± 8.1% at the low density, 55.1 ± 2.1% at the medium density, and 34.2 ± 5.8% at the high density ( $p < 0.05$ ) (Fig. 10.2). On the whole, cell number decreased with time ( $p < 0.05$ ) throughout the culture period (Fig. 10.1B). The higher density groups had more cells than the lower density groups (5M < 25M < 50M) ( $p < 0.05$ ). The low density group maintained cell number over the 6-week culture time, the medium density group decreased in cell number only from weeks 0 to 3 ( $p < 0.05$ ), and the high density group decreased in cell number at both weeks 3 and 6 ( $p < 0.05$ ). It is interesting that with the drastic drop in the volume of the low density group, the cellularity (cells per volume) in the medium and high density groups was significantly lower than in the low density group at week 6 ( $p < 0.05$ ). There was no significant difference in cellularity between the medium and high density groups.

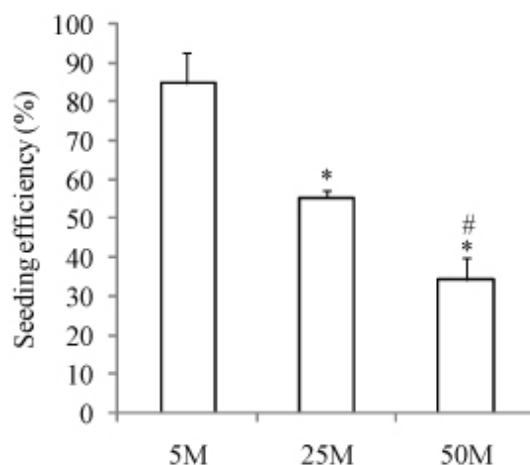


**Figure 10.2:** Seeding efficiency ( $n = 4$ ). \* = statistically significant difference ( $p < 0.05$ ) from the low density group (5M). # = statistically significant difference between the medium density (25M) and high density (50M) groups. Error bars represent standard deviations.

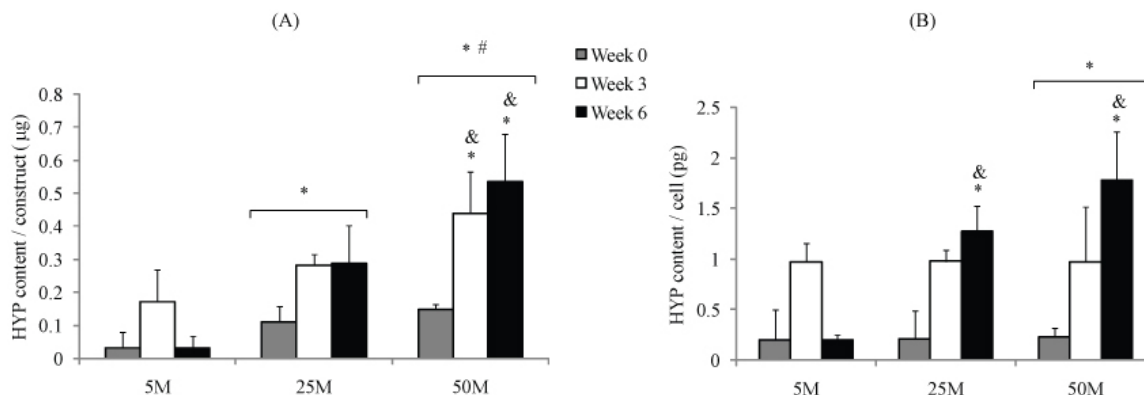


**Figure 10.3:** Hydroxyproline (HYP) content per construct (A) and per cell (B) ( $n = 4$ ). \* = statistically significant difference ( $p < 0.05$ ) from the low density group (25M). & = statistically significant difference from week 0. # = statistically significant difference between the medium density (25M) and high density (50M) groups. The symbols in top brackets represent significant differences between the different density groups throughout the whole culture period. Error bars represent standard deviations.

### ***HYP content***

The higher density group maintained a higher HYP content per construct during the 6-week culture period ( $5M < 25M < 50M$ ) ( $p < 0.05$ ) (Fig. 10.3A). The high density group had 2.3 and 17 times more HYP content per construct than the low density group at weeks 3 and 6 ( $p < 0.05$ ), respectively, while there was no significant difference between the low density and medium density groups at weeks 3 and 6. In the high density group, HYP content per construct increased by 2.0 and 2.6 times at weeks 3 and 6 relative to week 0 ( $p < 0.05$ ), respectively. With regard to HYP content per cell, the high density group had significantly higher content than the low density

group ( $p < 0.05$ ), while no significant difference was detected between the medium and high density groups (Fig. 10.3B). At week 6, the medium and high density groups had 6.4 and 9.0 times more HYP content per cell, respectively, than the low density group ( $p < 0.05$ ). Both the medium and high density groups had more HYP content per cell at week 6 than at week 0 ( $p < 0.05$ ), while there were no significant differences between weeks 3 and 6. It was interesting that in the low density group, the highest HYP content per construct and per cell were observed at week 3, although there were no significant difference among weeks 0, 3, and 6.

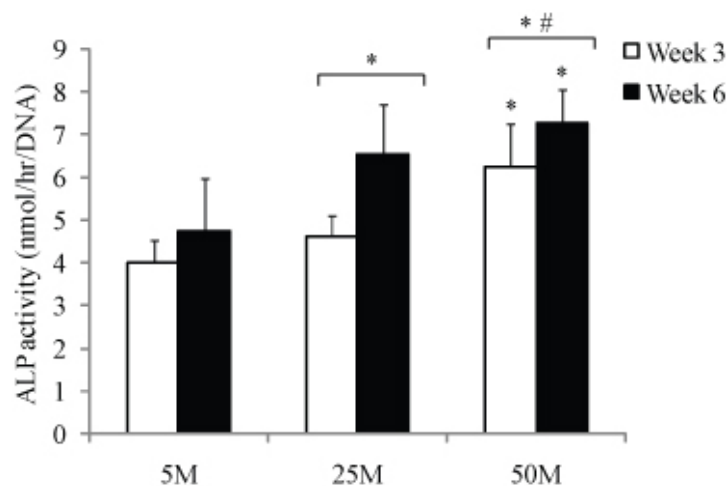


**Figure 10.4:** Alkaline phosphatase (ALP) activity at weeks 3 and 6 ( $n = 4$ ). \* = statistically significant difference ( $p < 0.05$ ) from the low density group (5M). # = statistically significant difference between the medium density (25M) and high density (50M) groups. The symbols in top brackets represent significant differences between the different density groups throughout the whole culture period. Error bars represent standard deviations.

### *ALP activity*

The higher density groups had a higher level of ALP activity (measured on a per DNA basis) than the lower density groups (5M < 25M < 50M) ( $p < 0.05$ ) (Fig. 10.4). At week 6, the medium and high density groups had 38.1% ( $p > 0.05$ ) and 53.9% ( $p < 0.05$ ) more ALP activity than the low density group, respectively. From weeks 3 to 6, mean values of ALP activities increased for all three groups, although these differences were not statistically significant.

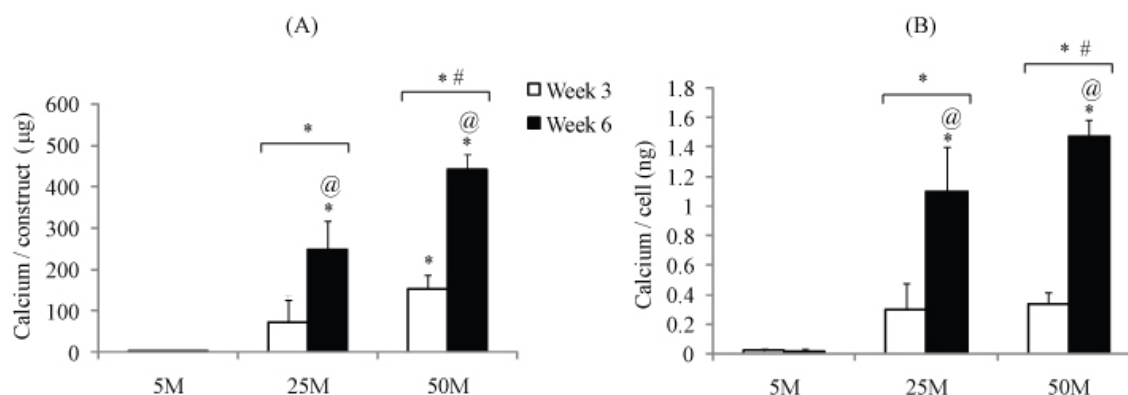


**Figure 10.5:** Calcium content per construct (A) and per cell (B) at weeks 3 and 6 ( $n = 4$ ). \* = statistically significant difference ( $p < 0.05$ ) from the low density group (5M). # = statistically significant difference between the medium density (25M) and high density (50M) groups. @ = statistically significant difference between weeks 3 and 6. The symbols in top brackets represent significant differences between the different density groups throughout the whole culture period. Error bars represent standard deviations.

### ***Calcium content and von Kossa staining***

In general, the higher density constructs had higher calcium content both per construct (Fig. 10.5A) and per cell (Fig. 10.5B) than at a lower density ( $p < 0.05$ ) (5M

< 25M < 50M). Only a small amount of calcium (less than 4  $\mu\text{g}$  per construct and 0.02 ng per cell) was detected in the low density group. Both the medium and high density groups at week 6 had 2.9 times more calcium content per construct than at week 3 ( $p < 0.05$ ). Calcium content per cell in the medium and high density groups at week 6 was 3.7 and 4.4 times higher than at week 3 ( $p < 0.05$ ), respectively. The low density group maintained calcium content at a low level between weeks 3 and 6, both per construct and per cell. von Kossa staining suggested that mineralization increased with time and with seeding density (Fig. 10.6), which was consistent with calcium quantification.

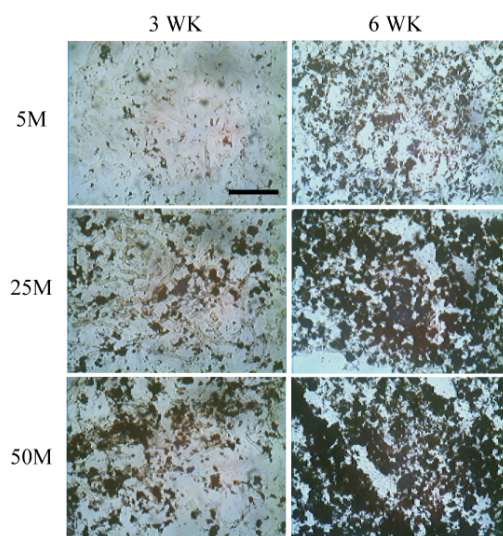


**Figure 10.6:** von Kossa staining at 3 and 6 weeks ( $n = 2$ ). The mineralization increased with time and seeding density. The scale bar is 50  $\mu\text{m}$ . 5M, 25M, and 50M means the low, medium, and high density groups, respectively.

## DISCUSSION

In this decade, there has been an increasing interest in new cell sources for tissue engineering and regenerative medicine. Mesenchymal stem cells (MSCs) with multilineage potential have been identified in various tissues including bone marrow,<sup>318</sup> adipose tissue,<sup>188</sup> blood,<sup>189, 354</sup> synovial fluid,<sup>190</sup> dermis,<sup>191</sup> muscle,<sup>355</sup> dental pulp,<sup>356</sup> and umbilical cord stroma.<sup>80</sup> In the present study, we demonstrated for the first time that hUCMSCs harvested from umbilical cord stroma formed bone-like tissues *in vitro* in a 3D biomaterial-based environment. Biochemical assays and histological staining revealed the positive ALP activities of hUCMSCs in osteogenic medium and the deposition of bone-specific extracellular matrix (calcium and phosphate groups) throughout the constructs. We also showed that a higher seeding density promoted osteogenic differentiation and matrix production by hUCMSCs in PGA scaffolds. These results validated our hypothesis that hUCMSCs can differentiate along osteogenic lineage showed that a higher density is results in better osteogenic differentiation and matrix biosynthesis than lower densities.

hUCMSCs are a promising cell source for tissue engineering for numerous compelling reasons.<sup>200</sup> First, hUCMSCs are developmentally primitive cells that have been shown to differentiate along mesenchymal lineages and cross into the ectodermal germ layer with neural differentiation.<sup>64, 66, 75-77, 80, 195, 202-204, 208, 210, 225</sup> Second, umbilical cords are in abundant supply and easily accessible, therefore these cells have practical advantages over both embryonic stem cells and BMSCs. Thirdly, following cell harvesting, hUCMSCs can be expanded 300-fold for over seven passages without the loss of differentiation potential.<sup>195</sup> The rapid proliferation rate

and availability make it possible to obtain a large amount of cells in a short time (orders of magnitude larger than BMSCs). Fourthly, there is no donor site morbidity and there are no sensitive political issues. hUCMSCs can be frozen at birth (as is commonly done with cord blood) as an autologous cell source. Fifth, as an allogeneic source, several studies have supported their immunocompatibility and even immunosuppressive nature of hUCMSCs.<sup>77, 78, 80, 254</sup> In fact, Weiss and colleagues<sup>78, 80, 357</sup> have demonstrated that UCMSCs survived in the extreme case of xenotransplantation, with no evidence of a host immune response for up to 12 weeks. All of these characteristics make hUCMSCs a suitable, attractive, and potentially preferred cell source for tissue engineering. However, the application of hUCMSCs for tissue engineering is virtually unexplored with only a few studies conducted in the past 3 years, some of which have focused on cardiovascular tissue engineering.<sup>65, 205, 222, 240, 241, 324</sup> Our group has focused on the application of hUCMSCs in cartilage<sup>66, 207</sup> and now bone tissue engineering (the current study).

In the current study, different seeding densities led to noticeable differences in seeding efficiency. The lower seeding efficiency at higher density was explained by cell aggregation (the formation of cell clusters) in the medium during the initial seeding period. We have improved the seeding efficiency at high densities by pipetting the cell solution in two-hour intervals for 8 hours to prevent the formation of cell clusters for the future studies. Nonetheless, the higher density groups had more cells after seeding and maintained the higher cell numbers compared to the lower density groups over the duration of the culture period. The cell number decreased

over time in the medium and high density groups. There are several possible explanations for this reduction. First, dexamethasone is known to inhibit cell proliferation. Second, the degradation rate of PGA scaffolds was faster than the rate of matrix production, leading to a decrease in volume over time (the contraction of scaffolds). During the contraction, many cells and PGA debris fell into the medium, which was observed under a microscope. This cell loss due to degradation has been observed in other studies with PGA scaffolds in cartilage tissue engineering<sup>207</sup> and with collagen scaffolds in bone tissue engineering.<sup>138</sup> A scaffold with a slower degradation rate (e.g. poly(L-lactic acid) (PLLA), poly(lactic-co-glycolic acid) (PLGA)) might help to retain cells in scaffolds. In fact, we have observed in our unpublished work that PLLA with hUCMSCs results in over 80% seeding efficiency and maintains its original shape in over 6 weeks of culture with hUCMSCs.

The formation of extracellular matrix and the osteogenic differentiation of hUCMSCs were clearly influenced by the initial seeding densities. The constructs in the higher density groups had noticeably more HYP and calcium than the lower density groups. More importantly, the higher density groups had more HYP and calcium content per cell than the lower density groups, indicating that the high density promoted extracellular matrix production for the average cell. In addition, the high calcium content per cell and ALP activities in the high density group suggest that high seeding density improved the osteogenic differentiation of hUCMSCs. It was unexpected that the level of ALP activities at week 6 was slightly higher than at week 3, since ALP is typically an earlier marker in osteogenic differentiation.

However, there were no statistically significant differences between these two time points for the different seeding densities. Given that ALP activity is an early osteogenic indicator of stem cells,<sup>358</sup> we anticipated that ALP activities of hUCMSCs before week 3 would be remarkably higher than the ALP level we reported here, which illustrates a need for further investigation of ALP activities over time.

Cell-cell interaction influences cell behavior and extracellular matrix synthesis in both 2D<sup>359</sup> and 3D<sup>349</sup> environments. In this study, cell densities were determined by the initial seeding density and scaffold volume. Throughout the 6 weeks of culture, the low density group formed a dense pellet with highly packed cells in a small amount of extracellular matrix, indicating a high cellularity might hinder extracellular matrix synthesis. In contrast, the medium and high density groups with a lower cellularity had more active bone-like extracellular matrix synthesis as evidenced by the high HYP and calcium content per cell and higher ALP activities. In the future, it will be interesting to determine the effect of hUCMSCs cell density on osteogenic differentiation by using a more slowly degrading scaffold that provides a fixed volume.

In summary, the osteogenic differentiation of hUCMSCs in a 3D biomaterial-based environment provides the foundation for future applications of this new cell source for bone tissue engineering. A higher seeding density in PGA scaffolds is a critically important factor to promote extracellular matrix synthesis and osteogenic differentiation. Given the clear advantages of hUCMSCs discussed earlier, and their capacity for osteogenic differentiation shown here, we therefore conclude that

hUCMSCs are indeed a highly desirable cell source for bone tissue engineering, and that a high seeding density is desirable for matrix production and osteogenic differentiation in 3D PGA scaffolds. Following this initial proof of concept, the optimization of osteogenic culture environment and the use of a scaffold with a slower degradation rate should be investigated in the future, with an in depth analysis of the quality of mineralization.

## **CHAPTER 11: Signaling Strategies for Osteogenic Differentiation of Human Umbilical Cord Mesenchymal Stromal Cells for 3D Bone Tissue Engineering\***

### **ABSTRACT**

Human umbilical cord mesenchymal stromal cells (hUCMSCs) have recently shown the capacity to differentiate into multiple cell lineages in all three embryonic germ layers. The osteogenic differentiation of hUCMSCs in monolayer culture has been reported, while the differentiation in three-dimensional biomaterials has not yet been reported for tissue engineering applications. Thus, the aim of this study was to evaluate the feasibility of using hUCMSCs for bone tissue engineering. hUCMSCs were cultured in poly(L-lactic acid) (PLLA) scaffolds in either an osteogenic medium (OM) or a control medium (CM) for 3 weeks, after which there were five different conditions: 1) continuing culture in the CM, 2) continuing culture in the OM, 3) shift from culturing in the OM, to a mineralization medium (MM) 4) shift from culturing in the OM to the MM with 10 ng/ml insulin-like growth factor (IGF)-I (I10), or 5) shift from culturing in the OM, to the MM with 100 ng/ml IGF-I (I100). The osteogenic differentiation was confirmed by the up-regulation of Runx2 and OCN, calcium quantification, and bone histology. Switching from the OM to the MM promoted collagen and calcium per cell, while continuing in the OM retained more cells in the constructs and had higher osteogenic gene expression. The addition of IGF-I into the MM had no effect on cell proliferation and differentiation and matrix synthesis. These results suggest that hUCMSCs seeded on PLLA scaffolds are

---

\*Chapter submitted to J Tissue Eng Regen Med as Wang, Bonewald, and Detamore. "Signaling strategies for osteogenic differentiation of human umbilical cord mesenchymal stromal cells for 3D bone tissue engineering," August 2008.

suitable for bone tissue engineering and culturing in the OM throughout the entire period is beneficial for bone tissue engineering.

## INTRODUCTION

Bone tissue engineering is a promising interdisciplinary field, in which cells can be integrated into biomaterials to provide a substitute for bone grafts. Indeed, human bone marrow mesenchymal stromal cells (hBMSCs) have been translated into clinical trials via a tissue engineering approach to treat bone defects successfully in a 7-year clinical trial.<sup>246, 247</sup> However, there are some known disadvantages associated with hBMSCs such as the relative number of hBMSCs in the marrow, a limited proliferation ability, and inferior differentiation potential in aged individuals.<sup>248</sup> Moreover, the invasive and painful harvesting procedure may cause donor site morbidity and complications.<sup>249</sup>

Recent evidence has shown that human umbilical cord mesenchymal stromal cells (hUCMSCs) are a primitive and multipotent stromal population that shares similar characteristics with hBMSCs.<sup>196, 200</sup> hUCMSCs are isolated from the Wharton's Jelly of umbilical cords, a routinely discarded tissue after delivery. They are non-hematopoietic cells that can adhere to plastic surfaces for *in vitro* expansion and have many surface markers that are identical to hBMSCs, such as CD73, CD90, and CD105.<sup>76, 77, 195, 199, 202, 204</sup> They are multipotent, differentiating along a variety of cell lineages in all germ layers such as chondrocytes, osteoblasts, adipocytes,

myocytes, neurons, and hepatocytes.<sup>76, 77, 195, 199, 202, 204</sup> Apart from the similarity to hBMSCs, hUCMSCs have a number of particular advantages over hBMSCs such as extensive availability and supply, no donor site morbidity, fast proliferation, and great *in vitro* expansion ability like other fetus-derived stem cells. All of these features render hUCMSCs attractive for tissue engineering as a mesenchymal stromal cell (MSC) source.

hUCMSCs have demonstrated their osteogenic differentiation in two-dimensional (2D) monolayer culture after exposure to chemical signals containing dexamethasone and  $\beta$ -glycerophosphate,<sup>76, 77, 195, 204, 208, 225</sup> and osteoinductive biomaterials such as demineralized bone matrix.<sup>239</sup> However, most studies regarding osteogenic differentiation of hUCMSCs are reported briefly in a qualitative way with histological stains such as Alizarin Red S staining and von Kossa staining.<sup>76, 77, 195, 204, 208, 225</sup> In addition, osteogenic differentiation of hUCMSCs in three-dimensional (3D) biomaterials is still unexplored in the literature. In our group, we have previously revealed that osteogenic differentiation can be achieved in polyglycolic acid (PGA) scaffolds, although the rapid degradation rate of PGA led to a loss of cells and construct integrity (unpublished data). Like PGA, poly(L-lactic acid) (PLLA) has been extensively investigated in tissue engineering applications with good biodegradability, biocompatibility, and mechanical properties, but is more slowly degraded. In a phosphate-buffered solution (PBS) at 37 °C, quenched PGA demonstrated a rapid decrease in mass after 10 days,<sup>325</sup> while in another study,<sup>360</sup> PLLA meshes almost had no loss of mass after 35 weeks in the same buffer.

Therefore, non-woven PLLA meshes were used in the current study as support for cell growth and bone formation during the *in vitro* osteogenesis of hUCMSCs.

The majority of bone tissue engineering studies using BMSCs have been conducted with an osteogenic medium (OM) throughout the entire culture period (up to 6 weeks),<sup>138, 361</sup> although osteogenic differentiation of BMSCs can be accomplished in 2-3 weeks with extensive mineralization.<sup>58, 351, 358</sup> However, it is unknown how the OM affects the differentiated MSCs. Thus, in the current study, we cultured hUCMSCs with the OM in slowly degrading PLLA scaffolds for 3 weeks, and then removed osteogenic components (dexamethasone and Vitamin D<sub>3</sub>) to expose pre-differentiated hUCMSCs to a mineralization medium (MM) and an insulin-like growth factor (IGF)-I-containing MM for another 3 weeks. The negative and positive controls were no and continued exposure to osteogenic components, respectively. The goal of this study was to examine *in vitro* osteogenesis with both qualitative and quantitative data and determine the effects of the medium shift on osteogenically-induced hUCMSCs.

## **MATERIALS AND METHODS**

### ***Isolation and culture of hUCMSCs***

IRB approval was obtained for human umbilical cord collection and hUCMSC isolation from KU-Lawrence (no. 15402) and the KU Medical Center (no. 10951). In this study, two human umbilical cords (both female, 15 and 23 cm long) were first cut

into 3-5 cm segments, from which vessels were then removed. Cord segments were cut into 1-2 mm<sup>3</sup> pieces and incubated at 37°C in 0.75 mg/ml type II collagenase (298 U/mg; Worthington Biochemical; Lakewood, NJ). A 5-hr incubation yielded a homogenous gelatinous solution, which was then diluted (1:8) in sterile phosphate buffered saline (PBS). hUCMSCs were obtained by centrifugation and then resuspended in an expansion medium containing low-glucose Dulbecco's modified Eagle's medium (DMEM-LG; Invitrogen, Carlsbad, CA), 10% MSC-qualified fetal bovine serum (FBS; StemCell Technologies, Vancouver, BC, Canada), and 1% penicillin/streptomycin (PS; Invitrogen). Cells were plated in cell culture flasks at 8000 cells/cm<sup>2</sup>, expanded to 80-90% confluence (recorded as P0 cells) and detached by 1X trypsin (Invitrogen). Following a previously described procedure,<sup>207</sup> P0 cells were cryogenically stored in liquid nitrogen at -196°C for future use.

### ***Scaffold preparation, cell seeding and differentiation***

hUCMSCs were thawed and expanded in the expansion medium to P4 for cell seeding. Cylinder-shaped scaffolds (n = 83), 5 mm in diameter and 2 mm in thickness, were cut out of non-woven PLLA meshes (> 95% porosity and 45–55% crystallinity; Biomedical Structures, Warwick, RI, USA). The scaffolds were sterilized in a sterile pouch using ethylene oxide and then placed in a fume hood. Before seeding, scaffolds were wetted with sterile-filtered ethanol followed by two PBS washes, and then immersed for one day in the expansion medium. P4 hUCMSCs were resuspended in the expansion medium and then seeded at 25 x10<sup>6</sup> cells per ml of

scaffold into PLLA scaffolds using an orbital shaker at 150 RPM according to a previously described protocol<sup>340</sup>. The expansion medium was referred as to the control medium (CM) over the following culture period. After a 2-day seeding period (week 0), some of the scaffolds were continually cultured in the CM and the remaining were cultured in the OM by replacing the CM with 1.5 ml of the OM, consisting of the CM supplemented by 100 nM dexamethasone (DEX; Sigma, St. Louis, MO), 5 mM  $\beta$ -glycerophosphate ( $\beta$ -GP; Sigma), 10 nM  $1\alpha,25$ -Dihydroxyvitamin D3 (VD3; BIOMOL International, Plymouth Meeting, PA), and 50  $\mu$ g/ml ascorbic acid 2-phosphate (AA2P; Sigma). After 3 weeks, there were five different culture conditions: (1) continue culture in the CM, (2) continue culture in the OM, (3) change culture from the OM to the MM, which consisted of the OM without DEX and VD3, (4) change culture from the OM to the MM with 10 ng/ml IGF-I (I10), or (5) change culture from the OM to the MM with 100 ng/ml IGF-I (I100). 1 ml of medium was changed every other day, except for the complete replacement at weeks 0 and 3.

### ***Biochemical assays***

Constructs (n = 4) were homogenized in 1.2 ml papain solution (120  $\mu$ g/ml) and then incubated at 60 °C overnight. A PicoGreen kit (Invitrogen) was used to determine DNA contents according to the manufacturer's protocol. A hydroxyproline (HYP) assay was used to obtain HYP content by using as described previously.<sup>207</sup> A conversion factor of 8.5 pg DNA/cell was used to convert DNA content to cell

number, and a conversion factor of 11.5 can be used to convert HYP mass to collagen mass, based on our preliminary studies.

Calcium content was quantified by an OCPC (ortho-cresolphthalein complexone) method as described in the literature.<sup>353</sup> Constructs (n = 4) were homogenized and suspended in 1N acetic acid (Sigma) overnight. 50  $\mu$ l of this culture sample or a standard solution (0–100 mg/ml CaCl<sub>2</sub>; Sigma) was added into 250  $\mu$ L of working solution. The working solution contained 0.05 mg/ml OCPC solution (1 mg/ml OCPC, 0.0063 N KOH and 0.0031 N acetic acid) (Sigma), 0.74M ethanolamine/boric acid buffer (pH 11; Sigma), and 2% 8-hydroxyquinoline (5 g in 100 mL of 95% ethanol; Sigma). This mixture was incubated at room temperature for 10 min and then read at 575 nm.

### ***Histology***

Frozen sections (10  $\mu$ m, n = 2) were used for histological analysis. Alizarin Red S and von Kossa staining were used to visualize the mineralization. Sections were fixed in 10% phosphate-buffered formalin for 20 min and then rinsed in ultrapure water before staining. For Alizarin Red S staining, sections were incubated with 2% Alizarin Red S reagent (PH = 4.1 - 4.3; Sigma) for 5 min. For von Kossa staining, sections were incubated with 1% silver nitrate solution (Sigma) under ultraviolet light for 20 minutes and then with 5% sodium thiosulfate (Sigma) for 5 minutes to remove un-reacted silver. Finally, all sections were rinsed in ultrapure water and dehydrated through graded alcohol (95% and 100% twice each).

### ***RNA isolation and real-time RT-PCR***

Total RNA was extracted from cells using 1 ml of Trizol reagent (Invitrogen) following the manufacturer's instructions (n = 4). Total RNA concentration and purity were determined on a spectrophotometer (Nanodrop; Wilmington, DE). The mRNA samples were then converted to cDNA using a High-Capacity cDNA Archive kit (Applied Biosystems, Foster City, CA) following the supplier's procedure. TaqMan gene expression assay kits (Applied Biosystems) were used for transcript levels of type I collagen (CI), runt-related transcription factor 2 (Runx2), and osteocalcin (OCN) using a real-time reverse transcriptase polymerase chain reaction (real time RT-PCR) in an Applied Biosystems 7500 System. TaqMan gene expression assay kits (Applied Biosystems) were Hs00164004\_m1 for type I collagen, Hs00231692\_m1 for Runx2, Hs01587813\_g1 for OCN, and Hs99999905\_m1 for glyceraldehyde 3-phosphate dehydrogenase (GAPDH). A  $2^{-\Delta\Delta Ct}$  method was used to evaluate relative the mRNA expression level for each target gene.<sup>312</sup> Briefly,  $\Delta Ct$  values were obtained by the difference between the Ct values of target genes and the GAPDH gene. They were then normalized by subtracting the  $\Delta Ct$  value of the calibrator sample, their respective Ct values in the CM groups, to obtain  $\Delta\Delta Ct$  values.

### ***Statistical analysis***

All data were expressed as means  $\pm$  one standard deviation, and analyzed by one-way ANOVAs followed by Tukey's Honestly Significant Difference post hoc tests. Statistical significance was determined by a statistical threshold of  $p < 0.05$ .

## RESULTS

### *Cell number*

Over the 6-week culture period, cell number decreased in all groups ( $p < 0.05$ ) compared to week 0 (Fig. 11.1). Despite the cell loss throughout the culture period,

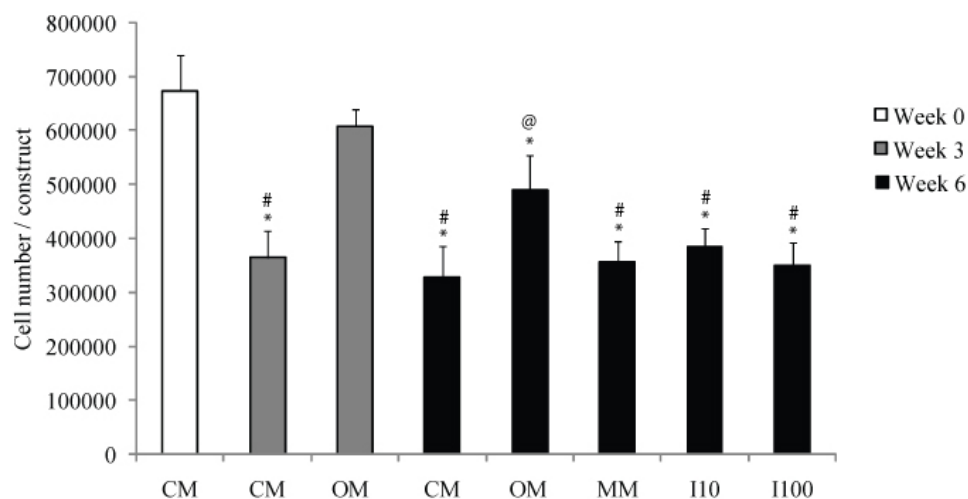


**Figure 11.1:** Cell number per construct ( $n = 4$ ). CM = control medium, OM = osteogenic medium, MM = mineralization medium, I10 = MM containing 10 ng/ml IGF-I, and I100 = MM containing 100 ng/ml IGF-I. \* = statistically significant difference ( $p < 0.05$ ) from week 0. # = statistically significant difference ( $p < 0.05$ ) from the OM group at weeks 3 or 6. @ = statistically significant difference ( $p < 0.05$ ) in the OM group between weeks 3 and 6. Error bars represent standard deviations. A conversion factor of 8.55 pg DNA/cell was used to convert DNA content to cell number.

the OM groups at weeks 3 and 6 retained 1.67 and 1.50 times more cells in the constructs than the CM groups, respectively ( $p < 0.05$ ). From weeks 0 to 3, the cell number decreased by 46% in the CM group ( $p < 0.05$ ), while only decreasing by 10% in the OM group without statistical significance. In contrast, from weeks 3 to 6, the cell number decreased in the CM group only by 10% without statistical significance, while decreasing by 19% in the OM group ( $p < 0.05$ ). The medium change at week 3 (from OM to MM, I10, and I100) caused a decrease in cell number ( $p < 0.05$ ) and there were no significant differences in cell number between the MM, I10, and I100 groups.

### ***HYP content***

In all groups but the CM group, the HYP content per construct and per cell increased over time, with a substantial leap from weeks 0 to 3 ( $p < 0.05$ ) (Fig. 11.2). In the CM groups, the HYP content per construct did not vary over the 6-week culture period and the HYP content per cell had a slight increase without statistical significance. The OM group had 4.2 and 3.5 times more HYP per construct than the CM group at weeks 3 and 6, respectively ( $p < 0.05$ ), and had 2.5 and 2.4 times more HYP per cell than the CM group at weeks 3 and 6, respectively ( $p < 0.05$ ). The shift from OM to MM, I10, or I100 did not affect the total HYP content per construct, while this change did lead to an up-regulation of HYP synthesis, given that the HYP content per cell was approximately 50% greater in the MM, I10 and I100 groups

compared to the OM group at week 6 ( $p < 0.05$ ). Like the cell number, HYP synthesis was not influenced by the addition of IGF-I into the MM.

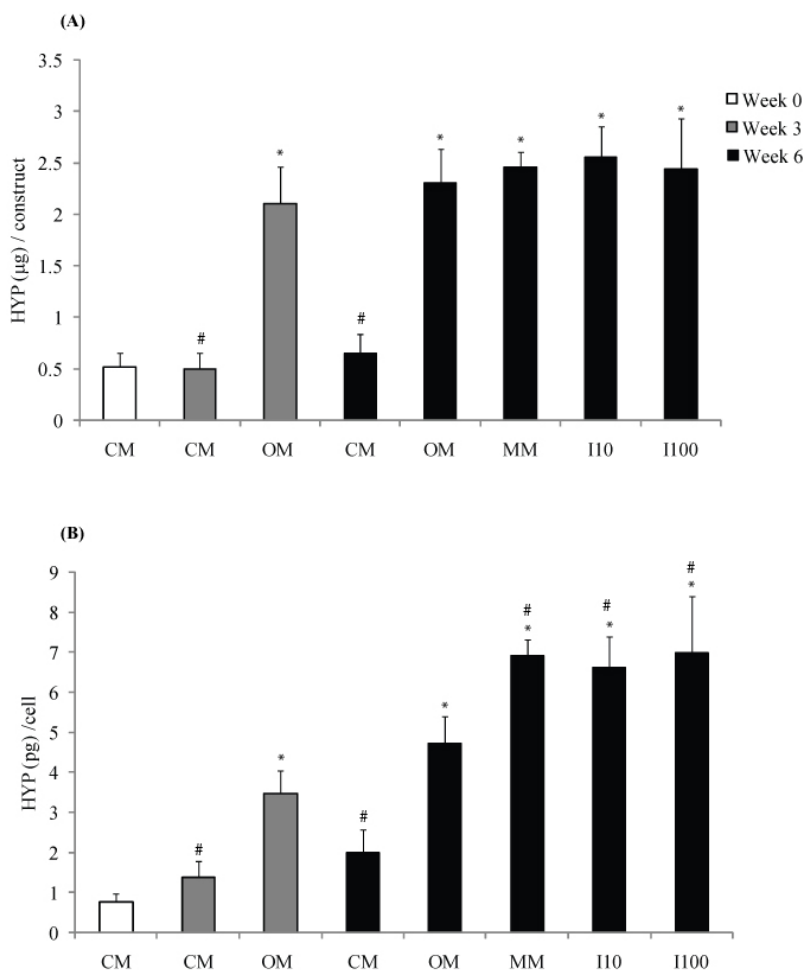


**Figure 11.2:** Hydroxyproline (HYP) content per construct (A) and per cell (B) ( $n = 4$ ). CM = control medium, OM = osteogenic medium, MM = mineralization medium, I10 = MM containing 10 ng/ml IGF-I, and I100 = MM containing 100 ng/ml IGF-I. \* = statistically significant difference ( $p < 0.05$ ) from week 0. # = statistically significant difference ( $p < 0.05$ ) from the OM group at weeks 3 or 6. Error bars represent standard deviations.

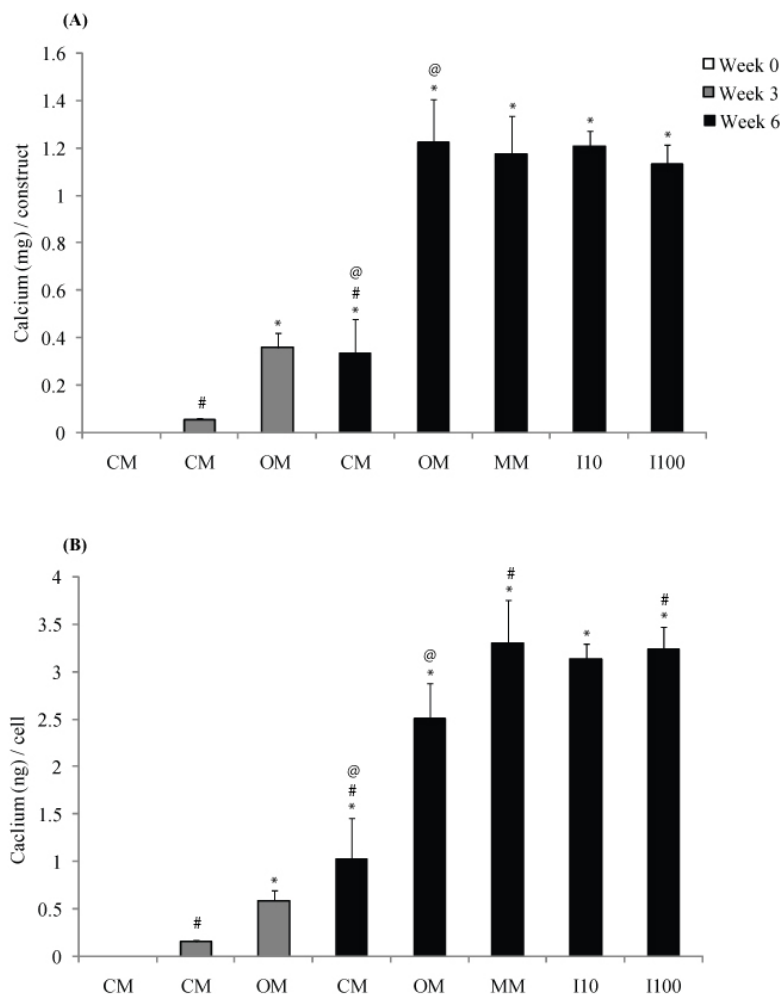


**Figure 11.3:** Calcium content per construct (A) and per cell (B) (n = 4). CM = control medium, OM = osteogenic medium, MM = mineralization medium, I10 = MM containing 10 ng/ml IGF-I, and I100 = MM containing 100 ng/ml IGF-I. \* = statistically significant difference (p < 0.05) from week 0. # = statistically significant difference (p < 0.05) from the OM group at weeks 3 or 6. @ = statistically significant difference (p < 0.05) between weeks 3 and 6. Error bars represent standard deviations.

### *Calcium content*

There was a considerable increase in calcium content per construct and per cell with time in all groups over the culture period ( $p < 0.05$ ) (Fig. 11.3). Calcium deposition was also observed in the CM group, albeit at a low level. However, the OM group did exhibit more calcium per construct and per cell than the CM group at weeks 3 and 6 ( $p < 0.05$ ). At week 6, there was no significant difference in calcium content per construct among the OM, MM, I10, and I100 groups, while the MM and I100 groups had 1.32 and 1.29 more times calcium content per cell than the OM group, respectively ( $p < 0.05$ ). No significant differences were observed in calcium content per cell among the MM, I10, and I100 groups.

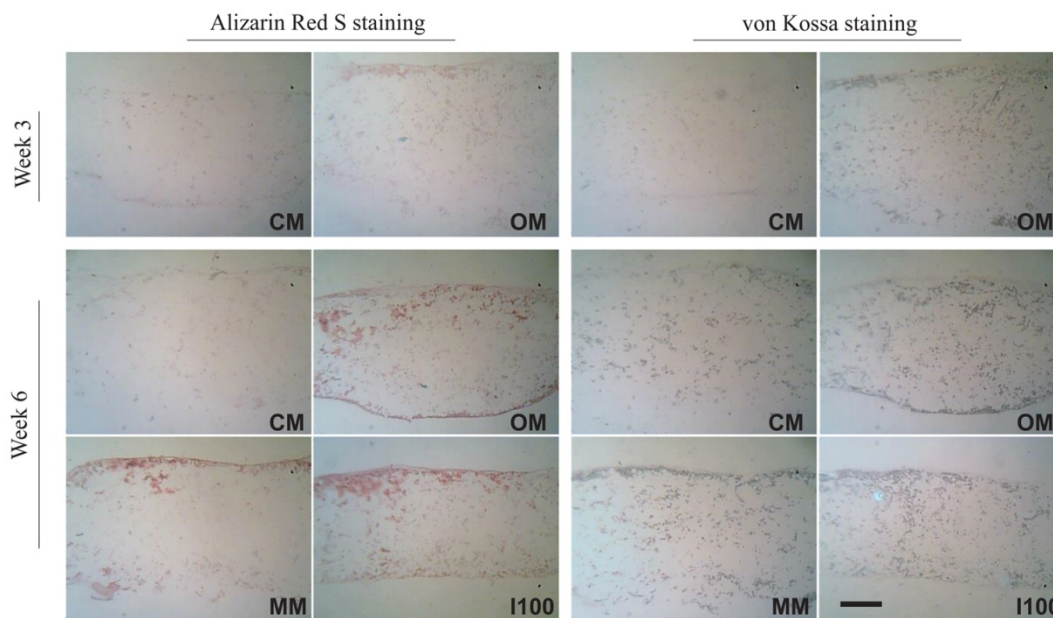


**Figure 11.4:** Alizarin Red S staining and von Kossa staining at 3 and 6 weeks ( $n = 2$ ).

CM = control medium, OM = osteogenic medium, MM = mineralization medium, and I100 = MM containing 100 ng/ml IGF-I. The scale bar is 500  $\mu\text{m}$ .

### *Histology*

Alizarin Red S staining was consistent with von Kossa staining, both of which revealed a positive mineral deposition that increased with time (Fig. 11.4). The CM groups had weaker staining than the OM groups, which was consistent with the calcium quantification. It must be noted that there was a stronger staining at the peripheral area of the constructs than inside the constructs. There were no discernible differences among the OM, MM, and I100 groups.

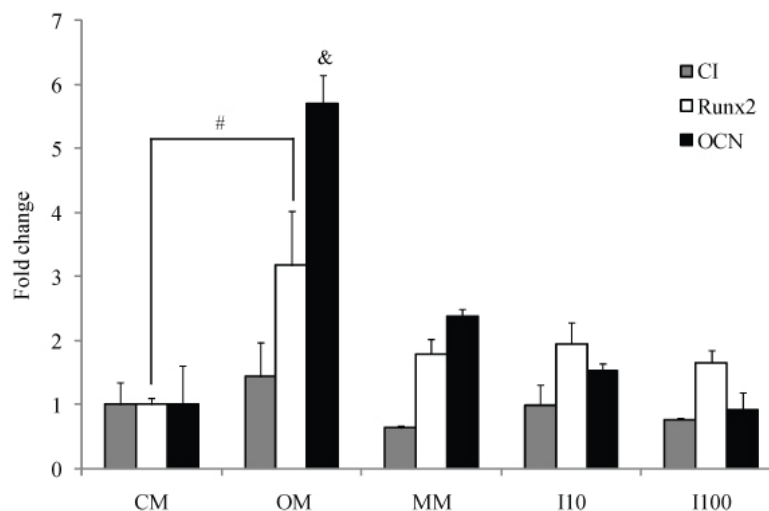


**Figure 11.5:** Gene expression (normalized to the CM group) for type I collagen (CI), runt-related transcription factor 2 (Runx2), and osteocalcin (OCN) at week 6 (n = 4). CM = control medium, OM = osteogenic medium, MM = mineralization medium, I10 = MM containing 10 ng/ml IGF-I, and I100 = MM containing 100 ng/ml IGF-I. # = statistically significant difference in Runx2 gene expression between the OM and CM groups ( $p < 0.05$ ). & = statistically significant difference in OCN gene expression between the OM group and all other groups ( $p < 0.05$ ). Error bars represent standard deviations.

### ***Gene expression levels of CI, Runx2, and OCN***

Runx2 and OCN gene expression was up-regulated in the OM group ( $p < 0.05$ ) (Fig. 11.5). There were no statistically significant differences in type I collagen gene expression among all groups. After a change from the OM, the MM group had a lower gene expression of CI, Runx2 ( $p < 0.05$ ), and OCN when compared to continuing treatment with the OM medium. The addition of IGF-I into the MM did not statistically affect the gene expression level of Runx2, OCN, or type I collagen.

## **DISCUSSION AND CONCLUSION**

In the field of tissue engineering, it is critical to select a promising cell source that is easy to obtain, and provides sufficient cell numbers. hUCMSCs undoubtedly meet these requirements. There is an abundant supply of umbilical cords, with 4.1 million births in the United States alone in 2005.<sup>257</sup> After cell isolation, hUCMSCs can achieve a 300-fold cell increase in 7 passages while maintaining differentiation potential.<sup>195</sup> *In vivo* transplantation of these cells has demonstrated their regenerative effects on brain injuries and retinal disease in animal models, while immunorejection was not observed in these studies.<sup>213, 214</sup> All previous osteogenic differentiation studies with hUCMSCs have been performed in monolayer (2D).<sup>76, 77, 195, 204, 208, 225</sup> In the current study, we presented the osteogenesis of hUCMSCs *in vitro* in a 3D biomaterial-based environment, thus supporting the use of hUCMSCs for bone tissue engineering.

The Runx2 gene is known to play an essential role in osteoblast differentiation and bone formation.<sup>362, 363</sup> The disruption of Runx2 leads to the termination of intramembranous and endochondral ossification due to the maturational arrest of osteoblasts.<sup>364</sup> The *in vitro* osteogenic differentiation of MSCs is accompanied by the up-regulation of Runx2 gene expression at the early stage.<sup>365</sup> The OCN gene is mainly expressed by mature osteoblasts and responsible for the mineralization at the late stage of differentiation. Exposed to the OM, hUCMSCs did show an up-regulation of the gene expression of Runx2 and OCN compared to the CM group, indicating osteogenic differentiation of these cells. Compared to the MM, I10 and I100 groups, the OM is also beneficial for the osteogenic differentiation due to the higher Runx2 and OCN gene expression. The positive staining of Alizarin Red S and von Kossa staining confirmed the presence of mineralization, suggesting that the hUCMSCs were progressing down an osteogenic lineage. In contrast to mineralization, collagen content increased mainly between weeks 0 to 3 and was maintained between weeks 3 to 6. In native normal bone, the nucleation and development of mineral crystals interacts principally with collagen.<sup>366</sup> The abundant collagen production may have contributed to the boost of mineralization between weeks 3 and 6.

The OM also promoted cell proliferation and/or inhibited cell loss compared to other media. This effect was mainly due to the presence of DEX and VD3 in the OM, rather than AA2P and  $\beta$ -GP, based on the observation that the MM group had a comparable cell number range with the CM group after switching the medium at

week 3. A few studies have demonstrated an inhibitory effect of either DEX or Vitamin D3 on cell proliferation,<sup>367-369</sup> although they can induce osteogenic differentiation.<sup>358, 370, 371</sup> In monolayer culture, we also observed in a previous study that DEX inhibited hUCMSC proliferation (unpublished data). Thus, the increase in cell number with the OM group in the current study indicated that the combination of DEX and VD3 might have a synergetic effect on hUCMSC proliferation and/or survival. It must be noted that this stimulation decreased with time (Fig. 11.1) and might achieve a plateau in cell number similar to the CM group after a longer culture period, which would be of interest to investigate in the future.

The MM had no impact on the total collagen and calcium content in the constructs, although they had a slight higher collagen and calcium per cell. Moreover, the shift from the OM to the MM led to a decrease in osteogenic gene expression including CI, Runx2 and OCN. IGF-I plays an important role as an anabolic agent in bone development at all stages,<sup>337, 338, 372</sup> and regulates MSC proliferation and biosynthesis.<sup>373, 374</sup> In the current study, the addition of IGF-I into the MM had no beneficial effects on cell proliferation, matrix production or gene expression. In the future, the incorporation of IGF-I at an earlier stage, and/or in addition to osteogenic signals as opposed to in lieu of them, might facilitate the osteogenic differentiation of MSCs.<sup>374</sup>

In summary, the results demonstrated the osteogenic differentiation of hUCMSCs in PLLA scaffolds with the up-regulation of bone-specific genes and

mineral deposition, thus supporting the feasibility of applying hUCMSCs to bone tissue engineering. Therefore, given the numerous advantages over adult stem cells and the successful osteogenesis in 3D biomaterials, hUCMSCs may be a promising alternative for bone tissue engineering. A future side-by-side comparison between hUCMSCs and hBMSCs in a 3D biomaterial environment will be interesting and meaningful to further evaluate the potential of hUCMSCs in bone tissue engineering. In the current study, there was no advantage to removing DEX and VD3 after 3 weeks, as in fact the only group to retain these factors (i.e., the OM group) produced a greater number of cells and expressed the highest level of osteogenic genes. Future strategies may include earlier introduction of IGF-I and/or extended exposure of DEX and VD3.

## CHAPTER 12: Conclusion

This thesis was motivated by the need for new cell sources for TMJ condyle tissue engineering. The osteochondral structure of the TMJ condyle necessitates engineering cartilage and bone tissue concurrently, and hUCMSCs provide a single cell source to fulfill that task. Indeed, this thesis presented evidence of the successful differentiation of fibro-chondrocytes and osteoblasts in 3D biomaterials, which filled a major void in the literature regarding the use of hUCMSCs for musculoskeletal tissue engineering. The refinement of cell-scaffold culture parameters, including seeding densities and signaling strategies, resulted in a biologically and mechanically closer substitute for native TMJ tissues that provides more cells, better differentiation, and a more abundant extracellular matrix. These results undoubtedly validated the overall hypothesis that TMJ condyle tissue engineering would be achieved *in vitro* using hUCMSCs.

hUCMSCs differentiated along chondrogenic and osteogenic lineages in scaffolds, as evidenced by the existence of type II collagen and aggrecan with chondrogenesis and the presence of mineralization, ALP activity, and up-regulation of osteogenic gene expression with osteogenesis. hUCMSCs surpassed mature TMJ cells and hBMSCs for TMJ cartilage regeneration with more cells and matrix content. In addition, as a mature cell source, *in vitro* culture of hyaline cartilage cells formed a TMJ-like fibrocartilage tissue with superior biosynthesis. Therefore, both hUCMSCs and hyaline cartilage cells provided superior alternatives to TMJ cells themselves. In the future, the comparison between hyaline cartilage and hUCMSCs can be made. An

advantage that mature cells possess over various types of stem cells is the absence of the variable of differentiation and the reduced possibility of metaplasia. However, even if hUCMSCs have a performance that is comparable to that of hyaline cartilage cells, hUCMSCs will be preferred because of their extensive availability and their non-invasive harvest among other reasons.

A higher cell seeding density ( $> 25M$ ) was recommended for both cartilage and bone tissue engineering. Higher densities promoted greater cell proliferation and differentiation and extracellular matrix synthesis than the lower densities and, more importantly, helped to retain the mechanical integrity of scaffolds. In both studies, PGA scaffolds experienced massive degradation and caused cell and matrix loss into the medium from the constructs. Therefore, in the future, more slowly degrading scaffolds, such as PLLA and PLGA, will need to be investigated for maintaining the original shape of the scaffolds, which will facilitate the integration of cartilage and bone to create an osteochondral TMJ condyle. In fact, PLLA scaffolds did maintain their initial shape during osteogenic differentiation over a 6-week period (Chapter 11).

Switching from differentiation media to anabolic media containing (IGF-I) was beneficial for cartilage tissue engineering using hUCMSCs, while it was not rewarding when attempting bone tissue engineering. When compared to the continued use of TGF- $\beta$ 3 for cartilage tissue engineering, switching to IGF-I increased collagen production and type II collagen gene expression and immunostaining. However, in bone tissue engineering, IGF-I did not affect the osteogenic differentiation and matrix

synthesis with hUCMSCs. Continuing in osteogenic media resulted in more cells, comparable matrix content, and a higher gene expression level of bone-specific markers than switching to mineralization media containing IGF-I or no IGF-I. In the future, an IGF-I concentration larger than 100 ng/ml may be warranted to investigate the manifestation of its anabolic effects on osteogenically induced hUCMSCs. Moreover, the incorporation of IGF-I at an earlier stage, and/or in addition to osteogenic signals as opposed to in lieu of them, might facilitate the osteogenic differentiation of MSCs. Finally, the sequential signaling strategy of initial differentiation followed by anabolic signaling might be beneficial for any other tissue engineering area involving the use of stem cells.

In summary, tissue engineering of TMJ condylar cartilage and bone was accomplished *in vitro* separately with refined culture parameters. The immediate next step will be to integrate tissue-engineered cartilage and bone to create an osteochondral construct that mimics the native structure of TMJ condyle. It must be noted that the application of these findings includes, but is not limited to, TMJ condylar cartilage and bone and can be translated to a broader area in orthopedic research, including other fibrocartilage tissues, such as TMJ discs, intervertebral discs, knee menisci, tendons and ligaments, and bone tissue in other joints, such as the knee, shoulder, and hip. In addition, with the modification of bioactive signals in chondrogenic differentiation, hUCMSCs can be used for hyaline cartilage tissue engineering and osteochondral tissues consisting of hyaline cartilage and bone tissues (e.g., femoral and tibial condyles).

## REFERENCES

1. Mann, B. K. Biologic gels in tissue engineering. *Clin Plast Surg* **30**, 601, 2003.
2. Oakes, B. W. Orthopaedic tissue engineering: from laboratory to the clinic. *Med J Aust* **180**, S35, 2004.
3. Gao, J., Dennis, J. E., Solchaga, L. A., Awadallah, A. S., Goldberg, V. M. and Caplan, A. I. Tissue-engineered fabrication of an osteochondral composite graft using rat bone marrow-derived mesenchymal stem cells. *Tissue Eng* **7**, 363, 2001.
4. Vunjak-Novakovic, G., Meinel, L., Altman, G. and Kaplan, D. Bioreactor cultivation of osteochondral grafts. *Orthod Craniofac Res* **8**, 209, 2005.
5. Alhadlaq, A. and Mao, J. J. Tissue-engineered neogenesis of human-shaped mandibular condyle from rat mesenchymal stem cells. *J Dent Res* **82**, 951, 2003.
6. Li, W. J., Laurencin, C. T., Caterson, E. J., Tuan, R. S. and Ko, F. K. Electrospun nanofibrous structure: a novel scaffold for tissue engineering. *J Biomed Mater Res* **60**, 613, 2002.
7. Poshusta, A. K. and Anseth, K. S. Photopolymerized biomaterials for application in the temporomandibular joint. *Cells Tissues Organs* **169**, 272, 2001.
8. Cao, T., Ho, K. H. and Teoh, S. H. Scaffold design and in vitro study of osteochondral coculture in a three-dimensional porous polycaprolactone scaffold fabricated by fused deposition modeling. *Tissue Eng* **9 Suppl 1**, S103, 2003.
9. Schek, R. M., Taboas, J. M., Segvich, S. J., Hollister, S. J. and Krebsbach, P. H. Engineered osteochondral grafts using biphasic composite solid free-form fabricated scaffolds. *Tissue Eng* **10**, 1376, 2004.
10. Hollister, S. J., Lin, C. Y., Saito, E., Lin, C. Y., Schek, R. D., Taboas, J. M., Williams, J. M., Partee, B., Flanagan, C. L., Diggs, A., Wilke, E. N., Van Lenthe, G. H., Muller, R., Wirtz, T., Das, S., Feinberg, S. E. and Krebsbach, P. H. Engineering craniofacial scaffolds. *Orthod Craniofac Res* **8**, 162, 2005.
11. Williams, J. M., Adewunmi, A., Schek, R. M., Flanagan, C. L., Krebsbach, P. H., Feinberg, S. E., Hollister, S. J. and Das, S. Bone tissue engineering using

- polycaprolactone scaffolds fabricated via selective laser sintering. *Biomaterials* **26**, 4817, 2005.
12. Rahaman, M. N. and Mao, J. J. Stem cell-based composite tissue constructs for regenerative medicine. *Biotechnol Bioeng* **91**, 261, 2005.
  13. Appleton, J. The ultrastructure of the articular tissue of the mandibular condyle in the rat. *Arch Oral Biol* **20**, 823, 1975.
  14. Piette, E. Anatomy of the human temporomandibular joint. An updated comprehensive review. *Acta Stomatol Belg* **90**, 103, 1993.
  15. Blackwood, H. J. Growth of the mandibular condyle of the rat studied with tritiated thymidine. *Arch Oral Biol* **11**, 493, 1966.
  16. Klinge, R. F. The structure of the mandibular condyle in the monkey (*Macaca mulatta*). *Micron* **27**, 381, 1996.
  17. Werner, J. A., Tillmann, B. and Schleicher, A. Functional anatomy of the temporomandibular joint. A morphologic study on human autopsy material. *Anat Embryol (Berl)* **183**, 89, 1991.
  18. Dolwick, M. F., Lipton, J. S., Warner, M. R. and Williams, V. F. Sagittal anatomy of the human temporomandibular joint spaces: normal and abnormal findings. *J Oral Maxillofac Surg* **41**, 86, 1983.
  19. Luder, H. U. and Schroeder, H. E. Light and electron microscopic morphology of the temporomandibular joint in growing and mature crab-eating monkeys (*Macaca fascicularis*): the condylar articular layer. *Anat Embryol (Berl)* **181**, 499, 1990.
  20. Copray, J. C. and Duterloo, H. S. A comparative study on the growth of craniofacial cartilages in vitro. *Eur J Orthod* **8**, 157, 1986.
  21. Luder, H. U., Leblond, C. P. and von der Mark, K. Cellular stages in cartilage formation as revealed by morphometry, radioautography and type II collagen immunostaining of the mandibular condyle from weanling rats. *Am J Anat* **182**, 197, 1988.
  22. Mizoguchi, I., Takahashi, I., Nakamura, M., Sasano, Y., Sato, S., Kagayama, M. and Mitani, H. An immunohistochemical study of regional differences in the distribution of type I and type II collagens in rat mandibular condylar cartilage. *Arch Oral Biol* **41**, 863, 1996.

23. Silbermann, M. and Frommer, J. The nature of endochondral ossification in the mandibular condyle of the mouse. *Anat Rec* **172**, 659, 1972.
24. Zhao, Z., Rabie, A. B., Urban, H. and Shen, G. [Image analysis of condylar cartilaginous adaptation to mandibular protrusion in rats]. *Hua Xi Kou Qiang Yi Xue Za Zhi* **17**, 155, 1999.
25. Durkin, J. F., Heeley, J. D. and Irving, J. T. The cartilage of the mandibular condyle. *Oral Sci Rev* **2**, 29, 1973.
26. Hansson, T. and Nordstrom, B. Thickness of the soft tissue layers and articular disk in temporomandibular joints with deviations in form. *Acta Odontol Scand* **35**, 281, 1977.
27. Hansson, T., Oberg, T., Carlsson, G. E. and Kopp, S. Thickness of the soft tissue layers and the articular disk in the temporomandibular joint. *Acta Odontol Scand* **35**, 77, 1977.
28. Mizuno, I., Saburi, N., Taguchi, N., Kaneda, T. and Hoshino, T. The fine structure of the fibrous zone of articular cartilage in the rat mandibular condyle. *Shika Kiso Igakkai Zasshi* **32**, 69, 1990.
29. Copray, J. C. and Liem, R. S. Ultrastructural changes associated with weaning in the mandibular condyle of the rat. *Acta Anat (Basel)* **134**, 35, 1989.
30. Silva, D. G. and Hart, J. A. Ultrastructural observations on the mandibular condyle of the guinea pig. *J Ultrastruct Res* **20**, 227, 1967.
31. Bibb, C. A., Pullinger, A. G. and Baldioceda, F. The relationship of undifferentiated mesenchymal cells to TMJ articular tissue thickness. *J Dent Res* **71**, 1816, 1992.
32. Bibb, C. A., Pullinger, A. G. and Baldioceda, F. Serial variation in histological character of articular soft tissue in young human adult temporomandibular joint condyles. *Arch Oral Biol* **38**, 343, 1993.
33. Mao, J. J., Rahemtulla, F. and Scott, P. G. Proteoglycan expression in the rat temporomandibular joint in response to unilateral bite raise. *J Dent Res* **77**, 1520, 1998.
34. de Bont, L. G., Boering, G., Havinga, P. and Liem, R. S. Spatial arrangement of collagen fibrils in the articular cartilage of the mandibular condyle: a light microscopic and scanning electron microscopic study. *J Oral Maxillofac Surg* **42**, 306, 1984.

35. Delatte, M., Von den Hoff, J. W., van Rheden, R. E. and Kuijpers-Jagtman, A. M. Primary and secondary cartilages of the neonatal rat: the femoral head and the mandibular condyle. *Eur J Oral Sci* **112**, 156, 2004.
36. Teramoto, M., Kaneko, S., Shibata, S., Yanagishita, M. and Soma, K. Effect of compressive forces on extracellular matrix in rat mandibular condylar cartilage. *J Bone Miner Metab* **21**, 276, 2003.
37. Poikela, A., Kantomaa, T., Pirttiniemi, P., Tuukkanen, J. and Pietila, K. Unilateral masticatory function changes the proteoglycan content of mandibular condylar cartilage in rabbit. *Cells Tissues Organs* **167**, 49, 2000.
38. Roth, S., Muller, K., Fischer, D. C. and Dannhauer, K. H. Specific properties of the extracellular chondroitin sulphate proteoglycans in the mandibular condylar growth centre in pigs. *Arch Oral Biol* **42**, 63, 1997.
39. Mow, V. C., Kuei, S. C., Lai, W. M. and Armstrong, C. G. Biphasic creep and stress relaxation of articular cartilage in compression? Theory and experiments. *J Biomech Eng* **102**, 73, 1980.
40. Yanagishita, M. Function of proteoglycans in the extracellular matrix. *Acta Pathol Jpn* **43**, 283, 1993.
41. Del Santo, M., Jr., Marches, F., Ng, M. and Hinton, R. J. Age-associated changes in decorin in rat mandibular condylar cartilage. *Arch Oral Biol* **45**, 485, 2000.
42. Kang, H., Bao, G., Dong, Y., Yi, X., Chao, Y. and Chen, M. [Tensile mechanics of mandibular condylar cartilage]. *Hua Xi Kou Qiang Yi Xue Za Zhi* **18**, 85, 2000.
43. Kuboki, T., Shinoda, M., Orsini, M. G. and Yamashita, A. Viscoelastic properties of the pig temporomandibular joint articular soft tissues of the condyle and disc. *J Dent Res* **76**, 1760, 1997.
44. Hu, K., Radhakrishnan, P., Patel, R. V. and Mao, J. J. Regional structural and viscoelastic properties of fibrocartilage upon dynamic nanoindentation of the articular condyle. *J Struct Biol* **136**, 46, 2001.
45. Patel, R. V. and Mao, J. J. Microstructural and elastic properties of the extracellular matrices of the superficial zone of neonatal articular cartilage by atomic force microscopy. *Front Biosci* **8**, a18, 2003.
46. Tanaka, E., Yamano, E., Dalla-Bona, D. A., Watanabe, M., Inubushi, T., Shirakura, M., Sano, R., Takahashi, K., van Eijden, T. and Tanne, K.

- Dynamic compressive properties of the mandibular condylar cartilage. *J Dent Res* **85**, 571, 2006.
47. Giesen, E. B., Ding, M., Dalstra, M. and van Eijden, T. M. Mechanical properties of cancellous bone in the human mandibular condyle are anisotropic. *J Biomech* **34**, 799, 2001.
  48. van Eijden, T. M., van der Helm, P. N., van Ruijven, L. J. and Mulder, L. Structural and mechanical properties of mandibular condylar bone. *J Dent Res* **85**, 33, 2006.
  49. Giesen, E. B., Ding, M., Dalstra, M. and van Eijden, T. M. Reduced mechanical load decreases the density, stiffness, and strength of cancellous bone of the mandibular condyle. *Clin Biomech (Bristol, Avon)* **18**, 358, 2003.
  50. Nomura, T., Gold, E., Powers, M. P., Shingaki, S. and Katz, J. L. Micromechanics/structure relationships in the human mandible. *Dent Mater* **19**, 167, 2003.
  51. Schwartz-Dabney, C. L. and Dechow, P. C. Variations in cortical material properties throughout the human dentate mandible. *Am J Phys Anthropol* **120**, 252, 2003.
  52. Jiang, J., Nicoll, S. B. and Lu, H. H. Co-culture of osteoblasts and chondrocytes modulates cellular differentiation in vitro. *Biochem Biophys Res Commun* **338**, 762, 2005.
  53. Takigawa, M., Okada, M., Takano, T., Ohmae, H., Sakuda, M. and Suzuki, F. Studies on chondrocytes from mandibular condylar cartilage, nasal septal cartilage, and spheno-occipital synchondrosis in culture. I. Morphology, growth, glycosaminoglycan synthesis, and responsiveness to bovine parathyroid hormone (1-34). *J Dent Res* **63**, 19, 1984.
  54. Tsubai, T., Higashi, Y. and Scott, J. E. The effect of epidermal growth factor on the fetal rabbit mandibular condyle and isolated condylar fibroblasts. *Arch Oral Biol* **45**, 507, 2000.
  55. Shieh, A. C. and Athanasiou, K. A. Biomechanics of single zonal chondrocytes. *J Biomech* 2005.
  56. Darling, E. M., Hu, J. C. and Athanasiou, K. A. Zonal and topographical differences in articular cartilage gene expression. *J Orthop Res* **22**, 1182, 2004.

57. Mao, J. J. Stem-cell-driven regeneration of synovial joints. *Biol Cell* **97**, 289, 2005.
58. Pittenger, M. F., Mackay, A. M., Beck, S. C., Jaiswal, R. K., Douglas, R., Mosca, J. D., Moorman, M. A., Simonetti, D. W., Craig, S. and Marshak, D. R. Multilineage potential of adult human mesenchymal stem cells. *Science* **284**, 143, 1999.
59. Jiang, Y., Jahagirdar, B. N., Reinhardt, R. L., Schwartz, R. E., Keene, C. D., Ortiz-Gonzalez, X. R., Reyes, M., Lenvik, T., Lund, T., Blackstad, M., Du, J., Aldrich, S., Lisberg, A., Low, W. C., Largaespada, D. A. and Verfaillie, C. M. Pluripotency of mesenchymal stem cells derived from adult marrow. *Nature* **418**, 41, 2002.
60. Gerson, S. L. Mesenchymal stem cells: no longer second class marrow citizens. *Nat Med* **5**, 262, 1999.
61. Kawaguchi, J., Mee, P. J. and Smith, A. G. Osteogenic and chondrogenic differentiation of embryonic stem cells in response to specific growth factors. *Bone* **36**, 758, 2005.
62. Tanaka, H., Murphy, C. L., Murphy, C., Kimura, M., Kawai, S. and Polak, J. M. Chondrogenic differentiation of murine embryonic stem cells: effects of culture conditions and dexamethasone. *J Cell Biochem* **93**, 454, 2004.
63. Wakitani, S., Aoki, H., Harada, Y., Sonobe, M., Morita, Y., Mu, Y., Tomita, N., Nakamura, Y., Takeda, S., Watanabe, T. K. and Tanigami, A. Embryonic stem cells form articular cartilage, not teratomas, in osteochondral defects of rat joints. *Cell Transplant* **13**, 331, 2004.
64. Eblenkamp, M., Aigner, J., Hintermair, J., Potthoff, S., Hopfner, U., Jacobs, V., Niemeyer, M. and Wintermantel, E. [Umbilical cord stromal cells (UCSC). Cells featuring osteogenic differentiation potential]. *Orthopade* **33**, 1338, 2004.
65. Kadner, A., Zund, G., Maurus, C., Breymann, C., Yakarisik, S., Kadner, G., Turina, M. and Hoerstrup, S. P. Human umbilical cord cells for cardiovascular tissue engineering: a comparative study. *Eur J Cardiothorac Surg* **25**, 635, 2004.
66. Bailey, M. M., Wang, L., Bode, C. J., Mitchell, K. E. and Detamore, M. S. A comparison of human umbilical cord matrix stem cells and temporomandibular joint condylar chondrocytes for tissue engineering temporomandibular joint condylar cartilage. *Tissue Eng* **13**, 2003, 2007.

67. Alhadlaq, A. and Mao, J. J. Mesenchymal stem cells: isolation and therapeutics. *Stem Cells Dev* **13**, 436, 2004.
68. Alhadlaq, A., Elisseeff, J. H., Hong, L., Williams, C. G., Caplan, A. I., Sharma, B., Kopher, R. A., Tomkoria, S., Lennon, D. P., Lopez, A. and Mao, J. J. Adult stem cell driven genesis of human-shaped articular condyle. *Ann Biomed Eng* **32**, 911, 2004.
69. Heng, B. C., Cao, T. and Lee, E. H. Directing stem cell differentiation into the chondrogenic lineage in vitro. *Stem Cells* **22**, 1152, 2004.
70. Hwang, N. S., Kim, M. S., Sampattavanich, S., Baek, J. H., Zhang, Z. and Elisseeff, J. The Effects of Three Dimensional Culture and Growth Factors on the Chondrogenic Differentiation of Murine Embryonic Stem Cells. *Stem Cells* 2005.
71. Nakayama, N., Duryea, D., Manoukian, R., Chow, G. and Han, C. Y. Macroscopic cartilage formation with embryonic stem-cell-derived mesodermal progenitor cells. *J Cell Sci* **116**, 2015, 2003.
72. zur Nieden, N. I., Kempka, G., Rancourt, D. E. and Ahr, H. J. Induction of chondro-, osteo- and adipogenesis in embryonic stem cells by bone morphogenetic protein-2: effect of cofactors on differentiating lineages. *BMC Dev Biol* **5**, 1, 2005.
73. Tai, G., Polak, J. M., Bishop, A. E., Christodoulou, I. and Buttery, L. D. Differentiation of osteoblasts from murine embryonic stem cells by overexpression of the transcriptional factor osterix. *Tissue Eng* **10**, 1456, 2004.
74. Buttery, L. D., Bourne, S., Xynos, J. D., Wood, H., Hughes, F. J., Hughes, S. P., Episkopou, V. and Polak, J. M. Differentiation of osteoblasts and in vitro bone formation from murine embryonic stem cells. *Tissue Eng* **7**, 89, 2001.
75. Mitchell, K. E., Weiss, M. L., Mitchell, B. M., Martin, P., Davis, D., Morales, L., Helwig, B., Beerenstrauch, M., Abou-Easa, K., Hildreth, T., Troyer, D. and Medicetty, S. Matrix cells from Wharton's jelly form neurons and glia. *Stem Cells* **21**, 50, 2003.
76. Wang, H. S., Hung, S. C., Peng, S. T., Huang, C. C., Wei, H. M., Guo, Y. J., Fu, Y. S., Lai, M. C. and Chen, C. C. Mesenchymal stem cells in the Wharton's jelly of the human umbilical cord. *Stem Cells* **22**, 1330, 2004.

77. Sarugaser, R., Lickorish, D., Baksh, D., Hosseini, M. M. and Davies, J. E. Human umbilical cord perivascular (HUCPV) cells: a source of mesenchymal progenitors. *Stem Cells* **23**, 220, 2005.
78. Weiss, M. L., Mitchell, K. E., Hix, J. E., Medicetty, S., El-Zarkouny, S. Z., Grieger, D. and Troyer, D. L. Transplantation of porcine umbilical cord matrix cells into the rat brain. *Exp Neurol* **182**, 288, 2003.
79. Barker, J. N. and Wagner, J. E. Umbilical-cord blood transplantation for the treatment of cancer. *Nat Rev Cancer* **3**, 526, 2003.
80. Weiss, M. L., Medicetty, S., Bledsoe, A. R., Rachakatla, R. S., Choi, M., Merchav, S., Luo, Y., Rao, M. S., Velagaleti, G. and Troyer, D. Human umbilical cord matrix stem cells: preliminary characterization and effect of transplantation in a rodent model of Parkinson's disease. *Stem Cells* **24**, 781, 2006.
81. Kadner, A., Hoerstrup, S. P., Tracy, J., Breymann, C., Maurus, C. F., Melnitchouk, S., Kadner, G., Zund, G. and Turina, M. Human umbilical cord cells: a new cell source for cardiovascular tissue engineering. *Ann Thorac Surg* **74**, S1422, 2002.
82. Schmidt, D., Mol, A., Neuenschwander, S., Breymann, C., Gossi, M., Zund, G., Turina, M. and Hoerstrup, S. P. Living patches engineered from human umbilical cord derived fibroblasts and endothelial progenitor cells. *Eur J Cardiothorac Surg* **27**, 795, 2005.
83. Hoerstrup, S. P., Kadner, A., Breymann, C., Maurus, C. F., Guenter, C. I., Sodian, R., Visjager, J. F., Zund, G. and Turina, M. I. Living, autologous pulmonary artery conduits tissue engineered from human umbilical cord cells. *Ann Thorac Surg* **74**, 46, 2002.
84. Darling, E. M. and Athanasiou, K. A. Retaining zonal chondrocyte phenotype by means of novel growth environments. *Tissue Eng* **11**, 395, 2005.
85. Darling, E. M. and Athanasiou, K. A. Rapid phenotypic changes in passaged articular chondrocyte subpopulations. *J Orthop Res* **23**, 425, 2005.
86. Benya, P. D. and Shaffer, J. D. Dedifferentiated chondrocytes reexpress the differentiated collagen phenotype when cultured in agarose gels. *Cell* **30**, 215, 1982.
87. von der Mark, K., Gauss, V., von der Mark, H. and Muller, P. Relationship between cell shape and type of collagen synthesised as chondrocytes lose their cartilage phenotype in culture. *Nature* **267**, 531, 1977.

88. Hauselmann, H. J., Masuda, K., Hunziker, E. B., Neidhart, M., Mok, S. S., Michel, B. A. and Thonar, E. J. Adult human chondrocytes cultured in alginate form a matrix similar to native human articular cartilage. *Am J Physiol* **271**, C742, 1996.
89. van Osch, G. J., van der Veen, S. W. and Verwoerd-Verhoef, H. L. In vitro redifferentiation of culture-expanded rabbit and human auricular chondrocytes for cartilage reconstruction. *Plast Reconstr Surg* **107**, 433, 2001.
90. Chang, J., Ma, X., Wei, M., Wang, J. and Jiao, Y. Application of alginate three-dimensional culture system for in vitro culture of mandibular condylar chondrocytes from human osteoarthritic temporomandibular joint. *Zhonghua Kou Qiang Yi Xue Za Zhi* **37**, 246, 2002.
91. Weng, Y., Cao, Y., Silva, C. A., Vacanti, M. P. and Vacanti, C. A. Tissue-engineered composites of bone and cartilage for mandible condylar reconstruction. *J Oral Maxillofac Surg* **59**, 185, 2001.
92. Hollister, S. J., Levy, R. A., Chu, T. M., Halloran, J. W. and Feinberg, S. E. An image-based approach for designing and manufacturing craniofacial scaffolds. *Int J Oral Maxillofac Surg* **29**, 67, 2000.
93. Liu, Y., Chen, F., Liu, W., Cui, L., Shang, Q., Xia, W., Wang, J., Cui, Y., Yang, G., Liu, D., Wu, J., Xu, R., Buonocore, S. D. and Cao, Y. Repairing large porcine full-thickness defects of articular cartilage using autologous chondrocyte-engineered cartilage. *Tissue Eng* **8**, 709, 2002.
94. Chu, C. R., Douchis, J. S., Yoshioka, M., Sah, R. L., Coutts, R. D. and Amiel, D. Osteochondral repair using perichondrial cells. A 1-year study in rabbits. *Clin Orthop Relat Res* **220**, 1997.
95. Douchis, J. S., Bae, W. C., Chen, A. C., Sah, R. L., Coutts, R. D. and Amiel, D. Cartilage repair with autogenic perichondrium cell and polylactic acid grafts. *Clin Orthop Relat Res* **248**, 2000.
96. Jikko, A., Harris, S. E., Chen, D., Mendrick, D. L. and Damsky, C. H. Collagen integrin receptors regulate early osteoblast differentiation induced by BMP-2. *J Bone Miner Res* **14**, 1075, 1999.
97. Mizuno, M. and Kuboki, Y. Osteoblast-related gene expression of bone marrow cells during the osteoblastic differentiation induced by type I collagen. *J Biochem (Tokyo)* **129**, 133, 2001.

98. Moursi, A. M., Globus, R. K. and Damsky, C. H. Interactions between integrin receptors and fibronectin are required for calvarial osteoblast differentiation in vitro. *J Cell Sci* **110 ( Pt 18)**, 2187, 1997.
99. He, W., Ma, Z., Yong, T., Teo, W. E. and Ramakrishna, S. Fabrication of collagen-coated biodegradable polymer nanofiber mesh and its potential for endothelial cells growth. *Biomaterials* **26**, 7606, 2005.
100. Ho, M. H., Wang, D. M., Hsieh, H. J., Liu, H. C., Hsien, T. Y., Lai, J. Y. and Hou, L. T. Preparation and characterization of RGD-immobilized chitosan scaffolds. *Biomaterials* **26**, 3197, 2005.
101. Ma, Z., Kotaki, M., Inai, R. and Ramakrishna, S. Potential of nanofiber matrix as tissue-engineering scaffolds. *Tissue Eng* **11**, 101, 2005.
102. Yang, X. B., Roach, H. I., Clarke, N. M., Howdle, S. M., Quirk, R., Shakesheff, K. M. and Oreffo, R. O. Human osteoprogenitor growth and differentiation on synthetic biodegradable structures after surface modification. *Bone* **29**, 523, 2001.
103. Kuo, C. K., Li, W. J., Mauck, R. L. and Tuan, R. S. Cartilage tissue engineering: its potential and uses. *Curr Opin Rheumatol* **18**, 64, 2006.
104. Elisseff, J., Puleo, C., Yang, F. and Sharma, B. Advances in skeletal tissue engineering with hydrogels. *Orthod Craniofac Res* **8**, 150, 2005.
105. Randolph, M. A., Anseth, K. and Yaremchuk, M. J. Tissue engineering of cartilage. *Clin Plast Surg* **30**, 519, 2003.
106. Tuli, R., Li, W. J. and Tuan, R. S. Current state of cartilage tissue engineering. *Arthritis Res Ther* **5**, 235, 2003.
107. Calvert, J. W., Weiss, L. E. and Sundine, M. J. New frontiers in bone tissue engineering. *Clin Plast Surg* **30**, 641, 2003.
108. Rose, F. R., Hou, Q. and Oreffo, R. O. Delivery systems for bone growth factors - the new players in skeletal regeneration. *J Pharm Pharmacol* **56**, 415, 2004.
109. Rezwan, K., Chen, Q. Z., Blaker, J. J. and Boccaccini, A. R. Biodegradable and bioactive porous polymer/inorganic composite scaffolds for bone tissue engineering. *Biomaterials* **27**, 3413, 2006.
110. Mistry, A. S. and Mikos, A. G. Tissue engineering strategies for bone regeneration. *Adv Biochem Eng Biotechnol* **94**, 1, 2005.

111. Salgado, A. J., Coutinho, O. P. and Reis, R. L. Bone tissue engineering: state of the art and future trends. *Macromol Biosci* **4**, 743, 2004.
112. Liu, X. and Ma, P. X. Polymeric scaffolds for bone tissue engineering. *Ann Biomed Eng* **32**, 477, 2004.
113. Katti, D. S., Robinson, K. W., Ko, F. K. and Laurencin, C. T. Bioresorbable nanofiber-based systems for wound healing and drug delivery: optimization of fabrication parameters. *J Biomed Mater Res* **70B**, 286, 2004.
114. Kim, K., Yu, M., Zong, X., Chiu, J., Fang, D., Seo, Y. S., Hsiao, B. S., Chu, B. and Hadjiargyrou, M. Control of degradation rate and hydrophilicity in electrospun non-woven poly(D,L-lactide) nanofiber scaffolds for biomedical applications. *Biomaterials* **24**, 4977, 2003.
115. Bhattarai, S. R., Bhattarai, N., Yi, H. K., Hwang, P. H., Cha, D. I. and Kim, H. Y. Novel biodegradable electrospun membrane: scaffold for tissue engineering. *Biomaterials* **25**, 2595, 2004.
116. Badami, A. S., Kreke, M. R., Thompson, M. S., Riffle, J. S. and Goldstein, A. S. Effect of fiber diameter on spreading, proliferation, and differentiation of osteoblastic cells on electrospun poly(lactic acid) substrates. *Biomaterials* **27**, 596, 2006.
117. Shin, M., Yoshimoto, H. and Vacanti, J. P. In vivo bone tissue engineering using mesenchymal stem cells on a novel electrospun nanofibrous scaffold. *Tissue Eng* **10**, 33, 2004.
118. Li, W. J., Danielson, K. G., Alexander, P. G. and Tuan, R. S. Biological response of chondrocytes cultured in three-dimensional nanofibrous poly(epsilon-caprolactone) scaffolds. *J Biomed Mater Res A* **67**, 1105, 2003.
119. Jiao, Y., Wang, D. and Han, W. L. [Effects of various growth factors on human mandibular condylar cartilage cell proliferation]. *Zhonghua Kou Qiang Yi Xue Za Zhi* **35**, 346, 2000.
120. Fuentes, M. A., Opperman, L. A., Bellinger, L. L., Carlson, D. S. and Hinton, R. J. Regulation of cell proliferation in rat mandibular condylar cartilage in explant culture by insulin-like growth factor-1 and fibroblast growth factor-2. *Arch Oral Biol* **47**, 643, 2002.
121. Delatte, M. L., Von den Hoff, J. W., Nottet, S. J., De Clerck, H. J. and Kuijpers-Jagtman, A. M. Growth regulation of the rat mandibular condyle and femoral head by transforming growth factor- $\beta$ 1, fibroblast growth factor-2 and insulin-like growth factor-I. *Eur J Orthod* **27**, 17, 2005.

122. Ogawa, T., Shimokawa, H., Fukada, K., Suzuki, S., Shibata, S., Ohya, K. and Kuroda, T. Localization and inhibitory effect of basic fibroblast growth factor on chondrogenesis in cultured mouse mandibular condyle. *J Bone Miner Metab* **21**, 145, 2003.
123. Yang, H., Luo, S., Li, F. and Zhou, Z. [Study on IGF-I regulation the proliferation of rat condylar chondrocytes in vitro]. *Hua Xi Yi Ke Da Xue Xue Bao* **31**, 365, 2000.
124. Delatte, M., Von den Hoff, J. W., Maltha, J. C. and Kuijpers-Jagtman, A. M. Growth stimulation of mandibular condyles and femoral heads of newborn rats by IGF-I. *Arch Oral Biol* **49**, 165, 2004.
125. Suzuki, S., Itoh, K. and Ohyama, K. Local administration of IGF-I stimulates the growth of mandibular condyle in mature rats. *J Orthod* **31**, 138, 2004.
126. Song, J., Luo, S. and Fan, Y. [Effects of static tension-stress and TGF-beta 1 on proliferation of mandibular condylar chondrocytes]. *Hua Xi Kou Qiang Yi Xue Za Zhi* **21**, 61, 2003.
127. Zhang, L. H. and Zhang, Q. Q. [Study on the osteoblast and the growth factors of bone tissue engineering]. *Zhongguo Yi Xue Ke Xue Yuan Xue Bao* **23**, 631, 2001.
128. Gittens, S. A. and Uludag, H. Growth factor delivery for bone tissue engineering. *J Drug Target* **9**, 407, 2001.
129. Giannobile, W. V., Hernandez, R. A., Finkelman, R. D., Ryan, S., Kiritsy, C. P., D'Andrea, M. and Lynch, S. E. Comparative effects of platelet-derived growth factor-BB and insulin-like growth factor-I, individually and in combination, on periodontal regeneration in *Macaca fascicularis*. *J Periodontal Res* **31**, 301, 1996.
130. Giannobile, W. V., Finkelman, R. D. and Lynch, S. E. Comparison of canine and non-human primate animal models for periodontal regenerative therapy: results following a single administration of PDGF/IGF-I. *J Periodontol* **65**, 1158, 1994.
131. Rutherford, R. B., Ryan, M. E., Kennedy, J. E., Tucker, M. M. and Charette, M. F. Platelet-derived growth factor and dexamethasone combined with a collagen matrix induce regeneration of the periodontium in monkeys. *J Clin Periodontol* **20**, 537, 1993.
132. Rosen, C. J. and Donahue, L. R. Insulin-like growth factors and bone: the osteoporosis connection revisited. *Proc Soc Exp Biol Med* **219**, 1, 1998.

133. Lazowski, D. A., Fraher, L. J., Hodsman, A., Steer, B., Modrowski, D. and Han, V. K. Regional variation of insulin-like growth factor-I gene expression in mature rat bone and cartilage. *Bone* **15**, 563, 1994.
134. Zellin, G. and Linde, A. Effects of recombinant human fibroblast growth factor-2 on osteogenic cell populations during orthopic osteogenesis in vivo. *Bone* **26**, 161, 2000.
135. Darling, E. M. and Athanasiou, K. A. Articular cartilage bioreactors and bioprocesses. *Tissue Eng* **9**, 9, 2003.
136. Vunjak-Novakovic, G. The fundamentals of tissue engineering: scaffolds and bioreactors. *Novartis Found Symp* **249**, 34, 2003.
137. Gooch, K. J., Kwon, J. H., Blunk, T., Langer, R., Freed, L. E. and Vunjak-Novakovic, G. Effects of mixing intensity on tissue-engineered cartilage. *Biotechnol Bioeng* **72**, 402, 2001.
138. Meinel, L., Karageorgiou, V., Fajardo, R., Snyder, B., Shinde-Patil, V., Zichner, L., Kaplan, D., Langer, R. and Vunjak-Novakovic, G. Bone tissue engineering using human mesenchymal stem cells: effects of scaffold material and medium flow. *Ann Biomed Eng* **32**, 112, 2004.
139. Martin, I., Obradovic, B., Freed, L. E. and Vunjak-Novakovic, G. Method for quantitative analysis of glycosaminoglycan distribution in cultured natural and engineered cartilage. *Ann Biomed Eng* **27**, 656, 1999.
140. Vunjak-Novakovic, G., Obradovic, B., Martin, I. and Freed, L. E. Bioreactor studies of native and tissue engineered cartilage. *Biorheology* **39**, 259, 2002.
141. Detamore, M. S. and Athanasiou, K. A. Use of a rotating bioreactor toward tissue engineering the temporomandibular joint disc. *Tissue Eng* **11**, 1188, 2005.
142. Freed, L. E., Hollander, A. P., Martin, I., Barry, J. R., Langer, R. and Vunjak-Novakovic, G. Chondrogenesis in a cell-polymer-bioreactor system. *Exp Cell Res* **240**, 58, 1998.
143. Gooch, K. J., Blunk, T., Courter, D. L., Sieminski, A. L., Bursac, P. M., Vunjak-Novakovic, G. and Freed, L. E. IGF-I and mechanical environment interact to modulate engineered cartilage development. *Biochem Biophys Res Commun* **286**, 909, 2001.

144. Pei, M., Solchaga, L. A., Seidel, J., Zeng, L., Vunjak-Novakovic, G., Caplan, A. I. and Freed, L. E. Bioreactors mediate the effectiveness of tissue engineering scaffolds. *Faseb J* **16**, 1691, 2002.
145. Martin, I., Obradovic, B., Treppo, S., Grodzinsky, A. J., Langer, R., Freed, L. E. and Vunjak-Novakovic, G. Modulation of the mechanical properties of tissue engineered cartilage. *Biorheology* **37**, 141, 2000.
146. Bancroft, G. N., Sikavitsas, V. I. and Mikos, A. G. Design of a flow perfusion bioreactor system for bone tissue-engineering applications. *Tissue Eng* **9**, 549, 2003.
147. Wendt, D., Jakob, M. and Martin, I. Bioreactor-based engineering of osteochondral grafts: from model systems to tissue manufacturing. *J Biosci Bioeng* **100**, 489, 2005.
148. Pazzano, D., Mercier, K. A., Moran, J. M., Fong, S. S., DiBiasio, D. D., Rulfs, J. X., Kohles, S. S. and Bonassar, L. J. Comparison of chondrogenesis in static and perfused bioreactor culture. *Biotechnol Prog* **16**, 893, 2000.
149. Davisson, T., Sah, R. L. and Ratcliffe, A. Perfusion increases cell content and matrix synthesis in chondrocyte three-dimensional cultures. *Tissue Eng* **8**, 807, 2002.
150. Sikavitsas, V. I., Bancroft, G. N., Holtorf, H. L., Jansen, J. A. and Mikos, A. G. Mineralized matrix deposition by marrow stromal osteoblasts in 3D perfusion culture increases with increasing fluid shear forces. *Proc Natl Acad Sci U S A* **100**, 14683, 2003.
151. Sikavitsas, V. I., Bancroft, G. N., Lemoine, J. J., Liebschner, M. A., Dauner, M. and Mikos, A. G. Flow perfusion enhances the calcified matrix deposition of marrow stromal cells in biodegradable nonwoven fiber mesh scaffolds. *Ann Biomed Eng* **33**, 63, 2005.
152. Wendt, D., Marsano, A., Jakob, M., Heberer, M. and Martin, I. Oscillating perfusion of cell suspensions through three-dimensional scaffolds enhances cell seeding efficiency and uniformity. *Biotechnol Bioeng* **84**, 205, 2003.
153. Anselme, K. Osteoblast adhesion on biomaterials. *Biomaterials* **21**, 667, 2000.
154. Schinagl, R. M., Kurtis, M. S., Ellis, K. D., Chien, S. and Sah, R. L. Effect of seeding duration on the strength of chondrocyte adhesion to articular cartilage. *J Orthop Res* **17**, 121, 1999.

155. Darling, E. M. and Athanasiou, K. A. Biomechanical strategies for articular cartilage regeneration. *Ann Biomed Eng* **31**, 1114, 2003.
156. Hughes-Fulford, M. Signal transduction and mechanical stress. *Sci STKE* **2004**, RE12, 2004.
157. Almarza, A. J. and Athanasiou, K. A. Effects of hydrostatic pressure on TMJ disc cells. *Tissue Eng* **12**, 1285, 2006.
158. Portner, R., Nagel-Heyer, S., Goepfert, C., Adamietz, P. and Meenen, N. M. Bioreactor design for tissue engineering. *J Biosci Bioeng* **100**, 235, 2005.
159. Venkat, R. V., Stock, L. R. Chalmers, J. J. Study of Hydrodynamics in Microcarrier Culture Spinner Vessels: A Particle Tracking Velocimetry Approach. *Biotechnol Bioeng* **49**, 456, 1996.
160. Sucusky, P., Osorio, D. F., Brown, J. B. and Neitzel, G. P. Fluid mechanics of a spinner-flask bioreactor. *Biotechnol Bioeng* **85**, 34, 2004.
161. Bilgen, B., Chang-Mateu, I. M. and Barabino, G. A. Characterization of mixing in a novel wavy-walled bioreactor for tissue engineering. *Biotechnol Bioeng* **92**, 907, 2005.
162. Begley, C. M. and Kleis, S. J. The fluid dynamic and shear environment in the NASA/JSC rotating-wall perfused-vessel bioreactor. *Biotechnol Bioeng* **70**, 32, 2000.
163. Lappa, M. Organic tissues in rotating bioreactors: fluid-mechanical aspects, dynamic growth models, and morphological evolution. *Biotechnol Bioeng* **84**, 518, 2003.
164. Boschetti, F., Raimondi, M. T., Migliavacca, F. and Dubini, G. Prediction of the micro-fluid dynamic environment imposed to three-dimensional engineered cell systems in bioreactors. *J Biomech* **39**, 418, 2006.
165. Vunjak-Novakovic, G., Obradovic, B., Martin, I., Bursac, P. M., Langer, R. and Freed, L. E. Dynamic cell seeding of polymer scaffolds for cartilage tissue engineering. *Biotechnol Prog* **14**, 193, 1998.
166. Feinberg, S. E., Hollister, S. J., Halloran, J. W., Chu, T. M. and Krebsbach, P. H. Image-based biomimetic approach to reconstruction of the temporomandibular joint. *Cells Tissues Organs* **169**, 309, 2001.
167. Chen, F., Mao, T., Tao, K., Chen, S., Ding, G. and Gu, X. Bone graft in the shape of human mandibular condyle reconstruction via seeding marrow-

- derived osteoblasts into porous coral in a nude mice model. *J Oral Maxillofac Surg* **60**, 1155, 2002.
168. Abukawa, H., Terai, H., Hannouche, D., Vacanti, J. P., Kaban, L. B. and Troulis, M. J. Formation of a mandibular condyle in vitro by tissue engineering. *J Oral Maxillofac Surg* **61**, 94, 2003.
  169. Ueki, K., Takazakura, D., Marukawa, K., Shimada, M., Nakagawa, K., Takatsuka, S. and Yamamoto, E. The use of polylactic acid/polyglycolic acid copolymer and gelatin sponge complex containing human recombinant bone morphogenetic protein-2 following condylectomy in rabbits. *J Craniomaxillofac Surg* **31**, 107, 2003.
  170. Chen, F., Chen, S., Tao, K., Feng, X., Liu, Y., Lei, D. and Mao, T. Marrow-derived osteoblasts seeded into porous natural coral to prefabricate a vascularised bone graft in the shape of a human mandibular ramus: experimental study in rabbits. *Br J Oral Maxillofac Surg* **42**, 532, 2004.
  171. Alhadlaq, A. and Mao, J. J. Tissue-engineered osteochondral constructs in the shape of an articular condyle. *J Bone Joint Surg Am* **87**, 936, 2005.
  172. Schek, R. M., Taboas, J. M., Hollister, S. J. and Krebsbach, P. H. Tissue engineering osteochondral implants for temporomandibular joint repair. *Orthod Craniofac Res* **8**, 313, 2005.
  173. Detamore, M. S. and Athanasiou, K. A. Motivation, characterization, and strategy for tissue engineering the temporomandibular joint disc. *Tissue Eng* **9**, 1065, 2003.
  174. Gerstenfeld, L. C., Cruceta, J., Shea, C. M., Sampath, K., Barnes, G. L. and Einhorn, T. A. Chondrocytes provide morphogenic signals that selectively induce osteogenic differentiation of mesenchymal stem cells. *J Bone Miner Res* **17**, 221, 2002.
  175. Mow, V. C., Ratcliffe, A., Rosenwasser, M. P. and Buckwalter, J. A. Experimental studies on repair of large osteochondral defects at a high weight bearing area of the knee joint: a tissue engineering study. *J Biomech Eng* **113**, 198, 1991.
  176. Wakitani, S., Goto, T., Pineda, S. J., Young, R. G., Mansour, J. M., Caplan, A. I. and Goldberg, V. M. Mesenchymal cell-based repair of large, full-thickness defects of articular cartilage. *J Bone Joint Surg Am* **76**, 579, 1994.
  177. Angele, P., Kujat, R., Nerlich, M., Yoo, J., Goldberg, V. and Johnstone, B. Engineering of osteochondral tissue with bone marrow mesenchymal

- progenitor cells in a derivatized hyaluronan-gelatin composite sponge. *Tissue Eng* **5**, 545, 1999.
178. Yaylaoglu, M. B., Yildiz, C., Korkusuz, F. and Hasirci, V. A novel osteochondral implant. *Biomaterials* **20**, 1513, 1999.
  179. Schaefer, D., Martin, I., Shastri, P., Padera, R. F., Langer, R., Freed, L. E. and Vunjak-Novakovic, G. In vitro generation of osteochondral composites. *Biomaterials* **21**, 2599, 2000.
  180. Schaefer, D., Martin, I., Jundt, G., Seidel, J., Heberer, M., Grodzinsky, A., Bergin, I., Vunjak-Novakovic, G. and Freed, L. E. Tissue-engineered composites for the repair of large osteochondral defects. *Arthritis Rheum* **46**, 2524, 2002.
  181. Tuli, R., Nandi, S., Li, W. J., Tuli, S., Huang, X., Manner, P. A., Laquerriere, P., Noth, U., Hall, D. J. and Tuan, R. S. Human mesenchymal progenitor cell-based tissue engineering of a single-unit osteochondral construct. *Tissue Eng* **10**, 1169, 2004.
  182. Kajiwara, R., Ishida, O., Kawasaki, K., Adachi, N., Yasunaga, Y. and Ochi, M. Effective repair of a fresh osteochondral defect in the rabbit knee joint by articulated joint distraction following subchondral drilling. *J Orthop Res* **23**, 909, 2005.
  183. Kim, T. K., Sharma, B., Williams, C. G., Ruffner, M. A., Malik, A., McFarland, E. G. and Elisseeff, J. H. Experimental model for cartilage tissue engineering to regenerate the zonal organization of articular cartilage. *Osteoarthritis Cartilage* **11**, 653, 2003.
  184. Tuan, R. S., Boland, G. and Tuli, R. Adult mesenchymal stem cells and cell-based tissue engineering. *Arthritis Res Ther* **5**, 32, 2003.
  185. Choumerianou, D. M., Dimitriou, H. and Kalmanti, M. Stem cells: promises versus limitations. *Tissue Eng Part B Rev* **14**, 53, 2008.
  186. Secco, M., Zucconi, E., Vieira, N. M., Fogaca, L. L., Cerqueira, A., Carvalho, M. D., Jazedje, T., Okamoto, O. K., Muotri, A. R. and Zatz, M. Mesenchymal stem cells from umbilical cord: do not discard the cord! *Neuromuscul Disord* **18**, 17, 2008.
  187. Prockop, D. J. Marrow stromal cells as stem cells for nonhematopoietic tissues. *Science* **276**, 71, 1997.

188. Zuk, P. A., Zhu, M., Ashjian, P., De Ugarte, D. A., Huang, J. I., Mizuno, H., Alfonso, Z. C., Fraser, J. K., Benhaim, P. and Hedrick, M. H. Human adipose tissue is a source of multipotent stem cells. *Mol Biol Cell* **13**, 4279, 2002.
189. Childs, R., Chernoff, A., Contentin, N., Bahceci, E., Schrupp, D., Leitman, S., Read, E. J., Tisdale, J., Dunbar, C., Linehan, W. M., Young, N. S. and Barrett, A. J. Regression of metastatic renal-cell carcinoma after nonmyeloablative allogeneic peripheral-blood stem-cell transplantation. *N Engl J Med* **343**, 750, 2000.
190. Jones, E. A., English, A., Henshaw, K., Kinsey, S. E., Markham, A. F., Emery, P. and McGonagle, D. Enumeration and phenotypic characterization of synovial fluid multipotential mesenchymal progenitor cells in inflammatory and degenerative arthritis. *Arthritis & Rheumatism* **50**, 817, 2004.
191. Huelsken, J., Vogel, R., Erdmann, B., Cotsarelis, G. and Birchmeier, W. beta-Catenin controls hair follicle morphogenesis and stem cell differentiation in the skin. *Cell* **105**, 533, 2001.
192. Seale, P., Asakura, A. and Rudnicki, M. A. The potential of muscle stem cells. *Dev Cell* **1**, 333, 2001.
193. Gronthos, S., Brahim, J., Li, W., Fisher, L. W., Cherman, N., Boyde, A., DenBesten, P., Robey, P. G. and Shi, S. Stem cell properties of human dental pulp stem cells. *J Dent Res* **81**, 531, 2002.
194. Guilak, F., Awad, H. A., Fermor, B., Leddy, H. A. and Gimple, J. M. Adipose-derived adult stem cells for cartilage tissue engineering. *Biorheology* **41**, 389, 2004.
195. Karahuseyinoglu, S., Cinar, O., Kilic, E., Kara, F., Akay, G. G., Demiralp, D. O., Tukun, A., Uckan, D. and Can, A. Biology of stem cells in human umbilical cord stroma: in situ and in vitro surveys. *Stem Cells* **25**, 319, 2007.
196. Troyer, D. L. and Weiss, M. L. Wharton's jelly-derived cells are a primitive stromal cell population. *Stem Cells* **26**, 591, 2008.
197. Hadidian, Z. and Pirie, N. W. The preparation and some properties of hyaluronic acid from human umbilical cord. *Biochem J* **42**, 260, 1948.
198. Bowles, H. E. and Mc, K. R. Ruptures of the umbilical cord with a case of intrapartum rupture of all three vessels. *Calif Med* **70**, 422, 1949.

199. Campard, D., Lysy, P. A., Najimi, M. and Sokal, E. M. Native umbilical cord matrix stem cells express hepatic markers and differentiate into hepatocyte-like cells. *Gastroenterology* **134**, 833, 2008.
200. Can, A. and Karahuseyinoglu, S. Concise review: human umbilical cord stroma with regard to the source of fetus-derived stem cells. *Stem Cells* **25**, 2886, 2007.
201. Carlin, R., Davis, D., Weiss, M., Schultz, B. and Troyer, D. Expression of early transcription factors Oct4, Sox2 and Nanog by porcine umbilical cord (PUC) matrix cells. *Reprod Biol Endocrinol* **4**, 8, 2006.
202. Fu, Y. S., Cheng, Y. C., Lin, M. Y., Cheng, H., Chu, P. M., Chou, S. C., Shih, Y. H., Ko, M. H. and Sung, M. S. Conversion of human umbilical cord mesenchymal stem cells in Wharton's jelly to dopaminergic neurons in vitro: potential therapeutic application for Parkinsonism. *Stem Cells* **24**, 115, 2006.
203. Fu, Y. S., Shih, Y. T., Cheng, Y. C. and Min, M. Y. Transformation of human umbilical mesenchymal cells into neurons in vitro. *J Biomed Sci* **11**, 652, 2004.
204. Lu, L. L., Liu, Y. J., Yang, S. G., Zhao, Q. J., Wang, X., Gong, W., Han, Z. B., Xu, Z. S., Lu, Y. X., Liu, D., Chen, Z. Z. and Han, Z. C. Isolation and characterization of human umbilical cord mesenchymal stem cells with hematopoiesis-supportive function and other potentials. *Haematologica* **91**, 1017, 2006.
205. Schmidt, D., Mol, A., Odermatt, B., Neuenschwander, S., Breymann, C., Gossi, M., Genoni, M., Zund, G. and Hoerstrup, S. P. Engineering of biologically active living heart valve leaflets using human umbilical cord-derived progenitor cells. *Tissue Eng* **12**, 3223, 2006.
206. Seshareddy, K., Troyer, D. and Weiss, M. L. Method to isolate mesenchymal-like cells from Wharton's Jelly of umbilical cord. *Methods Cell Biol* **86**, 101, 2008.
207. Wang, L., Seshareddy, K., Weiss, M. L. and Detamore, M. S. The effect of initial seeding density on human umbilical cord matrix mesenchymal stromal cells for fibrocartilage tissue engineering. *Tissue Eng, Part A* **In Press**, 2008.
208. Wu, K. H., Zhou, B., Lu, S. H., Feng, B., Yang, S. G., Du, W. T., Gu, D. S., Han, Z. C. and Liu, Y. L. In vitro and in vivo differentiation of human umbilical cord derived stem cells into endothelial cells. *J Cell Biochem* **100**, 608, 2007.

209. Wu, K. H., Zhou, B., Yu, C. T., Cui, B., Lu, S. H., Han, Z. C. and Liu, Y. L. Therapeutic potential of human umbilical cord derived stem cells in a rat myocardial infarction model. *Ann Thorac Surg* **83**, 1491, 2007.
210. Yang, L. Y., Zheng, J. K., Wang, C. Y. and Xu, M. D. [Stromal cells from human Wharton's jelly differentiate into neural cells]. *Sichuan Da Xue Xue Bao Yi Xue Ban* **36**, 13, 2005.
211. Pereira, W. C., Khushnooma, I., Madkaikar, M. and Ghosh, K. Reproducible methodology for the isolation of mesenchymal stem cells from human umbilical cord and its potential for cardiomyocyte generation. *J Tissue Eng Regen Med* 2008.
212. Kestendjieva, S., Kyurkchiev, D., Tsvetkova, G., Mehandjiev, T., Dimitrov, A., Nikolov, A. and Kyurkchiev, S. Characterization of mesenchymal stem cells isolated from the human umbilical cord. *Cell Biol Int* **32**, 724, 2008.
213. Lund, R. D., Wang, S., Lu, B., Girman, S., Holmes, T., Sauve, Y., Messina, D. J., Harris, I. R., Kihm, A. J., Harmon, A. M., Chin, F. Y., Gosiewska, A. and Mistry, S. K. Cells isolated from umbilical cord tissue rescue photoreceptors and visual functions in a rodent model of retinal disease. *Stem Cells* **25**, 602, 2007.
214. Jomura, S., Uy, M., Mitchell, K., Dallsen, R., Bode, C. J. and Xu, Y. Potential treatment of cerebral global ischemia with Oct-4+ umbilical cord matrix cells. *Stem Cells* **25**, 98, 2007.
215. Chao, K. C., Chao, K. F., Fu, Y. S. and Liu, S. H. Islet-like clusters derived from mesenchymal stem cells in Wharton's Jelly of the human umbilical cord for transplantation to control type 1 diabetes. *PLoS ONE* **3**, e1451, 2008.
216. Ennis, J., Gotherstrom, C., Le Blanc, K. and Davies, J. E. In vitro immunologic properties of human umbilical cord perivascular cells. *Cytotherapy* **10**, 174, 2008.
217. Weiss, M. L., Anderson, C., Medicetty, S., Seshareddy, K., Weiss, R. J., VanderWerff, I., Troyer, D. and McIntosh, K. R. Immune properties of human umbilical cord Wharton's jelly-derived cells. *Stem Cells* **Accept**, 2008.
218. Ennis, J., Sarugaser, R., Gomez, A., Baksh, D. and Davies, J. E. Isolation, characterization, and differentiation of human umbilical cord perivascular cells (HUCPVCs). *Methods Cell Biol* **86**, 121, 2008.

219. Karahuseyinoglu, S., Kocaefe, C., Balci, D., Erdemli, E. and Can, A. Functional structure of adipocytes differentiated from human umbilical cord stroma-derived stem cells. *Stem Cells* **26**, 682, 2008.
220. Friedman, R., Betancur, M., Boissel, L., Tuncer, H., Cetrulo, C. and Klingemann, H. Umbilical cord mesenchymal stem cells: adjuvants for human cell transplantation. *Biol Blood Marrow Transplant* **13**, 1477, 2007.
221. Sodian, R., Lueders, C., Kraemer, L., Kuebler, W., Shakibaei, M., Reichart, B., Daebritz, S. and Hetzer, R. Tissue engineering of autologous human heart valves using cryopreserved vascular umbilical cord cells. *Ann Thorac Surg* **81**, 2207, 2006.
222. Schmidt, D., Asmis, L. M., Odermatt, B., Kelm, J., Breymann, C., Gossi, M., Genoni, M., Zund, G. and Hoerstrup, S. P. Engineered living blood vessels: functional endothelia generated from human umbilical cord-derived progenitors. *Ann Thorac Surg* **82**, 1465, 2006.
223. Weiss, M. L. and Troyer, D. L. Stem cells in the umbilical cord. *Stem Cell Rev* **2**, 155, 2006.
224. McElreavey, K. D., Irvine, A. I., Ennis, K. T. and McLean, W. H. Isolation, culture and characterisation of fibroblast-like cells derived from the Wharton's jelly portion of human umbilical cord. *Biochem Soc Trans* **19**, 29S, 1991.
225. Baksh, D., Yao, R. and Tuan, R. S. Comparison of proliferative and multilineage differentiation potential of human mesenchymal stem cells derived from umbilical cord and bone marrow. *Stem Cells* **25**, 1384, 2007.
226. Nanaev, A. K., Kohnen, G., Milovanov, A. P., Domogatsky, S. P. and Kaufmann, P. Stromal differentiation and architecture of the human umbilical cord. *Placenta* **18**, 53, 1997.
227. Kobayashi, K., Kubota, T. and Aso, T. Study on myofibroblast differentiation in the stromal cells of Wharton's jelly: expression and localization of alpha-smooth muscle actin. *Early Hum Dev* **51**, 223, 1998.
228. Simmons, P. J., Gronthos, S., Zannettino, A., Ohta, S. and Graves, S. Isolation, characterization and functional activity of human marrow stromal progenitors in hemopoiesis. *Prog Clin Biol Res* **389**, 271, 1994.
229. Gao, J., Yao, J. Q. and Caplan, A. I. Stem cells for tissue engineering of articular cartilage. *Proc Inst Mech Eng [H]* **221**, 441, 2007.

230. Johnstone, B., Hering, T. M., Caplan, A. I., Goldberg, V. M. and Yoo, J. U. In vitro chondrogenesis of bone marrow-derived mesenchymal progenitor cells. *Exp Cell Res* **238**, 265, 1998.
231. Mackay, A. M., Beck, S. C., Murphy, J. M., Barry, F. P., Chichester, C. O. and Pittenger, M. F. Chondrogenic differentiation of cultured human mesenchymal stem cells from marrow. *Tissue Eng* **4**, 415, 1998.
232. Im, G. I., Jung, N. H. and Tae, S. K. Chondrogenic differentiation of mesenchymal stem cells isolated from patients in late adulthood: the optimal conditions of growth factors. *Tissue Eng* **12**, 527, 2006.
233. Spagnoli, A., Longobardi, L. and O'Rear, L. Cartilage disorders: potential therapeutic use of mesenchymal stem cells. *Endocr Dev* **9**, 17, 2005.
234. Longobardi, L., O'Rear, L., Aakula, S., Johnstone, B., Shimer, K., Chytil, A., Horton, W. A., Moses, H. L. and Spagnoli, A. Effect of IGF-I in the chondrogenesis of bone marrow mesenchymal stem cells in the presence or absence of TGF-beta signaling. *J Bone Miner Res* **21**, 626, 2006.
235. Naughton, B. A., San Roman, J., Liu, K., Purchio, A., Pavelec, R. and Rekettye, L. Cells isolated from Wharton's jelly of the human umbilical cord develop a cartilage phenotype when treated with TGF- $\beta$  *in vitro*. *FASEB J* **11:A19 (Abstr. No. 108)**, 1997.
236. Barry, F., Boynton, R. E., Liu, B. and Murphy, J. M. Chondrogenic differentiation of mesenchymal stem cells from bone marrow: differentiation-dependent gene expression of matrix components. *Exp Cell Res* **268**, 189, 2001.
237. Motoki, D. S. and Mulliken, J. B. The healing of bone and cartilage. *Clin Plast Surg* **17**, 527, 1990.
238. Habal, M. B. Bone repair by regeneration. *Clin Plast Surg* **23**, 93, 1996.
239. Honsawek, S., Dhitiseith, D. and Phupong, V. Effects of demineralized bone matrix on proliferation and osteogenic differentiation of mesenchymal stem cells from human umbilical cord. *J Med Assoc Thai* **89 Suppl 3**, S189, 2006.
240. Breymann, C., Schmidt, D. and Hoerstrup, S. P. Umbilical cord cells as a source of cardiovascular tissue engineering. *Stem Cell Rev* **2**, 87, 2006.
241. Schmidt, D. and Hoerstrup, S. P. Tissue engineered heart valves based on human cells. *Swiss Med Wkly* **137 Suppl 155**, 80S, 2007.

242. Patrick, C. W., Jr. Tissue engineering strategies for adipose tissue repair. *Anat Rec* **263**, 361, 2001.
243. Gomillion, C. T. and Burg, K. J. Stem cells and adipose tissue engineering. *Biomaterials* **27**, 6052, 2006.
244. Okita, K., Ichisaka, T. and Yamanaka, S. Generation of germline-competent induced pluripotent stem cells. *Nature* **448**, 313, 2007.
245. Yu, J., Vodyanik, M. A., Smuga-Otto, K., Antosiewicz-Bourget, J., Frane, J. L., Tian, S., Nie, J., Jonsdottir, G. A., Ruotti, V., Stewart, R., Slukvin, II and Thomson, J. A. Induced pluripotent stem cell lines derived from human somatic cells. *Science* **318**, 1917, 2007.
246. Quarto, R., Mastrogiacomo, M., Cancedda, R., Kutepov, S. M., Mukhachev, V., Lavroukov, A., Kon, E. and Marcacci, M. Repair of large bone defects with the use of autologous bone marrow stromal cells. *N Engl J Med* **344**, 385, 2001.
247. Marcacci, M., Kon, E., Moukhachev, V., Lavroukov, A., Kutepov, S., Quarto, R., Mastrogiacomo, M. and Cancedda, R. Stem cells associated with macroporous bioceramics for long bone repair: 6- to 7-year outcome of a pilot clinical study. *Tissue Eng* **13**, 947, 2007.
248. Mueller, S. M. and Glowacki, J. Age-related decline in the osteogenic potential of human bone marrow cells cultured in three-dimensional collagen sponges. *J Cell Biochem* **82**, 583, 2001.
249. Lee, S. Y., Miwa, M., Sakai, Y., Kuroda, R., Matsumoto, T., Iwakura, T., Fujioka, H., Doita, M. and Kurosaka, M. In vitro multipotentiality and characterization of human unfractured traumatic hemarthrosis-derived progenitor cells: A potential cell source for tissue repair. *J Cell Physiol* **210**, 561, 2007.
250. Guillot, P. V., Gotherstrom, C., Chan, J., Kurata, H. and Fisk, N. M. Human first-trimester fetal MSC express pluripotency markers and grow faster and have longer telomeres than adult MSC. *Stem Cells* **25**, 646, 2007.
251. Drukker, M. Immunogenicity of human embryonic stem cells: can we achieve tolerance? *Springer Semin Immunopathol* **26**, 201, 2004.
252. Drukker, M. and Benvenisty, N. The immunogenicity of human embryonic stem-derived cells. *Trends Biotechnol* **22**, 136, 2004.

253. Chen, X., McClurg, A., Zhou, G. Q., McCaigue, M., Armstrong, M. A. and Li, G. Chondrogenic differentiation alters the immunosuppressive property of bone marrow-derived mesenchymal stem cells, and the effect is partially due to the upregulated expression of B7 molecules. *Stem Cells* **25**, 364, 2007.
254. Cho, P. S., Messina, D. J., Hirsh, E. L., Chi, N., Goldman, S. N., Lo, D. P., Harris, I. R., Popma, S. H., Sachs, D. H. and Huang, C. A. Immunogenicity of umbilical cord tissue derived cells. *Blood* **111**, 430, 2008.
255. Mannello, F. and Tonti, G. A. Concise review: no breakthroughs for human mesenchymal and embryonic stem cell culture: conditioned medium, feeder layer, or feeder-free; medium with fetal calf serum, human serum, or enriched plasma; serum-free, serum replacement nonconditioned medium, or ad hoc formula? All that glitters is not gold! *Stem Cells* **25**, 1603, 2007.
256. Galban, C. J. and Locke, B. R. Analysis of cell growth kinetics and substrate diffusion in a polymer scaffold. *Biotechnol Bioeng* **65**, 121, 1999.
257. Martin, J. A., Hamilton, B. E., Sutton, P. D., Ventura, S. J., Menacker, F., Kirmeyer, S. and Munson, M. L. Births: Final data for 2005. *National Vital Statistics Reports* **56**, 1, 2007.
258. Detamore, M. S. and Athanasiou, K. A. Effects of growth factors on temporomandibular joint disc cells. *Arch Oral Biol* **49**, 577, 2004.
259. Detamore, M. S. and Athanasiou, K. A. Evaluation of three growth factors for TMJ disc tissue engineering. *Ann Biomed Eng* **33**, 383, 2005.
260. Dodge, G. R. and Jimenez, S. A. Glucosamine sulfate modulates the levels of aggrecan and matrix metalloproteinase-3 synthesized by cultured human osteoarthritis articular chondrocytes. *Osteoarthritis Cartilage* **11**, 424, 2003.
261. Bassleer, C., Rovati, L. and Franchimont, P. Stimulation of proteoglycan production by glucosamine sulfate in chondrocytes isolated from human osteoarthritic articular cartilage in vitro. *Osteoarthritis Cartilage* **6**, 427, 1998.
262. Varghese, S., Theprungsirikul, P., Sahani, S., Hwang, N., Yarema, K. J. and Elisseeff, J. H. Glucosamine modulates chondrocyte proliferation, matrix synthesis, and gene expression. *Osteoarthritis Cartilage* 2006.
263. Hwang, N. S., Varghese, S., Theprungsirikul, P., Canver, A. and Elisseeff, J. Enhanced chondrogenic differentiation of murine embryonic stem cells in hydrogels with glucosamine. *Biomaterials* **27**, 6015, 2006.

264. Uitterlinden, E. J., Jahr, H., Koevoet, J. L., Bierma-Zeinstra, S. M., Verhaar, J. A., Weinans, H. and van Osch, G. J. Glucosamine reduces anabolic as well as catabolic processes in bovine chondrocytes cultured in alginate. *Osteoarthritis Cartilage* **15**, 1267, 2007.
265. Uitterlinden, E. J., Jahr, H., Koevoet, J. L. M., Jenniskens, Y. M., Bierma-Zeinstra, S. M. A., DeGroot, J., Verhaar, J. A. N., Weinans, H. and van Osch, G. Glucosamine decreases expression of anabolic and catabolic genes in human osteoarthritic cartilage explants. *Osteoarthritis and Cartilage* **14**, 250, 2006.
266. Detamore, M. S. and Athanasiou, K. A. Tensile properties of the porcine temporomandibular joint disc. *J Biomech Eng* **125**, 558, 2003.
267. Terry, D. E., Rees-Milton, K., Smith, P., Carran, J., Pezeshki, P., Woods, C., Greer, P. and Anastassiades, T. P. N-acylation of glucosamine modulates chondrocyte growth, proteoglycan synthesis, and gene expression. *J Rheumatol* **32**, 1775, 2005.
268. Lippiello, L. Glucosamine and chondroitin sulfate: biological response modifiers of chondrocytes under simulated conditions of joint stress. *Osteoarthritis and Cartilage* **11**, 335, 2003.
269. Wang, L. and Detamore, M. S. Tissue engineering the mandibular condyle. *Tissue Eng* **13**, 1955, 2007.
270. Eyre, D. Collagen of articular cartilage. *Arthritis Res* **4**, 30, 2002.
271. Wang, L. and Detamore, M. S. Effects of growth factors and glucosamine on porcine mandibular condylar cartilage cells and hyaline cartilage cells for tissue engineering applications. *Arch Oral Biol*, **Epub ahead of print**, 1, 2008.
272. Freed, L. E., Vunjak-Novakovic, G., Biron, R. J., Eagles, D. B., Lesnoy, D. C., Barlow, S. K. and Langer, R. Biodegradable Polymer Scaffolds for Tissue Engineering. *Bio/Technology* **12**, 689, 1994.
273. Vunjak-Novakovic, G., Martin, I., Obradovic, B., Treppo, S., Grodzinsky, A. J., Langer, R. and Freed, L. E. Bioreactor cultivation conditions modulate the composition and mechanical properties of tissue-engineered cartilage. *Journal of Orthopaedic Research* **17**, 130, 1999.
274. Almarza, A. J. and Athanasiou, K. A. Effects of initial cell seeding density for the tissue engineering of the temporomandibular joint disc. *Ann Biomed Eng* **33**, 943, 2005.

275. Detamore, M. S., Athanasiou, K. A. and Mao, J. A call to action for bioengineers and dental professionals: directives for the future of TMJ bioengineering. *Ann Biomed Eng* **35**, 1301, 2007.
276. Herring, S. W., Decker, J. D., Liu, Z. J. and Ma, T. Temporomandibular joint in miniature pigs: anatomy, cell replication, and relation to loading. *Anat Rec* **266**, 152, 2002.
277. Herring, S. W. TMJ anatomy and animal models. *J Musculoskel Neuronal Interactions* **3**, 391, 2003.
278. Hidaka, C., Cheng, C., Alexandre, D., Bhargava, M. and Torzilli, P. A. Maturation differences in superficial and deep zone articular chondrocytes. *Cell Tissue Res* **323**, 127, 2006.
279. Hylander, W. L. The human mandible: lever or link? *Am J Phys Anthropol* **43**, 227, 1975.
280. Girdler, N. M. The behaviour of mandibular condylar cartilage in cell culture. *Int J Oral Maxillofac Surg* **22**, 178, 1993.
281. Kim, T. G. and Park, T. G. Biomimicking extracellular matrix: cell adhesive RGD peptide modified electrospun poly(D,L-lactic-co-glycolic acid) nanofiber mesh. *Tissue Eng* **12**, 221, 2006.
282. Chen, R., Curran, S. J., Curran, J. M. and Hunt, J. A. The use of poly(l-lactide) and RGD modified microspheres as cell carriers in a flow intermittency bioreactor for tissue engineering cartilage. *Biomaterials* **27**, 4453, 2006.
283. Venn, M. and Maroudas, A. Chemical composition and swelling of normal and osteoarthrotic femoral head cartilage. I. Chemical composition. *Ann Rheum Dis* **36**, 121, 1977.
284. Richardson, D. W. and Clark, C. C. Biochemical changes in articular cartilage opposing full- and partial-thickness cartilage lesions in horses. *Am J Vet Res* **51**, 118, 1990.
285. Brama, P. A., Tekoppele, J. M., Bank, R. A., Barneveld, A. and van Weeren, P. R. Functional adaptation of equine articular cartilage: the formation of regional biochemical characteristics up to age one year. *Equine Vet J* **32**, 217, 2000.
286. Homicz, M. R., Chia, S. H., Schumacher, B. L., Masuda, K., Thonar, E. J., Sah, R. L. and Watson, D. Human Septal Chondrocyte Redifferentiation in

- Alginate, Polyglycolic Acid Scaffold, and Monolayer Culture. *The Laryngoscope* **113**, 25, 2003.
287. Schulze-Tanzil, G., de Souza, P., Villegas Castrejon, H., John, T., Merker, H. J., Scheid, A. and Shakibaei, M. Redifferentiation of dedifferentiated human chondrocytes in high-density cultures. *Cell Tissue Res* **308**, 371, 2002.
288. Yaeger, P. C., Masi, T. L., de Ortiz, J. L., Binette, F., Tubo, R. and McPherson, J. M. Synergistic action of transforming growth factor- $\alpha$  and insulin-like growth factor-I induces expression of type II collagen and aggrecan genes in adult human articular chondrocytes. *Exp. Cell Res* **237**, 318, 1997.
289. van Osch, G., van der Veen, S. W. B. and Verwoerd-Verhoef, H. L. In Vitro Redifferentiation of Culture-Expanded Rabbit and Human Auricular Chondrocytes for Cartilage Reconstruction. *Plastic and Reconstructive Surgery* **107**, 433, 2001.
290. Mroz, P. J. and Silbert, J. E. Effects of [3H]glucosamine concentration on [3H]chondroitin sulphate formation by cultured chondrocytes. *Biochem J* **376**, 511, 2003.
291. Mroz, P. J. and Silbert, J. E. Use of 3H-glucosamine and 35S-sulfate with cultured human chondrocytes to determine the effect of glucosamine concentration on formation of chondroitin sulfate. *Arthritis Rheum* **50**, 3574, 2004.
292. Landesberg, R., Proctor, R. L., Rosier, R. N. and Puzas, J. E. The mandibular condylar growth center: separation and characterization of the cellular elements. *Calcif Tissue Int* **56**, 71, 1995.
293. Springer, I. N., Fleiner, B., Jepsen, S. and Acil, Y. Culture of cells gained from temporomandibular joint cartilage on non-absorbable scaffolds. *Biomaterials* **22**, 2569, 2001.
294. Almarza, A. J. and Athanasiou, K. A. Seeding techniques and scaffolding choice for tissue engineering of the temporomandibular joint disk. *Tissue Eng* **10**, 1787, 2004.
295. Guo, J. F., Jourdian, G. W. and MacCallum, D. K. Culture and growth characteristics of chondrocytes encapsulated in alginate beads. *Connect Tissue Res* **19**, 277, 1989.
296. Risbud, M. V. and Shapiro, I. M. Stem cells in craniofacial and dental tissue engineering. *Orthod Craniofac Res* **8**, 54, 2005.

297. Uematsu, K., Hattori, K., Ishimoto, Y., Yamauchi, J., Habata, T., Takakura, Y., Ohgushi, H., Fukuchi, T. and Sato, M. Cartilage regeneration using mesenchymal stem cells and a three-dimensional poly-lactic-glycolic acid (PLGA) scaffold. *Biomaterials* **26**, 4273, 2005.
298. Romanov, Y. A., Svintsitskaya, V. A. and Smirnov, V. N. Searching for alternative sources of postnatal human mesenchymal stem cells: candidate MSC-like cells from umbilical cord. *Stem Cells* **21**, 105, 2003.
299. French, M. M., Rose, S., Canseco, J. and Athanasiou, K. A. Chondrogenic differentiation of adult dermal fibroblasts. *Ann Biomed Eng* **32**, 50, 2004.
300. Kim, J. W., Kim, S. Y., Park, S. Y., Kim, Y. M., Kim, J. M., Lee, M. H. and Ryu, H. M. Mesenchymal progenitor cells in the human umbilical cord. *Ann Hematol* **83**, 733, 2004.
301. Kang, T. J., Yeom, J. E., Lee, H. J., Rho, S. H., Han, H. and Chae, G. T. Growth kinetics of human mesenchymal stem cells from bone marrow and umbilical cord blood. *Acta Haematol* **112**, 230, 2004.
302. Yang, S. E., Ha, C. W., Jung, M., Jin, H. J., Lee, M., Song, H., Choi, S., Oh, W. and Yang, Y. S. Mesenchymal stem/progenitor cells developed in cultures from UC blood. *Cytotherapy* **6**, 476, 2004.
303. Lee, M. W., Choi, J., Yang, M. S., Moon, Y. J., Park, J. S., Kim, H. C. and Kim, Y. J. Mesenchymal stem cells from cryopreserved human umbilical cord blood. *Biochem Biophys Res Commun* **320**, 273, 2004.
304. Lee, O. K., Kuo, T. K., Chen, W. M., Lee, K. D., Hsieh, S. L. and Chen, T. H. Isolation of multipotent mesenchymal stem cells from umbilical cord blood. *Blood* **103**, 1669, 2004.
305. Tondreau, T., Meuleman, N., Delforge, A., Dejeneffe, M., Leroy, R., Massy, M., Mortier, C., Bron, D. and Lagneaux, L. Mesenchymal stem cells derived from CD133-positive cells in mobilized peripheral blood and cord blood: proliferation, Oct4 expression, and plasticity. *Stem Cells* **23**, 1105, 2005.
306. Fuchs, J. R., Hannouche, D., Terada, S., Zand, S., Vacanti, J. P. and Fauza, D. O. Cartilage engineering from ovine umbilical cord blood mesenchymal progenitor cells. *Stem Cells* **23**, 958, 2005.
307. Gang, E. J., Jeong, J. A., Hong, S. H., Hwang, S. H., Kim, S. W., Yang, I. H., Ahn, C., Han, H. and Kim, H. Skeletal myogenic differentiation of mesenchymal stem cells isolated from human umbilical cord blood. *Stem Cells* **22**, 617, 2004.

308. Lu, F. Z., Fujino, M., Kitazawa, Y., Uyama, T., Hara, Y., Funeshima, N., Jiang, J. Y., Umezawa, A. and Li, X. K. Characterization and gene transfer in mesenchymal stem cells derived from human umbilical-cord blood. *J Lab Clin Med* **146**, 271, 2005.
309. Detamore, M. S., Orfanos, J. G., Almarza, A. J., French, M. M., Wong, M. E. and Athanasiou, K. A. Quantitative analysis and comparative regional investigation of the extracellular matrix of the porcine temporomandibular joint disc. *Matrix Biol* **24**, 45, 2005.
310. Tondreau, T., Lagneaux, L., Dejeneffe, M., Delforge, A., Massy, M., Mortier, C. and Bron, D. Isolation of BM mesenchymal stem cells by plastic adhesion or negative selection: phenotype, proliferation kinetics and differentiation potential. *Cytotherapy* **6**, 372, 2004.
311. Edwards, C. A. and O'Brien, W. D. Modified assay for determination of hydroxyproline in a tissue hydrolyzate. *Clin Chim Acta* **104**, 161, 1980.
312. Livak, K. J. and Schmittgen, T. D. Analysis of Relative Gene Expression Data Using Real-Time Quantitative PCR and the  $2^{-(\Delta\Delta C(T))}$  Method. *Methods* **25**, 402, 2001.
313. Nehring, D., Adamietz, P., Meenen, N. M. and Pötner, R. Perfusion cultures and modelling of oxygen uptake with three-dimensional chondrocyte pellets. *Biotechnology Techniques* **13**, 701, 1999.
314. Adesida, A. B., Grady, L. M., Khan, W. S., Millward-Sadler, S. J., Salter, D. M. and Hardingham, T. E. Human meniscus cells express hypoxia inducible factor-1alpha and increased SOX9 in response to low oxygen tension in cell aggregate culture. *Arthritis Res Ther* **9**, R69, 2007.
315. Yoo, J. U., Barthel, T. S., Nishimura, K., Solchaga, L., Caplan, A. I., Goldberg, V. M. and Johnstone, B. The chondrogenic potential of human bone-marrow-derived mesenchymal progenitor cells. *J Bone Joint Surg Am* **80**, 1745, 1998.
316. Benjamin, M. and Evans, E. J. Fibrocartilage. *J Anat* **171**, 1, 1990.
317. Benjamin, M. and Ralphs, J. R. Biology of fibrocartilage cells. *Int Rev Cytol* **233**, 1, 2004.
318. Bianco, P., Riminucci, M., Gronthos, S. and Robey, P. G. Bone Marrow Stromal Stem Cells: Nature, Biology, and Potential Applications. *Stem Cells* **19**, 180, 2001.

319. Owen, M. and Friedenstein, A. J. Stromal stem cells: marrow-derived osteogenic precursors. *Ciba Found Symp* **136**, 42, 1988.
320. Zuk, P. A., Zhu, M., Mizuno, H., Huang, J., Futrell, J. W., Katz, A. J., Benhaim, P., Lorenz, H. P. and Hedrick, M. H. Multilineage cells from human adipose tissue: implications for cell-based therapies. *Tissue Eng* **7**, 211, 2001.
321. Kavalkovich, K. W., Boynton, R. E., Murphy, J. M. and Barry, F. Chondrogenic differentiation of human mesenchymal stem cells within an alginate layer culture system. *In Vitro Cell Dev Biol Anim* **38**, 457, 2002.
322. Seghatoleslami, M. R. and Tuan, R. S. Cell density dependent regulation of AP-1 activity is important for chondrogenic differentiation of C 3 H 10 T 1/2 mesenchymal cells. *J Cell Biochem* **84**, 237, 2002.
323. Fung, Y. *Biomechanics: Mechanical Properties of Living Tissues*. Springer, 1993.
324. Schmidt, D. and Hoerstrup, S. P. Tissue engineered heart valves based on human cells. *Swiss Med Wkly* **136**, 618, 2006.
325. Hurrell, S. and Cameron, R. E. Polyglycolide: degradation and drug release. Part I: changes in morphology during degradation. *J Mater Sci Mater Med* **12**, 811, 2001.
326. Lu, H. H., Cooper, J. A., Jr., Manuel, S., Freeman, J. W., Attawia, M. A., Ko, F. K. and Laurencin, C. T. Anterior cruciate ligament regeneration using braided biodegradable scaffolds: in vitro optimization studies. *Biomaterials* **26**, 4805, 2005.
327. Chung, C., Mesa, J., Miller, G. J., Randolph, M. A., Gill, T. J. and Burdick, J. A. Effects of auricular chondrocyte expansion on neocartilage formation in photocrosslinked hyaluronic acid networks. *Tissue Eng* **12**, 2665, 2006.
328. Bryant, S. J., Durand, K. L. and Anseth, K. S. Manipulations in hydrogel chemistry control photoencapsulated chondrocyte behavior and their extracellular matrix production. *J Biomed Mater Res A* **67**, 1430, 2003.
329. Seidel, J. O., Pei, M., Gray, M. L., Langer, R., Freed, L. E. and Vunjak-Novakovic, G. Long-term culture of tissue engineered cartilage in a perfused chamber with mechanical stimulation. *Biorheology* **41**, 445, 2004.
330. Campbell, M. A., Handley, C. J., Hascall, V. C., Campbell, R. A. and Lowther, D. A. Turnover of proteoglycans in cultures of bovine articular cartilage. *Arch Biochem Biophys* **234**, 275, 1984.

331. Bolis, S., Handley, C. J. and Comper, W. D. Passive loss of proteoglycan from articular cartilage explants. *Biochim Biophys Acta* **993**, 157, 1989.
332. Bilgen, B., Orsini, E., Aaron, R. K. and Ciombor, D. M. FBS suppresses TGF-beta1-induced chondrogenesis in synoviocyte pellet cultures while dexamethasone and dynamic stimuli are beneficial.
333. Vunjak-Novakovic, G., Freed, L. E., Biron, R. J. and Langer, R. Effects of mixing on the composition and morphology of tissue-engineered cartilage. *AIChE Journal* **42**, 850, 1996.
334. Davisson, T. Static and dynamic compression modulate matrix metabolism in tissue engineered cartilage. *Journal of Orthopaedic Research* **20**, 842, 2002.
335. Kelly, D. J., Crawford, A., Dickinson, S. C., Sims, T. J., Mundy, J., Hollander, A. P., Prendergast, P. J. and Hatton, P. V. Biochemical markers of the mechanical quality of engineered hyaline cartilage. *J Mater Sci Mater Med* **18**, 273, 2007.
336. Allen, K. D. and Athanasiou, K. A. Scaffold and growth factor selection in temporomandibular joint disc engineering. *J Dent Res* **87**, 180, 2008.
337. Ross, R. J., Rodriguez-Arno, J., Bentham, J. and Coakley, J. H. The role of insulin, growth hormone and IGF-I as anabolic agents in the critically ill. *Intensive Care Med* **19 Suppl 2**, S54, 1993.
338. Kasukawa, Y., Miyakoshi, N. and Mohan, S. The anabolic effects of GH/IGF system on bone. *Curr Pharm Des* **10**, 2577, 2004.
339. Schulze, P. C. and Spate, U. Insulin-like growth factor-1 and muscle wasting in chronic heart failure. *Int J Biochem Cell Biol* **37**, 2023, 2005.
340. Wang, L., Lazebnik, M. and Detamore, M. S. Hyaline cartilage cells outperform mandibular condylar cartilage cells in a TMJ fibrocartilage tissue engineering application. *Osteoarthritis Cartilage* **In Press**, 2008.
341. Worster, A. A., Brower-Toland, B. D., Fortier, L. A., Bent, S. J., Williams, J. and Nixon, A. J. Chondrocytic differentiation of mesenchymal stem cells sequentially exposed to transforming growth factor-beta1 in monolayer and insulin-like growth factor-I in a three-dimensional matrix. *J Orthop Res* **19**, 738, 2001.
342. Indrawattana, N., Chen, G., Tadokoro, M., Shann, L. H., Ohgushi, H., Tateishi, T., Tanaka, J. and Bunyaratvej, A. Growth factor combination for

- chondrogenic induction from human mesenchymal stem cell. *Biochem Biophys Res Commun* **320**, 914, 2004.
343. Makower, A. M., Wroblewski, J. and Pawlowski, A. Effects of IGF-I, rGH, FGF, EGF and NCS on DNA-synthesis, cell proliferation and morphology of chondrocytes isolated from rat rib growth cartilage. *Cell Biol Int Rep* **13**, 259, 1989.
344. Kretlow, J. D. and Mikos, A. G. Review: mineralization of synthetic polymer scaffolds for bone tissue engineering. *Tissue Eng* **13**, 927, 2007.
345. Dawson, J. I. and Oreffo, R. O. Bridging the regeneration gap: stem cells, biomaterials and clinical translation in bone tissue engineering. *Arch Biochem Biophys* **473**, 124, 2008.
346. Rose, F. R. and Oreffo, R. O. Bone tissue engineering: hope vs hype. *Biochem Biophys Res Commun* **292**, 1, 2002.
347. Siddappa, R., Fernandes, H., Liu, J., van Blitterswijk, C. and de Boer, J. The response of human mesenchymal stem cells to osteogenic signals and its impact on bone tissue engineering. *Curr Stem Cell Res Ther* **2**, 209, 2007.
348. Stenderup, K., Justesen, J., Clausen, C. and Kassem, M. Aging is associated with decreased maximal life span and accelerated senescence of bone marrow stromal cells. *Bone* **33**, 919, 2003.
349. Bitar, M., Brown, R. A., Salih, V., Kidane, A. G., Knowles, J. C. and Nazhat, S. N. Effect of cell density on osteoblastic differentiation and matrix degradation of biomimetic dense collagen scaffolds. *Biomacromolecules* **9**, 129, 2008.
350. Holy, C. E., Shoichet, M. S. and Davies, J. E. Engineering three-dimensional bone tissue in vitro using biodegradable scaffolds: investigating initial cell-seeding density and culture period. *J. Biomed. Mater. Res* **51**, 376, 2000.
351. Sumanasinghe, R. D., Osborne, J. A. and Lobo, E. G. Mesenchymal stem cell-seeded collagen matrices for bone repair: Effects of cyclic tensile strain, cell density, and media conditions on matrix contraction in vitro. *J Biomed Mater Res A* 2008.
352. Boyan, B. D., Schwartz, Z., Bonewald, L. F. and Swain, L. D. Localization of 1, 25-(OH) 2D3-responsive alkaline phosphatase in osteoblast-like cells (ROS 17/2.8, MG 63, and MC 3T3) and growth cartilage cells in culture. *Journal of Biological Chemistry* **264**, 11879, 1989.

353. ter Brugge, P. J. and Jansen, J. A. In Vitro Osteogenic Differentiation of Rat Bone Marrow Cells Subcultured with and without Dexamethasone. *Tissue Eng* **8**, 321, 2002.
354. Broxmeyer, H. E., Douglas, G. W., Hangoc, G., Cooper, S., Bard, J., English, D., Arny, M., Thomas, L. and Boyse, E. A. Human umbilical cord blood as a potential source of transplantable hematopoietic stem/progenitor cells. *Proc Natl Acad Sci U S A* **86**, 3828, 1989.
355. Seale, P., Asakura, A. and Rudnicki, M. A. The Potential of Muscle Stem Cells. *Developmental Cell* **1**, 333, 2001.
356. Gronthos, S., Mankani, M., Brahimi, J., Robey, P. G. and Shi, S. Postnatal human dental pulp stem cells (DPSCs) in vitro and in vivo. *Proceedings of the National Academy of Sciences* 240309797, 2000.
357. Medicetty, S., Bledsoe, A. R., Fahrenholtz, C. B., Troyer, D. and Weiss, M. L. Transplantation of pig stem cells into rat brain: proliferation during the first 8 weeks. *Exp Neurol* **190**, 32, 2004.
358. Jaiswal, N., Haynesworth, S. E., Caplan, A. I. and Bruder, S. P. Osteogenic differentiation of purified, culture-expanded human mesenchymal stem cells in vitro. *J Cell Biochem* **64**, 295, 1997.
359. Neuhuber, B., Swanger, S. A., Howard, L., Mackay, A. and Fischer, I. Effects of plating density and culture time on bone marrow stromal cell characteristics. *Exp Hematol* 2008.
360. Yuan, X., Arthur, F. T. M. and Yao, K. *In vitro* degradation of poly(L-lactic acid) fibers in phosphate buffered saline. *Journal of Applied Polymer Science* **85**, 936, 2002.
361. Yoshimoto, H., Shin, Y. M., Terai, H. and Vacanti, J. P. A biodegradable nanofiber scaffold by electrospinning and its potential for bone tissue engineering. *Biomaterials* **24**, 2077, 2003.
362. Ducy, P., Zhang, R., Geoffroy, V., Ridall, A. L. and Karsenty, G. *Osf2/Cbfa1*: a transcriptional activator of osteoblast differentiation. *Cell* **89**, 747, 1997.
363. Schroeder, T. M., Jensen, E. D. and Westendorf, J. J. *Runx2*: a master organizer of gene transcription in developing and maturing osteoblasts. *Birth Defects Res C Embryo Today* **75**, 213, 2005.
364. Komori, T., Yagi, H., Nomura, S., Yamaguchi, A., Sasaki, K., Deguchi, K., Shimizu, Y., Bronson, R. T., Gao, Y. H., Inada, M., Sato, M., Okamoto, R.,

- Kitamura, Y., Yoshiki, S. and Kishimoto, T. Targeted disruption of *Cbfa1* results in a complete lack of bone formation owing to maturational arrest of osteoblasts. *Cell* **89**, 755, 1997.
365. Tou, L., Quibria, N. and Alexander, J. M. Transcriptional regulation of the human *Runx2/Cbfa1* gene promoter by bone morphogenetic protein-7. *Mol Cell Endocrinol* **205**, 121, 2003.
366. Landis, W. J. An overview of vertebrate mineralization with emphasis on collagen-mineral interaction. *Gravit Space Biol Bull* **12**, 15, 1999.
367. Walsh, S., Jordan, G. R., Jefferiss, C., Stewart, K. and Beresford, J. N. High concentrations of dexamethasone suppress the proliferation but not the differentiation or further maturation of human osteoblast precursors in vitro: relevance to glucocorticoid-induced osteoporosis. *Rheumatology (Oxford)* **40**, 74, 2001.
368. Murata, H., Tanaka, H., Taguchi, T., Shiigi, E., Mizokami, H., Sugiyama, T. and Kawai, S. Dexamethasone induces human spinal ligament derived cells toward osteogenic differentiation. *J Cell Biochem* **92**, 715, 2004.
369. Campbell, M. J., Reddy, G. S. and Koeffler, H. P. Vitamin D3 analogs and their 24-oxo metabolites equally inhibit clonal proliferation of a variety of cancer cells but have differing molecular effects. *J Cell Biochem* **66**, 413, 1997.
370. Partridge, N. C., Frampton, R. J., Eisman, J. A., Michelangeli, V. P., Elms, E., Bradley, T. R. and Martin, T. J. Receptors for 1,25(OH)<sub>2</sub>-vitamin D<sub>3</sub> enriched in cloned osteoblast-like rat osteogenic sarcoma cells. *FEBS Lett* **115**, 139, 1980.
371. Beresford, J. N., Joyner, C. J., Devlin, C. and Triffitt, J. T. The effects of dexamethasone and 1,25-dihydroxyvitamin D<sub>3</sub> on osteogenic differentiation of human marrow stromal cells in vitro. *Arch Oral Biol* **39**, 941, 1994.
372. Linkhart, T. A., Mohan, S. and Baylink, D. J. Growth factors for bone growth and repair: IGF, TGF beta and BMP. *Bone* **19**, 1S, 1996.
373. Jeong, W. K., Park, S. W. and Im, G. I. Growth factors reduce the suppression of proliferation and osteogenic differentiation by titanium particles on MSCs. *J Biomed Mater Res A* **86A**, 1137, 2008.
374. Koch, H., Jadlowiec, J. A. and Campbell, P. G. Insulin-like growth factor-I induces early osteoblast gene expression in human mesenchymal stem cells. *Stem Cells Dev* **14**, 621, 2005.